NEW YORK STATE OF OPPORTUNITY | NYSERDA

Regional Model Estimates of Acidic and Mercury Depositions over Refined Spatial Scales in Northeastern U.S. and the Contribution from New York Power Production Point Sources

Final Report

October 2016

Report Number 16-31

NYSERDA's Promise to New Yorkers:

NYSERDA provides resources, expertise, and objective information so New Yorkers can make confident, informed energy decisions.

Mission Statement:

Advance innovative energy solutions in ways that improve New York's economy and environment.

Vision Statement:

Serve as a catalyst – advancing energy innovation, technology, and investment; transforming New York's economy; and empowering people to choose clean and efficient energy as part of their everyday lives.

Regional Model Estimates of Acidic and Mercury Depositions over Refined Spatial Scales in Northeastern U.S. and the Contribution from New York Power Production Point Sources

Final Report

Prepared for:

New York State Energy Research and Development Authority

Albany, NY

Gregory Lampman
Senior Project Manager

Prepared by:

SEDEFIAN Consulting

Malta, NY

Leon Sedefian,
Principal Investigator

and

New York State Department of Environmental Conservation

Albany, NY

Mike Ku,
Kevin Civerolo
Winston Hao
Eric Zalewsky
Project Team

NYSERDA 16-31 NYSERDA Contract 50774 October 2016

Notice

Preferred Citation

New York State Energy Research and Development Authority (NYSERDA). 2016. "Regional Model Estimates of Inorganic Pollutant Depositions over Refined Spatial Scales in Northeastern U.S. and the Contribution from New York Power Production Sources". NYSERDA Report 16-31. nyserda.ny.gov/publications

Abstract

As recent U.S. Environmental Protection Agency (EPA) and New York State (NYS or the State) policy and regulatory approaches have emphasized the importance of the interaction of multi-pollutants, the need has shifted to more comprehensive techniques to ascertain their impacts. Requirements to reduce toxics such as mercury from power plants and the importance of sulfate and nitrate transport in the eastern United States have taken center stage as the EPA revisits the secondary national ambient standard for sulfur and nitrogen. These rules have relied on regional-scale photochemical models, which reflected emissions from over a decade ago, have a level of uncertainly due to the coarse grid resolution used and need to be updated in their technical capabilities.

The purpose of the current study was to address at least two of the limitations in previous regional modeling assessments by first, refining the previous coarse grid resolutions down to a 4km grid level in a novel application of the Community Multiscale Air Quality (CMAQ) Eulerian grid modeling system on an annual timescale. To that end, the latest available National Emissions Inventory (NEI) for 2011 and Weather Research and Forecasting (WRF) simulated meteorological data were generated on a 4km grid domain over the Northeastern U.S. centered on NYS. In addition to "natural" emissions of precursors, the NEI emissions data includes all anthropogenic point, area, and mobile sources. The second issue addressed was the study's determination of the contribution of the NYS major power generation sector point sources to the overall acidic and mercury depositions. For mercury, emissions of the elemental, oxidized and particulate species were characterized using available stack test and technology based data to properly assess the relative contribution of significant power sources such as Energy Generation Units (EGUs) and waste to energy (WTE) facilities. The speciation allowed CMAQ to account for the relative species dependent wet removal and dry deposition velocities in calculating total depositions.

The results of the CMAQ modeling for annual and seasonal deposition levels are presented over the modeling domain and, in particular, over NYS portion for the relative impact of power production sources. The results show the importance of both dry and wet deposition for the oxidized form of mercury, which has the largest contribution to the total mercury levels. The contribution of the State's power sector is deemed relatively small and very localized. The impact of emissions outside the modeling domain are found to dominate total Hg depositions in and around NYS, confirming the importance of regional and global transport into the State. For acidic deposition, the importance of wet deposition is noted for sulfates and nitrates, but dry deposition becomes dominant for total sulfur deposition. Larger summer vs. winter contributions for sulfate is noted, but for nitrate and mercury, no real distinction by

season is found. The reduction of emissions from the NYS power sector is determined to have an important effect in reducing total sulfur, but not sulfate or nitrate deposition over extensive areas of the State, while large reduction in EGUs and other sources modeled in a "future" 2018 scenario causes large reductions in sulfate and nitrate levels. A comparison of wet deposition observations to CMAQ results indicates remarkably good model performance for mercury and acidic deposition species.

Keywords

Regional modeling, CMAQ model, emission inventory, acidic deposition, mercury deposition, Adirondacks, Catskills, EGUs, WTEs, power production, AERMOD modeling, model evaluation.

Acknowledgments

We greatly appreciate the assistance of NYS Department of Environmental Conservation (DEC) Division of Air Resources (DEC/DAR) staff Tom Gentile, Steve DeSantis, Julia Stuart, Ruby Tian, Margaret Valis, and Central Office and Regional staff in providing valuable information, data and graphics and review of sections of the report. We also thank NYSERDA Project Manager, Gregory Lampman, for his valuable guidance throughout the project completion.

Table of Contents

List of Figures

List of Tables

Acronyms and Abbreviations

AAI: Aquatic Acidification Index
AERMOD: AMS/EPA Regulatory Model
AMAD: Atmospheric Modeling and Analysis Division
ANC: Acid Neutralizing Capacity
ASTRAP: Advanced Statistical Trajectory Regional Air Pollution
CAMD: Clean Air Markets Division
CAMR: Clean Air Mercury Rule
CAMx: Comprehensive Air Quality Model with Extensions
CASTNET: Clean Air Status and Trends Network
CCR: Combustion Residuals from Electric Utilities
CISWI: Commercial and Industrial Solid Waste Incineration
CMAQ: Community Multiscale Air Quality
CMAS: Community Modeling and Assessment System
CSAPR: Cross-State Air Pollution Rule
DAR: Division of Air Resources
DEC: New York State Department of Environmental Conservation
DRH: Deliquescence Relative Humidity
EGU: Energy Generation Unit
EPA: U.S. Environmental Protection Agency
ETV: Environmental Threshold Value
HAPs: Hazardous air pollutants
HNO_3: Nitric acid
Hg, Hg0, Hg2, HgP: mercury, its elemental, oxidized and particulate forms
ISC: Industrial Source Complex
LAI: Leaf area index
MAGIC: Model of Acidification of Groundwater in Catchments
MAP: Mercury Action Plan
MATS: Mercury and Air Toxics Standards
MDN: Mercury Deposition Network
MM5: Penn State/NCAR 5th generation Mesoscale Model
MWh: megawatt-hours
NADP: National Atmospheric Deposition Program
NAMMIS: North American Mercury Model Intercomparison Study
NAPAP: National Acid Precipitation Assessment Program
NED: National Elevation Dataset
NEG-ECP: New England Governors and Eastern Canadian Premiers
NEI: National Emissions Inventory

NERL: National Exposure Research Laboratory
NESCAUM: Northeast States for Coordinated Air Use Management
NESHAPS: National Emissions Standards for Hazardous Air Pollutant standards
NH4: particulate ammonium
NHx: reduced Nitrogen
NME: normalized mean error
NMB: normalized mean bias
NOx: Nitrogen oxides
NSPS: New Source Performance Standard
NTN/AIRMON: National Trends Network/Atmospheric Integrated Research Monitoring Network
NWS: National Weather Service
OTC: Ozone Transport Commission
PCA: Portland Cement Association
PM2.5: Particulate Matter of size less than 2.5 um
RADM: Regional Acid Deposition Model
RATA: Relative Accuracy Test Audit
RELMAP: Regional Lagrangian Model of Air Pollution
RRF: Resource Recovery Facility
SADCA: State Acidic Deposition Control Act
SMOKE: Sparse Matrix Operator Kernel Emissions
SOx: Sulfur oxides
TDEP: Total Deposition Science Committee
TRI: EPA's Toxics Release Inventory
TS: Total sulfur
TSD: EPA's Technical Support Document
WRF: Weather Research and Forecasting
WTE: Waste to energy

Summary

The importance of atmospheric processes and the response of the underlying land and water surface to anthropogenic air pollutant input has been studied considerably in recognition of the importance of this controlling pathway for acidic and mercury deposition. As more recent EPA and NYS policy and regulatory approaches have emphasized an interest in the interaction of multi-pollutant mixtures and their consequences on the ecological systems, the need for more comprehensive approaches has surfaced. This shift has been brought about by requirements to reduce toxics such as mercury from power plants and regulations to reduce regional scale emissions of acidic deposition precursors. These requirements have been supported by technical documents with heavy reliance on regional photochemical modeling assessments. In addition, research studies have used the results of similar modeling analyses to guide and verify the consequences of emissions changes on acidic and mercury deposition levels.

Many national and NYS requirements affect the emissions and interactions of pollutants from energy production sources such as Energy Generation Units (EGUs) and waste to energy (WTE) facilities. However, technical assessments to carry out these requirements, and to understand the multi-pollutant system have not been commensurate with the latest emissions data and the techniques or approaches necessary to properly assess the implementation of these requirements. In addition, the quantification of the impacts from important source categories is either lacking or outdated by reliance on older modeling simulation results, including past emission inventories, older chemical modules, and relatively coarse meteorological and modeled grid data. The latter limitation has not allowed the proper resolution of the spatial distribution of acidic and mercury deposition in some areas with the complex terrain setting of the Adirondacks and the Catskills. Further complications arise such as the finding that mercury impacts on the ecosystem by anthropogenic emissions are obscured by the interaction of atmospheric deposition and “naturally” occurring reemissions from the underlying surfaces.

The objective of our study was to use the most recent emissions data and meteorological fields to project acidic and mercury deposition on a refined grid across the northeast with emphasis on NYS, and to determine the contribution of major energy production sources to these levels. In particular, the following updates and refinements were carried out:

1. The latest version of the EPA Community Multiscale Air Quality (CMAQ) regional modeling system was used to project annual levels of acidic and mercury deposition over a 4km refined grid covering the upper eastern portion of the U.S. The CMAQ version included updates to both the mercury physical and chemical module and to the simulation of acidic aerosols. Previous modeling assessments had, at best, relied on a 12km resolution grid.
2. The CMAQ simulations used the latest available 2011 National Emissions Inventory (NEI) to generate the source specific data on the 4km grid by its emissions processor. Previous regulatory analysis had relied on the 2005 NEI. Furthermore, the study used the latest meteorological processor, the Weather Research and Forecasting (WRF), to refine the simulation of the necessary dynamic (e.g., wind flow) and static (temperature) parameter fields on the 4km grid.
3. Most germane for the study was the lack of full determination of the NYS power generation sector's major source contributions to statewide acidic and mercury deposition. Source categories of importance for both deposition species, such as EGUs and WTEs, were identified in the NYS inventory and detailed data review conducted to assure the most reliable emissions parameters were used in the study. CMAQ modeling was then conducted to determine deposition levels from the overall 2011 NEI, as well as the relative contribution of the energy production sector to these levels. In addition, for acidic deposition, another CMAQ analysis was conducted for a projected 2018 "future" emissions inventory to determine the consequences of ongoing/proposed reductions in emissions from the 2011 NEI.

To carry out these tasks, it was first prudent to review previous modeling assessments for regulatory emphasis and implementation of pollutant specific emission reductions to ascertain expectations and potential pitfalls in the current modeling approaches. This review is outlined in Section 2, with specific reference to the regional modeling assessments carries out by the EPA and by/for the Northeastern United States over the last three decades. It is natural that the assessments and the techniques used have evolved over time in both sophistication and abilities, starting with the first in the nation regulation by NYS for acidic deposition and a corresponding assessment for mercury in line with the EPA's Mercury Report to Congress. As CMAQ applications became more practical and comprehensive, it became the model of choice for many regional analyses for the background documentations for EPA regulations and the states implementation of these regulations. Thus, CMAQ was chosen as the platform for performing the study.

Section 3 provides a summary of the pertinent aspects of the CMAQ modeling approach, including the emission inventory processing module, the meteorological simulation module and the kernel of the physical and chemical processes included in the latest version. The refined 4km modeling domain and the outer "nested" 12km domain are shown in Section 3, with the latter serving to generated boundary conditions for the CMAQ refined grid. The refined grid is found to better represent the terrain features as well as the spatial distribution of meteorological parameters such as precipitation. However, the 4km grid is still deemed too coarse for specific terrain features such as Whiteface and Hunter Mountains. Thus, limited supplemental pollutant patterns near these features were generated by the EPA's AERMOD

(AMS/EPA Regulatory Model) system. The purpose of this latter analysis was exclusively to determine potential gradients around the terrain features and not for any comparisons to the CMAQ results due to the relatively simplistic treatment of transport, dispersion, and chemical transformation in AERMOD. Both models, however, rely on the same basic approaches to the calculation of dry and wet deposition by the use of, respectively, the resistance model approach that generates dry deposition velocities from pollutant specific characteristics, combined with land use data, and wet removal due to precipitation in the column through which the plume is transported. A summary of the approach is presented in Section 3.

An important consideration in any modeling assessment is the adequacy of the emission inventory data, which is one of the critical inputs. In regional modeling studies, this inventory contains essentially all known anthropogenic source types and their pollutant specific emission rates and stack parameters or release configurations. In addition, known pertinent “naturally” occurring emissions of pollutants, such as forest fires, are included in the inventory used for the study. The assurance of the validity of all the data used, especially for sources outside of NYS, is an enormous and impractical task. Thus, for the current study, the approach was to identify major point sources in NYS of importance to acidic and mercury deposition and to perform as comprehensive of a review as possible with available data from the DEC. Certain of these source types were identified from previous modeling and field studies, such as EGUs for both deposition species and WTEs specific to mercury deposition. In this study, some additional point sources with relatively high mercury emissions were identified in the review of NYS inventory data. These sources included cement plants and metal processing facilities and, in fact, had higher mercury emissions than the coal EGUs and WTEs combined. Thus, these sources were classified as “other” important mercury sources and included in the stack emission and parameter review. Details on the emission inventory review are presented in Section 4.

The result was a set of about three dozen facilities for which detailed data from DEC files were reviewed. The locations of these facilities are shown in Figure S-1. The review concluded with revisions to both emission rates and stack parameters for about one-quarter of the facilities, including a reduction in mercury emissions from the large NYS point sources. A simple review of known area sources of mercury in NYS also was conducted with a reduction of about one-third in emissions from specific residual oil burning sources.

Figure S-1. Locations of Potential Large Point Sources in NYS based on 2011 NEI data

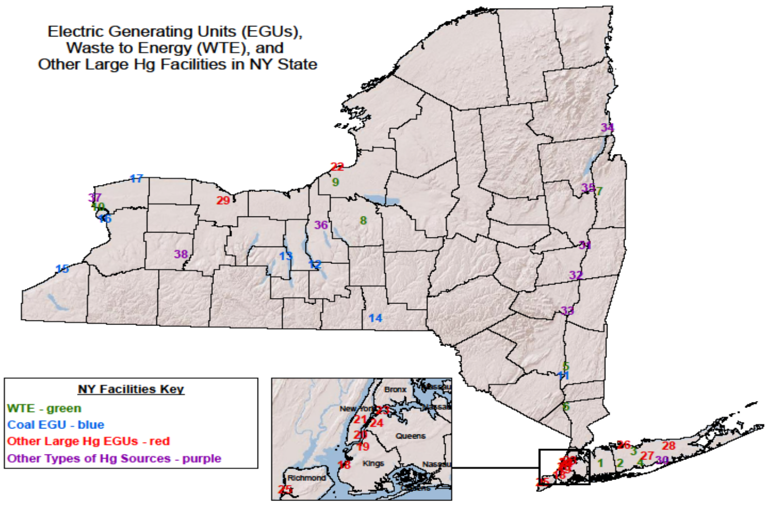

Another important aspect of the emission data review dealt with the speciation of mercury into its elemental (Hg0), oxidized (Hg2) and particulate (HgP) forms. The specification of percent of emissions of these three species for the various source types was deemed necessary because of the large differences previously found for the dry deposition velocities and wet washout factors between the species. Available emission speciation studies were reviewed and the determination was made to use the factors from an older EPA and Northeast states study due to their reliance on actual data for coal burning EGUs and WTEs and the identification of "default" breakdowns for other source types. For cement plants, additional data was invoked for the speciation for NYS sources, including stack test data for one plant. Details are given in Subsection 4.3.

In the review of the supporting information for the 2011 NEI data, it was noted that certain coal burning EGUs and WTE have been shut down or curtailed since the 2011 inventory. Thus, the consequences of these modifications were considered in the discussion of the results. Furthermore, these and other major sources in the 2011 NEI were missing in a "future" 2018 inventory based on the EPA's emissions modeling to reflect the implementation of two major regulations affecting the EGUs, and to a smaller extent, WTEs. Thus, CMAQ was run for the whole 2011 data year for the base case 2011 NEI, then for a "zero out" case wherein the major power production sources were eliminated so as to determine their relative effect and for the 2018 "future" inventory. The results are then presented for the acidic and mercury deposition patterns on the modeling domain for three scenarios: 1) the base 2011 NEI case; 2) the consequences of the NYS power sector major point sources, which is determined by dividing the difference between the base case and the "zero out" case by the base case results; and 3) the difference between the "future" 2018 inventory and the base case, divided by the base 2011 case. For the power sector contribution, the normalized or relative differences calculated provide the fraction of the total 2011 base case due to the EGUs, WTEs, and "other" large emitters in NYS. The results are detailed in Section 5. Additionally, a comparison of the CMAQ predicted acidic and mercury wet deposition for the base 2011 case are compared to corresponding data collected at numerous National Atmospheric Deposition Program (NADP)'s and Mercury Deposition Network (MDN) sites. No similar robust data exists for the dry deposition component due to monitoring difficulties with direct and surrogate methods, such that a comprehensive evaluation is not possible for the whole results.

Maps of deposition patterns for sulfate, SO4eq defined as particulate SO4 plus gas-phase H2SO4, total sulfur (TS, as sulfate equivalent) defines as SO4 plus 1.5 times gaseous SO2), nitrate, NO3eq defined asparticulate NO3 plus gas-phase HNO3), ammonium (NH4), and reduced Nitrogen (NHx as ammonium equivalent) defined as particulate NH4 plus gas phase NH3), and for the three species (elemental (Hg0), oxidized gaseous (Hg2) and particulate (HgP), and total mercury (THG) were generated for the CMAQ modeling scenarios noted above. Limited maps of the dry and wet components of the total deposition were also generated, plus some summer vs. winter season differences for the base case results. A subset of the more pertinent results discussed in Section 5 are summarized here. Also, one of the findings from the AERMOD modeling results presented in Section 6 is provided.

One aspect of the CMAQ modeling was some initial testing to guide the rest of the assessment. This initial CMAQ run used three months of "summer" 2011 meteorological data over the 12km grid resolution and indicated that the Hg impacts in the modeling domain from all of the State's sources, and, in fact, due to all of the in-domain sources were a small fraction of the overall deposition results when all sources outside of the domain were included as influx to the domain and the bi-directions option described in the methods section was invoked. The graphical presentation for this summer Hg modeling is repeated in Figure S-2. This refined modeling result of the dominance of out-of-state sources confirm the "crude" modeling performed in 2002 for NYS receptors described in Section 2, which indicated the clear dominance of out of the region, and in fact, out of the U.S. sources. This result differs from the acidic deposition results described in Section 5 and is attributed to the distinct differences in the chemical and physical transformations and in dry and wet deposition factors in CMAQ for the two species. For example, the dominant elemental form of mercury in the emissions profiles for the majority of the source types modeled has a low dry deposition velocity and wet deposition scavenging factor.

Figure S-2. CMAQ predictions of weekly mercury wet deposition at all MDN sites for mid-May to end of July, 2011 with and without boundary conditions (BC) and bidirectional (Bi-di) flux

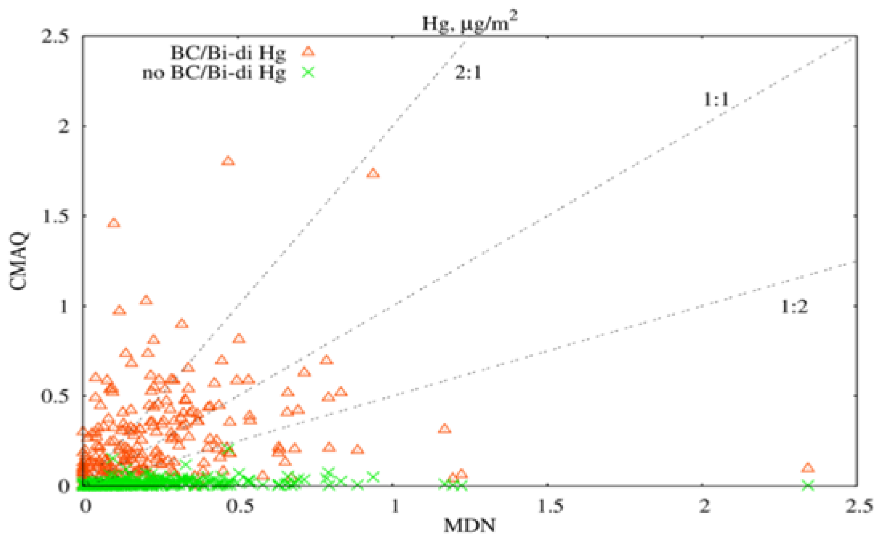

It is important to note that the deposition levels presented are accumulated values over the timeframes discussed. For example, the annual results are the amount of deposition accumulated by the model over a 11-month period of (instead of the full year) 2011 since most of the meteorological data for March was missing, as noted previously, thus, the month was not modeled. The CMAQ projected total annual SO4eq and its wet component are presented in Figure S-3(a) while total TS and its dry deposition fraction are shown in Figure S-3 (b). For SO4eq and sulfate, it was found that the wet component essentially controls the total impacts over the domain with overall maxima in southwestern PA and a relatively smooth pattern over NYS, at least on the scales used for the whole domain representation.

On the other hand, the inclusion of gaseous SO_2 deposition in TS results in expected overall larger impacts over the domain (left map in [a] vs. left map in [b] due to its higher dry deposition velocity). The dry component contributes above 50 percent to TS over most of the domain, as shown in the fraction map (i.e., over 0.5), but in NYS the dry component is less than 50 percent over extended areas, especially in the Adirondacks. The corresponding maps for NO_{3eq} (presented in section 5) show approximately the same level of deposition as for sulfate, but an equal importance of the wet and dry components due to the influence of the higher dry deposition for gaseous nitric acid (HN03). Maps of reduced Nitrogen (NHxeq) show much lower absolute impacts, confined mainly to areas of large ammonia (NH3) emissions from agricultural activities. However, it is recognized that on the relative Nitrogen deposition basis, the contribution of NHxeq becomes as, if not more important on a molar weighted scale. A comparison of summer vs. winter month total deposition shows the dominance of the former for TS, but less so for SO4eq and no difference for NO3eq.

Figure S-3. Annual accumulated total (left) and wet (right) SO4eq deposition in (a) and total sulfur (TS) (left) and its dry fraction (right) in (b)

(a)

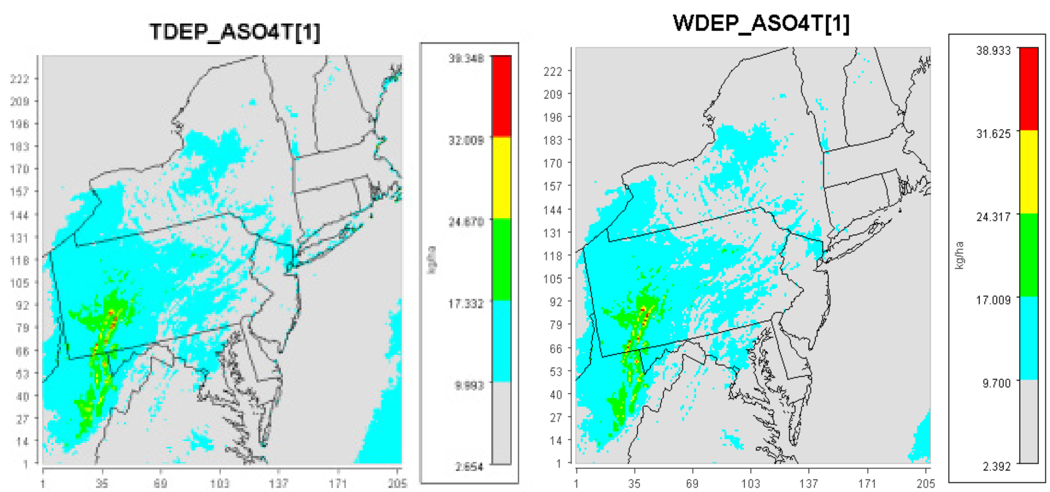

(b)

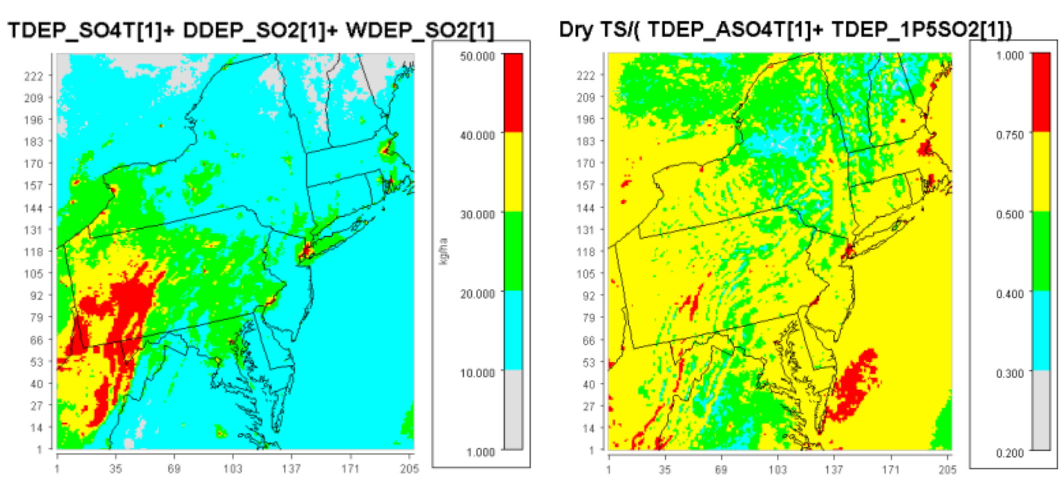

The contribution of the power sector's major point sources was determined as the relative difference between the CMAQ runs for the base 2011 NEI case and the "zero out" case, wherein these sources were eliminated in the latter case and the result divided (or normalized) by the base case levels. These plots were limited to NYS and its immediate surroundings since the domain scale maps showed no influence by the NYS power sector sources in other areas. Examples of this relative difference for SO4eq and TS are presented in Figure S-4. Similar plots for NO3eq and NHxeq showed very small differences. It shows that the power sector's influence on annual SO4eq deposition is essentially less than 7.5 percent, with very limited areas having somewhat higher reductions due to the elimination of these sources. On the other hand, the TS map shows a very distinct and extended areas of impacts due to the power sector as a direct result of reductions in SO2 emissions in the "zero out" CMAQ run. The reductions appear highest (over 40 percent) in areas of the large coal burning EGUs depicted in Figure S-1, with lesser, but still important reductions (about 25 percent) outwards from these facilities. In addition, it shows these reductions have an influence over the Catskills, but not over the Adirondacks. It was determined that many of the coal burning facilities have either eliminated or greatly reduced reliance on coal vs. cleaner fuels such as gas since the 2011 base case, which means that reductions in deposition has been realized in these areas.

Figure S-4. Relative difference in total SO4eq (top) and TS (bottom) deposition from the base case and the "zero out" case

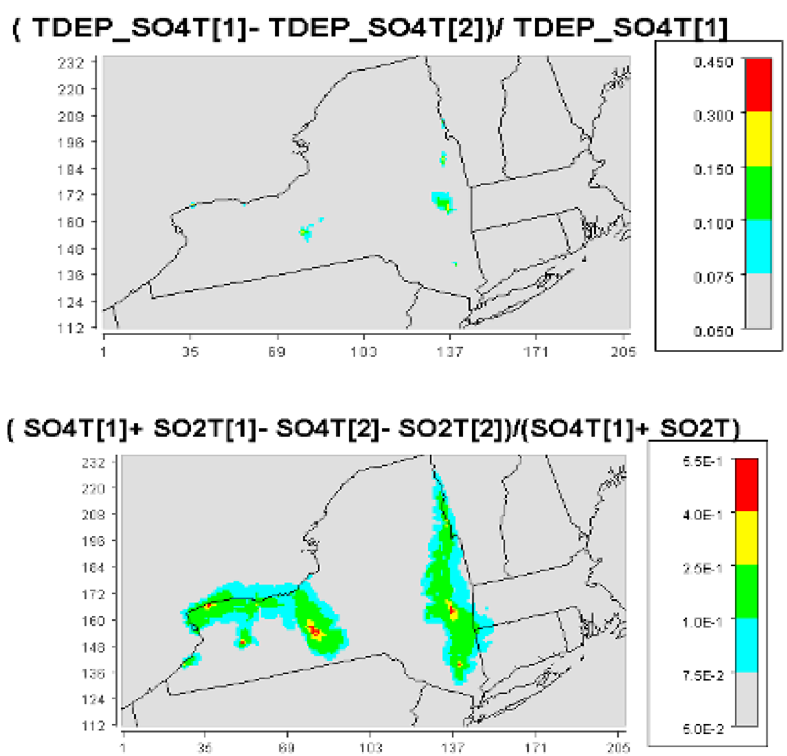

Turning to the mercury results, Figure S-5 shows the annual deposition of total mercury (THG) and its three species, elemental (Hg0), oxidized (Hg2) and particulate (HgP) forms for the 2011 NEI base case. These deposition plots have a scale in ug/m2 due to much smaller mercury levels and are on the same basis for ease of comparison (except for the upper limits set by the plotting routine, which are not consequential to the discussion). It is projected that annual THG deposition is contributed mostly by the oxidized form, followed by the elemental and, to a much lesser extent, by the particulate form. This result is a consequence of the known low washout factor and dry deposition velocity for Hg0, even though its emissions are in par with or higher than for Hg2 for the major point sources and other source categories. The low contribution by HgP is due to the low percentage (few percent) of this species in the emissions profile. These results are in line with other modeling studies discussed in Section 5, but seem contrary to other types of studies that identify Hg0 as the overwhelming contributor to deposition. The difference is the fact that the latter studies use ambient Hg0 concentrations to calculate deposition by simple schemes for deposition velocity, with observed Hg0 levels being two to three orders of magnitude higher than for Hg2 and HgP. These observations are contributed by continental scale transport and naturally occurring elemental mercury, or by the conversion of less stable Hg species to Hg0 in the atmosphere. The modeling exercise, on the other hand, accounts only for known anthropogenic emissions and also included the large re-emission of mercury to the atmosphere, which counteracts the surface deposition.

The contribution of the power sector point sources plus “other” major Hg sources was determined the same way it was calculated for the acidic deposition species. That is, relative difference maps were created for the species and the example for Hg2 is presented in Figure S-6. This map is similar to the TS one in Figure S-4 to the extent that it identifies areas where the “elimination” of the major point sources in CMAQ corresponds to reductions in deposition. In addition, for Hg, reductions have also occurred at some of the WTEs and the areal extent of the reductions is much smaller for Hg2 due to the much lower contribution of these sources to the overall mercury deposition, which is dominated by emissions influx from outside the modeling domain as demonstrated in Section 5. The relative difference for THG reflect the same general pattern as for Hg2, while the patterns for Hg0 is less distinguished on local scales than in Figure S-6, with wet component contributing to the localized deposition reductions. The corresponding map for HgP does not show any real effect by the power sector sources due to their very small emissions of this species.

Figure S-5. Annual species (Hg0, Hg2, HgP) and total (THG) Hg deposition for base case

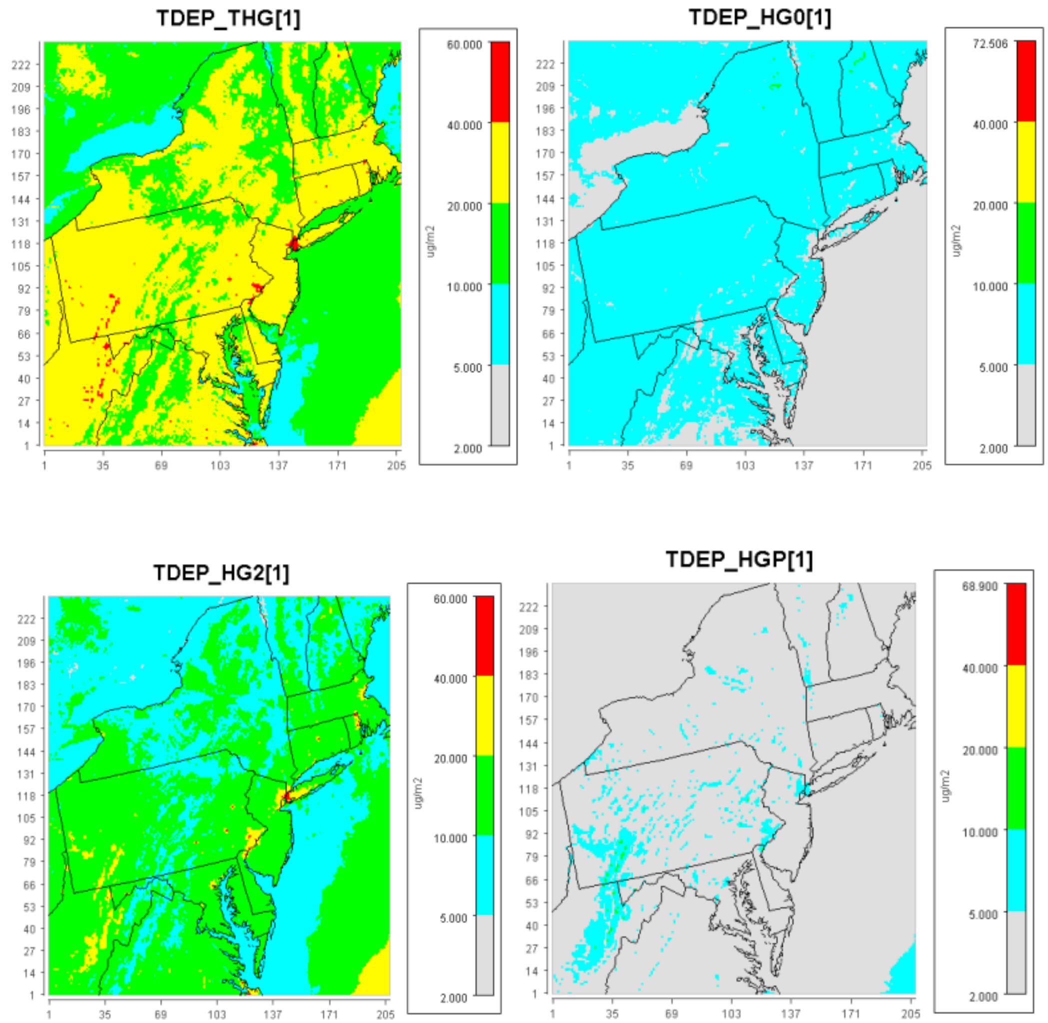

Figure S-6. Relative difference in annual total Hg2 deposition between the base and "zero out" cases

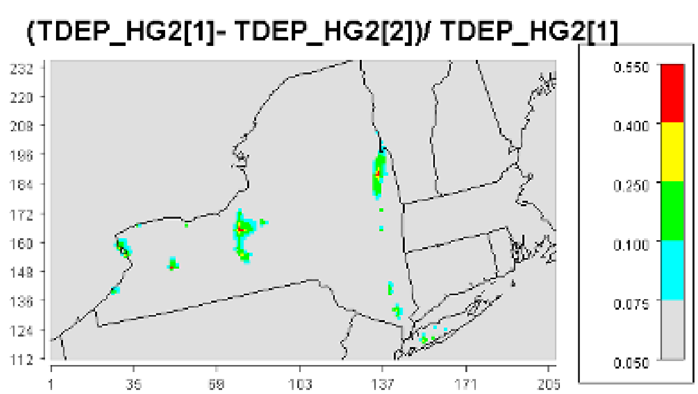

As is the case for general model applications, in order to gauge the appropriateness of these CMAQ estimates, it is necessary to test the model's performance again observational data. For acidic and mercury deposition, such data in the U.S. is collected at National Atmospheric Deposition Program (NADP)'s Mercury Deposition Network (MDN) and NTN (National Trends Network) sites. However, the spatial distribution of such monitoring is sparse and limited to only the wet deposition component. There are no robust and accurate direct measurements of the dry components and the surrogate methods used, such as litterfall, are limited to specific areas with forest cover, which lack the level of accuracy for proper model evaluations. Thus, only the wet deposition component can be compared to the corresponding observation, and then only to the sulfate, nitrate, or total mercury species. Such a comparison was performed for the seasonal and annual 2011 projections of these three species and the result for mercury is shown in Figure S-7. Also included in the plot are the corresponding simultaneous precipitation data from the NTN sites. The plots for SO4 and NO3 are very similar to the mercury plot.

It is clear that CMAQ underestimates the annual levels, mainly due to the underestimation of precipitation by the meteorological processor, especially in the summer months. This occurs even though CMAQ/WRF was applied with the subgrid convective option for simulating these small scale features. Similar underestimations of precipitation by CMAQ have been reported in most of the previous model evaluations referenced in Section 2. However, a limited assessment of the data indicates that the underestimation of deposition is not solely the result of the precipitation underestimation, but is likely a more complex mix with transformation and transport considerations. Statistics of model performance for each season and on the annual level indicates that the model errors and biases are all well within previous CMAQ evaluations, with the annual simulations within 30 percent of observations, with the lowest bias of -6.5% surprisingly for mercury. Clearly a number of important factors come into play such as the number of monitors and their locations, the uncertainly in the emissions inventory, and the physical and chemical processes in CMAQ simulations. To the uninitiated in modeling assessments, these results might be considered poor, but from the standpoint of the modeling community, these results are remarkably good.

Figure S-7. Comparisons of CMAQ to observed wet deposition of Hg at MDN sites (a) and precipitation at NADP NTN sites (b)

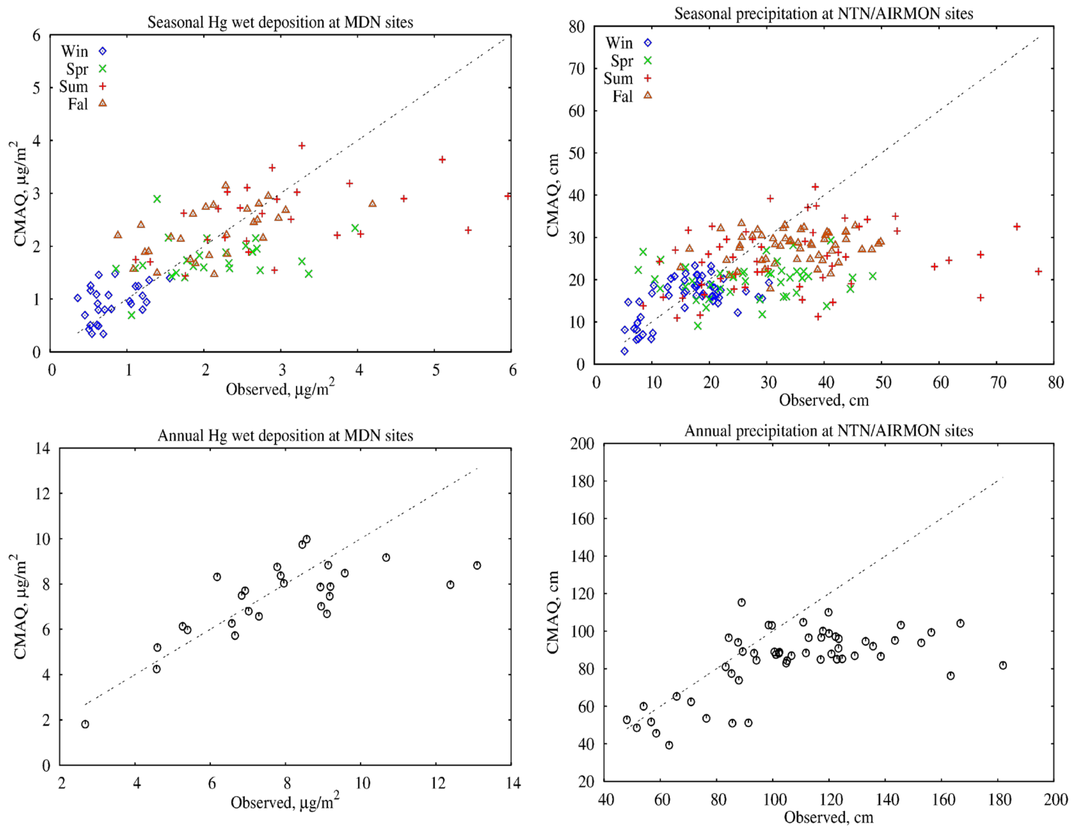

Another aspect to note is the comparisons of the "future" year 2018 inventory results in relation to the base 2011 NEI results. Normalized differences similar to the "zero out" vs. base case were plotted for total acidic deposition species; those for TS and NO_{3eq} are shown in Figure S-8. The results indicate about 40–50 percent reduction in TS deposition and about 20–30 percent reduction in NO_3 values. No such difference was found for the NHx results. Interestingly, relatively large reductions are seen in NYS, especially for NO3. The TS and NO_{3eq} reductions were found to be associated with both wet and dry components. The reductions are clearly related to current and future implementation of EPA regulations, which affect a large reduction in the emissions from coal burning EGUs, as well as expected reductions from other facilities.

Figure S-8. Total annual TS (left) and NO3eq (right) deposition difference between the 2011base case and the 2018 future cases

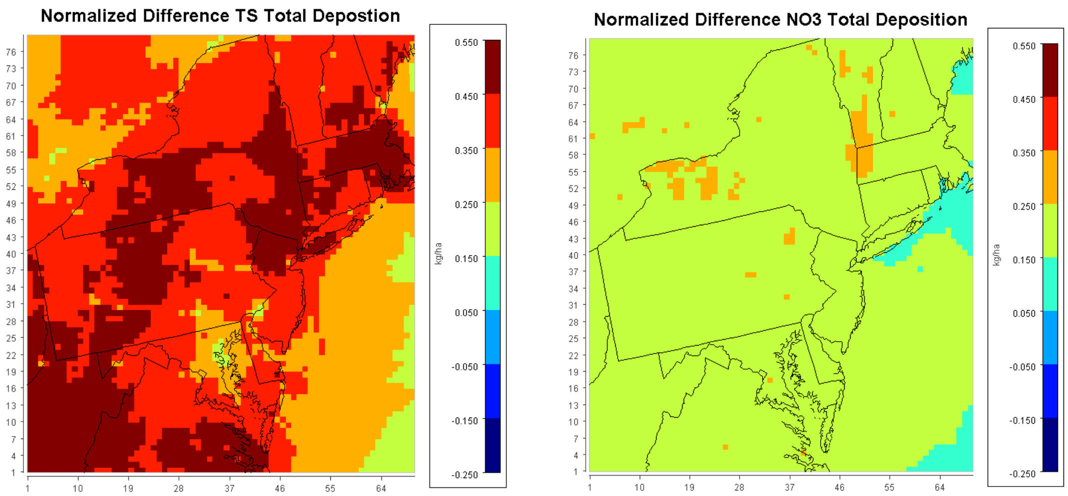

The last aspect of the study to note is the simplified AERMOD modeling conducted to determine the potential gradients on the level of complex terrain features of Whiteface and Hunter Mountains, which were obscured by even the refined 4km grid used in CMAQ. There were a number of source scenarios model, ranging from the simulation of the case of uniform concentration in the air parcel arriving at both mountains to instances of emissions from varied source heights. Example patterns were presented, such as the case of deposition from the Danskammer facility, located at 70km SE of the Catskill receptor grid, as depicted in Figure S-9. The gradients of Hg2 deposition are in terms of isopleths (lines of constant values) and seem to maximize at the northern edge of the grid where the terrain features are at heights relatively close to the plume height from the facility. An analysis of a set of 24-hour meteorological conditions from the AERMOD model to the corresponding data from the CMAQ/WRF system revealed that the maxima in concentrations do not occur on the same days. In general, the deposition maxima are associated with higher wind speed days, while the higher concentration days have low wind speed conditions. These corresponding surface layer scaling parameters follow the Monin-Obhukov relationships to a large extent, with few exceptions. In addition, the spatially varying wind speeds and directions simulated by the WRF meteorological processor are found to better represent observations at the Whiteface mountain sites rather than the single point representation by steady state models.

Figure S-9. Annual deposition patterns by AERMOD from Danskammer facility at the Catskills grid (facility 70km SE of grid)

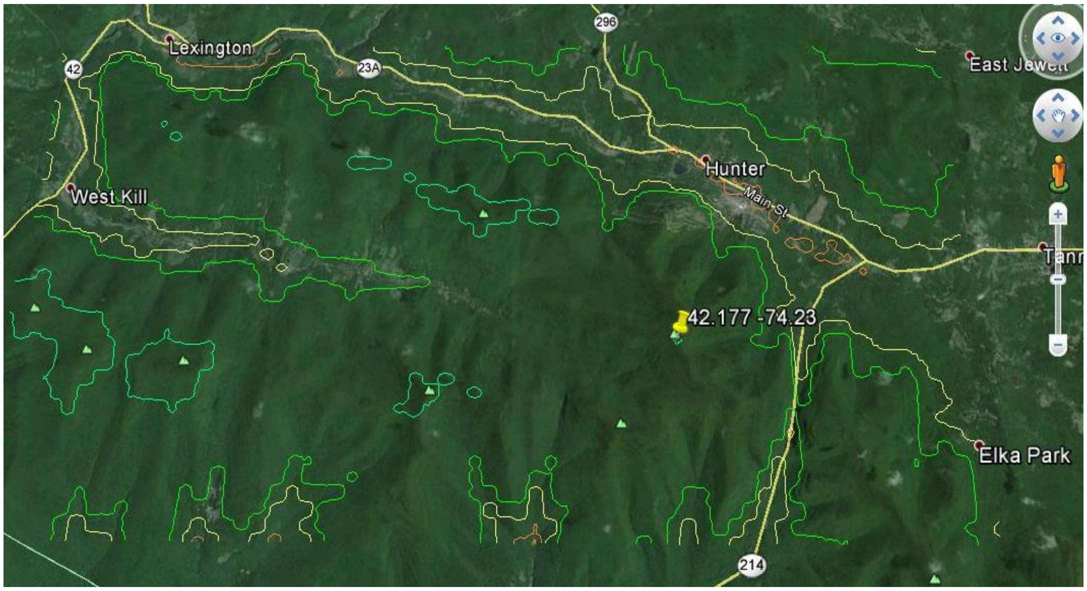

1 Project Purpose and Objectives

The response of the ecosystem to anthropogenic air pollutant input through the atmospheric processes has been studied considerably in recognition of the importance of this controlling pathway for acidic and mercury deposition to surface land and water. As more recent EPA and New York policy and regulatory approaches have emphasized an interest toward the interaction of multi-pollutant mixtures and their consequences on the ecological systems, the need for a more comprehensive approach has surfaced. This shift has been brought about by requirements to reduce toxics such as mercury generated from power plants (Mercury and Air Toxics Standards, MATS)[1] and the Supreme Court's determination[2] to reinstate the EPA's Cross-State Air Pollution Rule (CSAPR) to reduce regional scale emissions of pollutants which are the main acidic deposition precursors, as well as EPA policy[3]on secondary formation of Particulate Matter of size less than 2.5 um ($PM_{2.5}$) from sulfur oxides (SOx) and nitrogen oxides (NOx) down to the specific source permitting process. These and other regulatory requirements have been supported by technical documents, which have relied heavily on regional photochemical modeling assessments. In fact, research studies have also used the results of similar modeling analyses to guide and verify the consequences of emissions from a variety of source types on acidic and mercury deposition levels.

Many national and NYS requirements affect the emissions and interactions of multiple pollutants, especially from energy production sources such as EGUs and WTE facilities. However, as discussed fully in the next section, technical assessments to carry out these requirements and understand the multi-pollutant system have not been commensurate with the latest emissions data and the techniques or approaches necessary to properly assess the implementation of these requirements. In addition, the quantification of the impacts from these specific sources is either lacking or presently outdated. To date, the assessments carried out by the EPA, as well as some in the research community, have relied upon outdated modeling simulation results including past emission inventories, older chemical modules in the EPA's models, and relatively coarse meteorological and modeled grid data. The latter limitation has not allowed the proper resolution of the spatial distribution of acidic and mercury deposition in some areas. This is especially the case in the complex terrain setting of the Adirondacks and the Catskills where the influence of the landscape on the wind fields and the dry and wet deposition have not been resolved at the level of the biological "hot spots" identified in previous findings.[4] Even recent studies carried out by the research community have reported conflicting results or have relied upon extrapolation of the limited observations beyond their applicable realm. Results from both modeling assessments and measurement studies related to the spatial deposition patterns have lacked the necessary refinements to properly characterize the contribution of pollutant species, and most importantly, from the power production section on spatial scales throughout NYS. Thus, as some of the EPA regulations are currently being implemented or revisited, there is a clear need to update the technical foundations of policy needs relating to the ecological effects of deposition of inorganic pollutants associated with sulfur, nitrogen, ammonium and mercury.

More germane to the current study is the recognition that modeling studies to date have not properly identified the current and future contributions of the State's power generation sector to the regional acidic and mercury deposition. This limitation is important from at least two perspectives. First, although elemental mercury has been identified to comprise over 90 percent of total ambient mercury, the emissions from the power production sector have been monitored to comprise a more even mix of the elemental vs. divalent/particulate species, which can affect policy actions on related wet and dry deposition. In addition, there has been a shift in the fuel use in the EGU sector in and around NYS from coal to natural gas. The implications of this shift as well as expected further changes in the near future need to be fully understood not only in policy determinations, but also ongoing research. Answers to these issues can only be addressed practically by regional modeling assessments and, thus, photochemical modeling simulations will continue to play the focal point of quantifying the impacts of anthropogenic emissions.

With the finalization of the CSAPR by the EPA in April, 2015, states in the eastern part of the country will implement reductions in SO_2 and NOx emissions in order to meet the ozone and $PM_{2.5}$ standards. These reductions will also have a beneficial effect on acidic deposition levels and the projected benefits can be assessed by modeling. More directly related to these deposition levels is current preparatory work for the EPA's revisit to the secondary standard for SOx and NOx. The finalized secondary standard for ecological effects[5] in April, 2012 retained the previous ambient concentration based standard, but clearly recognized the inadequacy of that approach and proposed a five-year pilot study in order to further address the ecological effects from acidic deposition. The EPA's documentation clearly established aquatic acidification as an indicator of such effects and proposed to study a "surrogate" Acid Neutralizing Capacity (ANC) by relating a "critical load" ANC due to deposition to a parameter called Aquatic Acidification Index (AAI). The concept is to use a simplified steady state "model" that defines the AAI (as representation of deposition) in terms of "transfer" function of ambient concentrations of SOx and NOx, and the resultant deposition by linking modeled and observation levels. However, the EPA's pilot study to resolve its approach to the secondary standard for SOx and NOx was severely curtailed, with NYS sites funded by NYSERDA. Even then, the approach relies on limited information on surrogate "markers" of acidic deposition effects and is being studied at very limited locations in the Adirondacks. The EPA did not perform any regional or national deposition assessments for the rule, but rather relied on relationships established between ambient concentrations and sulfur and nitrogen deposition. The modeling mentioned in the EPA rule, Model of Acidification of Groundwater in Catchments (MAGIC), is for surface response of ANC to deposition. There does not appear to be a foreseeable plan by the EPA to perform any updated acidic deposition modeling.

It has been pointed out that there are great improvements in the acidic deposition levels and its ecological effects since the implementation of the national Acid Rain Program in 1990. These arguments cite studies indicating great reductions in sulfur and nitrogen depositions on sensitive receptor areas. In fact, the most recent 2011 National Acid Precipitation Assessment Program (NAPAP) report to Congress[6] indicated large reductions in acid deposition precursors emissions and consequent sulfur and nitrogen deposition throughout the country. Specifically, for the Northeast U.S., the Report indicates over 50 percent reductions in both wet sulfate and nitrate deposition since the imposition of emissions reductions through the Title IV (Acid Rain provisions) of the Clean Air Act amendments of 1990. Similar levels of reduction have been observed at specific monitors in NYS since the early 1990s, as exemplified by depictions for Whiteface Mountain in the Adirondacks and Biscuit Brook in the Catskills in Figure 1-1 using data from National Atmospheric Deposition Program (NADP). The levels of sulfate and nitrate deposition have been steadily declining as emission reduction measures have taken place. More recent data shows even higher reduction than 50 percent for sulfate and nitrate in NYS. On the other hand, the relatively lower deposition of ammonium has remained the same during this period.

The NAPAP Report also describes strides made in our understanding of the ecosystem's response to, and recovery from, the effects of acidic deposition and emphasizes that additional measures are needed to achieve necessary further improvements to both aquatic and terrestrial systems. One aspect the report discusses is the interaction of the multi-pollutant effects, including that of mercury with sulfate and nitrate deposition on the ecosystem. It also provides information on certain thresholds, such as "critical loads", which can be used to define levels below which significant harmful effects on sensitive ecosystem elements have not been identified. For example, using a critical load for sulfur and nitrogen deposition, the Report indicates ongoing "exceedances" specifically in the western part of the Adirondack Park in NYS. There is also a description for the ongoing adverse terrestrial ecological effects. The Report then goes on to provide modeled estimates of the impact, which further reductions in anthropogenic emissions are based on an EPA regional model.

Figure 1-1. Annual Levels of Wet Sulfate, Nitrate and Ammonium Deposition at Whiteface (WF) and Biscuit Brook (BB) NADP Sites in NYS

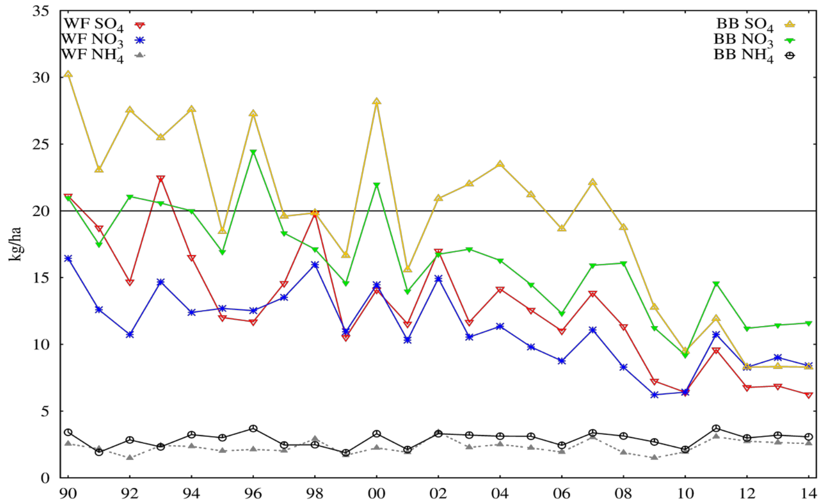

With respect to mercury impacts on the ecosystem, it appears that our understanding of the relative importance of anthropogenic emissions is obscured by such complexities as the interaction of the atmospheric deposition and “naturally” occurring reemissions from the underlying surfaces. The notion of “naturally” occurring is rather vague since these could represent previously deposited anthropogenic mercury over decades due to the long lifetime of elemental component, which by far dominates ambient concentrations. Coupled with the fact that the deposition of the mercury species behaves very differently, emissions reductions from certain source categories such as WTEs are already very significant, while for other sources such as EGUs have not occurred to a similar degree, has further complicated the findings and understanding of mercury deposition. For example, while studies[7] indicate reductions in wet Hg deposition downwind of a major coal plant in NYS, other studies[8] at a more remote monitoring site in Vermont, have not seen any such reductions during the period when overall regional emissions from EGUs were rather flat. A more comprehensive study[9] of Hg wet deposition at monitors in the Great Lakes region for the period between 2002–2008 found no consistent trend in levels, with some monitors showing decreases while others increased. A similar study[10] for a larger set of sites for the period between 1996–2005 indicated statistically significant decreases at most sites in the northeastern sector of the country, attributed to large reductions due to regulations in emissions from incineration sources.

Figure 1-2 shows plotted trends in mercury wet deposition using data reported by the national Mercury Deposition Network (MDN) for sites in the U.S. and Canada with at least 15 years of data. Also plotted are sites with greater than 10 years of data without indicating t the trend so the Underhill location in Vermont can be seen. The data indicated a different trend at some sites than reported by the second study, such as the indication of opposite trends for PA sites. This is likely due to the differences in the years of data used, with our data covering a larger time period from the 1990s to 2013. However, it hould be noted that for mercury, statistics of trends should be viewed within the relatively low values of observations and associated measurement accuracy difficulties. The differences do point to another level of complexity in such data comparisons when time periods of the trends vary, but it is clear that there is no consistent reduction in wet Hg deposition levels as in the case of acidic deposition, especially for the sites in NYS, which are of most interest for our study purposes.

Figure 1-2. Trends in annual Hg concentrations in precipitation at MDN sites with 15 or more years of data for the period 1990 to 2013 across the U.S. and Canada

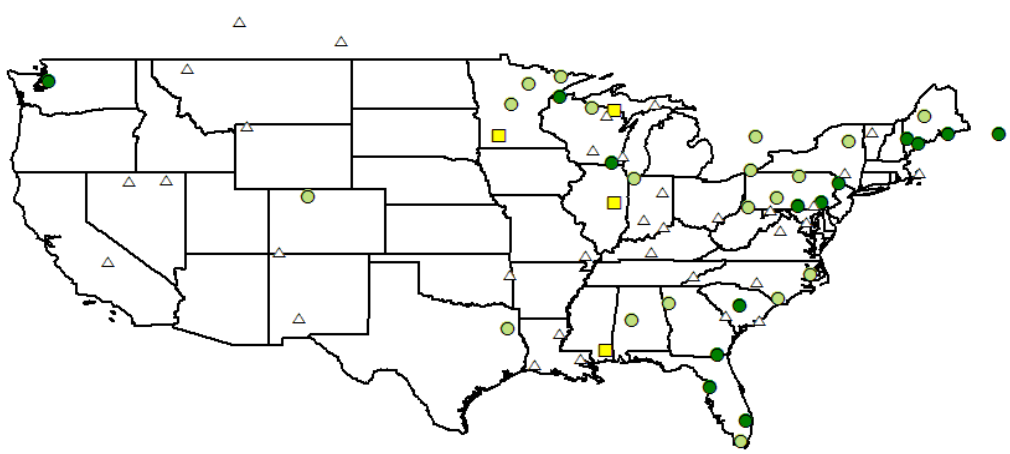

Decreasing trend, statistically significant

Decreasing trend, not statistically significant

Increasing trend, not statistically significant

Triangles denote sites with at least 10 years of data

As the EPA finalized the MATS rule's implementation for EGU sources over the next few years, it will be important to determine whether anticipated reductions in mercury emissions will translate to corresponding observed deposition reductions. NYS has invested considerable resources in monitoring the impacts of acidic and mercury deposition, and recently established ambient/deposition baselines for Hg, as it had established a similar baseline for acidic deposition over the last three decades. Decisions will need to be made with respect to multi-pollutant interactions and potential mitigation strategies should rely on the latest technical information, especially on the power production source sector which is the main focus of these regulations. That is, recent changes are expected to occur specifically in emissions from the power production sector and need to be quantified in resultant deposition impacts. Arguably, the only comprehensive and practical approach to undertaking such an assessment is the application of a photochemical regional model that can account for the various physical and chemical processes involved in the transformation and deposition of mercury species and the precursor emissions for acidic deposition. In addition, the projection of changes in the deposition fields by the modeling analysis accounting for future emissions reductions can assist with policy making decisions.

Thus, the objective of our study was to use the most recent emissions data and refined meteorological fields to project acidic and mercury deposition across NYS and determine the contribution of major energy production sources to these levels. The updates to the emission inventory and the refined grid resolution used in the study to address some of the issues noted in previous modeling assessment for regulatory purposes are discussed in the next section. In short, the EPA's use of the Community Multiscale Air Quality (CMAQ) regional modeling mercury deposition for the MATS regulations[11] relied upon an emission inventory from 2005, an older chemical module for toxics species and coarse (12 and 36 km) meteorological and modeling grids. Studies that have relied in part on these results also suffer from the older inventory limitations. For example, a recent research study[12] of soil mercury from dry deposition across the northeast used the EPA's 2005 generated mercury dry deposition data. More site specific studies using detailed spatial observation driven schemes have their own limitations as far as some of the assumptions used to extrapolate the data even to the nearby landscape. In addition, the applicability of these results to other settings and to the whole of NYS is not possible as the examples discussed in the next section indicate.

Similarly, the background documentation for the CSAPR rule indicates that supporting Comprehensive Air Quality Model With Extensions (CAMx) regional scale modeling[13] performed more recently in 2010 included all EGU sources. Arguably these results can be used to indirectly calculate estimate of acidic deposition, or at least relative incremental levels, using simplistic estimates of dry deposition velocities and washout/rainout for wet deposition from precipitation data, However, there are technical limitations as well with such modeling exercise used in deposition estimations, with the major ones being: 1) the 2005 emission inventory, projected to year 2012; 2) the meteorological and modeling grid at 12km resolution which cannot fully resolve complex terrain features in the Adirondacks and Catskills; 3) the use of meteorological data from 2005 generated by the Penn State/NCAR 5th generation Mesoscale Model (MM5) model, while more recent applications rely on the Weather Research and Forecasting (WRF)[14] modeling scheme; and 4) the use of a chemical transformation model that only accounted for limited precursors in the $PM_{2.5}$ modeling. Most germane for the current study's purposes is the fact that previous modeling and research studies lack a full determination of the State's power generation sector's contribution to statewide acidic and mercury deposition in NYS.

This lack of a current and comprehensive dry and wet deposition estimates over NYS and the contribution of major power production sources can be overcome with the most recent updates to the EPA emission inventory, the 2011 National Emissions Inventory (NEI), and better simulation of the chemistry of inorganic pollutants, coupled with refined meteorological and receptor grids possible by the latest CMAQ modeling system. The recent version of the model also allows for "source attribution" to identify the contribution from any subset of sources to the overall impacts. Furthermore, for the purposes of the study, the EPA's 2011 emission inventory for the modeling domain region was modified using verified refinements to the subset of power generation major point source emissions data for the State's sources. The results from this inventory provided a baseline against which power sector source impacts were gauged and anticipated projected future emissions inventory for the year 2018 were assessed. Due to known limitations in mercury emissions from all source sectors, it was deemed important to verify, to a practical extent, the emissions from at least the major power sector sources in NYS prior to undertaking the model simulations of dry and wet deposition of the three mercury species over the whole state. This source category has been identified as a major contributor to mercury emissions and the determination of its proper impacts should be assessed for use in policy making decisions.

Our CMAQ simulations also improved on previous modeling methods in a number of ways. An important aspect of the applied WRF/CMAQ module was the ability to simulate transport and dispersion at research grade resolution compared to what was previously possible for the EPA and state modeling of regional transport. The project used a nested 4km grid to better resolve the deposition patters over a finer scale than in previous modeling and allowed for better simulation of the effects of complex terrain and land surface-air-water interfaces on the wind, precipitation and temperature fields. The better simulation of the wind fields not only affects the transport of the plumes over terrain features, but also the associated wind speed levels in complex terrain, which is a critical parameter for dry deposition velocity calculations. The WRF/CMAQ modeling system relies on land-use data for these refinements in the Adirondacks and the Catskills, allowing for better simulation of the influence of complex terrain features on both the wind field pattern and deposition. Furthermore, the recent version of CMAQ incorporates improved chemical modules for acidic deposition precursors and mercury species. Specifically, the comprehensive chemical equilibrium ISORROPIA2.1 module[15] is used to predict sulfates, nitrates, ammonium, and crustal component (e.g., calcium, potassium) in the aqueous and solid phases to better define concentrations and deposition. The latter two components contribute to possible particulate formation and deposition as well as regulate the form of the primary contributors to acidic deposition (sulfates and nitrates). Additionally, improvements have been made to the modeling of mercury compounds[16] and their interaction with ammonia. Further details are provided in the technical descriptions section of the modeling components.

Given that local “hot spots” might still not be resolved by the WRF/CMAQ 4km scale simulations in complex terrain, a set of model simulations using the EPA AERMOD model were used for limited comparisons. Although AERMOD is a steady state model, it has been demonstrated to properly account for complex terrain simulations in comparison to the EPA’s CTDMPLUS model,[17] the latter having been formulated from comprehensive field studies. The AERMOD simulation of terrain effects are carried out using terrain data down to a 30m increment and are described below. The simulations were carried out for sample sources placed upwind of the Adirondacks and Catskills as ground level and elevated releases to simulate long range transport of both coherent plumes and well mixing plumes. These estimates were only used in the relative sense to test the effects of complex terrain on deposition, given that the AERMOD model incorporates state of the science methods for deposition of both gas and particulates.[18] However, the CMAQ 4km grid was deemed still too coarse for direct comparisons of patterns from AERMOD on the terrain grid scaled modeled.

One novel approach taken in the study with respect to the dissemination of the study approach and results was to include a social science student as a collaborator in the study. The student was tasked with formulating two documents and a presentation in layperson's language. One document summarized the results from a technical workshop held at the beginning of the study to discuss and solicit comments on the study approaches, while a subsequent, and more important document, provided a summary of the study findings. The latter aspect was also presented at a second policy maker oriented workshop at which the student provided a summary of the study findings. For this aspect of the study, information provided at the 2013 EMEP Conference session on how to effectively communicate the findings to policy makers[19] was implemented.

It was the expectation that the findings from the modeling simulations over NYS and the contribution of the major emitters of acidic deposition precursors and mercury in the State will provide information on current levels of deposition and the potential benefits of emissions reductions in the near future. These results can also disclose potential pitfalls, the effects of lack of information, or unexpected impacts from the multi-pollutant system. In addition, the research community might also benefit from the comprehensive modeling of current emissions and potential reduction of acidic deposition precursors and mercury emissions on a more localized level in the interpretation of observed ecological responses, as well as anticipated impacts in the future.

2 Summary of Previous Pertinent Modeling and Research Results

The use of regional photochemical transport and dispersion models has been the technical support basis of many regulatory actions for decades. Over time, these models and their applications have evolved considerably based on field research, computational improvements, and model performance exercises. These changes have allowed for refinements to the chemical processes, the meteorological data inputs and horizontal and vertical resolutions, which were previously not considered practical. The study's aim was to use the latest techniques in one of the EPA models (CMAQ) which has been relied upon for regional modeling assessments for many air pollutants and their regulations. Before describing basics of this modeling approach, it is informative to summarize some of the previous modeling analyses which formed the basis of specifically acidic and mercury deposition studies and associated regulatory actions. The examples are mainly of EPA and NYS related assessments and actions in keeping with the main interest of the current study. The examples provided are for acidic deposition first, followed by mercury deposition modeling assessments.

A noteworthy acidic deposition analysis was for the first in the nation regulatory action to reduce its precursor emissions; the New York State Acidic Deposition Control Act (SADCA)[20] in 1985. The purpose of the modeling analysis was to determine area wide emissions contributions to impacts on NY receptors using a long-term statistically based model, the Advanced Statistical Trajectory Regional Air Pollution (ASTRAP). The relatively crude 100km spatial resolution, with 12-hour incremental wind and precipitation fields provided relative contributions of different states and regions to annual wet deposition at a set of three "sensitive" receptor areas in New York. These impacts allowed the determination of the importance of source regions in relation to a "concern" adverse sulfate deposition level, which at that time was the Environmental Threshold Value (ETV) of 20 kg/ha-yr. These relative impacts allowed for the determination of emissions reductions necessary to achieve acceptable levels.

The SADCA was the precursor to the EPA action on the acid rain front in the 1990 Clean Air Act Amendments. A number of federal regulatory initiatives followed, including those by the Federal Land Managers (FLMs) who are given primary responsibility for the definition and corrective actions on air pollution effects in federal Class I Wilderness areas. Thus, the U.S. Forest Service finalized a Screening Procedure Report[21] to assist in the determination of the status of existing conditions and levels of adverse aquatic and terrestrial levels as guidance in the evaluation of future proposed emissions. The report relied upon observed wet deposition levels from the National Atmospheric Deposition Program (NADP) sites, while the lack of applicable dry deposition observations was overcome by modeled dry deposition estimates provide by EPA using the Regional Acid Deposition Model (RADM) for sulfate, plus estimated satellite data for nitrates, and high elevation cloud deposition “enhancement” factors. The corresponding Green and Red screening values determined for aquatic and terrestrial components were then related to acceptable (similar to the critical load concept) and adverse conditions, respectively. The screening procedures were a precursor to the FLM/EPA approach for modeling major sources in the permitting process. The Eulerian RADM modeling system was subsequently revised to include the scavenging of acidic precursors by wet removal due to precipitation, cloud processes, and simple aqueous phase chemical processes. The model was driven by the MM4 meteorological transport simulations available at the time.

As CMAQ modeling approaches were being enhanced and computational processes optimized, EPA performed a number of model evaluation studies to ensure that simulations performed for regulatory purposes were technically acceptable. Thus, a study[22] of CMAQ simulations of wet deposition of sulfates, nitrates and ammonium was carried out for the continental U.S. and compared to the wet deposition data from over 200 sites for the years between 2002–2006. The model was driven by both a 36km and 12km grid MM5, with the latter grid applied only for the eastern two-thirds of the country. Emissions data were based on the 2002 NEI, but were adjusted for the other years by emissions monitored at major EGUs, MOBILE6 modeling for mobile sources and ammonia emissions from the agricultural sector. Since errors in CMAQ wet deposition modeling had been related to errors in precipitation simulations, adjustments were made to the model estimates using available observations at discrete sites. The results indicated general overestimation of sulfates and underestimation of nitrates and ammonium in the eastern U.S., all connected to similar tendencies on a seasonal level, as well as poor representation of such factors as bidirectional exchange of ammonia and lightning generated NO emissions. Although some differences were noted in the comparison of the 36 km to 12km simulations, no “improvements” by the 12km grid simulations were identified.

However, these results cannot be interpreted as meaning that refined grid simulations do not provide improvements in the generated meteorological and emissions fields. In fact, some of these refinements could lead to predictions that would otherwise not be simulated by coarser grid simulations and to difficulties in matching observed levels from limited data in the simulated grid areas. Coupled with issues occurring with emissions data, incomplete understanding and simulation of chemical and physical transformation processes, result in complexities which cannot be easily discerned or understood in these results. Improvements to the model transport and chemical processes as well as to emissions data and deposition observations will likely lead to improved simulations. Thus, another study[23] by the EPA staff used a newer version (5.02) of CMAQ simulations for the years 2002–2011 included the use of WRF meteorology with improved convective parameterization, updated land use characteristics, improved emissions estimates accounting for yearly agricultural emissions with bi-directional NH_3 flux, and lightning emissions to project annual wet and dry sulfur and nitrogen deposition. Comparisons to annual wet deposition observations at NADP sites indicated very good agreements, at least for the eastern half of the country. These comparisons were further improved with adjustments to the CMAQ estimates for precipitation underestimation of observed values in some of the years. The errors in the estimation of wet deposition of sulfates, nitrates and ammonium at the northeast monitors were less than 20 percent, which can be considered very satisfactory with the precipitation unadjusted CMAQ nitrate deposition showing a remarkable performance for the eastern U.S. It is also important to note that the CMAQ model estimates of oxidized nitrogen and sulfur deposition indicated higher dry than wet annual values for both species in the northeastern U.S. region.

As in other modeling studies, this EPA study could not compare projected dry deposition to observed levels due to both qualitative and quantitative lack of robust observations. Nonetheless, it is important that the deposition estimates of the dry component be accounted for in total deposition estimates. Thus, part of the data made available at the NADP webpage are maps of total deposition generated by the Total Deposition Science Committee (TDEP) based on an assessment[24] performed by the EPA using CMAQ simulations. The analysis approach determined total sulfur and nitrogen deposition across the U.S. by combining wet deposition observations from NADP data, enhanced by PRISM model resolution of precipitation data, with estimated dry deposition values from CMAQ versions 4.7 and 4.7.1 using concentrations of available sulfur and nitrogen species through Clean Air Status and Trends Network (CASTNET) and two other more limited data networks for the years 2002–2009. Previously available CMAQ v.4.7 estimates were "adjusted" by re-gridding the 36km cell sizes to 12km, while for the years 2007–2009, the grids were already at 12km. In addition, while the 2002–2006 meteorology was provided by MM5, the 2007–2009 runs included the use of WRF generated fields. The 2002 NEI served as the basis for the 2002-6 modeling with yearly adjustments for major point sources, while for 2007 and 2008–2009, the 2005 NEI and 2008 NEI were used, respectively, with yearly adjustments for updated major point sources, mobile sources and agricultural and fire emissions.

These CMAQ inputs were used to generate hourly dry deposition velocities for six sulfur and nitrogen gaseous and particulate species, which were then averaged to the weekly periods of available ambient concentrations to generate dry deposition. To have more up-to-date data and in order to produce dry deposition for the years 2010 to 2012, weekly averaged and seasonal biased adjustments were made from the modeled years and finally, calculated annual averaged dry deposition were combined with wet deposition observations. Resultant total deposition for two of the years (2002 and 2010) were discussed and indicated the importance and even the dominance of dry nitrogen deposition in many parts of the country. Furthermore, noted large reductions in SO_2 emissions in 2010 vs. 2002 resulted in corresponding large sulfur deposition reductions, with dry deposition more important in 2010 due to less precipitation. Dry deposition for SO_2 was found to be more important than for sulfates due to its higher dry deposition velocity, while for nitrogen deposition dry deposition of the HNO_3 species was determined to be of most importance. One of the authors of the study[25] indicated that more recent CMAQ estimates have been made using the same model version as in the current study (v. 5.02) and for the more recent years through 2014 over a 12km grid, which are then scaled down to a "pseudo" 4km grid system. Finding details will be made available on the NADP site.

In addition to providing total sulfur and nitrogen deposition throughout the U.S., the earlier study did a limited comparison of these estimates to available throughfall data from forested sites in western U.S. Throughfall is the amount of deposition collected below the forest canopy after precipitation events and is thought to represent an estimate of total deposition, accounting for previously dry deposited materials through the forest. It was noted that throughfall should represent a lower limit of total deposition and the comparisons confirmed the expectation, with a factor of two models to observe throughfall nitrogen deposition.

The evaluation of these model estimates against actual data is especially important for regulatory applications due to the higher level of scrutiny these modeling exercises undergo in that arena. As noted, however, such model performance studies are limited by a number of factors, including the availability of necessary speciation data and the essential lack of any robust dry deposition observations. Thus, inferential evaluations are necessary for the application of regional photochemical modeling results, such as the comparison of predicted deposition velocities previously determined values in field observations. Some field study examples will be provided, but for current purposes the use of these modeling predictions in regulatory applications needs to be considered. A very timely and pertinent need is exemplified by the EPA's revisit to the sulfur and nitrogen secondary standard. As noted previously, the approach put in place by the EPA was to study the relationship between observed concentrations of sulfur and nitrogen and associated deposition at few sites such as the Adirondacks instead of any direct actions based on acidic deposition and the established adverse effects on aquatic ecosystems. Thus, the connection of atmospheric loading of acidic precursor pollutants to deposition was established through the Aquatic Acidification Index, which included the use of "transference ratios." These ratios were defined for total oxidized sulfur and nitrogen deposition to their corresponding species concentrations in air.

This method was evaluated[26] for a limited number of sites to determine its ability to provide a practical and useful approach. The evaluation was limited to eastern U.S. and to less than half of the 22 CASTNET/NADP sites (none in NYS) due to annual level data capture issues for the necessary observations. Furthermore, not all of the nitrogen species were available from the 1990–2004 period of the study. The observations were compared to previously available modeled deposition for the period, but these did not include predictions of cloud deposition that were noted as important for some of the high-elevation monitoring sites. The results indicated that transference ratios within acceptable confidence levels were possible only at the annual average levels and not on the weekly or seasonal basis. In addition, the findings emphasized the importance of site specific factors for the proper transference ratio determination. Arguably more recent modeling results from the NADP data bases described above can be substituted for by the model estimates and compared to corresponding observations to further test the method. However, it is clear that observational limitations and the results from this EPA study point to the limitation of broad brushing the general landscape from the available data. On the other hand, the results from more recent regional modeling can be revisited for better spatial and temporal resolution of acidic deposition.

Turning to the issue of mercury deposition, it can be said that many of the same and even more limitations found for acidic deposition also apply to the simulation of mercury deposition in NYS. As with the examples for acidic deposition, we will summarize those dealing with mercury deposition, which have been carried out in support of regulatory development and similar applications. Along a parallel track, as with supporting regional model application documentation for acidic deposition, the EPA performed regional scale Hg modeling for the 1997 EPA Mercury Report to Congress. Section III of the Report27 provides the approach and results from assessing the fate and transport of mercury using the Regional Lagrangian Model of Air Pollution (RELMAP) over the continental U.S. in recognition of the importance of long range transport aspects of mercury. The1989 meteorological data was generated by the Nested Grid Model and used by National Weather Service (NWS). Mercury emissions from 11-point source types and averaged emission area source representations for the smaller emitters were modeled, with the point sources "introduced" at the higher layer of the model to account for higher stack heights and plume elevations. Due to the rather coarse grid spacing of 40 by 40km, some localized impacts were also calculated using the steady state Industrial Source Complex (ISC3) model.

The study recognized the importance of treating the three species of mercury separately, but also realized the interdependence of chemical transformations and wet and dry deposition. In recognition of uncertainties, the modeling still accounted for elemental (Hg0) and divalent (gas, Hg2 and particle, HgP) forms, with Hg0 having small direct dry deposition (low vapor pressure) or wet (insoluble) deposition, while Hg2 being readily dry and wet deposited and HgP deposited through the wet process by rain/cloud scavenging. In forested areas some Hg0 dry deposition was recognized due to the large leaf area index (LAI). It was further noted that there is a mechanism of indirect deposition of these species, especially Hg0, controlled by interspecies chemical transformations: for example, Hg2 is reduced to Hg0 by sulfite, but oxidation of Hg0 to Hg2 was found to be much faster, thus resulting in steady state Hg2 concentrations in the air and not prone to full depletion. The importance of natural re-release of Hg0 and Hg2 back to the atmosphere was recognized, but not modeled. Instead, the outside the grid regional and natural impacts were assigned a constant concentration. The results of the modeling were subsequently used to develop control programs for such sources as incinerators and EGUs.

At the time the EPA was preparing the Mercury Report to Congress, the Northeast States for Coordinated Air Use Management (NESCAUM) were gathering information on mercury and its ecological effects, which then lead to the New England Governors and Eastern Canadian Premiers (NEG-ECP) release of a Mercury Action Plan (MAP) in 1998. One purpose of MAP was to reduce and eventually eliminate anthropogenic mercury emissions. Based on some of this information, a rather ambitious modeling exercise[28] was undertaken through NYSERDA funding to identify the contribution of global and regional scale emission areas on New York receptors. The study included a global scale estimated emissions modeling of NYS, the rest of the U.S., continental scale, and land/ocean over a 1000km grid driven by a general circulation model, plus a regional scale modeling with 100km grid, driven by 1989 meteorology from the standard weather forecasting model. For the latter, the results from the global scale modeling were used as boundary conditions. Wet and dry deposition at three receptor areas in NYS were simulated; Adirondacks, Catskills and Finger Lakes and the contribution from the various source regions and the three mercury species to the deposition estimates were determined. While for the global scale modeling, constant values of dry deposition velocities and washout ratios were used, the regional model relies on the resistance modeling approach for dry deposition and included precipitation data from NADP sites. Both models used the latest set of mercury chemical transformation and equilibrium equations. In addition, three scenarios were simulated in both models; a baseline case, a case were local impact were dominant by choice of parameters, and a regional impact case that reversed the local case assumptions.

The modeling recognized known large differences in the dry and wet deposition effects for the elemental vs. the oxidized forms of mercury. These differences were reflected in some of the modeling results summarized for the three receptor areas and the relative contribution of various source regions. Some of the pertinent findings were that NYS sources contributed at most 20 percent of the impacts, while the rest of the U.S. and far distance sources (e.g., Asia) accounted for significant portions of deposition as "background" sources in the regional modeling results. It was noted that dry deposition of Hg2 was much more than for Hg0, but the total deposition of mercury was due to wet deposition. The rest of U.S. and background sources were about two-thirds of the impacts depending on the receptor location. The contribution of local sources was dominant at a location like Catskills vs. the more remove Adirondack area. A limited model to observation wet deposition comparison was made which indicated a rather surprisingly acceptable performance, with most simulations within 50 percent error bounds.

Interim to further national regulatory actions, some of the EPA staff involved with the RELMAP modeling also tested a version of the CMAQ model which had incorporated a number of new features in the mercury module. These included chemical and aqueous phase reactions, with cloud water partitioning effects. A study[29] of a CMAQ application using 1995–1996 NEI and corresponding year MM5 meteorological data was performed for central and eastern U.S. over a 36km grid. Hg emissions were speciated, but dry deposition for Hg0 was assumed negligible. CMAQ Hg module results were tested against wet deposition observations over one month in the spring and summer seasons from Mercury Deposition Network (MDN) sites. The model was found to over predict in both seasons, but mainly in the summer due to issues with simulation of the precipitation depth. Further development and testing of the CMAQ model's abilities was undertaken as part of the more comprehensive North American Mercury Model Intercomparison Study (NAMMIS). The simulation of wet deposition across the U.S. and Canada by three models including CMAQ, were compared to MDN data, plus precipitation event based data from Underhill, VT by a collaborative study[30] including the EPA and DEC. The models used mercury emissions from the 2001NEI and 2001 meteorological data from MM5 simulations to predict deposition over a 36km grid. All three models were found to perform well on an annual basis, explaining over 50 percent of the site to site variances. CMAQ seemed to performed well due to its low (15 percent) overestimation of precipitation, while the other two model had much larger overestimations. Part of the overprediction in one of the models was related to inadequate chemical reduction of Hg2+ to Hg0 and the associated recognition of the low wet deposition of the latter. As would be expected, model prediction comparison to weekly observations at MDN sites did not produce favorable results due to low resolution of the models of weekly precipitation data. No comparison of modeled total deposition to observations was possible due to lack of adequate dry deposition observations. However, the results showed promise for regional models such as CMAQ for performing modeling exercises in support of regulatory efforts.

As the development of the technical approaches and their refinements in CMAQ continued, it became the model of choice for the assessment of mercury and other pollutants for two national regulatory initiatives. The first was the Clean Air Mercury Rule (CAMR) and the associated CSAPR rule. The technical support documents[31] for CAMR provides the details on how the emissions from sources such as EGUs, incinerators and other large mercury emitters were treated. The emission inventory used was for 2001 and included speciated Hg for a large set of source categories, with varying percentages of the three species. For coal EGUs, individual source percentages were used based on data gathered by the EPA in 1999 from an information request to industry. Further details on the speciation are provided in the emissions review section. The CMAQ model v4.3 was updated for certain chemical processes and was used with MM5 driven meteorological data over a 36km grid through the country. Instead of assuming a constant boundary concentration as in previous modeling, the global input of mercury was calculated by the GEOS-Chem system over a larger grid system. An evaluation of the wet deposition projections showed that the model underestimated observations from MDN sites in the east by 23 percent, but overestimated the corresponding values in the west.

CMAQ was also used for the assessment of mercury and other toxics in support of the Mercury and Toxics Standards (MATS) rule for coal and oil power plants. The rule was "finalized" in 2011, with subsequent challenges, which continue up to this writing. The modeling technical support document[32] for the rule provided the approach used with an updated 2005 emission inventory. Mercury emissions were taken from the National Air Toxics Assessment (NATA) 2005 inventory and some industrial boiler sector mercury emissions more consistent with the engineering analysis for the "Boilers" National Emissions Standards for Hazardous Air Pollutant standards (NESHAPs) rule. The speciation was essentially the same as used for the CAMR analysis. Simulations were performed with the 2005 MM5 meteorology over a12km grid in the east and another in the west, both nested within in a

36km grid. Updated CMAQ v4.7.1 included further refinements to both MM5 simulations and mercury chemical processes. An evaluation against MDN wet deposition data found overestimations in three of the four quarters in a year, more consistent with previous findings as opposed to the underestimation in the CAMR modeling. Projections were also made for a future year (2020) emissions scenario, which has not been revisited to check against potential recent changes.

Further details on the performance of the application of CMAQ v.4.7.1 and another regional model (CAMx) using the 2005 modeling platform is informative. These are presented in a study[33] by the EPA where both models were used to simulate mercury concentrations and deposition over the 12km grid and also over the 36km grid and the performances compared. The various chemical reactions in three phases of mercury are accounted in the version, including the inorganic pollutant module ISORROPIA, which is described in the next section. Important differences between the models included: CAMx ignoring dry and wet deposition of Hg0, while CMAQ include a dry deposition scheme. Thus, elemental mercury in CAMx deposits only through the indirect route of transformation from Hg2. The 2005 NEI included species specific data for area, EGU, non-EGU point sources, and relatively large land and ocean re-emissions of Hg0 to the atmosphere. As noted previously, the percentage of the oxidized form of mercury was almost the same as elemental form for the important EGU source category in contrast to the dominance of the latter (over 95 percent) in ambient concentrations in the country. The projected dry, wet and total deposition over the 36 km grid indicated that the dry and wet deposition in both models were dominated by Hg2 species which was not unexpected for wet deposition due to the modeling assumption of essentially nil wet deposition for the elemental component. In addition, total deposition in CAMx was predominately due to dry deposition, while for CMAQ, the distribution was more even; 57 percent dry vs. 43 percent wet. An interesting aspect to the CMAQ modeling was the use of its ability to calculate the flux of elemental mercury to and from land and water surfaces using a module developed for such "bidirectional" flux calculations.

One of the important aspects of model uncertainty recognized by the EPA's Mercury Report to Congress was the issue of rerelease of mercury back to the atmosphere from land and water surfaces. The relatively long lifetime for elemental mercury and its low direct deposition to the surface further highlights the importance of addressing this component of air-surface interaction in estimates of total mercury on a regional and global scale. In order to address this process, the EPA developed a bi-directional module[34] for Hg0 into the CMAQ model and tested it against the "standard" version for a month of meteorological data. It was noted in the study that both a stable mercury isotope study and other studies had previously indicated that from 20 to 70 percent of the global mercury loading could be rereleased to the atmosphere.

The CMAQ application for the short-term period with and without this module was not conclusive, but did show promise. However, for the 2005 CMAQ modeling platform, the annual deposition simulated over the 36km grid with the 2005 NEI and with the inclusion of the bidirectional module for Hg0 indicated essentially nil dry deposition for Hg0 and the reversal of the percentages above for the dry vs. wet contributions to the totals. Emission estimates provided in the study showed large reemissions from the underlying surfaces. Thus, reemissions of Hg0 did provide an effect not simulated by the “standard” model.

The model comparisons were also made for predictions over the 12km grids in the east and the west against MDN wet deposition data averaged over four seasons. CAMx was found to consistently underpredict for all seasons in the east and west, while CMAQ overpredicted in all seasons in the east and west, with the exception of a large underprediction for the summer months in the east. Data presented for the summer months indicated that the model projection of rainfall was mostly larger than observed and not likely the main cause of the underprediction. Another interesting item noted was that while initial conditions were not important in the modeling after a short time period, the boundary conditions were important especially for monitors near the edge of the domains.

The last example of regional scale mercury modeling is probably the most germane to the current study approach inasmuch as it was performed specifically for northeast states and identified NYS specific emission sector impacts. In response to the NEG-ECP MAP study, NESCAUM prepared a Mercury Modeling Study[35] report in 2007. The NESCAUM modeling used yet another model, the Regional Modeling System for Aerosols and Deposition (REMSAD), with the specific goal of determining mercury deposition in the NE region and to apportion the contribution to deposition by source regions and major source categories. REMSAD’s technical approaches were compatible to those used by the EPA models at the time, including wet and dry deposition approaches and chemical processes for the three mercury species. The meteorological data used was taken from the EPA’s MM5 runs for 1996 over a 36km grid over the U.S. The emissions for 1996 were from point, area, and mobile sources from the northeast states, rest of the U.S., and from Canada and Mexico, while global boundary conditions input came from the GEOS-Chem model.

One feature of the modeling was the tagging of source categories and regions for the determination of attributions. Thus, source sectors such as EGUs and incinerators were tagged to determine their contributions, specifically from the New England and NY/NJ regions. During the modeling process, a revised inventory for 2002 was developed that reflected specific regulatory affected reductions in mercury emissions from municipal waste and medical incinerators. These reductions were about 90 percent for the northeast and only 40 percent for the rest of the country. On the other hand, the inventory for 2002 did not show any reductions in EGU emissions either from the northeast or the rest of the country. The two inventories allowed the determination of the effects of the mercury reductions on the deposition levels. The three mercury species for the various source categories were taken from data which formed the basis of the EPA 2005 NEI and the CAMR. One major exception was the use of average percentages for the species for the EGUs instead of the source specific assignments of these species for coal plants. Further details on this are provided for specific species percentages in the inventory review section.

The modeling results showed the importance of the WTE (municipal waste) combustors located in the northeast as a major contributor to deposition in 1996, while for the 2002 inventory results, these WTE impacts dropped considerably in association with emissions reductions from this source category. The results also indicated the importance of EGUs outside of the northeast region in both 1996 and 2002, with these sources becoming the dominant contributors to deposition in the northeast. However, the percent contributions from outside the region EGUs were not commensurate with the order of magnitude higher emissions from these sources vs. those in the northeast. The contributions from sources outside the U.S. were found to be very important for both inventory results. In addition, although dry deposition had a substantial contribution to the totals, the model results could not be tested due to lack of observations. However, wet deposition estimates were compared to MDN data in terms of the ability of the model to predict annual values in the range of observations from 1997–2004 with relatively good results, although monitored observations during the period of emissions reductions did not show any noticeable reductions. Furthermore, the REMSAD deposition estimates were found to be comparable to the levels projected by the EPA’s RELMAP modeling, at least in terms of contributions from general NE regions to the NESCAUM area. Lastly, it was noted that the NESCAUM model deposition estimates were on par with levels projected in a previous global/regional scale modeling performed for NYS.

These examples for both acidic and mercury deposition modeling and the results reported indicate the continued attempts to improve the modeling modules as research on our understanding of the atmospheric chemical processes, improvements in meteorological data simulations and computational methods have evolved. However, the testing of these modeling predictions have suffered from the lack of adequate observations of all deposition forms, except possibly for wet acidic deposition where coverage of the modeled region by monitor sites seems to be achieved, at least on a regional scale. The paucity of wet mercury deposition sites is apparent from figure 1.2, especially for New York and its vicinity. What complicates the issue is the fact that these monitoring sites are established with a region's ecological sensitivity and importance in mind and not necessarily where modeled impacts are maximized. Model performance testing is a difficult process even when monitored data is deemed adequate due to various uncertainties in model inputs, formulations, and atmospheric processes. Even when the modeling exercise is for long-term averages and over large scales, such as the continental U.S., model to monitored comparisons have at times been prompted by certain adjustments in order to achieve good comparisons. For example, in an application of the GEOS-Chem model over North America on a 50km grid resolution for mercury simulations, the authors[36] had to invoke an adjustment to the inventory speciation from the EPA by arguing that the large percentage of the Hg2 component vs. Hg0 for EGUs and WTE was not demonstrated in coal fired plume observations. The argument used was that sulfur reduction of the oxidized to elemental mercury should result in the dominance of Hg0 in the emissions over the scales of the modeling. However, such adjustments might be viewed within the confines of large scale regional modeling where Hg2 conversion over large distances might be sufficient, it does not adequately address the fact that the assumption in the mercury emissions inputs for WTEs is not supported by the relatively low sulfur emissions from this source category, as discussed in a subsequent section, nor the applicability of in-plume oxidation to general atmospheric processes. Thus, an important consideration would be the need to address possible limits in the mercury chemical processes in the model or other processes.

At the same time, studies which have been undertaken on smaller scale features or areas have suffered from the same data limitations as the photochemical modeling applications. Thus, noted model assumption of homogeneity over at least the larger grids used in model assessments have been claimed to be overcome with more site specific data assimilations. In addition, questions on the proper chemical processes and meteorological simulations of complex terrain raised in some studies reference older model applications or more global scale applications and are not in line with the abilities of models such as CMAQ. The next section provides details on the CMAQ model's approaches. The current study was an attempt to refine the grid scale issue and the meteorological simulations. The important consideration for any study is the purpose and eventual use of the results in general terms. Thus, monitoring data based studies carried out in a specific region or with specific topographical or geographic features have to be viewed within the same context of their general applicability and the adequacy of the assumptions. Two examples of empirically driven modeling approaches in complex terrain settings will be provided to identify certain issues with inadequate data availability, some of which the authors themselves have identified. One study[37] was an attempt to use landscape features to characterize deposition patterns in national Parks at Acadia and Smoky Mountains. Using statistical measures on readily available variables that were likely to control deposition patterns, it was found that the two primary parameters were elevation and forest type, although the correlations with deposition patterns were rather weak. These features were noted to be related to other "indirect" variables such as orographic effects on precipitation and leaf area index (LAI), but the chosen parameters and the consequent approach were able to explain less than half of the variability. Based on these results, deposition scaling factors were identified in a generalized landscape-wide model for use in comparing predictions to "observed" sulfur deposition, with largest underestimations noted at the higher elevations at both sites. In addition, attempts to correlate LAI to deposition showed contradictory results when compared at the two parks. At the same time, "hot spots" identified by the landscape model indicated "underestimation" of these projected levels by the NADP observations. The applicability of the empirical model to other sites was not attempted, but such studies identify patterns of deposition in terrain setting which, when confirmed by other studies, can be used qualitatively to identify features against the regional scale models that can be tested. An example is the noted enhancement of deposition with increasing terrain height, which is noted further in the report.

Another more recent and pertinent example[38] of projected mercury deposition over the Adirondack Park relied on limited data essentially from one site in the region and averaged dry deposition values found by other researchers to estimate total deposition across the whole park. Interpolated wet deposition determined by precipitation and MDN site data were combined with dry deposition estimates using two databases. For non-forested areas and "leaf off" periods, dry deposition was essentially based on Huntington Forest mercury species concentrations and a form of the dry deposition velocity calculation scheme used in CMAQ and similar models. The assumption was made that ambient air concentrations of Hg from this site applied to the whole Park, especially since the elemental form dominated the total concentration, combined with a simple adjustment for wind speed and temperature variations with terrain height found by other researchers for Whiteface Mountain. These calculations also accounted for the effects of major land use categories on the dry deposition velocity estimates. For forested and leaf on periods, average dry deposition determined from data in previous studies for litterfall in the eastern U.S. and throughfall enrichment factors for two major tree "types" based on studies in the Adirondacks and a forest in Minnesota. The resultant wet, dry, and total deposition were then mapped across the Adirondack Park

It was found that dry deposition was essentially due to the elemental form, which is not surprising for this study since the corresponding average concentration used was three orders of magnitude higher than the oxidized forms and this factor overcame the two orders of magnitude lower dry deposition velocity for the elemental form. A comparison was made to the results from the EPA MATS modeling with the 2005 data platform previously discussed, which indicated that while Hg0 projections were similar between the two studies, the Hg2 dry deposition in the EPA study were essentially of the same order as the elemental form deposition. Even with possible underestimation of the oxidized form by the Tekran instrument, it was argued that the dominance of Hg0 dry deposition remained. However, there are at least two other reasons for this difference. First, while the mapping study relied on observed concentrations regardless of their source, the EPA study was essentially a determination of anthropogenic emission impacts wherein the oxidized form of mercury was important. Both studies accounted for elemental Hg evasion back to the atmosphere, although the data used from other research by the mapping study was not clarified. Furthermore, while the EPA study predicted small dry deposition contributions from the particulate Hg species due to its low anthropogenic emissions, the mapping study found that the particulate form to have larger dry deposition than Hg2, especially at higher elevations. This difference point to another possible explanation in the likelihood that the mapping study had potential underestimation of Hg2 dry deposition due to the use of a rather unrealistically low average wind speed reported at Huntington Forest (0.64m/s) compared to a value reported (2.4 m/s) for the same site in a study referenced and relied upon as the basis of the wind speed profile equation. The fact that single point wind speed and no wind direction adjustment due to terrain features was used, as is done in simpler steady state models like AERMOD, is yet another issue to be recognized. The study did predict larger deposition with increasing terrain height as found in other studies.

For our current purposes, however, these studies also point to the general lack of adequate observational data to provide better estimates than photochemical models, especially when the important dry deposition component is to be estimated. The germane question for our study is related to the influence of the State's power sector sources in the overall anthropogenic emissions impacts in the recent past and in the future, which the empirical studies cannot resolve while previous regional modeled estimates are not adequate. These important considerations can be tested by the regional modeling approach performed in our study allowing policy making decisions and guidance for further research. Details of the modeling assessment used and what has been addressed will be described after the next section where a summary of the CMAQ and AERMOD modeling approaches is provided.

3 Models and methodologies used for the study

Since the main purpose of the study is to determine the contribution of the State's energy sector relative to the total projected acidic and mercury deposition due to a large set of anthropogenic and pertinent "natural" source sectors, the chosen modeling system must be suited to address the multitude of emission source types and the multi-pollutant interactions over the large spatial scales of NYS, as well as beyond its borders. This is important for the particular pollutants addressed in the study since it has been well established that the influx of precursors and background levels from outside the State play an essential role in the determination of ambient concentrations and surface deposition within NYS. Thus, the model of choice needs to be able to simulate the complex set of source emission interactions and the meteorological conditions encountered on the transport scales up to hundreds of kilometers, as well as properly account for source contributions from outside and inside the modeling domain.

The main modeling approach used for the study is the state of the science photochemical regional Community Multi-Scale Air Quality (CMAQ) model, which has become the model of choice for regulatory and research modeling performed by the EPA and many states, including consortiums such as NESCAUM. As described in the previous section, the model has evolved over the years and currently can project regional impacts of many pollutants, including concentrations and deposition of acidic and mercury species. The model is a system of components, comprised of two main inputs dealing with emissions and meteorology and the dispersion and transport module that accounts for multi-pollutant chemical and physical interactions to produce a variety of desired outputs. In this study, the model has been applied at a refined horizontal scale not previously used in any regulatory applications or long-term averaging purposes necessary for deposition estimates. This level of refinement in horizontally heterogeneous areas such as at land-sea interfaces or complex terrain features, has not been tested as far as the abilities of both the meteorological processor and the deposition model to provide realistic predictions.

As such, it was decided that for two important complex terrain areas of the State, the Adirondacks and the Catskills, a limited set of simulations would be performed using the relatively simple the EPA AERMOD (AMS/EPA Regulatory Model) system to determine if the patterns of projections from CMAQ can be assessed from the standpoint of the effects of terrain features. The AERMOD modeling cannot address a number of refinements in simulations performed by CMAQ such as varying meteorological fields or chemical transformation and was not meant to quantify expected deposition levels from the multitude of sources. Its only purpose was to determine whether the level of complex terrain effects at the much finer receptor scales possible from AERMOD can add to the understanding of the CMAQ results. The next three subsections present a brief description of the pertinent aspects of the two models in simulating long-term acidic and mercury deposition from their respective precursor emissions, and the methods used for dry and wet deposition estimates.

3.1 CMAQ modeling system

Over the last two decades, CMAQ has become a standard modeling approach for the EPA and state regulatory assessments, including the demonstration of standards compliance and exposure assessments on the national level and in NYS. Over time, CMAQ has been further developed and enhanced by the EPA's Atmospheric Modeling and Analysis Division (AMAD) of the National Exposure Research Laboratory (NERL), which supports the EPA's mission to protect human health and the environment. CMAQ is an active open-source development project of the AMAD that consists of a suite of programs supported and distributed by the Community Modeling and Assessment System (CMAS) Center.[39] The set of programs and technical documents are available at the CMAS site, including the latest version 5.02 used for this study. The documentation includes the basic modeling approached such as advection-diffusion and cloud physics, plus more recent enhancements for bidirectional mercury exchange, source apportionment to track set of sources of interest, and enhancement of the inorganic aerosol chemistry module ISORROPIA II.

The CMAQ modeling system simulates various chemical and physical processes that are thought to be important in understanding atmospheric trace gas transformations and distributions. The CMAQ system contains three types of modeling components: a meteorological modeling system (WRF) to simulate atmospheric parameters and wind flow conditions, an emission model for projecting man-made and natural emissions that are injected into the atmosphere, and a chemistry-transport module within CMAQ for simulating chemical transformation and the fate of pollutants and their precursors. Because CMAQ is designed to handle scale dependent meteorological formulations and a large amount of flexibility, CMAQ's governing equations are expressed in a generalized coordinate system and this approach ensures consistency between CMAQ and the meteorological modeling system. The generalized coordinate system determines the necessary grid and coordinate transformations, and it can accommodate various vertical coordinates and map projections. The target grid resolutions and domain sizes for CMAQ range spatially and temporally over several orders of magnitude.

Throughout the development of the CMAQ modeling system, a number of modules have been incorporated to address pollutants of concern and associated chemical and physical transformations. In addition, testing these versions against available ambient data has allowed the tweaking and refinements to the various components. For example, section 2 described attempts to better simulate wet acidic deposition by improvements to precipitation predictions. With respect to hazardous air pollutants (HAPs) such as mercury, the development of a multipollutant version and its testing has been described by the EPA and other researchers. In particular, one study[40] evaluated CMAQ against observations for five HAPs in support of risk assessment studies on human exposure. Another study[41] describes this model development, particularly the mercury version, which includes a dry deposition approach and the aqueous chemistry in the cloud dynamics module. The data tests of these versions showed promise in comparison to observations, but also indicated areas where further research and refinements were necessary. Along with these internal the EPA model development steps, groups such as the CMAQ Model External Peer Review Panel[42] provided findings and recommendations to further improve the model performance.

For the current study, the aim was to address deposition levels in and around NYS at a refined horizontal scale well below the 12km level used in previous assessments. The hope was that with this refinement, better projections of impacts would be possible due to expected better simulation of meteorological fields as well as concentration fields. Since CMAQ is a Eulerian model where average impacts are determined within each grid cell, the smaller areas of the 4km grid used in our study vs. the 12km grid would be expected to produce better simulation of terrain features as well as more refined concentration fields. However, the grid refinement also comes at a computational expense and in order to assure practical simulation timescales by the three components of the CMAQ system, it was necessary to limit the horizontal extent of the 4km grid modeling domain. In doing so, it is possible to include this grid nested within a larger domain of 12km grid size to allow the simulation of the influence of sources outside the domain of interest.

The two grids, the 4km and the outer nested 12km, are shown in figure 3-1. The 12km grid corresponds to the grid used by DEC for the Ozone Transport Commission (OTC) and is 172 by 172 grid points with 34 vertical layers. The 4km grid encompasses all of NYS and the adjacent neighboring states. An example of the refinement provided by the 4km grid is demonstrated in Figure 3-2 where the terrain resolution in the Adirondack mountain area is depicted for the 12km and the 4km resolutions. It is seen that the 4km grid has a much better resolution of the terrain features; i.e., while the maximum terrain height in the 12km grid is about 800m, the 4km grid maximum height is about 1200m, much closer to the 1400m actual level in the Adirondacks. The resolution should ideally produce better impact estimates.

Figure 3-1. The OTC 12km grid (left) and the study's 4km grid (right) used in CMAQ simulations

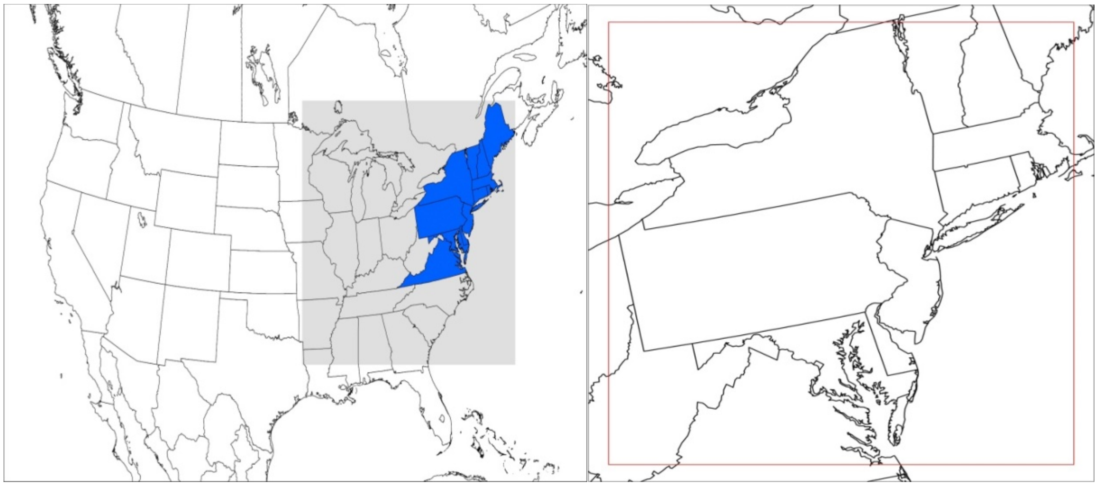

Figure 3-2. Terrain resolutions in meters at the 12km (left) and the 4km grids in the Adirondacks

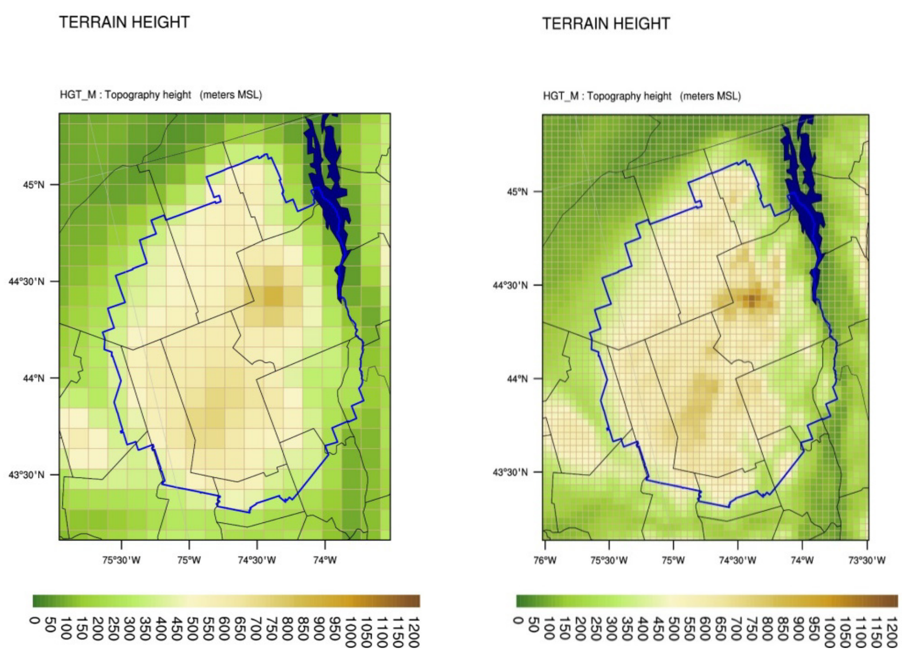

A schematic of the CMAQ modeling system is provided. A brief description of the meteorological, emissions, and inorganic aerosol chemistry modules pertinent to the current study is provided to assist in understanding the complexities encountered in a CMAQ model application.

Figure 3-3. CMAQ Modeling System

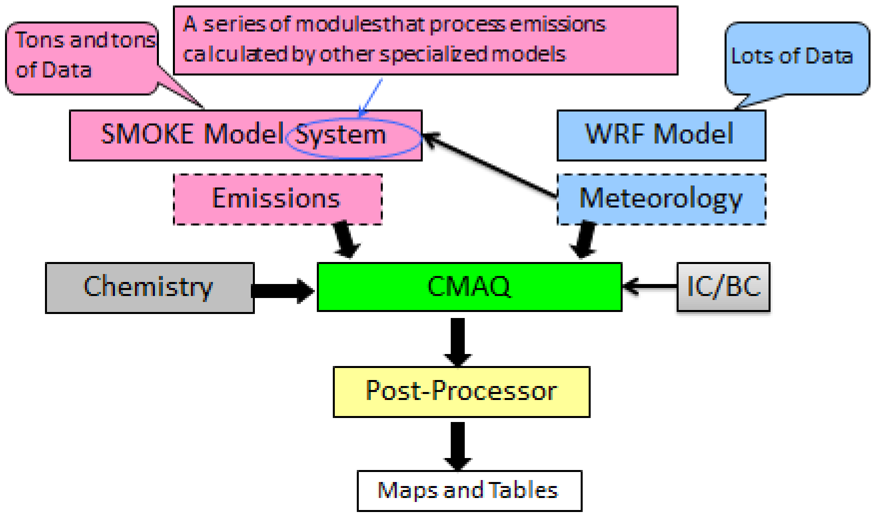

The current preferred meteorological processing system for CMAQ applications is the Weather Research Forecast (WRF)[43] v 3.4 module developed and supported by a consortium of federal agencies and universities. It is both an operational weather forecasting and research tool used to simulate hourly fields of a number of meteorological parameters over a chosen grid. While steady state plume models are limited by the use of representative meteorological data from single NWS stations per application over the grid under study, the important advantage of WRF/CMAQ system is that it can simulate spatially varying meteorological fields both in the horizontal and vertical dimensions over the relatively large grid domain. This simulation more closely resembles the varying conditions of both dynamic (e.g., winds) and static (e.g., temperature) parameters occurring over tens to hundreds of kilometers in a domain. WRF simulates conditions over a basic one-hour time step by incorporating all observed data from NWS sites in the modeling domain and other available information (e.g., precipitation network data) in the solution of atmospheric dynamic equations at the grid locations. Thus, by design, the WRF simulations over a smaller grid scale such as the 4km grid used in the study, should better simulate the various parameter variability. Hourly surface and upper level data for the year 2011 were obtained for the various observation sites for WRF simulations. However, it was discovered that many of the hours in March were missing from the data sets and the WRF simulations and CMAQ modeling had to be limited to the eleven months of valid data.

One factor affecting the simulation of meteorological conditions and underlying CMAQ parameters, especially for deposition calculations, is the land use data in its surface physics schemes. For this purpose, the WRF-CMAQ interface allows the use of three different options from the National Land Cover Database (NLCD). In our application we used the NLDC 2006 data. The use of this data over the 4km grid of the current study further enhances the ability to define more representative land use over the area of each grid. Another factor that needs discussion is the precipitation simulation in the WRF-CMAQ system and the use of this data to calculate wet deposition through the cloud dynamics and chemistry module. The wet deposition scheme involves the scavenging of pollutants which participate in the aqueous phase of cloud chemistry or are removed by precipitation over the vertical extent of the cloud.[44] This removal is dependent on the simulated precipitation by the cloud module containing a resolved and subgrid model. For large horizontal grid resolutions, the model requires the parameterization of the subgrid scheme to simulate convective conditions not otherwise resolved in the model. The convective cloud is simulated within the grid if precipitation clouds are detected over the grid.

The user's guide recommends this subgrid convective modeling be used for grid resolution on the order of 12km or more based on a referenced study which indicated that convective clouds are adequately resolved by the model for resolutions finer than 5km. As part of testing the WRF-CMAQ system for the current study, a preliminary set of calculations was performed where results of deposition over the 4km grid were compared to results from a 12km simulation. These results were limited to one month (July) to learn and obtain guidance on the overall study approach. For wet acidic deposition, CMAQ was applied with the subgrid convective cloud option for the 12km grid, but was not used for the 4km grid as recommended in the guidance. These results were compared to each other and to available observations of precipitation and wet acidic deposition at NADP sites in the modeling domain. As this preliminary study[45] indicated, the omission of the sub-grid convective modeling in the 4km grid run resulted in underestimation of precipitation and the associated wet deposition relative to the 12km results, and more importantly, relative to observed data. Thus, subsequent modeling of wet deposition was performed with the sub-grid module being used for the 4km grid.

Such "midstream" model adjustments are important for better understanding and simulation of the complexities involved in regional scale modeling. In some instances, these adjustments are clearly necessary and defensible, while in many cases, reliance must be made on studies that have resulted in further development of the CMAQ system. One example of the latter is the demonstration of the importance of bi-directional mercury flux discussed in the previous section. While in other instances, no such verification or indication of the latest model schemes is possible by regional scale studies. In these instances, the limited indirect evaluations of the improved scheme in the studies which have developed the scheme have to be considered adequate. One such area is the chemistry involved in the simulations of atmospheric transformations of acidic precursors and mercury simulations. In particular, a relatively recent development incorporated into CMAQ is a revised chemistry module to simulate inorganic particulate and gaseous pollutants. Through its aerosol module (AERO6), the model calculates the condensation/evaporation of volatile inorganic gases to/from the gas-phase concentrations from known particle surfaces and thermodynamic equilibrium between the gas phase and fine particle modes using the latest methods in ISORROPIA II.[46]

This revised chemistry scheme is important for the simulation of pollutants such as sulfate, nitrate, and ammonium, and has the updated ability to include the influence of sea salt and crustal aerosols in the thermodynamics of particulate formation. ISORROPIA II allows the calculation of aqueous, solid, and gas phase reactions for 27 reactions or equilibria through the use of the aerosol equilibrium thermodynamics for multicomponent mixtures by considering transformation between solid and aqueous phase (deliquescence) as a function of temperature and relative humidity. It uses the concept of Deliquescence Relative Humidity (DRH) and for mixtures it determines the mutual (M)DRH below which solid state is favored for mixture. Another factor considered is the "activity coefficient," which is the adjustment from the ideal state behavior of chemical substances for the aqueous solution of the electrolytes. This is important at lower RH where aqueous phase of mixture is concentrated and very non-ideal. For example, the model allows for the existence of aerosols such as nitrates below RH levels (e.g., 60 percent) where other schemes previously used in the EPA models assume these would not exist. These lead to a complex set of equations solved mostly numerically, but the other improvement in ISORROPIA against previous modules is the very large improvement in computational times for the components. The new scheme was indirectly revaluated against water activity measurements (i.e., mass fraction of solutes) for some mixtures and showed good results. Another test of the model was reported in a study[47] of nitrate projections with the CALPUFF plume model where improved model performance was reported, partly due to the inclusion of ISORROPIA II chemistry. Thus, it is believed that these improvements to the inorganic pollutant chemistry of acidic precursors would only add to better modeling of the constituents in all environments, especially where coarse size particulates are important.

Another critical data input to the CMAQ modeling is the emissions information. Ideally, this aspect of the modeling should be adequately represented by information available from the EPA, states, and industries. However, a number of issues have hindered the generation of the best possible data base in many applications involving multi-source configurations. Complicating the situation is the fact that regional scale assessments attempt to incorporate all known sources of precursors and pollutants of importance to a given application. Some of this data is better quantified than others, leading to uncertainties in emission estimates. In addition, data that should be easier to quantify is not appropriately resolved or provided leading to less than adequate inventory. The next section discusses some of the issues encountered in the review of the specific NYS sources this study has tracked for their contribution to deposition levels. This current study used the base case of the 2011 NEI, developed by the EPA from data supplied in part by state submittals. This data base contains emissions and stack information from a large set of anthropogenic sources represented as point (e.g., EGUs, WTEs), area (e.g., manufacturing, oil and gas exploration) and mobile (e.g., on-road and non-road) sources in the modeling domain. In addition, natural emissions such as from fires and wind-blown dust have been incorporated into the NEI. For sources outside the 4km modeling domain, the influence of emissions such as from Canada are accounted for in the modeling as initial and boundary conditions at the edges of the grid, as depicted in the CMAQ schematic diagram. It becomes clear that while most of the emission information should be well represented from available data, other aspects are not as easily or adequately defined.

In addition to the base case modeling of the 2011 NEI, the study also estimated potential changes to the inventory in a future scenario. Initially, the year chosen for this latter scenario was based on the available EPA 2018 NEI which was being developed for regulatory applications, such as the Ozone compliance demonstrations. However, this future year was switched to the 2017 NEI since this, subsequent to our plans, became the choice by the EPA for the regulatory demonstrations. As noted in the EPA Technical Support Document (TSD),[48] the year 2018 was used for the preliminary modeling performed since it aligned with the Ozone requirements for that year. Subsequently, the EPA issued the final Ozone NAAQS Rule that revised the attainment deadline based on rules vacated by a court ruling and the EPA adopted 2017 as the year for the updated ozone transport modeling in the 2011v6.2 platform. However, as of the time of the CMAQ modeling for the study, the EPA was still modifying the 2017 NEI. Because projected emission inventories had already been prepared for the year 2018, the study adopted that year as the "future" scenario. The study had proposed to limit the future year projection analysis to only acidic deposition and not to mercury since it was anticipated during the study plan that the 2018 inventory would have inadequate projections for mercury from all the modeled sectors. The TSD in fact notes that the EPA's interest was in establishing the modeling inventories was for criteria pollutants and a handful of HAPS not including mercury. A basic review of the 2017–2018 data indicates very little or no emissions for mercury in the set of sources of interest in our study. Details on some of the data reviews and what the study addressed for the future scenario using the 2018 NEI is discussed in the next section on emissions development.

The emissions processor used to put the large set of data from the 2011 NEI into the correct form for CMAQ applications is the Sparse Matrix Operator Kernel Emissions (SMOKE) Modeling System.[49] SMOKE input data consist of emissions inventories, temporal and chemical speciation profiles, spatial surrogates, gridded meteorology and land use data, and other ancillary files for specifying the timing, location, and chemical nature of emissions. The processor keeps track of the various source types as well as performs rudimentary checks of the parameters and assigns default values where necessary to these sources. For most sources, the emissions generally represent an average set of conditions, some are adjusted for seasonal effects, but certain source types, such as on-road mobiles and EGUs, SMOKE uses provided data or calculates more representative hourly emissions. For example, many point source emissions depend on atmospheric parameters such as temperature and relative humidity, which are used from the WRF projections to better characterize the hourly emissions. As such, SMOKE modeling of a set of source types follows the completion of the WRF analysis. For other sources such as those from Canada and Mexico, only larger scale emissions are available and for our study only data from 2010 were available instead of the 2011 base case. However, this limitation is determined not to be of major consequence since the representation of these emissions in the outer 12km grid is deemed adequate.

For the study, it was necessary to cast the EPA 12km grid emissions data down to the 4km grid in the modeling domain. This step involved few complexities, but was accomplished successfully for essentially all source types. The emission inventory can be processed for any grid cell size as long as the corresponding spatial surrogate, meteorology, and land use data are available. For biogenic and Canadian sources, we did not have a 4km land use data available, thus for these categories, the 12km sources data were divided up and allocated to the corresponding 4km cells. This step was more than adequate for our specific study given its focus on the explicit point sources types of importance for both the acidic and mercury deposition. One unexpected aspect of the results was the need to better define the emissions information from outside the modeling domain specific for the mercury modeling. It was known that the 2011 NEI contained certain hazardous air pollutant (HAPs) emissions for the sources, but it became clear that the EPA's development of both the 2011 NEI and the future scenario emissions (i.e., 2017–2018) was mainly focused on the criteria pollutants and certain HAPs, not including mercury. Although mercury data was included in the 2011 NEI that was available to DEC staff, the extraction of the mercury data from the inventory required further steps in order to properly assign the source information from the EPA 12km base data to the 4km grid of our study. This step was successfully accomplished for the sources in the 4km modeling domain, which was then included in the preliminary modeling noted above. In this instance, the modeling covered two and a half months of meteorological data, mid-May to end of July. A comparison of projected to observed wet deposition at Mercury Deposition Network (MDN) sites for this limited run (see Section 5 details) indicated very low projections relative to observations and the clear need to more fully define the impacts of mercury emissions into the domain from outside the 4km grid boundaries. Thus, further effort was put into extracting and processing mercury emissions for sources from the EPA 12km NEI data base as input boundary conditions to the modeling domain analysis. The recalculation of wet deposition with the inclusion of these outside the grid emissions showed much improved performance for wet deposition relative to observations.

It is clear that proper simulation of all sources of importance is essential for the determination of not only how well the model performs, and more importantly for our study, the correct interpretation of the relative contribution of the State's energy sector to the overall deposition levels. To this end, it was important for the project to review the emissions data for the NYS energy sector's major point sources to at least assure their proper and adequate representation in the modeling assessment. This review of the 2011 NEI and the future 2018 emissions scenario was undertaken as an important component of the project and the results are presented in the next section.

3.2 AERMOD modeling system

As noted previously, the use of the EPA AERMOD model had a very limited application in the current study. Although the refined 4km grid spacing used in the current CMAQ application provides a better representation than previous larger grid applications of the complex terrain features in NYS, there is still a limitation of the ability of this finer grid spacing to adequately represent the variability in the detailed terrain features, as seen in Figure 3-2 results. Previous studies had indicated the importance of understanding the variability of deposition on terrain features such as Whiteface mountain in the Adirondacks and it was determined that the application of the terrain approach of the simpler Gaussian plume models might assist in understanding the results of the CMAQ applications. The EPA AERMOD model was the practical choice from the standpoint that it contained the state of the science formulations for deposition and demonstrated good performance in complex terrain areas relative to the EPA model specifically formulated for such applications. AERMOD provided the opportunity to test two aspects of the projections in complex terrain in a relative sense; i.e., to calculate annual wet and dry deposition patterns on example terrain features and determine their relative importance to total deposition, and to check these patterns of acidic and mercury deposition to augment CMAQ predictions in the area of these specific features. That is, these results were meant to more fully represent the variability within the terrain features which likely be missed by the CMAQ simulations. As discussed in the results section, the CMAQ results are still too coarse for any detailed comparisons to the detailed gradients generated by AERMOD.

The choice of AERMOD was also appropriate from the standpoint of its current standing as the EPA recommended plume modeling approach for regulatory applications and its ongoing improvements and updates in the modeling community. At the same time, however, it was recognized that the terrain approach in AERMOD was only an approximation of some of the terrain flow complexities addressed by the EPA CTDMPLUS model. The letter model was specifically formulated based on intensive field studies around power plants in complex terrain settings and features a more complex simulation of streamline deformation and flow around terrain. However, the model application is tedious and does not contain the deposition algorithms of interest in our study. Although AERMOD has a simpler approach to the calculation of impacts on complex terrain than CTDMPLUS in that it does not simulate the terrain forced flow "plume deformation" along the stagnation streamline, it simulates the basic approaches of plume lifting over or wrapping around terrain based on atmospheric conditions and the critical streamline height which separates the two flow regimes. Furthermore, an evaluation of AERMOD against CTDMPLUS at some of the field study sites indicated a very good comparison to observed levels. Details on both model formulations, evaluations, and applications can be found at the EPA's SCRAM website.[50]

Similar to CMAQ, the AERMOD model is part of a modeling system with its own preprocessors for meteorology based on land use and receptor terrain setup for a given application. The main aspects of these will be briefly described as far as their use in the current application. First, the terrain approach in AERMOD needs to be outlined. Once the terrain features and heights have been defined by the terrain pre-processor (AERMAP) for a given application, AERMOD simulates flow over or around these features based on the hourly meteorological conditions. In general, AERMOD models a plume as a combination of two limiting cases: a horizontal plume with terrain impaction and a terrain-following plume where the plume flows over the terrain. AERMAP uses gridded terrain data to calculate a representative terrain-influence height (hc) for each receptor with which AERMOD computes receptor specific critical height (Hc) values. A plume embedded in the flow below Hc tends to remain horizontal;

it might go around the hill or impact on it, but a plume above Hc will ride over the hill. Associated with the latter is a tendency for the plume to be depressed toward the terrain surface and for flow to speed up and vertical turbulent intensities to increase. Essentially the plume behavior in the two regimes is determined by its ability to overcome the stable flow by comparison of its kinetic energy to the flow potential energy. The calculation of concentrations from the two regimes is based on a weighting factor, the formulation of which requires the computation of H_c. Using the receptor specific terrain height scale (h_c) from AERMAP, H_c is calculated from the same algorithms found in CTDMPLUS as:

Equation 1. $$1/2 \cdot u^2\{H_c\} = \int_{H_c}^{h_c} N^2 (h - z)dz$$ **where N is the Brunt-Vaisala frequency.**

For a receptor at an elevation *zt* and an effective plume at height *he,* the height that the streamlines must reach in order to be in the terrain-following state is *zt*+*he*. Therefore, the terrain height of importance, *hc*, in determining *Hc,* is simply equal to this local terrain-following height. These calculations are performed for each hour of the meteorological data. For areas with no or simple terrain, these formulations reduce to the standard AERMOD equations.

The application of AERMOD in our study was conducted for two distinct terrain settings in NYS, the Adirondack and Catskill mountains. These features are not only of interest from regulatory standpoint in understanding acidic and mercury deposition, but have been and continue to be important research sites. The central features at these two sites are Whiteface and Hunter mountains, respectively, and for the AERMOD application, the receptors were overlaid around these features with a balance between two factors: 1) the ability to determine deposition over a horizontal scales that would have at least two grid locations from the CMAQ modeling and 2) practicality of the size of the grids, which would not lead to computationally impractical times due to the large set of model runs to be performed for various source combinations. By using the results from AERMAP and an initial simulation, the final configuration of the receptors and corresponding heights were chosen to be rectangular in shape with both Whiteface and Hunter mountains as well as adjacent terrain features included in the simulations.

The receptor grids and corresponding terrain features used for the AERMOD analysis are depicted in Figure 3-3. Starting with the Adirondack Mountain area, the receptors were generated over a grid extending 20km in the east-west direction and 7.25km in the north-south direction. Although terrain data for NYS is available at a 30m increment for the AERMAP application, for the current study a receptor spacing of 250m increment was used and deemed more than adequate to resolve variations in impacts. The topography included Whiteface Mountain and the adjacent McKenzie and Esther mountains with a grid wide enough to contain at least two receptor grids from CMAQ's 4km grid. Based on modeling results for the Adirondack receptor grid, the Catskill Mountain grid was extended by 3km in the north-south direction to 11km while the east-west grid coverage was kept at 20km, as indicated in Figure 3.4. In order to retain a practical receptor set of approximately 2,500 points, the grid increment for the Catskill modeling was increased slightly to 300m with no expected consequence.

Figure 3-4. Receptors and terrain heights generated by AERMAP for Adirondacks and Catskills

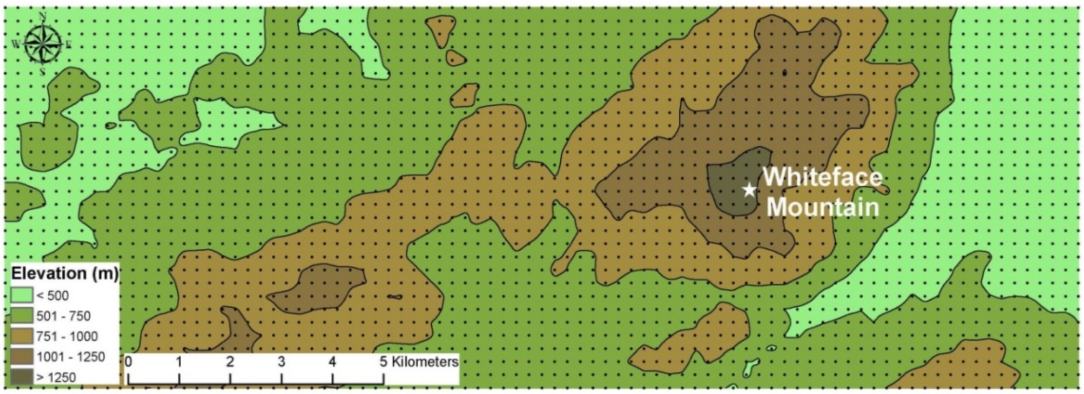

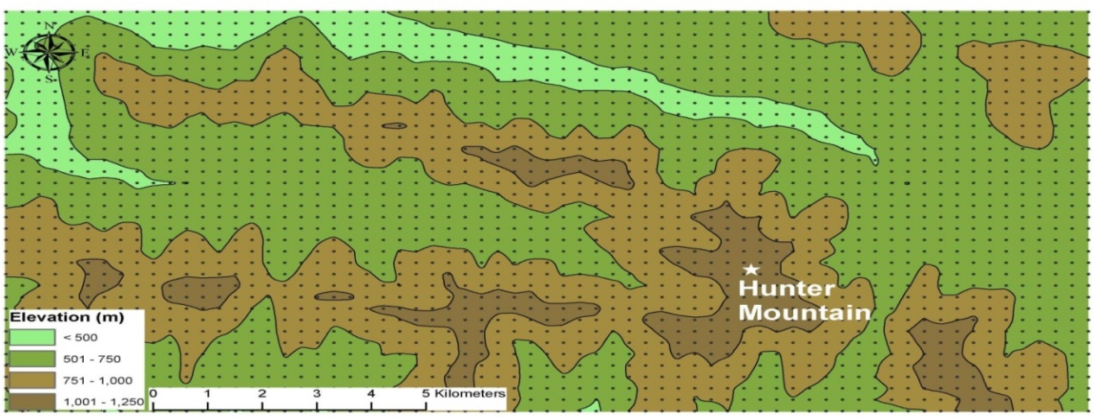

The AERMAP terrain processor for both areas was applied using more recent USGS GeoTIFF data format of the National Elevation Dataset (NED) files available from the Seamless Data Server. Data at 30m increments for the respective counties where Whiteface and Hunter mountains are located, as well as adjacent counties, were used in AERMAP to generate terrain elevations and critical hill heights. Spot checks were made of the elevations against values from Google Earth data to verify the proper generation of the terrain heights. The resultant terrain features are depicted in Figure 3.3 and resemble features documented through site visits at both locations. It is apparent that terrain rises from less than

500m to approximately 1250m and 1450m at the Whiteface and Hunter Mountains, respectively. For the AERMOD runs, a discrete receptor was also placed at the highest terrain location at both terrain features. These receptor and terrain data were then input to the AERMOD model, along with other inputs, to simulate terrain effects. The two terrain patterns for the sites show similarities, but also provide for potentially distinct effects by the complex terrain configurations at the two sites for the simulations.

For the meteorological data, the AERMET processor was applied to "raw" hourly data from the nearest NWS site, as is customary in AERMOD applications. These are the Saranac Lake and Poughkeepsie NWS sites located 20km west of the Adirondack grid and 70km south-southeast of the Catskills grid. The scarcity of data sites with all necessary parameters for plume modeling makes it difficult to use ideally representative data especially for complex terrain setting. Thus, the use of especially the Poughkeepsie data might be inadequate to represent flows in the chosen grid. However, these meteorological data were used in the current study to project patterns of impacts as influences by various source and wind flow sectors and not absolute values. This limitation was deemed acceptable for the purposes of the current AERMOD application.

Raw meteorological data for the two sites were obtained for the purposes of generating wind roses depicting the combination of wind direction and wind speed to guide in the placement of "generic" sources chosen for the AERMOD runs. These wind roses for the years 2011–2014 for the two sites are presented in Figure 3.5. It shows that annual wind flows at the Adirondack site is dominated with winds from the southwest to west-southwest sectors, with secondary peak in the west flow. On the other hand, the wind data use for the Catskills grid has relatively evenly distributed flows, with peaks in the north, southwest and southeast flows. The southeast flow sector has a large low wind speed component, but it is unknown if these latter flows are representative of the exact condition near Hunter Mountain.

Figure 3-5. Wind roses for the Saranac Lake (left) and Poughkeepsie NWS sites

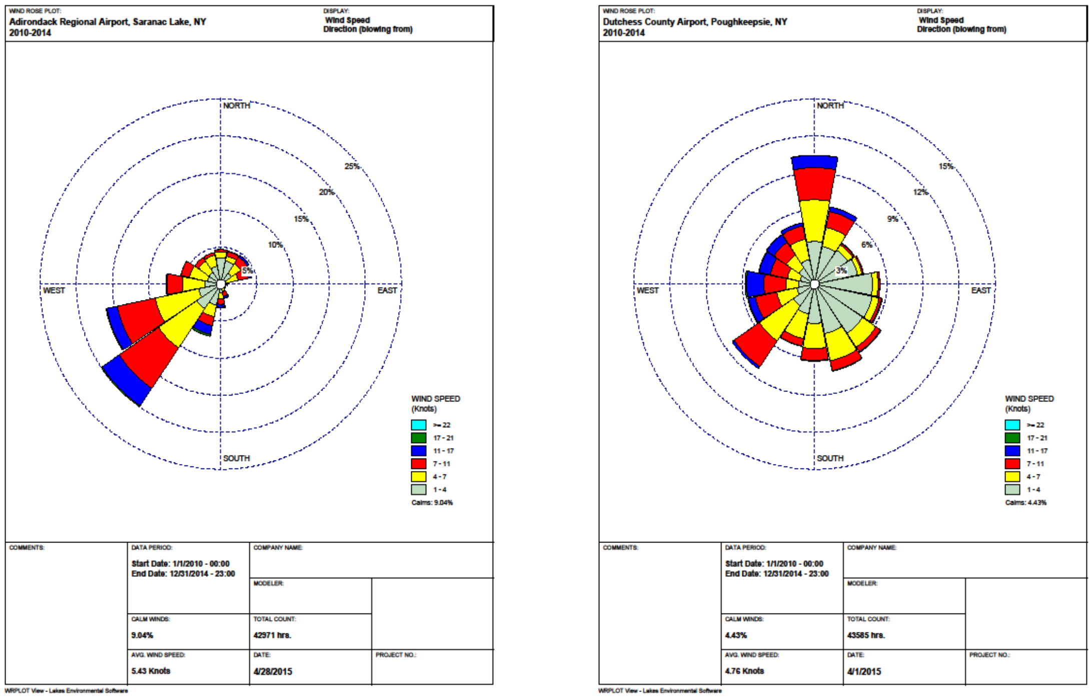

The hourly meteorological data for 2011 was extracted from the two data sets and processed using the AERMET meteorological pre-processor to generate the parameters necessary to run AERMOD. In addition to the standard set of parameters needed for concentration calculations, the AERMET processing also included precipitation and relative humidity data for use in the deposition estimates. In order to calculate the various turbulence scales and meteorological variables needed for the application of surface layer similarity and boundary layer dispersion simulations, the land use within 1km of the NWS sites were extracted by the use of AERSURFACE processor for the 36 wind flow directions. This is standard practice in regulatory applications and adequately represents flow conditions upwind of the receptor grid under study.

It has been noted that in areas with large variability in land use over the source and receptor sectors, the representativeness of some of the generated meteorological parameters might be better simulated using the data for the receptor area. Although this latter approach has not been tested as far as AERMOD model performance in complex terrain settings, it was decided to recast the meteorological data from the Saranac Lake site using the forested area surface parameters (e.g., roughness length of 1m in all directions) to determine if these resulted in significant differences for the study. The recast data for 2011 was used in one of the source scenarios for the Adirondacks; i.e., 10m source at the grid's edge. These results, when compared to the standard AERMET application data results, indicated the same patterns of impacts, although the absolute levels of impacts were different. However, since the study's focus is not the determination of absolute concentrations and deposition from AERMOD in comparison to the main CMAQ results, further assessments for the AERMOD sets were carried out using the standard approach meteorological data.

The next step in the AERMOD application was to choose the set of sources to model. Section 4 describes the steps taken to determine the set of energy production and other larger point sources of mercury and acidic precursor emissions explicitly tracked in the CMAQ modeling to determine their relative contribution to deposition levels. As described in that section, the final set of these sources are located at distances well outside the "applicability" of Gaussian plume models per the EPA guidance. However, for the current study, two sources each for the terrain grids were chosen to gauge the influence of these distant sources as far as projected patterns on the receptor grid. It was assumed that at these far distances, the plumes from these sources would be well mixed in the vertical transport layer and the patterns of impacts would not be specific to their plume heights. The sources chosen for the Adirondacks were Hudson Falls as the closest source at a distance of 70km due SE of the grid, and the Cayuga coal plant with its higher mercury emissions in the dominant southwest upwind direction from the grid, at a distance of about 270km. For the Catskills grid, the source choices were the LaFarge cement plant and Danskammer coal plant, both at a distance of 65km and in the northwest and south-southeast directions, respectively, from the receptor grid.

Arguably, at these distances, the dispersion patterns projected on the complex terrain grid from these specific sources have other limitations. One such limitation is the narrow horizontal plumes associated with point sources relative to the grid scales, even when assuming the plumes are likely well mixed in the vertical. Since the purpose of the AERMOD modeling was to simulate the effects of the multitude of sources in the CMAQ inventory and especially the influence of sources outside the modeling domain due to their significant influence on mercury levels, it was decided that a set of sources that could simulate this influence should be modeled. The choice of such sources was guided by two main factors: the representation of more "area-wide" emissions than afforded by a single point source to represent the likely larger scale distribution of concentrations resulting from distant sources and the placement of these sources in the upwind direction from the grids and at various vertical and horizontal distances. Due to the limitations of steady state models like AERMOD, these locations were limited to within 50km from the grids and at below the average heights of about 1000m expected for the boundary layer within AERMOD simulations are deemed more appropriate.

The choice of a "generic" source type dictated by these considerations was further guided by the fact that simulation of a multitude of point sources involves another consideration of importance in interpreting the results. General point source modeling involves the definition of stack parameters that determine the final plume height of the source by the calculation of plume rise which is then added to the physical stack height of the source. These heights are calculated on an hourly basis and can have a very large range of values, thus complicating the interpretation of long-term impacts. Of course, simulations of point sources could be performed by setting the plume rise to zero, but then the placement of the multiple point sources in the horizontal and vertical dimensions is still very tedious and is of no advantage over the use of other source types like line, area, and volume sources. It was determined that a long line source representation at various heights was the best choice for our purposes. An initial model run with a compatible area source representation resulted in the same impacts as for the corresponding line source configuration. Given the longer AERMOD run times for simulating area sources, all further modeling was performed using the line source configuration.

The AERMOD modeling for the Adirondack grid was performed first and the experience gained from the results guided the modeling for the Catskills grid. The line sources were modeled as a very long and narrow source of 4km long and 10m wide. A sample run with a 100m width line source did not influence the patterns seen with the 10m wide source and further modeling was carried out with the 10m width. The length of the line source was determined to adequately represent the wide-spread concentration patterns over the grid area due to the multitude of distant sources likely affecting the deposition patterns. The heights of the line sources were set from ground level (nominal 10m) to elevations at 100m, 400m, 700m and 1000m, with the last set at an average mixed layer height. These sources were placed at various upwind distances from the grid: the western "edge", 10km west, 30km west, and 30km southwest of the grid. These were meant to represent dominant flow directions, as well as cases of well mixed vs. "intact" plumes. Each source was modeled separately and also as a case of impacts from the combination of a subset or all sources simultaneously. Results were reviewed at each step of the modeling to guide the choice and approach to the rest of the runs.

These results for the Adirondack grid also helped guide the approach for the Catskills modeling. For the latter grid the same source heights were modeled, but instead of individual source runs, all sources were included in the same runs based on the results for the Adirondack grid. Further analysis was performed with the modeling including only the sources at and above the 400m level to test and understand some of the previous patterns. The locations of the sources were: at the western and southwestern “edges” of the grid, at 10km west of the grid and at 10km Southeast of the grid. Not all possible combinations of configurations were modeled and the discussions in the results sections provides the rationale for the choices made.

Since absolute values of concentrations or deposition were not the purpose of the study, an arbitrarily large emission rate was chosen to ensure distinct patterns of impacts would be observed. However, the purpose of the AERMOD model was also to test the relative contributions of wet vs. dry deposition in review of the CMAQ results. Thus, two distinct sets of deposition parameters were identified based on the AERMOD guidance document and other study finding. One set was for gaseous mercury simulations and the second set was for particulate sulfate simulations. The choice for the mercury deposition simulation started with the recommended deposition parameters corresponding to the elemental component due to its abundance in the atmosphere. However, the initial model estimates indicated essentially nil wet deposition and very low dry deposition. These results were in keeping with expectations from both guidance and previous pertinent studies. Thus, the rest of the modeling was conducted using the deposition parameters for the gaseous oxidized mercury, which are the basis of the discussions of the deposition schemes. For limited runs of particulate sulfates, the dry and wet deposition parameters from the AERMOD guidance document were used.

The set of projected annual deposition and some concentration patterns were reviewed to guide the understanding of the CMAQ results. In addition, the maximum 24-hour projected impacts were tabulated and the associated meteorological conditions reviewed and compared to corresponding set of data from the WRF simulations to provide further information and guidance in the interpretation of results.

3.3 Deposition approaches

The basic methods used in both the CMAQ and AERMOD modeling rely on essentially the same relationships between concentrations and the resultant deposition due to dry and wet processes and the parameters controlling these processes. At the same time, however, there are significant differences between the two models, including the steps taken and assumptions made to determine the average deposition parameters for specific meteorology, underlying surfaces and the integrated column concentration and precipitation. Coupled with differences in the plume and grid modeling approaches, there cannot be a comparison of the projected deposition. On the other hand, it is possible to determine the relative influence of wet and dry processes and the effects of calculated deposition parameters from both modeling approaches.

A summary is provided of the simpler dry and wet deposition approaches used in the AERMOD model for gases and particles. The details of these approaches are presented in the original document[51] on the parameterization of deposition and the science document[52] to adoption these methods for application in the AERMOD model. In order to be able to use these methods with the basic meteorological data input to AERMOD, as well as for parameters of importance in these calculations, certain assumptions have been made in the formulations and specific pollutant physical and chemical properties have been tabulated in the Appendices of the science document.

AERMOD deposition approach is separated into the dry and wet schemes and each of these invokes specific approaches for gas or particle pollutants of importance to given applications. For dry deposition, the basic calculation is performed for each hour of meteorology using the product of ambient concentration and a dry deposition velocity from:

Equation 2. $$Fd = Cd \times Vd$$

where Fd = dry deposition flux (µg/m2/s), Cd = concentration (µg/m3) calculated at a reference height and Vd = deposition velocity (m/s). The method then reduces to the appropriate calculation of the deposition velocity to account for various meteorological and surface conditions. These velocities are simulated as an analogy to resistances to deposition (or conductance) as an inverse relationship between the velocity and the various resistances to deposition as set in a series. The more resistance, the lower the deposition velocity and less consequent deposition. The importance of the various underlying conditions is highly dependent on whether the pollutant is in gaseous or in particulate form.

For gases, the dry deposition velocity is calculated from:

Equation 3. **Vdg = (Ra + Rb + Rc)-1**

where Ra is the aerodynamic resistance dependent of surface layer similarity parameters calculated by AERMOD, Rb represents the surface resistance to deposition in the quasilaminar sublayer in contact with surface elements, and Rc is the resistance of the surface itself to uptake. For Ra, the set of equations under stable and unstable conditions are determined from parameters input to AERMOD, such as roughness length and Monin-Obukhov scales. Rc is an important and multifaceted resistance for gases, especially in forested areas since it accounts for a number of physical/chemical processes at the underlying surface. It accounts for the surface leaf areas, the stomata and cuticle effects by the canopy, and other resistances at the ground surface by the formulation:

Equation 4. **Rc = [LAIr(Rs + Rm)-1 + LAIrRcut-1 + (Rac + Rg)-1]-1**

Where LAIr = relative leaf area index (unitless), Rs = canopy stomatal resistance, Rm = canopy mesophyll resistance, Rcut = canopy cuticular resistance, Rac = gas-phase resistance in the vegetative canopy, and Rg = resistance to uptake at the ground. These resistances, in turn, are functions of other physico-chemical and meteorological parameters such as radiation and reactivity. Because of the many parameters involved in its calculations, Rc is the most difficult of the resistances to estimate, but the Appendices to the parameterization document provide physical and chemical properties of many gaseous compounds for use in pollutant specific applications. Further specifications of select parameters are incorporated in the formulations to allow the practical application of the deposition method.

For dry deposition of particles, an analogous resistance formulation to equation (1) is used:

Equation 5. **Vdp = (Ra + Rp + RaRpVg)-1 + Vg**

Here Ra is again the aerodynamic resistance, but Rb in equation (1) is replaced by another sublayer resistance term, Rp, with the assumption that Rb for particles is either very small or is included in Rp estimations. One additional resistance for particles is the term Vg, which represents the gravitational settling velocity which has greater importance for the larger particle sizes. The modeling allows for the incorporation of any information on the particle size distribution in the Vdp calculations by two methods. For cases where there is no detailed size distribution, a simpler scheme is used. Method two was used for the Hg and sulfate calculations due to the limited data on the fine coarse modes of these particles and the relative aspect of this modeling. Limited data for sizes of mercury species are provided in Appendix B of the deposition document, as well as in some of the references noted in the next section on mercury speciation. The science document notes that the Rp relationship to the friction velocity used for method two is based on observations for sulfate.

The deposition of gases due to wet processes is essentially a function of the precipitation in the column through which it encounters the pollutant concentrations. It is determined from:

Equation 6. $$Fg = 10^{-3}\rho_g Wgr$$

where Fg = flux of gas by wet deposition (mg m-2 hr-1), Wg = gas washout ratio (equal to RTa/H-unitless), H = Henry's Law constant (Pa m3 mol-1), ρ_g= average column concentration of gaseous pollutant, and r = water or water-equivalent precipitation rate (mm hr-1). Thus, Wg represents a ratio of the concentration of a specific pollutant in precipitation to air and is also known as the scavenging ratio. For AERMOD applications, the removal of gases by snow and rain are assumed to be the same based on referenced studies indicating inconclusive results as to which is higher.

Wet deposition for particles is calculated by an equation analogous to (5), except for the use of particle washout ratio and its column averages concentration. Here again, the effects of snow are assumed equal to rain, even though certain studies indicate much lower removal by the former while some studies indicate higher removal. In addition, the washout ratio is dependent on collision efficiency and mean mass droplet distribution. Values for the latter for certain inorganic pollutants are given in the appendices, along with Henry's law constants and diffusivities in water and air. It must be noted that the scavenging and wet deposition are more complicated in CMAQ and depend on interaction of the pollutant in aqueous chemistry, Henry's Law equilibrium, and cloud water PH. Also, washout and rainout are integrated over time and precipitation rate with washout time depends on time it takes to remove the water from the cloud volume at a given precipitation rate. For convective clouds in the subgrid model, this time is about one hour.

The application of all the equations in AERMOD is carried out by assigning certain of the parameters to the seasonal variations in the underlying surfaces. For example, the AERMOD deposition science document provides a tabulation of the various resistances noted above for nine land use types ranging from urban to forested areas and for five "seasons" determined by the type of vegetation or the extent of snow cover. These values are meant as guidance for specific applications. For our study, the "forest" land use type was assigned to both grids since the receptor area is essentially covered by trees. In addition, the "seasons" were assigned similarly, except the "winter with snow cover" was extended to April in the Adirondacks where the "summer with lush vegetation" was limited to July and August. In addition, the parameterization document notes that care must be exercised in the determination of certain parameters for inorganic pollutants, such as for non-particulate forms of mercury. The document provides specific values for Henry's law constant, reactivity, cuticle resistance, and air diffusivity for elemental and oxidized forms of mercury. Some of these parameters differ by orders of magnitude for the two forms which can lead to significant differences in both dry and wet deposition between the two forms. The guidance document recommended values, along with water diffusivity from the literature, were used in the AERMOD application. As noted previously, due to its low solubility and low dry deposition velocity, low projected elemental mercury deposition was replaced by its oxidized form in all subsequent set of AERMOD runs used for relative comparisons of source and terrain combinations.

The methodologies, as well as the set of input data for each model, were used to project annual deposition estimates from the complete source inventory and from the set of large NYS point source emissions related to energy production were "tracked" in the CMAQ modeling. This allowed for the relative determination of the contribution of these larger NYS sources to the overall deposition levels in NYS, including the combined impacts from categories of EGUs, WTEs, and "other" large point sources. A large task of the study was to first identify these larger energy production point sources to be tracked and then to ensure the emissions data for mercury and acidic deposition precursors were appropriately defined in the 2011 NEI. In addition, the review included the determination of the adequacy of the stack parameters for this subset of chosen sources to minimize uncertainties introduced by emissions data in the results. Furthermore, mercury data review extended to the identification of the relative emissions of its three species for the various source types due to significant differences in the behavior of these species in dry and wet deposition. The next section details the steps taken in the review and identification of the sources tracked in the CMAQ modeling. In addition, a summary of the overall emissions within and outside of the modeling domain is provided for the 2011 NEI to provide a sense of relative emissions from source categories and regions.

4 Development of the Emissions Inventory for Sources to be Tracked in CMAQ Modeling

One of the more important, but at times overlooked, inputs to a modeling exercise is the set of emissions sources and the corresponding pollutant emission rates and stack parameters. Emission inventory development is a resource intensive and somewhat tedious task involving the gathering and massaging of data from various source types and federal and state agencies. These, in turn, rely on facility reported data, estimates using emission factors representing testing, or data from similar source types. The level and quality of such data depends on factors such as whether it is based on mandates by regulations or from requested estimates for rule or policy development and whether the sources being analyzed are point sources or area or mobile sources. For example, data on the “basic” acidic deposition precursors SO_2 and NOx from larger point sources such as Electric Generating Units (EGUs) are monitored “continuously” and reported by industry to satisfy regulations such as the acid rain program. On the other hand, there are no general requirements to have similar reporting of ammonia (NH3) or mercury (Hg) on an industry wide scale, but rather data reporting depends on the specific source federal requirements (e.g., regulations on Incinerators and the Prevention of Significant Deterioration rule) or state requirements (e.g., Hg from sources under DEC’s requirements in Part 219 for Incineration and Part 246 for Hg from coal burning EGUs).

As such, at times the reported data is either taken at face value or is missing important information necessary for modeling assessments. Furthermore, the emission rates used in the modeling depends on the purpose of the assessment. These emissions can reflect either short-term maximum values or, as in the case on the current study, long-term or annual levels. The latter situation is more tenable since deviations from the mean are less likely to influence the annual impacts and render the modeling exercise considerably more robust. Of course the argument can be made that “episodic” occurrences could be important in the determination of the longer term averages; however, from a modeling standpoint, simulations of such shorter term conditions would also have to incorporate all aspects of such model input parameters, which are far from well known. Thus, using representative long-term emissions and stack parameters in estimating long-term deposition is adequate within the recognized limitations on emissions data.

It has been long recognized, but not always addressed, that confidence in emission inventories is lacking the level of verification necessary to ensure reliable inventory development for a large scale modeling assessment. Thus, one of the major tasks of the current study was to review the data for the specific set of sources to be specifically tracked by the CMAQ model for their relative contributions to the overall deposition fields. By the study's design, that emissions data review was confined to point sources of importance for acidic and mercury deposition and to sources in NYS. Although other source sectors or regions in and outside the domain could be as important to the deposition levels in NYS, no attempt was made to review the emissions data from these and their emissions were taken as reported in the EPA 2011 NEI. However, in some instances, findings for NYS sources were also applied to the rest of the domain. For example, the mercury speciation information on coal EGUs used for NYS sources was also used for out of state coal EGUs.

The refined grid modeling of the 2011 NEI for both acidic and mercury deposition in NYS and the vicinity is the first such assessment for quantifying long-term impacts from the domain sources and the source sectors considered and represents the "base case" conditions. In addition to this case, we have also modeled a future projected year inventory for 2018 that incorporates expected emissions reductions due to mandated federal and NYS requirements, as well as State specific point source modifications that have taken place since the base year of 2011. The next subsections will detail the set of steps taken to verify the emissions data for NYS point sources explicitly tracked in the CMAQ modeling for the 2011 NEI, information on the other source sectors in the inventory, the mercury speciation used for the CMAQ tracked sources, and a description of the changes from the base case inventory to the 2018 emission scenario.

4.1 Modifications to the 2011 NEI for CMAQ tracked point sources

The EPA 2011 NEI includes a large set of anthropogenic and "natural" emissions used for many purposes, including modeling for criteria pollutants with national ambient standards and Hazardous Air Pollutants (HAPs) on regional scales to assess public health exposure and related secondary effects. The inventory incorporates the latest information from states, including data reported by facilities, estimates of regulatory imposed emissions, and emission sector testing data. The version used in this study features source types and assumptions summarized in Table 4-1. This information and the corresponding emissions estimates of acidic deposition precursors (SO_2, NOx and NH3) and mercury are processed with the EPA SMOKE program for preparing the necessary inputs to CMAQ.

Table 4-1. Set of Sources included in the 2011 NEI for the study domain

EPA 2011 V2 Modeling Platform

2011 CONUS modeling platform based on 2011 National Emission Inventory (NEI) v2

- **AREA SOURCE**
  - Agricultural emissions (primarily ammonia)
  - Area source fugitive dust emissions (only PM)
  - Residential wood combustion
  - Area source emissions from oil & gas drilling
  - Nonpoint emissions not in other sectors
- **EGU POINT SOURCE**
  - Electric generating unit emissions
- **NonEGU POINT SOURCE**
  - Point source emissions from oil and gas drilling
  - Industrial point sources
  - Fire emissions - includes wild and prescribed fires as point sources
- **ONROAD**: Onroad mobile source emissions from SMOKE-MOVES
- **NONROAD**: Off-road emissions from NONROAD2008
- **MAR** (Marine, Air & Rail)
  - c1c2rail: Category 1 and 2 commercial marine + railroads
  - c3marine: Category 3 commercial marine vessels in state waters
- **BIOGENIC**: biogenic emissions from BEIS3.6

Information contained in this document, such as web page addresses, are current at the time of publication.

Although the NEI contains a large set of source data, the current study aims only to determine the contribution of the NYS major point sources in the energy production sector to the projected deposition from the total inventory. Furthermore, the set of point sources which are of importance for acidic deposition impacts are not necessarily the same as for mercury deposition and a distinction has to be made in these sets of model "tracked" sources. For acidic deposition, a larger set of point sources have emissions of precursors such as NOx resulting from combustion of different fuels. On the other hand, based on previous studies and emissions data, it is less likely that some of these same sources burning gas have significant Hg emissions, resulting in different set of important point sources to be tracked. Thus, we have determined that the point sources of importance for CMAQ tracking of relative mercury impacts are a subset of those used for acidic deposition. At the same time, it became clear during data review that the study had to also consider certain other point sources which had larger Hg emissions, but which are not qualified as energy producers. This later subset is defined below and was also included in CMAQ source apportionment determinations as a separate group.

The starting point of reviewing the emission rates and stack parameters for the set of point sources was defined by a previous analysis conducted by DEC's Division of Air Resources (DAR) for mercury emissions from coal burning EGUs and WTEs facilities. That analysis was concerned with the annual emissions of Hg for the year 2009 and the corresponding capacity of the facilities in megawatt-hours (MWh). The data was obtained for 10 WTEs and eight coal EGUs and processed as a first step in the review of the corresponding information for these same facilities in the 2011 NEI. Since the Hg emissions were reviewed by the DEC staff for these sources for the year 2009, it provided a good threshold for checking the 2011 data in identifying any large differences and finding possible explanations. It was noted that the 2009 data for five of the ten WTEs were adjusted in DAR's study from what was in DEC's facility data base using stack test data provided by Covanta who owed/operated most of these units. These adjustments were relatively small, given the nature of Hg emission variations and the stack test methods, with three within 10 percent while the other two within 25 percent of the DEC data.

The next step involved extracting the Hg emissions from these 18 facilities from the 2011 NEI for comparison. In the process, it was discovered that the Toxics Section at the DEC-DAR had initiated a review of Hg data for 2010 from large point sources in their Air Facilities System (AFS) data base. Thus, a further comparison was possible for three consecutive years of Hg emissions from these facilities which allowed for a better understanding of yearly variations. Table 4-2 provides the Hg emissions from the 18 facilities for each of the three years and also data for the 2011 year from the AFS system, as another check of information. It became clear that the 2011 NEI data needed to be scrutinized for many of these facilities to assure proper representation of Hg emissions. The total Hg emissions from the EGUs varied considerably more between the years relative to the WTEs, but there were facility specific variations in need of resolution for both types. Some of the highlighted data in the table indicate relatively simple explanations on follow-up, such as facility shutdown or phase out during the three-year period (Westover, Niagara Generating) or installation of carbon injection for Hg control (Oswego RRF), while others did not have any reasonable explanation of variation (e.g., Danskammer). There were also instances where the data between the years were fairly consistent (e.g., Hempstead, Huntington) and could reflect yearly capacity differences as an explanation.

Table 4-2. Hg emissions and ratios for 10 coal EGUs and eight WTEs for 2009 to 2011

Facility Name Hg summed from all units	Hg (lb./yr) 2009 data	Hg (lb./yr) 2010 AFS	Hg (lb./yr)* 2011 NEI	Hg (lb./yr) 2011 AFS	ratio Hg 2010/ 2009	ratio Hg 2011/ 2009	ratio Hg 2011 NEI/ 2010	ratio Hg 2011 AFS /2011 NEI
WTEs								
Hempstead RRF	*36.7*	21.1	24.1	30.9	0.6	0.7	1.1	**1.3**
Babylon RRF	*28.4*	11.5	2.7	2.7	0.4	**0.1**	**0.2**	1.0
Huntington RRF	*4.2*	5	4.4	4.4	1.2	1.0	0.9	1.0
Islip-McCarthur RRF	1.8	5.4	1.5	1.5	3.0	0.8	**0.3**	1.0
Dutchess Co. RRF	7.2	9.7	6.3	6.3	1.3	0.9	0.6	1.0
Westchester RRF	18	9	27.4	27.4	0.5	1.5	3.0	1.0
Hudson Falls RRF	5.8	46	33.3	33.3	**7.9**	**5.7**	0.7	1.0
Onondaga Co. RRF	*2.1*	30.4	7.7	7.7	**14.5**	**3.7**	**0.3**	1.0
Oswego Co. RRF	0.0065	0.0061	0.0062	0.0062	0.9	1.0	1.0	1.0
Covanta Niagara RRF	*26.6*	28	13	13	1.1	0.5	0.5	1.0
Totals WTEs	**130.8**	**166.1**	**120.4**					
Coal EGUs								
Danskammer Generating	26	0.09	52.7	12	0.0	2.0	**585.6**	**0.2**
AES Westover	0.14	0.03	**0.00004**	**0.002**	0.2	0.0	0.0	1.0*
AES Cayuga	2.1	28.6	33.5	33.4	**13.6**	**16.0**	1.2	1.0
AES Greenidge	0.015	3.1	3.1	3.1	**206.7**	**206.7**	1.0	1.0
Dunkirk Generating	39	82	16.1	32	2.1	0.4	**0.2**	**2.0**
Huntley Generating	26	83	42	42	3.2	1.6	0.5	1.0
Niagara Generating	0.0094	0.3	0	0**	**31.9**	1.0*	**1.0***	1.0*
AES Somerset	0.15	1.1	7.7	7.7	**7.3**	**51.3**	**7.0**	1.0
Totals EGUs	**93.4**	**198.2**	**145.8**					

* Ratios inconsequential due to very small levels.

** Facility reported no fuel use in 2011.

To assist in the review of the latter aspect, emissions data for SO_2 and NOx were tabulated for the years 2009 and 2011 and compared to the Hg data. The ratios for Hg, SO_2, and NOx emissions are presented in Table 4-3. In general, there is less variability in the SO_2 and NOx emissions than in the Hg data and in some instances all three pollutants indicate good consistency between the years, especially for the WTEs (e.g., four of the facilities have ratios close to one). In cases where the emissions were higher for all three pollutants in 2011 vs. 2009, it was an indication of possible capacity increase (e.g., Westchester RRF) while, again, no real explanation was obvious for other cases. The table does indicate a distinct difference between the emissions of SO_2 vs. NOx for the two source types, with much higher SO_2 than NOx for the coal EGUs while the reverse situation exists for WTEs.

Table 4-3. Ratios of Hg, SO2 and NOx emissions for 18 facilities for 2009 and 2011

Facility Name	**Ratio Hg**	**Ratio SO2**	**Ratio NOx**	**Ratio SO2/NOx**
(emissions summed from all units at facility)	**2011 NEI /2009**	**2011 NEI /2009**	**2011 NEI /2009**	**2011 NEI**
WTEs				
Hempstead RRF	0.7	**0.4**	1.0	0.04
Babylon RRF	**0.1**	0.9	1.0	0.17
Huntington RRF	1.0	1.1	1.1	0.02
Islip-McCarthur RRF	0.8	0.8	0.9	0.11
Dutchess Co. RRF	0.9	0.7	1.0	0.12
Westchester RRF	1.5	**3.0**	1.6	0.16
Hudson Falls RRF	**5.7**	1.0	**2.1**	0.06
Onondaga Co. RRF	**3.7**	**1.6**	1.1	0.05
Oswego Co. RRF	1.0	0.8	1.0	0.11
Covanta Niagara RRF	0.5	0.9	1.1	0.12
Coal EGUs				
Danskammer Generating	2.0	1.2	1.3	3.77
AES Westover	0.0	0.0	0.0	1*
AES Cayuga	11.5	**4.8**	0.9	5.74
AES Greenidge	**206.**7	**0.2**	**0.4**	0.59
Dunkirk Generating	0.4	1.3	0.8	3.32
Huntley Generating	1.6	0.7	0.8	3.51
Niagara Generating	0.0		**0.0**	
AES Somerset	51.3	2.0	1.5	1.84

* Ratios inconsequential due to very small levels.

As the data was reviewed, a number of graphs were developed to test relationships between pollutants within the set of the 18 facilities that could assist not only in the identification of source specific concerns, but also in the review of identified other potential large Hg sources and their corresponding emission rates. Thus, if a simple and solid relationship can be established between Hg and another pollutant or facility capacity, then the appropriateness of identifying and verifying other sources' Hg emissions would be simplified. Here we present only sample graphs of various attempts at such relationships. Figure 4-1 presents plots of Hg emissions against SO_2 and NOx for all 18 facilities in the 2009 data set.

No relationship of any value is seen; in fact, the Hg emissions seem independent of the other pollutant rates. Since the purpose was to also review other facilities with Hg emissions, it was not useful to plot just the sector based values, especially since all WTEs were already identified in the 2009 data. A graph for the EGUs alone did not reveal any better relationship.

Figure 4-1. Hg emissions against SO2 and NOx for the WTEs and Coal EGUs in 2009

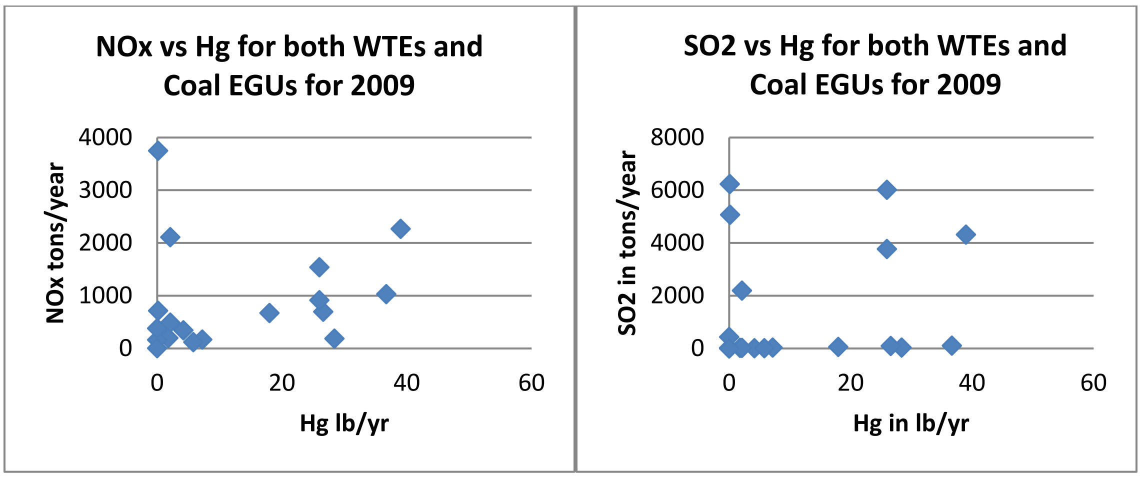

However, it is possible that a relationship can be established on a unit capacity basis. Data on the actual MWh for 2009 for these facilities were available and the emissions per MWh were calculated and presented in Figure 4-2. These graphs do not include some large and small "outlier" values which dominated the corresponding plots (not shown), but even with these removed, no useful relationship was obtained. In fact, a similar plot of SO_2 and NOx on a MWh basis, surprisingly, did not provide a reliable relationship.

Figure 4-2. Hg vs SO_2 and NOx on per MWh basis for WTEs and coal EGUs for 2009

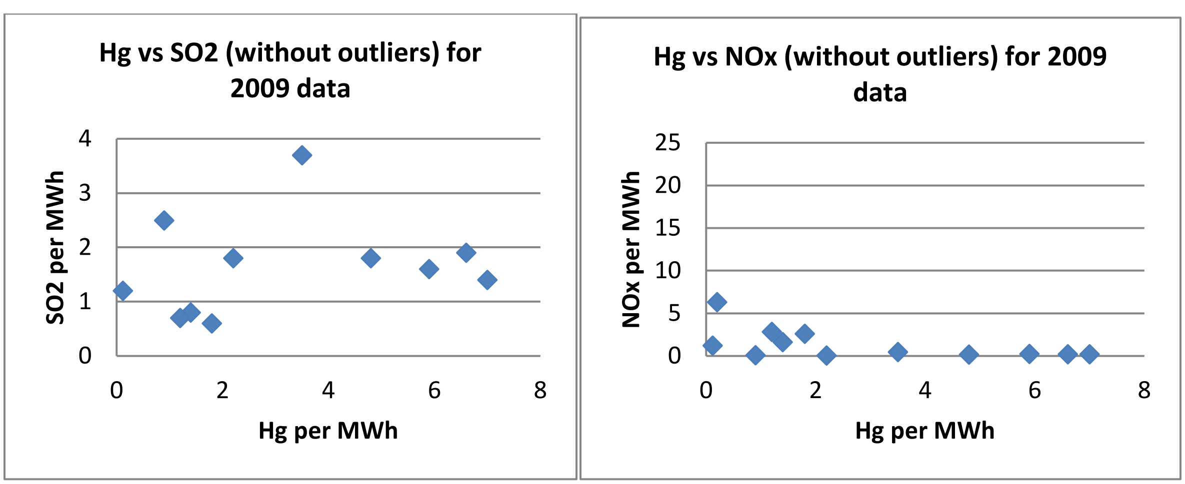

It became clear that the review of Hg emissions and the identification of other large Hg sources would require a number of other steps, including the review of all pertinent reports or data submissions to DEC. In order to identify other potentially large Hg emission sources in the CMAQ tracking set, the complete set of point sources in the 2010 AFS and 2011 NEI was reviewed. For practical reason, a minimum Hg emission rate was established to use in identifying these other large sources. For this purpose, the average Hg emission rate for the WTEs and coal EGUs was calculated separately from Table 4-2 data. Given the large range of values for both sectors, it was felt that a reasonably low average can be defined in order not to overstate a cutoff. The average for 2009 data was given preference since that data was reviewed previously, as shown in Table 4-2, the year provides a low end average especially for the EGUs. The calculated averages were 12.8 lb./yr and 11.7 lb./yr for the WTEs and EGUs, respectively. These values are rather similar and both were further reduced by a single factor of about six to arrive at an annual emission rate of 0.0001 lb./yr (units in the NEI and AFS) or 2 lb./yr, which was then used to scan the 2010 AFS and 2011 NEI point source data bases. The 2011 NEI included the Title V major sources, but also a separate file of capped point sources. The "minimum" value for large Hg source identification purposes was applied to the facility total emissions and not on a unit basis to be more conservative and inclusive.

The minimal rate identified 32 potential other large Hg sources combined from both data sets, with some appearing only in one of the sets. It was more important for obvious reasons for the study that the 2011 NEI reflected the correct list as well as emissions. Review of the potential set with readily known information on some of the facilities' status related to shutdowns, fuel use switches and facility modifications, resulted in nine of these sources being eliminated. The remaining 23 facilities were then further reviewed, in addition to the original set of 18, for their Hg emissions and stack parameters. It was noted that the identified potential large Hg sources included many additional EGUs burning oil or gas, plus a number of others which are not strictly energy production facilities, such as cement plants and metal works facilities. Although the aim of the study was to determine the contribution of energy production sources to the total deposition, it was determined prudent to include the "other" source types in a subset of sources to be tracked in the CMAQ modeling.

The set of potential sources and their Hg emissions from the 2010 AFS and 2011 NEI are presented in Table 4-4. Three sources appeared in the 2011 NEI Title V list, but not in the 2010 set, while two sources in the 2010 set were only in the capped list for 2011 with zero emissions (*sources in Table 4-4). The table also provides the ratios between the two years and further indicates the level of inconsistency in the Hg emissions and a large difference in total emissions, which do not appear to be readily explainable.

Another attempt was made at establishing relationships between Hg and the acidic deposition precursor pollutant rates (SO_2, NOx, NH3) for at least the EGUs since the additional set of Hg sources revealed 10 more facilities in combination of the seven coal burning facilities (Niagara Generating was removed from the original set since it was shut down).

Table 4-4. Set of other potential large 23 Hg sources inclusive of 2010 and 2011 data

Source Name	**Hg (lb./yr)**	**Hg (lb./yr)**	**Ratio**
	2010 AFS	**2011 NEI**	**2011/2010**
Other Potential Sources			
Holtsville GT/LNG	13.5	9	0.67
Wadding River	7.5	3.3	0.44
Gershow Recycling	56	66	1.18
Northport Power	7.4	2.2	0.30
Narrows Generating	5.5	4.8	0.87
Con Ed 74th street	4	2.9	0.73
Con Ed East River	6.6	2.9	0.44
Ravenswood	1	5.2	5.20
Arthur Kill	3	2.8	0.93
Algonquin Gas	4.7	0*	0.00
Norlite	5.2	2.1	0.40
Bethlehem Energy	12.6	0*	0.00
Holcim Catskill	23	0.004	0.00
Intern. Paper-Ticonderoga	2.3	2.2	0.96
Lehigh Northeast Cement	48	58	1.21
Globe Metallurgical	17.4	18.3	1.05
Morton Salt	21.7	21.5	0.99
Lafarge Buildings	91	143	1.57
Nucor Steel	126	240	1.90
Independent Station	74	60	0.81
Brooklyn Navy Yard	NA	83	
Astoria Generating	NA	4.1	
Kodak Park Power	NA	13	
Total	**534**	**744.4**	

In addition to emission rates, normalized values with readily available design capacities for 2011 NEI data (actuals were not obtained for this purpose) were plotted to establish not only the likely Hg inconsistencies, but also the possible identification of the type of fuel use.

As in the 2009 data set, Hg vs. SO_2 or NOx emissions for all 18 EGUs did not reveal any practical relationships. However, there was a linear, but weak relationship between SO2 and NOx as would be expected (these plots are not presented). Some other plots are presented in Figures 4-3 and 4-4 with further information. During the review of facility data down to the emission unit basis, it became clear that while SO2 and NOx emissions for the facilities were associated with all combustion units, the same was not the case for Hg in situations where there were multiple units. Only a subset of these units contributed to the total Hg emissions – Figure 4-3 presents the plots of Hg against the facility total capacity and the capacity of units contributing to the Hg emissions. It is clear that neither plot reveals an expected relationship, but rather the reverse where emissions increased with lower capacities, possibly indicating the effects of other factors at lower loads. It is known that lower capacities facilities such as EGUs experience less efficient start up conditions and have larger initial emissions than normal operations.

Figure 4-3. Mercury emissions vs. total facility capacity (left) and only for units with Hg emissions (right) for all EGUs for 2011 data

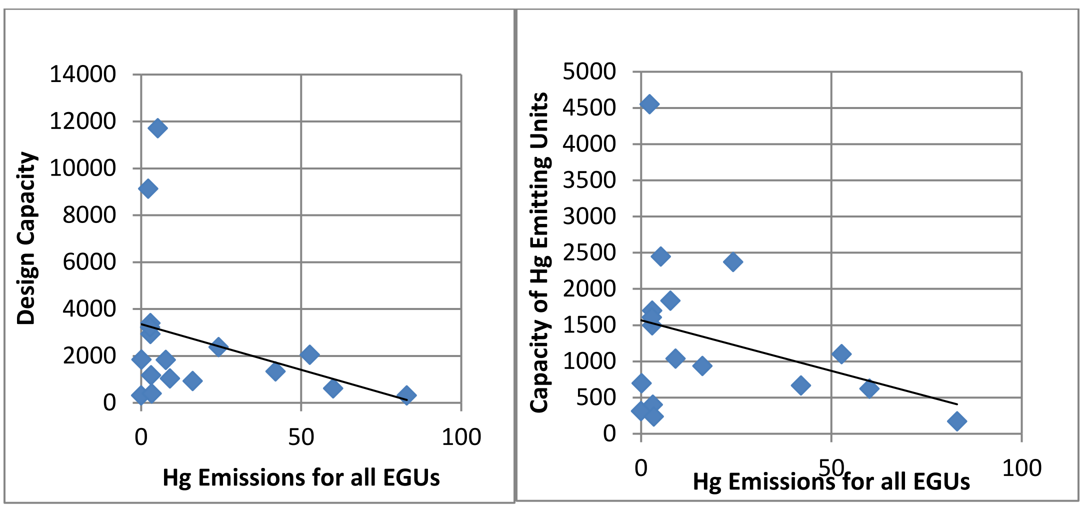

For the 17 EGUs, it was informative to look at the ratios of SO_2 to NOx and NH3 to NOx; the former providing possible information on dominant fuel type while the latter about either NH3 use or "slip" as an agent for the control of NOx. Figure 4-4 presents these plots. The facilities numbered 1 to 7 are the coal EGUs while the rest are the additional potentially large Hg oil and gas EGUs identified. As indicated previously in Table 4-3, the coal plants have large SO_2 emissions relative to NOx as expected (with one exception) while the rest have approximately the same or much lower SO_2 vs. NOx emissions. These additional EGUs were deemed dominated by oil or gas use, respectively, and this information was confirmed with further review. On the other hand, the NH3 to NOx ratios were variable, with three of the facilities not reporting any NH3 emissions (one of the these was coal EGU number 4), while the other two are not plotted. The other three coal EGUs with indistinguishable values near zero are in contrast to the relatively large values for the previous three, indicating either actual low NH3 emissions or reporting inconsistencies. For the other EGUs, the NH3 to NOx ratios do not show a pattern similar to the SO_2 to NOx ratios, indicating reporting issues or differences in the fact that certain newer facilities that had been reconfigured for gas use have imposed NH3 "slip" limits, which are more closely monitored and reported.

Figure 4-4. Ratios of SO2 to NOx and NH3 to NOx for the large Hg EGUs from Table 4-3 for the 2011 data

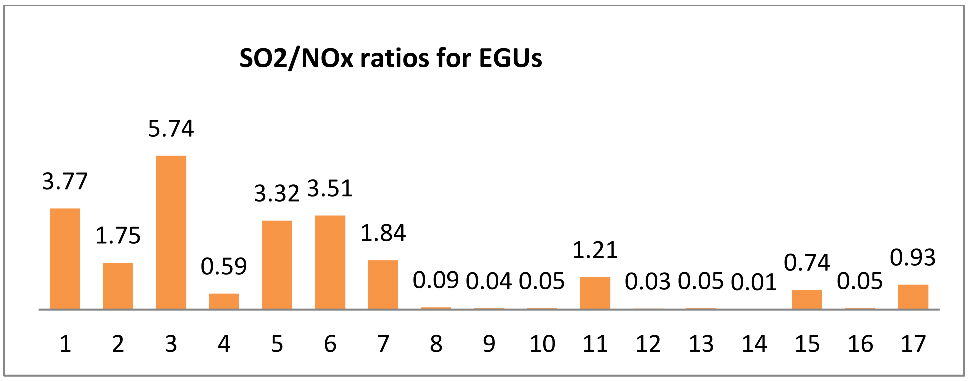

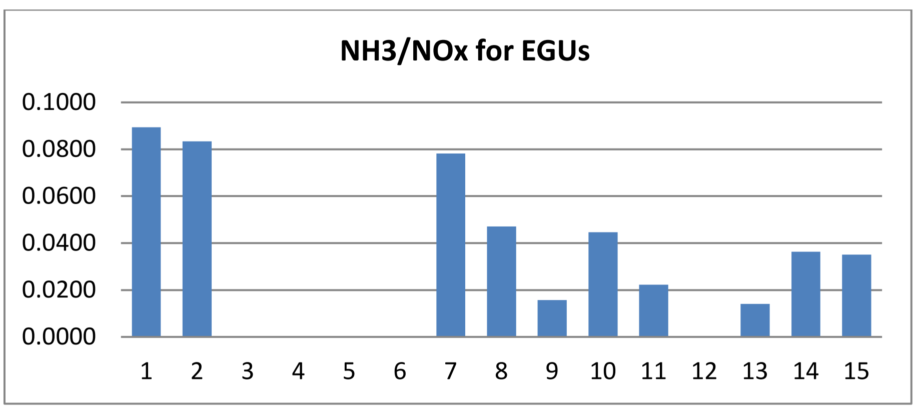

These preliminary findings on the potential set of large Hg point sources revealed the need to carefully review certain information available in DEC files and from the EPA. Again, the emphasis was on the Hg emission point sources since it was felt many of these had relatively less scrutiny in terms of assuring the emission rates from the regulatory standpoint, many not being covered by federal or DEC regulations. That is, a number of regulatory requirements have been in place for decades for the direct and indirect control of the acidic deposition precursors, at least SO_2 and NOx, and there are various reporting and monitoring requirements. That same level of reporting and verification is relatively low for the Hg emissions, except for coal EGUs, WTEs, and certain other individual facilities. However, for the modeling exercise, it is also necessary to assure that the stack parameters are proper, but, at times, these are either not fully verified or ever required to be reported. The 2011 NEI data set includes the stack parameters necessary for the modeling and these were included as part of the review process. Thus, our review also included the verification of the stack parameters to the practical extent possible based on readily available and obtainable information.

Data sets and reports that the DEC-DAR provided for the review of emission rates and stack parameters included: 1) annual emissions statement (ES); 2) compliance stack tests; 3) Relative Accuracy Test Audit (RATA) for coal EGUs; and 4) certain individual source data from the AFS. In addition, a subset of facilities was provided to the DAR Toxics Section for verification of the Hg emissions, which seemed clearly questionable. For the SO_2 and NOx emissions for the EGU sources, an additional check was made using the data in the EPA's Clean Air Markets Division's (CAMD) Program Data query site. It was important to obtain the emissions for the 2011 year modeled, but not all stack tests or available reports reflected that year. In addition, it was not necessary to check all information for the 37 facilities in the remaining set of potential large Hg sources for few reasons, including a) previously reviewed facilities such as WTEs for which Hg emissions were consistent over the years 2009–2011; b) low Hg emissions in the 2011 NEI (vs. 2010), which were attributes to facility shutdown or intermittent use; and c) known gas burning facilities whose permit modifications did not readily reflect the proper Hg emissions in the AFS data and similar simply verified conditions. In all, only 15 of the facilities were chosen to require a closer look and had the necessary 2011 emissions data in the requested information. A small number of this set also had many stack parameters either missing or were obviously incorrect and in need of resolution.

The data checks using the various available reports and information inquiries and their outcomes will be only summarized. The use of 2011 annual ES data essentially replicated what was in the 2011 NEI, with exceptions only for two EGUs for Hg emissions (Narrows, Arthur Kill) and one WTE (Covanta Niagara) for NH3 emissions. It should be noted that not all ES reviewed included NH3 data, specifically for other than EGU source type facilities. The replication of almost all of the emissions was as expected since the facility reported data is loaded by DAR to the AFS system, which then forms the basis of the NEI as reported by the states to the EPA. However, the check was made since differences between the two systems were noted previously. It also identified the potential issue of not having a complete NH3 data base for these facilities, with no readily available means of obtaining the information within the constraints of the study. Thus, the ES check step was not conclusive in resolving known errors that were clear on face value. The check of SO_2 and NOx data for the EGUs in the CAMD database also confirmed the information in the 2011 NEI within five percent for the subset of the source inquiries, except for one case. However, the exception was for a source with very small emissions and could also relate to the fact that not all units at this facility had to report emissions to the EPA. The confirmation of the SO_2 and NOx emissions was also as expected since this data is continuously stack monitored for these larger EGUs as required by the federal acid rain program.

The next check of compliance stack tests and RATA data was more productive, but had to be limited to eight facilities which had reports for 2011 readily available. These facilities were essentially WTEs and EGUs requiring regular testing. Inquiries indicated that there could be additional reports from the companies or from the DEC regional files for other years or tests, but no attempt was made to obtain similar data since it was not the aim of the study to verify every single data point associated with the study's set of point sources. As discussed below, there were other means by which Hg emissions and stack parameters were reviewed to assure that obvious incorrect data were modified. In terms of the stack test and RATA reports, only six provided Hg emissions data and corresponding stack parameters, while the other two provided SO_2 and NOx emissions. It is important to note that the test method used for Hg emissions reports only the vapor phased as required by the DEC regulations and could underestimate total emissions. This limit was judged to be not essential since gaseous Hg emissions are the larger of the species, as discussed later on speciation. Furthermore, the Hg stack concentrations during a set of "runs" varied by a factor of three in some cases, but are averages to determine the emission rate for regulatory compliance purposes.

This Hg variability could be important in some instances, but not likely for the long-term average deposition calculated for this study. The more important issue for the latter is the representativeness of such short-term tests for annual conditions. A similar question surfaces about the stack velocity and temperature during these tests conducted during high or maximum load conditions, while the deposition modeling relies on annual averages for these parameters. This difference was taken into consideration in judging the appropriate data to be used in the modeling; in the simple case where many of the stack data were not found in the 2011 NEI, the stack test results had to be used (e.g., Huntington RRF). The Hg data from the RATA reports was compared to the corresponding 2011 NEI data and good agreement found for four of the six facilities. The other two cases had one lower and one higher rate, which were incorporated in the data corrections.

While the above data checks were conducted, two additional data reviews were made by DAR staff independent of the research team. One group provided stack parameter and facility status information for five cases where there were large gaps in stack parameter data in the 2011 NEI, while staff from the Toxics Section reviewed the Hg emissions against information available to them, but not in the AFS system, as well as checks with regional permit staff on operations of a limited set of facilities with questionable data in the 2011 NEI. The results of the first group's checks were used to correct or populate the 2011 NEI data base. The corrections were rather significant in some instances, raising issues about the stack data for the other sources. The Hg emissions data for the set of facilities provided to the Toxics Section was reviewed along with other sources that were not necessarily large point sources, rather which fuel type information allowed for necessary modifications. These additional sources were smaller generation facilities with Title V or capped permits. This larger set contained 51 facilities for which the Hg emissions in the AFS were tabulated for comparison to the 2011 NEI data, but not all facility emissions could be reviewed for accuracy of Hg emissions.

The review was concentrated on the larger Hg emission sources, to checking the status of those with large reductions in emissions in the data from 2009 to 2011, and the EGUs burning oil or gas. The latter source type review was important from two standpoints; first, unlike the coal EGUs, these facilities were not previously scrutinized in any detail; and second, a report was available that provided sulfur and metal contents of oils and gas used in NYS. A study [53] conducted by NESCAUM for NYSERDA provided State specific data on the Hg content of both residual and distillate oils and contained valuable information on Hg content of gas throughout the world. It is common practice for facilities and regulatory agencies to rely on average emission factors provided by the EPA in their AP42 documentation.[54] The data is used in instances where more refined source specific or sector based emission factors are not available and is rated by quality and quantity. Since the data is used for regulatory purposes, such as permitting, it is also common practice by the EPA to provide conservative (higher) emission factors in many instances. It is known that very little data was available on oil and gas Hg emissions on which the EPA relied upon to generate its emission factors in AP42. Therefore, the NESCAUM report was used to determine more appropriate factors. For oil, it was noted that the data in NYS indicated Hg concentrations were 30 and seven times lower than the EPA factors for # 2 (residual) and #6 (distillate) oils, respectively. For gas burning, the difference was even larger. Data in the report indicate that the Hg concentration rages from 0.1 to 3000 ug/m^3, with the higher end representing untreated gas manly outside the U.S. Gas use in the U.S. is essentially treated to avoid corrosion of aluminum parts and other effects and for that gas, the concentration range was closer to the lower end. Although there is considerable variability even for treated gas, the factor the DEC used for gas units was from one of the references in the NESCAUM report. That concentration (0.2 ug/m^3) is 200 times lower than the EPA's, which is generally used by facilities and incorporated by states in their data systems.

The EGU plants in the set reviewed by the Toxics Section and burning gas and oil were adjusted by the factors previously discussed. It was noted that only three of the 14 facilities in the list had oil use and then mainly as either backup fuel or intermittent use as peaking units. The results of all adjustments to the Hg emission rates in the potential set of large Hg facilities are presented in Table 4-5. The table includes the 2010 AFS, 2011 NEI, the revised 2011 NEI for the study, and the ratio of the latter two data sets. The revisions seem to confirm that the level of previous review and scrutiny by DAR of the WTEs and coal EGUs has been productive in assuring a good data base, with only three cases in which the stack test data indicate a different Hg emission than in the 2011 NEI. Furthermore, for these two sectors, the total emissions in the 2011 NEI needed to be modified slightly in the context of all the changes. As expected, there was a major reduction in the Hg emissions from the mainly gas and backup oil burning EGUs. There is an order of magnitude reduction in the total emissions from 193.2 to 17.5 lb./yr. The 2011 NEI entries for Independent Station and Brooklyn Navy Yard were clearly in error and prompted the detailed review of this EGU sector. The total Hg emissions for the "other types" of large emitters was reduced about the same percentage as the coal EGUs due to revisions to about half of the facilities. However, it is important to note that for other half of these facilities, there was no practical alternative means of verifying the reported Hg values. For example, it was determined that the Hg emissions for Gershow Recycling was incorrectly reported as combustion related when, in fact, this facility only scraps the cars and any switches that might contain Hg are not processed in a way to release the mercury. On the other hand, Nucor does process switches in a way that could emit Hg, although it reported a lower value to the EPA than in Table 4-5. For consistency, the study used what was reported to DEC.

The total emissions in Table 4-5 for the three categories (WTEs, EGUs, and "other" sources) indicate that the decision to identify other than energy production point sources with high Hg emissions was productive. These "other" sources have about twice as much Hg emissions as the WTEs and EGUs combined and these emissions are dominated by the contribution from three sources. There is stack test data to confirm large Hg emissions from the Lafarge facility, while the other cement plant (Lehigh) and the auto scrap facility (Nucor) did not have readily available stack test data to confirm their estimates. Based on the revised Hg emissions, modified sets of facilities in the WTE, EGU, and "other" source categories were developed for CMAQ modeling. It was decided to retain four of the facilities with emissions below the 2 lb./yr cutoff used since the stack data corrections to these were already accomplished and also since three had emissions at or above a 1 lb./yr values used by the Toxics Section as a cutoff other purposes, while one (independence Station) with 0.3 lb./yr was the closest plant west of the Adirondacks. It is also important to note that, while a set of nine smaller facilities (with less than 2 lb./yr emissions in the 2011 NEI) reviewed by the Toxics Section were not included in our CMAQ tracking list, the corrected Hg emissions from this set was nonetheless modified and provided for SMOKE emissions processing. In addition, these smaller Hg emitters, especially the gas burning EGUs, are potential large sources of acidic deposition precursor NOx and were retained in the review of their stack parameters.

It is helpful to know the spatial distribution of this set of 38 original potential large Hg facilities contained in Table 4-5 and these are depicted in Figure 4-5. The location of the different types of sources is color coded and reveals that many of the facilities are adjacent to water sources, with the coal EGUs confined to the western part of NYS, while a large portion of the EGU plants serve the more populated NYC metropolitan and Long Island areas. There are only a few facilities near the Catskills and the Adirondacks, but these are located generally downwind of these areas based on annual wind direction frequencies for these locations. The category of “other” types of Hg point to sources distributed mostly along the Hudson River and in western NYS.

Based on the revisions to the Hg emissions, a modified final list of large Hg sources tracked in the CMAQ modeling was generated. There were 26 facilities left on the potential list of 38, with one of he WTEs (Oswego) and two of the coal EGUs (Westover and Niagara Generating) from the original list from the 2009 data set dropped due to very low corrected Hg emissions. This final set of facilities and their Hg emissions are presented in Table 4-6 and depicted in Figure 4-6. The table indicates that a large portion of the potential EGUs with gas/oil as fuel are no longer considered large Hg facilities for the study’s purposes, while a comparison of Figure 4-5 and 4-6 shows that many of these “eliminated” facilities are located in the NYS Metropolitan area, with gas usage as a reason for the reduction in emissions. The reduction in Hg emissions from the 12 gas/oil facilities in Table 4-6 is a factor of 11 and contributes significantly to the overall Hg reductions from the CMAQ “tracked” set of sources in NYS. The table reveals that the review process resulted in about 25 percent reduction in total Hg emissions.

Table 4-5. Hg emissions for potential set of large Hg facilities from 2010 AFS, 2011 NEI and the revised 2011 NEI for the study (* ratios inconsequential since emissions zero or very low)

Facility Name Hg summed for all unit)	Hg (lb./yr) 2010 AFS	Hg (lb./yr) 2011 NEI	Hg (lb./yr) Revised for study	Ratio Revised/2011 NEI
WTEs				
Hempstead RRF	21.1	24.1	24.3	1.0
Babylon RRF	11.5	2.7	2.7	1.0
Huntington RRF	5	4.4	**3.15(stack test)**	**0.7**
Islip-McCarthur RRF	5.4	1.5	1.54	1.0
Dutchess Co. RRF	9.7	6.3	6.26	1.0
Westchester RRF	9	27.4	27.4	1.0
Hudson Falls RRF	46	33.3	33.3	1.0
Onondaga Co. RRF	30.4	7.7	7.7	1.0
Covanta Niagara RRF	28	13	**17.5(stack test)**	**1.3**
Sub-total	**166.1**	**120.4**	**123.9**	
Coal EGUs				
Danskammer Generating	0.09	52.7	12	**0.2**
AES Westover	0.03	0.00004	0	**1.0***
AES Cayuga	28.6	33.5	33.2	1.0
AES Greenidge	3.1	3.1	3.1	1.0
Dunkirk Generating	82	16.1	**32 (stack test)**	**2.0**
Huntley Generating	83	42	42	1.0
AES Somerset	1.1	7.7	7.7	1.0
Sub-total	**197.9**	**155.1**	**130.0**	
Oil and Gas EGUs				
Holtsville GT/LNG	13.5	9	0.8	**0.1**
Wadding River	7.5	3.3	0.05	**0.0**
Northport Power	7.4	2.2	0.21	**0.1**
Narrows Generating	5.5	4.8	0.28	**0.1**
Con Ed 74th street	4	2.9	1.33	**0.5**
Con Ed East River	6.6	2.9	0.26	**0.1**
Ravenswood	1	5.2	0.38	**0.1**
Arthur Kill	3	2.8	0.22	**0.1**
Independent Station	74	60	0.29	**0.0**
Brooklyn Navy Yard	NA	83	0.24	**0.0**
Astoria Generating	NA	4.1	0.48	**0.1**
Kodak Park Power	NA	13	13	1.0
Sub-total	**122.5**	**193.2**	**17.5**	

Table 4-5 continued

Facility Name Hg summed for all unit)	Hg (lb./yr) 2010 AFS	Hg (lb./yr) 2011 NEI	Hg (lb./yr) Revised for study	Ratio Revised/2011 NEI
<u>**Other types of Sources**</u>				
Norlite	5.2	2.1	3.1	**1.5**
Holcim Catskill	23	0.004	0	**1.0***
Intern. Paper-Ticonderoga	2.3	2.2	1.37	**0.6**
Lehigh Northeast Cement	48	58	58	1.0
Globe Metallurgical	17.4	18.3	18.3	1.0
Morton Salt	21.7	21.5	21.5	1.0
Lafarge Buildings	91	143	143	1.0
Nucor Steel	126	240	239.9	1.0
Gershow Recycling	56	66	0.001	**0**
Sub-total	**390.6**	**551.4**	**485.2**	
Total	**877.1**	**1020.1**	**756.6**	

Figure 4-5. Location of Potential Large Point Sources in NY based on 2011 NEI data

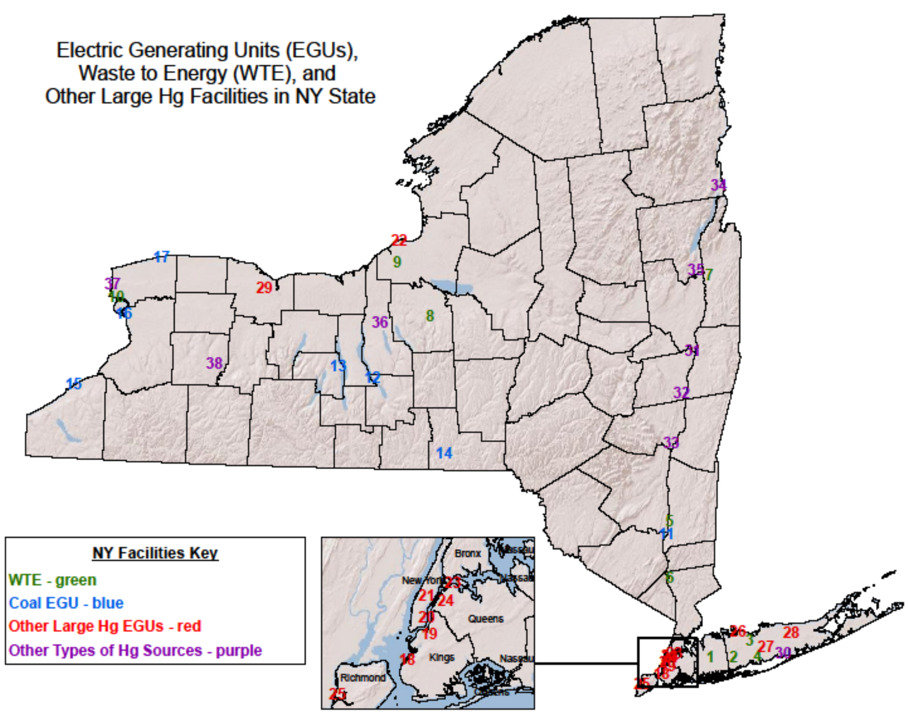

Figure 4-6. Locations of the Final Set of Large Hg Sources in NY for CMAQ Tracking

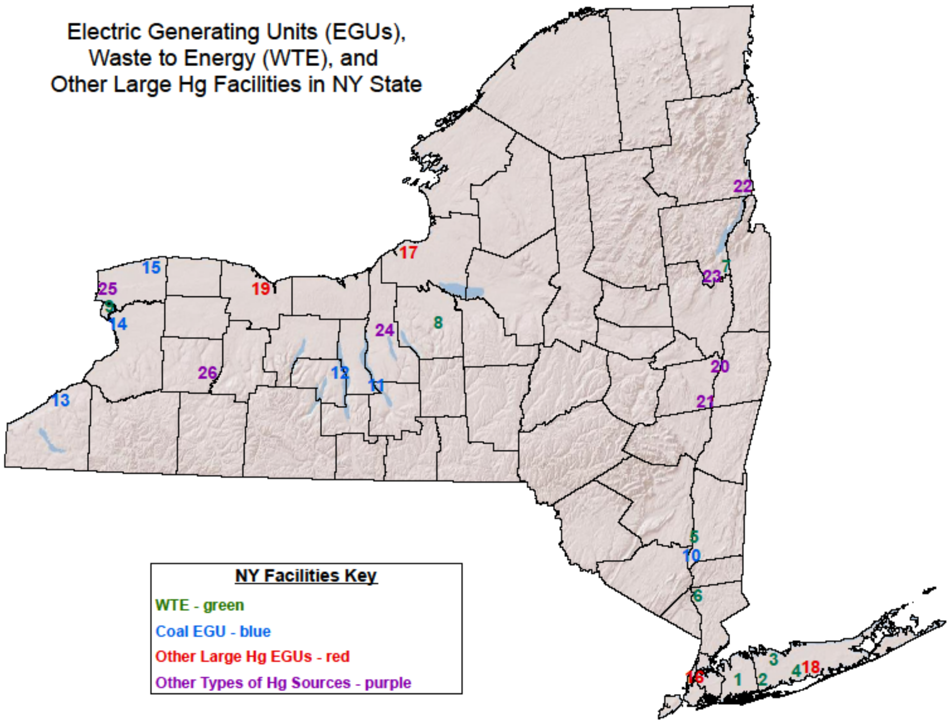

Table 4-6. Final Set of 26 Large Hg Point Sources Tracked in CMAQ Modeling

	FINAL SET OF FACILITIES WITH HG EMISSIONS FOR CMAQ TRACKING	
	Facility name	**Revised Hg For 2011 NEI**
	Waste To Energy (WTEs)	
1	HEMPSTEAD RESOURCE RECOVERY FACILITY	24.3
2	BABYLON RESOURCE RECOVERY FACILITY	2.7
3	HUNTINGTON RESOURCE RECOVERY FACILITY	3.2
4	ISLIP MCARTHUR RESOURCE RECOVERY FACIL	1.5
5	DUTCHESS CO RESOURCE RECOVERY FACILITY	6.3
6	WHEELABRATOR WESTCHESTER LP	27.4
7	WHEELABRATOR HUDSON FALLS	33.3
8	ONONDAGA CO RESOURCE RECOVERY FACILITY	7.7
9	COVANTA NIAGARA LP	17.5
	Subtotal	**123.9**
	Energy Generating Units (Coal EGUs)	
10	DANSKAMMER GENERATING STATION	12.0
11	AES CAYUGA	33.2
12	AES GREENIDGE LLC	3.1
13	DUNKIRK STEAM GENERATING STATION	32.0
14	HUNTLEY STEAM GENERATING STATION	42.0
15	AES SOMERSET LLC	7.7
	Subtotal	**130.0**
	Additional Hg EGUs (gas/oil)	
16	CON ED-74TH STREET STATION	1.3
17	INDEPENDENCE STATION	0.3
18	HOLTSVILLE GT FACILITY	0.9
19	KODAK PARK POWER DIVISION	13.0
	Subtotal	**15.5**
	"Other" large Hg Facilities	
20	NORLITE CORP	3.1
21	LAFARGE BUILDING MATERIALS INC	143.0
22	INTERNATIONAL PAPER TICONDEROGA MILL	1.4
23	LEHIGH NORTHEAST CEMENT COMPANY	58.0
24	NUCOR STEEL AUBURN INC	240.0
25	GLOBE METALLURGICAL INC	18.3
26	MORTON SALT DIVISION	21.5
	Subtotal	**485.3**
	Total Emissions	**754.7**

Although the review process did not answer all questions on the individual sources in the final set, it is important to recognize that this level of effort is essentially all that is practically achievable in the review of large set of source specific information. Other information such as emissions factors in EPA's AP-42 can be used as a further step in the review, but these factors are average and by design, conservative. The EPA document recognizes the preference for source or category specific data when available. Such category level data from mercury testing at a large set of coal EGUs have been established by the EPA for the gaseous and particulate forms, and that information is used in concert with other data, in the discussions of Hg specific percentages assigned to source categories. However, source specific data is still preferred. Another source of such information at the facility level was identified as the EPA Toxics Release Inventory (TRI), which each facility must report to the EPA. The TRI contains all emissions of a set of toxic contaminants including point and fugitive emissions. Thus, it could establish an upper limit to the Hg emissions for the facilities under review. Before requesting the TRI data for all 26 facilities, it was found that the total Hg emissions reported for 2013 (nearest year to 2011 readily available) from the EGU sector in NYS was 15 percent of the sum for the facilities' reported data in Table 4-5 (348 lb./yr) and was one-third of the corrected value in that Table (147.5 lb./yr). It is highly unlikely that differences in the years compared could explain such a large discrepancy. Thus, it was decided not to pursue obtaining the facility level TRI information for our purposes.

The total Hg emissions for the set of facilities in Table 4-5 with revisions had to be distributed to the individual units that emitted Hg in the 2011 NEI data. For facilities with single or identical multi-units, the task was simply to distribute the total emissions equally. For facilities where Hg emissions from different types of coded units with varying emission rates, the equitable approach was to distribute the revised Hg to these units in proportion to the unrevised emission percentages of the units. However, in cases where individual unit stack test data was available (e.g., Dunkirk), the modifications reflected the proper values.

The set of large Hg sources in Table 4-6 were included in the acidic deposition modeling, but the types of facilities tracked was expanded to include all point source (i.e., Title V) EGUs in NYS regardless of their size or Hg emissions (i.e., Table 4-5). That is, for acidic deposition the three types of sources included in the tracked set for CMAQ modeling were: 1) EGUs; 2) combined WTEs plus "other" sources in Table 4-5; and 3) all point sources in NYS. The rationale to include the third set will be clarified below in discussing the total 2011 NEI acidic deposition precursor emissions. The emissions from WTEs and "other" sources were combined with EGUs since the emissions of SO_2 and NOx from the former categories were about one and 19 percent of the corresponding NY EGU emissions and these are not expected to have large contribution to the projected deposition as individual sectors. The acidic deposition precursor SO_2 and NOx emissions for the EGUs were noted previously to be well documented as far as the 2011 NEI values, with minor exceptions. There were NH3 emissions estimates in the 2011 NEI for almost all of the EGUs in Table 4-5, but an independent verification of all the data could not be made.

The next step in the review process was for the stack parameters for the set of potential large point sources, which was undertake concurrent with the emission rate review. Thus, data review occurred for some of the initial set of potential large Hg facilities that were eventually dropped from the CMAQ tracking list. However, any corrections to these data only helped the improvement of the inventory for the acidic deposition modeling. The stack parameters used in a modeling analysis include stack height, diameter, velocity, temperature, and location. In the 2011 NEI the flow rate is also included in the data and is used when available or calculated from the stack velocity and diameter. Unfortunately, not all of these parameters are required to be reported by the Title V program and, as such, there is missing information for even these larger facilities in the DAR AFS system and the 2011 NEI. Specifically, although stack temperature and velocity are optional reporting parameters, there were data entries for these parameters in the NEI as a result of source specific permitting and other regulatory requirements. In addition, for a small set of the facilities in Table 4-5 (mostly EGUs), relatively recent permit modeling data was readily available and was accessed for the review process. These were in addition to the data found in the review of the stack test and RATA reports.

Nonetheless, in very few instances essentially no stack data were available and DAR staff provided the necessary information. The stack diameter and velocity or the flow rate are used in combination with the temperature to calculate the plume rise out of the stack, which is then added to the actual stack height to determine the layer of the atmosphere in which the effective plume will be transported and dispersed in the CMAQ model. Thus, these parameters must at least be reasonably representative of the type of source reviewed. One means to check this reasonableness is to perform simple engineering calculations as described in DAR's guidance[55] on source data verification. For example, the relationship between flow rate (V) and exit velocity (v_s) and stack cross sectional area was used: $V=\pi R^2 * v_s$, where R is the radius of the stack. In some instances, where the flow rate and exit velocity were both missing and the design capacity was given, the flow rate was calculated with the use of combustion F factors given in DAR document. It should be noted that in addition to the manual checks made of the flow rates, there is another level of check made in the SMOKE processor whereby any inconsistent or missing data is then replaced with a "default" value. Of course, a proper representation of facility specific information is preferred, including stack parameter data.

With respect to the stack locations, the data in the 2011 NEI is in longitude and latitude and these values were checked using Google Earth maps, augmented in few cases by USGS's mapping site. Where a stack was found on the facility property, it longitude/latitude was used if it was different from the NEI data base. It is to be noted that for regional modeling exercises such as in the present study, the correct location of the facility is adequate given the large transport distances involved. Although more than half of the locations for the 38 facilities in Table 4-5 were modified, these changes were not substantial for the current modeling purposes. The largest difference found in facility location was about 1km, but in vast majority of cases the differences were less than 100m. Any location changes were assigned to all units at the facility regardless of the distribution of stacks on the property.

The verification of other stack parameters resulted in changes ranging from major corrections, including missing data substitution and clearly erroneous information, to minor alterations of the data. An example was a consistent error found for flow rates, but fortunately both a simple equation to fix these errors and the SMOKE program's check rendered these errors less problematic. The other parameters were either fixed or filled in were the stack temperature and velocity, which was not surprising since these are not required to be provided by facilities. Only few stack heights and diameters were found to be in need of significant changes, but roughly one-third of the set of stack parameters for the 157 units at the 38 facilities were in need of correction. As noted above, not all of these changes were based on source specific information and, thus, not down to the unit specific level. In instances where multiple units of the same process code were present, missing data was substituted from information for units with data. In addition, certain of these units were clearly not a source of Hg and were not scrutinized as carefully for the stack parameters. All of the changes were provided to DAR staff in charge of SMOKE processing to replace the corresponding 2011 NEI data.

4.2 Identification and basic review of other potential sources of Hg emissions in the 2011 NEI

The process of identifying, reviewing and verifying emissions and stack parameters from the larger point sources was important, but influenced by various practical limitations. However, an attempt was also made to ensure that the inventory did not miss potential other major source sectors that have been identified in other studies and inventories. It was necessary to also consider the fact that for our 2011 “base case” year, inventory, and source categories such as steel production and aluminum reduction were no longer as prominent in NYS as in the past. There are also no large smelter operations in NYS, which have been previously identifies as another large source of Hg, while our inventory includes two remaining cement plants. Previous studies have also identified or inferred two other source types which were associate with at least large observed concentrations of Hg deviations from the mean.

The first was wood/biomass burning was identified as a possible source in wet deposition in Underhill by a study[56] using potassium (K) as a marker and back trajectories of air mass transport. It was inferred that significant biomass burning and use as fertilizer in the Northeast could be a source of observed Hg. The issue for our study was whether there are individual large Hg wood burning sources which our inventory search did not find or are wood burning emissions relatively small in NYS and are part of the area source emissions. The level of Hg concentrations in wood chips and pellets were analyzed previously by NESCAUM in a study for NYSERDA[57] in which the levels of Hg were the lowest of the elements analyzed and five orders of magnitude less than K concentrations. The emission factor for Hg from this analysis was essentially what was found for wood combustion in boilers in a study,[58] which noted higher ambient levels of oxidized Hg in areas of such combustion. Although large scale and area wide wood burning could be a source of ambient Hg, the emissions from individual source are likely of small magnitude and part of the area source category.

The other potential sources of Hg inferred by researchers[59] as contributing to at least the generation of the oxidized form of Hg from its elemental form were mobile sources. Although this sector would not be included in our CMAQ tracking, it raised the issue of possible direct emissions of mercury from the mobile sector. The emissions of Hg from various source types were updated in a NESCAUM inventory report[60] prepared for Massachusetts DEP. The study concluded that Hg emissions from the mobile sector were minimal, even as an upper estimate.

It is instructive to look at the relative contributions of our major source emissions for both Hg and acidic deposition precursors within the context of other source categories as well as total NYS and modeling domain emissions in the 2011 NEI. This step could also help determine what percentage of total point sources are represented by the CMAQ tracking list. Table 4-7 presents the various source sectors and regions, which contribute to the acidic deposition precursors and Hg emissions. It is important to note that in this as well as in many of the other emissions tables, the representation of the emissions down to the pound or a tenth of a pound are merely the results of calculations, such as from the SMOKE processor, and do not reflect data precision, as is clear from the discussions of uncertainties in even the larger sources. As noted previously, the sets of large NYS emitters for the two different deposition have categories in common, but are not the same. For Hg, the set is as described previously: list of 26 WTEs, large Hg emission coal EGUs and "other" large Hg sources, while for acidic deposition the set is: all EGUs, combined with WTEs and "others" sources from the Hg list. The difference in the sets recognize that the set of EGUs tracked for Hg purposes represents only a portion of the acidic deposition precursor emissions.

Table 4-7. Anthropogenic emissions summaries from 2011 NEI for mercury and acid deposition precursors (* means 96 percent of NH3 emissions in NY are agricultural sources)

Pollutant → Source Category ↓	**SO2 (TPY)**	**NOx (TPY)**	**NH3 (TPY)**	**Pollutant → Source Category ↓**	**Mercury (lb./year)**
All Point Sources in NY (includes Oil & Gas-NOx)	66,559	61,714	2,296	All Point Sources in NY	816
All EGUs in NYS	41,344	26,755	1,370	NY WTEs in list CMAQ	123.9
NY EGUs in 26 Hg Source list	37,043	17,393	697	NY EGUs in CMAQ list	145.5
NY WTEs and "other" sources in CMAQ list	440	4,660	287	NY "other" large Hg sources in CMAQ list	485.3
Study sources (all NY EGU, plus WTEs and "others") as percent of point sources	62.8%	50.9%	72.2%	Study source emissions (list of 26 NY sources) as % of point sources	92.5%
Area Sources in NY (e.g., oil & gas, RWC, agriclt.)	43,046	[illegible]	44,589*	Area Sources in NY	1130
Mobile Sources in NY	1,439	160,472	4,573	Mobile Sources in NY	NA
All NY Anthropogenic Emissions	114,852	386,743	51,569	All NY Anthropogenic Emissions	1942
Rest of domain emissions	795,727	2,042,566	208,234	Rest of domain emissions	12,088
Rest of states in 2011 NEI Inventory domain	1,537,805	2,341,052	325,468	Rest of states in 2011 NEI Inventory domain	19,753

Table 4-7 data shows that for Hg, the identified major point source categories essentially make up all the NY point source sector emissions (92.5 percent). This is reassuring and allows the identification of the point source contributions to the Hg deposition due to NYS sources. On the other hand, for acidic deposition, the sources make up from 50 to 72 percent of all NYS source emissions for the three precursors. However, the emissions from the large Hg coal EGUs relative to emissions from all NYS EGUs are 90, 65, and 60 percent for SO_2, NOx, and NH3, respectively. Thus, tracking all NYS EGUs for acidic deposition also reflects the coal EGU contributions to a large extent. For the other source categories, it is seen that there are no Hg emissions in the NEI for mobile sources, but this category dominates NOx emissions from NYS sources. For the area sources, the acidic precursors are on par with the point sources, except for the dominance of agricultural emissions for NH3, none of which is surprising. On the other hand, the relatively large area source emissions for Hg, a factor of about 1.4 higher than point source emissions, was further investigated.

It was decided to determine if any specific area source categories dominated these emissions. A scan of the 2011 NEI indicated that three source types essentially controlled the total area source emissions: 1) residential fuel use at 450 lb./yr; 2) scrap metal works at 300 lb./yr; and 3) crematories at 143 lb./yr. The latter was essentially at the level of the WTEs emissions, while the scrap metal category was at the level of the single scrap metal point source in Table 5 (Nucor). Area source emissions in the 2011 NEI are only presented as county level sums, thus, no further resolution of source contributions to these categories was pursued. It was further determined that for both the scrap metal and crematory emissions, the largest three contributing counties were in the NYC and Long Island areas, with 10 percent contribution from each country to these categories. No further review of these two source categories' emissions was conducted.

On the other hand, it was recognized that the residential fuel use category can be refined based on the data discussed previously provided in the NESCAUM studyon oil Hg content in NYS. The concentrations of Hg in both residual and distillate oils were noted to be well below the factors in the EPA's AP42 that forms the basis of the NYS74 2011 NEI. A check of the NEI indicated that residential fuel use was confined to the distillate fuel category, which is not surprising given the continued reduction of sulfur content in fuel due to regulatory actions and refining of the fuels. In addition, residential fuel use has been preferentially of the distillate type in NYS. Thus, we applied the factor from the NESCAUM study of seven for distillate fuel use vs. EPA AP-42 emission factor to reduce the Hg emissions for this area source category. The result was a total Hg emission of 64.3 lb./yr. The reduction factor was used to adjust all counties in which that source category emissions were found. This adjustment resulted in total area source Hg emissions in NY of 742.3lb./yr, which was now less than the total point source value by 11 percent.

It was also informative to provide two other aspects of the total point source facilities. First, Figure 4-7 shows the location of all EGUs in the NYS and in the modeling domains. It indicates the lack of EGUs in the immediate western "upwind" vicinity of the Adirondacks and Catskills and shows the preponderance of these large point sources in the NYC/Long Island area and in Pennsylvania. However, the corresponding level of emissions is not discerned from the figure.

Figure 4-7. Location of EGUs in the CMAQ modeling domain

The second item to note is from a 2011 EPA emission inventory[61] memorandum for Hg emissions. The data is replicated in Table 4-8, which shows the dominance of EGUs in Hg emissions even in the projected 2016 year.

Table 4-8. Anthropogenic Hg emissions and projections in the U.S. from the EPA

Category	2005 Mercury(tons)	2016 Base Mercury (tons)
Electric Generating Units	53	27
Portland Cement Manufacturing	7.5	1.1
Stainless and Non-stainless Steel Manuf.: Electric Arc Furnaces	7.0	4.6
Industrial, Commercial, Institutional Boilers & Process Heaters	6.4	4.6
Chemical Manufacturing	3.3	3.3
Hazardous Waste Incineration	3.2	2.1
Mercury Cell Chlor-Alkali Plants	3.1	0.3
Gold Mining	2.5	0.7
Municipal Waste Combustors	2.3	2.3
Sum of other source categories (each emits less than 2 tons)	17	16
Total	**105**	**62**

4.3 Mercury speciation for point sources emissions for CMAQ deposition assessment

An important consideration in the deposition modeling for Hg was the issue of whether speciation of mercury into its known gaseous and particulate forms was necessary. The predicted deposition estimates in many studies, including the current one, are meant to determine the total loading of mercury on the earth surface and its eventual uptake into the water bodies containing fish. In addition, Hg ambient concentrations from various parts of the U.S. show the clear dominance of the elemental form that makes up over 95 percent of the observed levels. However, for the specific purposes of deposition estimate, the assignment of mercury species to various source types becomes important from at least two standpoints. First, limited stack test data have shown that the emissions from important source categories such as EGUs and WTEs are more evenly distributed between the elemental and oxidized forms. This, coupled with the fact that the deposition of elemental mercury has been predicted and confirmed to be rather low from both dry and wet deposition pathways relative to the considerably larger rates for the oxidized form, makes it necessary to consider the level of these specific distributions for at least the larger Hg point sources.

Furthermore, this speciation becomes more important within the context of the refined grid used in the current study whereby relatively localized impacts can be identified. In more large scale and global modeling assessments,[62] the forcing of this speciation to the elemental component to achieve better model performance might be acceptable, but for the current purposes the conversion process of the various species is confined to the chemical transformations in CMAQ. The model equations contain a large set of gaseous and aquatic conversions from elemental to the oxidized form and the reverse. Thus, any indirect deposition of the elemental form of Hg, as it converts to the oxidized form in the modeling, is controlled by these set of transformations.

We have assigned a percentage for the three species of mercury to the three main categories of sources tracked in CMAQ using available data from the EPA, the literature and facility specific data in one case. Some of the data were developed for EPA regulatory purposes, especially for mercury controls, while others were not used on such broad scale. The data are not comprehensive, but have been used in regional modeling of mercury by the EPA for their technical support documents for regulations and by other entities for specific regions, such as by NESCAUM for the Northeast states. It should be noted that most of the more complete data available represent facility testing from over a decade ago, but it is still used as the basis for more recent regulations and modeling assessments. These data show considerable variability even within sector based results, but for our regional modeling purposes, the averages used are deemed appropriate. Source specific results for the facilities in the CMAQ tracking list in NYS are preferred for speciation, but only one such data set was found to be more recent than the coal plant data relied upon by the EPA for their regulatory applications. Most source specific testing for regulation such as the RATA test noted previously for the DEC's Part 246 and similar purposes only provide total vapor form Hg emissions.

It was noted that past and recent EPA regulatory use of Hg speciation data relied on information collected from certain source categories during the original assessments for mercury. Thus, it was decided to review other data sets and reports that had specifically addressed the issue of Hg speciation from the set of major emitters determined important for CMAQ tracking in the study. This review was not comprehensive, but did provided adequate information to best choose the speciation profiles for the three species for at least the main point sources for the study. A summary of the data for

Hg speciation found is presented in Table 4-9. The Hg forms are elemental-Hg0, gaseous oxidized-Hg2 and particulate-HgP. At face value, it might appear that there is considerable information on speciation, but the large number of entries is somewhat misleading. Many of these reports and studies have relied on limited stack testing data or mainly EPA data for coal EGUs and WTEs and even less data for the "other" categories. A quick discussion of the data sets will clarify the limitation.

Table 4-9. Mercury speciation data for the three categories of point sources in CMAQ

Study/Data Source	Coal burning (EGUs)			WTEs			"others" (e.g., cement plants)			Comment
	Hg0	Hg2	HgP	Hg0	Hg2	HgP	Hg0	Hg2	HgP	
Walcek, et. al (2003) EPA NTI, 1996	50	30	20*	20	60	20	80	10	10	EGU data included oil burners, coal ICBs.
EPA CAMR Inventory Hg Speciation (2005)	Source specific assignments			22	58	20	50 80	30 10	20 or 10	EGU oil plants used 50/30/20 breakdown.
Edgerton, et. al.(2006) EPA 1999 ICR and EPRI	62 78	37 20	1.5 2.0	NA			NA			Average data for three coal plants, bituminous coal &ESP.
NESCAUM, Oct. 2007 EPA 2002, except coal	66	29	4	22	58	20	80	10	10	For EGUs on oil, used EPA 50/30/20 factors.
Baker and Bash (2012) Used EPA 2005 NEI data (11/14/11 EPA memo)	57	40	3.0	NA			64	23	13	Non-EGU area source values essentially same as "other" point.
Gustin et. al. (2012). EPA 2002 NEI, except Florida coal EGU 2009 data	40	58	2.0	24	57	19	NA			Individual facilities from FLDEP for coal burning EGUs.
	(oil burning facilities had 50/30/20 split)									
EPA 2011 NEI and MATS rule (the 12/1/11 memo references 11/14/11 data)	66.3	29.5	4.2	NA			NA			Same emissions testing as for CAMR. Averages only, see text.
	Ranges (15-97), (2 -82), and (.04-42)									
Two Reports on Cement Plant Testing (2007, 2008)	NA			NA			31 >93	60 <7	8 <1	Ash Grove facility. Four sources (see text)

There is no specific order to the table entries, but one of the earliest attempts to assign species of Hg to emissions in the eastern half of the country started with the EPA's 1996 data as reported through the National Toxics Inventory. The reported percentages for the three source categories are presented in the first row of Table 4-9. The asterisk is to note that the authors also reported more recent stack test data at the time indicated that the particulate form of mercury was found to be considerable lower at about one percent for coal EGUs. The second entry is the original mercury speciation assessment on which a number of subsequent regulatory actions followed. It reflect the work performed for the Clean Air Mercury Rule (CAMR)[63] in which the EPA augmented data developed for the CAIR rule with stack test and projected category specific mercury data for the large set of sources in the 2001 NEI. The mercury speciation was based on data collected from specific coal burning facilities as part of the 1999 NEI, subsequently augmented in July, 2003. Since a large enough data base was available, the stack test data were segregated in bins reflection type of coal, controls, and type of combustion process and then assigned to individual plants in the inventory. For WTEs, the EPA 1999 inventory was replaced by more facility specific data and projections from the 2002 NEI. The speciation is given in Table 4-9 and indicates a significant variation from the values used for other categories. For other point source, a combination of data and projections were used to assign mercury species to the large set of categories. These are listed in Appendices B1 and B2 of the EPA report. For our purposes, it is noted that the oil burning facilities were assigned a 50/30/20 breakdown which as the "default" set used where no information was available. The same values were used for other source types such as internal combustion boilers and turbines. On the other hand, other point and area source categories were assigned an 80/10/10 breakdown. It was also noted that for Portland cement, a 75/13/12 speciation was used.

The third row entry in Table 4-9 reports data from a study[64] of three coal EGUs in the Southeast where stack test data reported to the EPA based on statistical projected speciation were compared to observed levels of Hg species in the vicinity of the plants. The EPA data was the result of 1999 information collection request (ICR) from a large set of coal burning facilities. The average percentages for the three facilities are provided on the top of the row, while the average across all bituminous coal facilities with electro-static precipitation (ESP) are at the bottom of the table entry. The data indicate variability in speciation even with the same type of coal use and controls. The next data set presents the results of a detailed review and modeling conducted by NESCAUM[65] for the northeast states in response to New England Governors and Eastern Canadian Premiers (NEG-ECP) 1998 Mercury Action Plan (MAP). The Hg speciation used by the study was essentially based on the EPA's data from the 1999 ICR and the 2002NEI, except for reassessment of the speciation for coal plants through the SMOKE processor. These speciation profiles were found to replicate the data from the EPA's set for the 2005 Clean Air Mercury Rule CAMR) assessment, which was not surprising. The NESCAUM report presents speciation breakdowns for other Hg source sectors, with EGUs using oil or gas at 50/30/20 breakdown, while for "other" source types the data was representative of cement plants and other point sources.

The data entry from the EPA's 2005 NEI was used in the technical support document for the Clean Air Mercury Rule (CAMR) and subsequently for the Mercury and Toxics Standards (MATS) rule. In addition, the referenced modeling assessment[66] for the country was performed by the EPA staff using CMAQ and another regional model for comparison purposes. The entry from the modeling study for WTEs is omitted since only "non-EGU point source" data was used, while WTE data is known to have a more distinct profile. Again, the basis of the 2005 NEI speciation was statistical reassessment of the data used in the previous NEI from 69 coal plant tested, as described in an EPA staff memo.[67] The profile has been used in other recent regional and global modeling studies.

The sixth row of data reported in Table 4-9 is from a study[vii] for Florida facilities that used information provided by the FLDEP for two coal plants for 2009, while for other sectors the EPA 2002 NEI data base was used. Although the data is rather limited, it confirms the variability that can occur for speciation of the elemental vs. the oxidized forms of mercury. The next row entry in the table reflecting only coal plants data is from the EPA final rule documentation for the Mercury and Toxics Standards (MATS).[68] However, the data for this rule comes from the previously generated statistical data base used for the CAMR rule, even though the EPA revised data on total mercury emissions using a 2010 ICR for coal and oil EGUs. The entry is provided to show the averages calculated for the three species using the EPA raw data table and the very large ranges these averages represent.

In addition to coal burning EGU facility tests, there have been other sectors tested for mercury emissions. For the study purposes, possible speciation tests for the two source categories in Table 4-6 with the higher Hg emissions were reviewed; that is, cement plants and scrap/steel processing. In one study from 2007, the EPA reported on testing at eight electric arc furnaces for use in steel/scrap iron source control regulations. However, these tests only reported total Hg emissions and were not useful for our speciation purposes. In the case of cement plants, in 2006 the EPA considered control regulations which prompted testing of a handful of facilities. Two of these tests were available to the DAR's Toxics Section and indicated varied results. For the Ashe Grove facility entry in Table 4-9, a set of tests in two separate months resulted in the average speciation profile shown, wherein the oxidized species dominated the emissions.[69] The values in the table represent the weighted average of the results for raw mill "on" for 85 percent and "off" 15 percent of the time. On the other hand, data reported by the Portland Cement Association (PCA)[70] for four facilities in three states indicated the clear dominance of the elemental form of Hg during both mill on and off conditions. The Table 4-9 entries from these tests provide percentage limitations since a number of data errors were noted in the report, rendering the determination of averages unstable.

As noted previously, if source specific data on Hg species were available, these would be generally preferred over sector averages and other emission factors. However, for our modeling purposes, such data must also be representative of the NYS source operations and conditions similar to the 2011 NEI period. To our knowledge, more recent speciated Hg data than those used to develop the averages for the early CAMR period are not available for the New York large Hg sources, except for the LaFarge plant that has information from 2008 stack tests. The test indicated a 98.7/1.3/0.1 percentage breakdown for Hg0, Hg2, and HgP averaged over three tests and these values were used for this facility in the modeling. For the rest of the sources, it was determined that the use of average values per sector were appropriate, given both the lack of source specific data, as well as the large variability in available data. Thus, although two of the NYS coal facilities (Cayuga and Dunkirk) had data from 1999 that were included in the EPA data tables, it was more prudent to use the robust averages for these plants as well due to the limited and dated data specific to these plants and the nature of the modeling conducted for this study. In addition, although cement plant sector test data were found for the period 2006–2007, these were deemed divergent and not representative for the only other cement facility (Lehigh) in the large Hg list.

Table 4-9 values for the three sectors were reviewed and the determination made that the most appropriate averages to use for the coal EGU values were the EPA MATS /NESCAUM (essentially based on the 2002 NEI data), while for the WTEs and "others" category, the limited test data from the EPA during the same era and which were used by NESCAUM and other studies were adopted for our study. Thus, the percentages in the NESCAUM row of Table 4-9 were used, with the understanding that other variable percentages for the cement plants have been reported. In addition, it is recognized that a 50/30/20 breakdown was reported in some of the studies referencing EPA data for oil EGUs, while the EPA MATS memo provides a 57/40/3 percent breakdown for all EGUs. However, no distinction was made for the oil/gas units as far as the Hg speciation in our modeling, given the relatively small Hg emissions from the small set of these particular EGUs. Again, given the purpose of the study and the limited and variable data reported within even the same sectors, the use of the chosen averages was deemed more than adequate for the regional modeling study.

In addition to assigning Hg speciation to the source categories tracked for our purposes, the rest of the sources were assumed to have the profiles as these appeared in the EPA 2011 NEI. This included sources both inside and outside of the modeling domain, with the latter being modeled as boundary conditions from the 12km EPA grid. It was noted that while the speciation for the WTEs in these regions were the same as the values in Table 4-9 used for the NYS sources, the corresponding sets for the EGUs ranged from the source specific data for the coal plants to the default 50/30/20 breakdown. No other modifications were made to any other sources than as described in this section.

4.4 Future scenario using the EPA 2018 emissions inventory and the effects on the New York subset of sources

In addition to determining the contribution of the subset of large NYS emitting sources to both mercury and acidic deposition levels using the 2011 NEI, the study also considered potential future levels of the relative impacts of reduced emissions using an inventory available for the year 2018. As noted in the previous section, the EPA officially revised the year of the future inventory for regulatory modeling assessments due to revised regulatory timeframes imposed by court actions. Both inventories, however, were developed mainly to test consequences of expected future reductions of emissions on Ozone levels and are within the 2011 NEI "version 6.2 platform." The details of how emissions from a set of source categories for both years developed are presented in the EPA Technical Support Document (TSD).[71] Since the main purpose of these NEIs were for Ozone standards compliance demonstrations purposes, the EPA only focused on data for only six HAPS that did not include mercury. In order to model mercury, DEC staff had to extract the information for the 2011 NEI from supplemented data files.

However, it was clear from a basic review of the 2017 and 2018 versions of the NEI that limited, if any, data for mercury was developed by the EPA or the states. Therefore, the study proposal was to only consider the impacts of future emissions in for acidic deposition, but for mercury impacts, the study would only qualify the relative impact from the change in mercury emissions from the set of large Hg emitters developed for the base case modeling for the 2011 NEI. Data reviewed from the 2017 and 2018 NEI for the set of these large NYS Hg emitters confirmed the limitations of the data, but also pointed to other issues which needed to be corrected for these sources. In sum, the review confirmed the decision to limit the future scenario modeling for mercury to only the relative impacts from the energy production sources, with added adjustments based on information provided by the DEC.

The EPA TSD details the steps taken to adjust the 2011 NEI and the use of the 2018 data to project the 2017 NEI. These inventories generally account for expected reductions in emissions of pertinent pollutants resulting from regulations, either on the books or expected to take effect within the timeframe of the inventory. Where appropriate, projected “growth” factors are accounted for using projection methods that are specific to the type of emission source. Future 2017/18 emissions were projected from the 2011 base case either by running models to estimate emissions (e.g., EGUs and on-road mobile sources) or by adjusting the base year emissions according to the best estimate of changes expected to occur in the intervening years (non-EGU point sources). Furthermore, the 2017/2018 inventories include federal regulatory imposed changes affecting overall emissions levels in the years between the base case and the future scenario.

For the specific point sources categories of interest in our study, the EPA 2017/2018 NEI used the following regulatory assumptions, models and adjustments:

1. For EGUs, the Integrated Planning Model (IPM) for power production was used assuming the implementation of the Cross-State Air Pollution Rule (CSAPR), the Mercury and Air Toxics Standards (MATS), the final EPA actions for the Regional Haze Rule, the Cooling Water Intakes Rule, and Combustion Residuals from Electric Utilities (CCR) rule.
2. For non-EGU point sources, facility/unit closures information, and growth factors and/or controls were applied to certain categories presented in Table 4.1 of the TSD.
3. For cement plants, the Industrial Sectors Modeling Platform (ISMP) was used to project the cement industry reductions of criteria and select hazardous air pollutants through Portland Cement NESHAPs and the NSPS for the Portland cement manufacturing industry.
4. For Commercial and Industrial Solid Waste Incineration (CISWI) units, the EPA promulgated revised NSPS and 2011 was applied, but was limited to two states not including NYS.

In addition to these assumptions, a number of other rules affecting smaller points and some area sources were imposed, such as New Source Performance Standards (NSPS) for boilers and turbines. The assumptions raise two issues for the 2017/2018 NEI specific to the coal EGUs. The IPM model used by the EPA has not been widely accepted by states as reflecting likely shifts in power production levels in various areas of the country or potential facility shutdowns. In addition, the assumption that the MATS rule will be in effect in 2017 or 2018 is questionable due to the Supreme Court decision in summer of 2015 remanding the rule to the EPA to include cost considerations in its regulatory decision. On the other hand, the CSAPR rule to achieve ambient standards for Ozone and PM2.5 will result in reductions of SO_2 and NOx emissions from major sources, which will have concomitant beneficial effect on acidic deposition levels.

However, for the study purposes it is of no major consequence whether these rules will affect the changes considered by the EPA within the timeframe for the 2017/2018 NEI. In addition, as noted in the last section, delays by the EPA in finalizing the 2017 NEI beyond the timeframe of the study necessitated the use of the 2018 inventory data, with minor consequence to the study's results. As long as the underlying assumptions used for the future case data are understood, this scenario is adequate for our specific purpose of projecting potential changes in overall acidic deposition in NYS from the modified inventory and the relative changes from the subset of large Hg emitters on mercury deposition. To that end, the 2018 NEI data for the 26 sources in Table 4-6 were reviewed. The review also included information supplied by DEC regional staff on known or expected changes to these facilities since 2011. Data for the 26 sources were extracted from the 2018 NEI files for comparison to the corresponding values for the 2011 NEI.

For the three types of sources in Table 4-6, the foreseen low quality of the Hg emissions data became apparent. Essentially all data for the WTEs and EGUs was either missing or the facility was not in the inventory. Surprisingly for the "other" source category sources, the Hg emissions were identical to the 2011 NEI values with minor changes for two sources. Since these latter source types were not affected by regulatory changes since 2011, their data was apparently carried over from the 2011 NEI. For the majority of WTEs and EGUs it was also noted that for facilities remaining in the 2018 inventory, the SO_2 and NOx emissions were either missing or close to zero. Table 4-10 presents the emissions of Hg, SO_2 and NOx for these sources from the 2011 and 2018 inventories. For the nine WTEs, two were missing, five had no data, two had "nil" emissions, and only one seemed appropriate. This was unexpected considering no major changes were noted in the EPA TDS for this source category. For the 10 EGUs, three were missing, three were in the non-EGU files, two of the latter had no emissions data. It was noted that the units for Danskammer and Dunkirk in the 2018 data were not the coal units, but some ancillary equipment. On the other hand, the Kodak Power unit was the same as the 2011 NEI unit and was apparently placed in the incorrect subfile.

Table 4-10. Comparison of emissions for WTEs and EGUs for the 2011 and 2018 NEIs

	SET OF WTE and EGU FACILITIES FROM Table 4-6				
	Waste To Energy (WTEs)	Hg (lb./yr) 2011 NEI	Hg (lb./yr) 2018 NEI	SO_2 2011/2018	NOx 2011/2018
1	HEMPSTEAD RESOURCE RECOVERY FACILITY	24.3	0[a]	44/0	981/0.5
2	BABYLON RESOURCE RECOVERY FACILITY	2.7	ND[b]	30/ND	181/ND
3	HUNTINGTON RESOURCE RECOVERY FACILITY	3.2	NS[c]	6/NS	361/NS
4	ISLIP MCARTHUR RESOURCE RECOVERY FACIL	1.5	ND	19/0	173/1.3
5	DUTCHESS CO RESOURCE RECOVERY FACILITY	6.3	NS	20/NS	173/NS
6	WHEELABRATOR WESTCHESTER LP	27.4	ND	171/ND	1050/ND
7	WHEELABRATOR HUDSON FALLS	33.3	0	15/0	246/0
8	ONONDAGA CO RESOURCE RECOVERY FACILITY	7.7	ND	27/0	558/0.3
9	COVANTA NIAGARA LP	17.5	13.0	91/91	774/746
	Energy Generating Units (Coal EGUs)				
10	DANSKAMMER GENERATING STATION[4]	12.0	ND	4598/ND	1219/ND
11	AES CAYUGA	33.2	NS	10,492/NS	1827/NS
12	AES GREENIDGE LLC	3.1	NS	82/NS	138/NS
13	DUNKIRK STEAM GENERATING STATION[4]	32.0	ND	5653/ND	1703/ND
14	HUNTLEY STEAM GENERATING STATION	42.0	1.1	4316/378	1230/205
15	AES SOMERSET LLC	7.7	28.8	10,024/3935	5437/7126
	Additional Hg EGUs				
16	CON ED-74TH STREET STATION	1.3	NS	NS	NS
17	INDEPENDENCE STATION	0.3	0	7/0	205/474
18	HOLTSVILLE GT FACILITY	0.9	0	9/0	180/0.2
19	KODAK PARK POWER DIVISION[d]	13.0	13.0	4293/ 4240	2593/895

a Zero means there is a very low number in the 2017/2018 NEI (for example, Hg for Heampstead=7E-5 lb./yr.).

b ND means No Data for the pollutant in the 2017/2018 NEI.

c NS means the source in NOT in the 2018 NEI.

d These EGU sources were in the EPA's non-EGU source files.

For the EGUs, it is clear that the EPA's 2018 inventory assumptions and modeling have resulted in many of the coal plants being shut down or converting to other fuels. The timeframe for the MATS implementation is not clear as of this report since the Supreme Court on June 13, 2016 did not act to review the lower court decision not to stay the MATS rule. Thus, the EPA 2018 inventory assumptions might be appropriate for many of these facilities, but since this assumption affects all other coal units in and out of the modeling domain, it was decided to retain these assumptions for the NYS sources in our study for consistency. In order to verify and understand some of the other apparent inconsistencies, DEC staff were provided information on these facilities with respect to any changes since 2011, including “current” permit modifications. Since the EPA’s NEI is mainly based on information supplied by states, most of the basic data should reflect DEC data. In particular, DEC staff were asked for information on actual changes that occurred or were imminent for any of these facilities, but not any speculative modifications. In addition, it was known that over the last few years, a number of these facilities have either reduced or eliminated coal use due to NYS requirements and other factors. For example, the AES Westover facility had minimal Hg emissions in 2009 (Table 2) and was no longer operating in the 2011 NEI (Table 4-6). Thus, particular attention was given to the status of coal use in the EGUs.

Information provided by DEC staff indicated that for the majority of sources in table 4-5, no significant changes have occurred or were being considered by the facilities during the study timeframe, which could significantly affect emissions. Specifically, the discrepancies noted for the WTE facilities for the 2018 data relative to the 2011 base case was explained mainly as a result of the fact that DEC had not completed populating the 2018 NEI data base. Thus, many of the missing or low emissions were not due to some regulatory program to be implemented for these sources. However, it is noted from Table 4-7 that the emissions of the acidic precursors from the WTEs (as well as the “other” source category) are a small fraction of the NYS point source and power sector emissions. Thus, it was decided that the modifications in the 2018 NEI were adequate for the study’s purposes. For the Hg emissions, the paucity of data in the 2018 inventory necessitated the further review of recent information on the New York sources. Based on the data in Table 4-10 for the WTEs, the two missing facilities (Huntington and Dutchess Co.) in the projected EPA 2018 NEI were assumed to be correct. For the rest of the facilities, missing or “nil” data should be replaced by the 2011 NEI data with the exception for Covanta Niagara, which apparently had realistic data. For the EGUs, the same approach was taken for the three missing facilities projected by the EPA as no longer operating. In addition, the Danskammer and Dunkirk facilities were projected by the EPA to no longer use coal and information noted below supported the omission of these facilities. As noted above, for the “other” source category of Table 4-6, the 2018 inventory data was essentially the same as for the 2011 NEI, except data for the Lafarge plant, which is being currently replaced with a new facility.

Based on information from DEC files and regional staff, emissions data for six of the 26 facilities were reviewed for comparison to their disposition in the EPA 2018 inventory and the results were as follows:

1. AES Greenidge facility was shut down in December 2012 eliminating the 3.1 lb. of Hg emission in Table 4-5 and its SO_2 and NOx emissions. This confirmed it being missing in the EPA inventory.
2. The Danskammer station eliminated coal use in 2012 and switched to natural gas as reflected in its permit of 2/24/15. However, gas use at the facility has been minimal due to an emissions cap. Since no long-term data is available, it was decided to not retain this facility in study, as projected by the EPA's 2018 NEI.
3. Based on an agreement in 2005 with NYS, the Dunkirk and Huntley facilities switched to low sulfur coal use. Subsequently, Dunkirk mothballed three of its four units, with only unit two still operating on coal. This unit has 18 percent relative contribution to the total emissions in the 2011 inventory. In addition, it was noted that the Dunkirk facility was considering bringing in gas firing capability for possible use by the mothballed units, but no details were available, and thus, were not considered for the study. Per the EPA's projection, Dunkirk coal facility was not included in the 2018 inventory. The Huntley station still uses coal as fuel, although at much lower capacity in recent years. This is reflected by the large reductions in emissions noted in Table 4-10 for this plant as compared to the 2011 NEI. Thus, Huntley emissions in the 2018 NEI were modeled without revision.
4. The Lafarge cement plant has a new permit and is constructing a replacement facility with a dry kiln state of the science facility. It must meet the EPA Portland Cement NESHAPS requirements, which will reduce its Hg emissions from 143 to 59.1 lb./yr. In addition, the new facility will have much lower SO_2 and NOx annual emissions and reflects the 2018 NEI conservative values.
5. The Hg emissions in the 2018 inventory for the Somerset facility seemed too high compared to the 2011 NEI relative to differences for other facilities. The DEC staff review of data for the facility from 2012 to 2014 gave a rage from seven to 13 lb./yr. and noted that the Hg emission factor used for the facility's 2017 data reflected an overly conservative value. Thus, for this facility, Hg emission was modified to 13 lb./yr. at the upper end of the data range.

It was also noted that other facilities might add gas firing capabilities, but these were not specific enough for consideration. In the case of the Kodak Park Power, the additional capability was almost completed, but the permit retained the coal burning capability and the emissions in Table 4-10 were kept for this source. In sum, the 2018 inventory with the explanation of the acidic precursors reflected the CMAQ modeling of acidic deposition. On the other hand, for mercury, only the relative change in the emissions from the 2011 NEI to the 2018 inventory were used to "scale" the CMAQ Hg deposition to indicate potential future case reductions. The Hg emissions reduction from 2011 to 2018 for the sources in Table 4-10 was 172.9 lb., mostly due to assumption of coal EGUs being shut down or converted to gas. This represents a 23 percent reduction in Hg emissions from the 754.7 lb. value n Table 4-6 for large point sources being tracked by CMAQ.

As to the overall emissions in the domain, the resultant 2018 inventory of acidic deposition precursor emissions from various source sectors and regions are presented in Table 4-11. Comparison to the 2011 NEI emissions in Table 4-7 indicates a general reduction in the SO_2 and NOx emissions, but none for NH3. In fact, there is a projected increase in overall NH3 emissions, but these are not associated with the major point sources of interest to the study. For SO_2, emissions in 2018 are only one-fifth (20 percent) of the 2011 values for the study sources and one-third for the totals for all states in the domain. For NOx, there is a reduction of 70 percent for the study sources, but only a 14 percent reduction in the overall total for the domain states due to the large mobile source influence. The consequences of these projected changes were modeled to determine the corresponding deposition fields in the CMAQ domain and are discussed in the next section.

Table 4-11. Anthropogenic emissions summaries from 2018 NEI for acid deposition precursors

Pollutant → Source Category ↓	SO2 (TPY)	NOx (TPY)	NH3 (TPY)
All Point Sources in NY (includes Oil & Gas-NOx)	20,298	46,427	2,250
All EGUs in NY	4,834	15,130	1,312
Study sources: all NY EGU emissions, plus WTEs and "other"	8644	9448	1657
Area Sources in NY (e.g. oil & gas, RWC, Agricult.)	8,609	61,924	45,040*
Mobile Sources in NY	605	89,037	3,567
All NY Anthropogenic Emissions	29,772	283,178	50,976
Rest of states in the 2018NEI Inventory domain	506,535	2,025,429	381,680
Ratio of 2018 to 2011 emissions for NYS study sources	0.21	0.30	1.0
Ratio of 2018 to 2011 emissions for all emissions in rest of states in the domain	0.33	0.86	1.17

* means 96 percent of NH3 emissions in NY are agricultural sources

5 Resultant CMAQ Deposition

The modeling methods and the 2011 meteorological and emissions input data described in the previous two sections were used to simulate annual concentration and deposition patterns of acidic and mercury species over the CMAQ 4km modeling domain. A limited assessment was also made of the total deposition patterns on a 12km grid over the domain for comparison to demonstrate the influence of the grid refinement. The main aim of the current study was to determine the impact of the emissions from sources within the domain from the 2011 NEI over the 4km grid, augmented by emissions outside the domain as influx through boundary conditions and, specifically, to determine the relative contribution of the State's "power sector" major point sources to the total deposition. The refinements and corrections made to these NYS major point sources described in the previous section were to ensure that at least for these larger sources, data for mercury and acidic deposition precursors and their modeling stack parameters were reasonably accurate and representative. In addition to these power sector sources, it was deemed necessary to include emissions from "other" large point sources to the mercury inventory due to their large Hg emissions. For acidic deposition, the emissions from all NYS EGUs, not just the coal plants, were determined and these were also included in the set of contributing "tracked sources."

The initial thinking was to attempt to track the influence of all subsets of the NYS point source categories on the overall emissions impacts, but it was soon clear this would be an enormous computer resources issue from a runtime standpoint. That is, the approach added to CMAQ to track source attributions was tested previously on a short-term scale of days, but the same approach applied on an annual timeframe would mean increases by factors, not percentages, for each subgroup. While a basic run for the full inventory for one month would take about a week of running time, the addition of just one subset would at least double that runtime. Given the unpractical runtime, these subsets would add, it was determined that the contribution of the total subset of all NYS large point sources to the overall 2011 NEI impacts would provide the desired outputs for acidic and Hg deposition without affecting the purpose of the study. Another approach in CMAQ was used wherein the emissions from the set of NYS sources of interest are eliminated and CMAQ rerun and these results were then compared to the base case run where all sources were included, with the contribution of these NYS point sources determined as the difference in the annual results from the two runs. This is the "zero out" approach in CMAQ, which provides the relative impact from the NYS sources not accounted for in the CMAQ run.

To ensure that the CMAQ results from the base 2011 NEI case and the "zero out" case provide the deposition information of interest to the study and at the same time minimize the necessary number of CMAQ runs, an approach was taken which, nonetheless, did not alter the desired results. Specifically, a comparison was made of the emissions data in Table 4-6, which includes the State's large Hg sources, to the corresponding set in Table 4-5 that includes additional oil and gas EGU emissions of importance to acidic deposition, and to the relative percent of these source contributions to the overall NYs emissions in Table 4-7. As noted previously, the subset of all NY EGUs comprise a large portion of the "study sources" category for acidic deposition in Table 4-7 while for Hg, the contribution of the oil and gas EGUs (not in the Table 4-5 list) to the corresponding study source category totals is small, with these additional oil/gas facilities adding less than ten percent to the emissions. Furthermore, for the acidic deposition precursors, the emissions from the WTEs and "other" source in the large Hg subsets are very low as indicated in Table 4-7. Therefore, by performing one CMAQ run with all the EGUs (not just the set of 26 large Hg sources from Table 4-5) plus the WTE and "other" sources "zeroed out" accomplishes the relative contribution determination for both acidic and mercury deposition for the State's study sources. The inclusion of all oil and gas EGUs in addition to the Hg emission sources does not alter the inventory sums for Hg to any real extent, but provides the means to limit the NYS "power sector" contribution assessment to one CMAQ run. In addition, as noted in section three modeling methods, initial CMAQ runs[72] for three months of "summer" 2011 meteorological data over the 12km grid resolution indicated the Hg impacts in the modeling domain from all NYS sources and, in fact, due to all of the in-domain sources were, a small fraction of the overall deposition results when all sources outside of the domain were included as influx to the domain and the bi-directions option for Hg0 described in the methods section invoked. The graphical presentation for this summer Hg modeling is repeated in Figure 5-1. These refined modeling results of the dominance of out of state sources confirm the "crude" modeling performed in 2002 for NYS receptors described in Section 2, which indicated the clear dominance of sources both out of the region and the U.S. Thus, although the subset of NYS sources modeled includes the relatively large Hg emissions from the "other" source category, further explicit modeling to separate the "power sector" contribution to the rather small impacts was deemed unwarranted. Rather, a qualitative assessment of the combined subsets can be made.

Figure 5-1. CMAQ predictions of weekly mercury wet deposition at all MDN sites for mid-May to end of July, 2011 with and without boundary conditions (BC) and bidirectional (Bi-di) flux

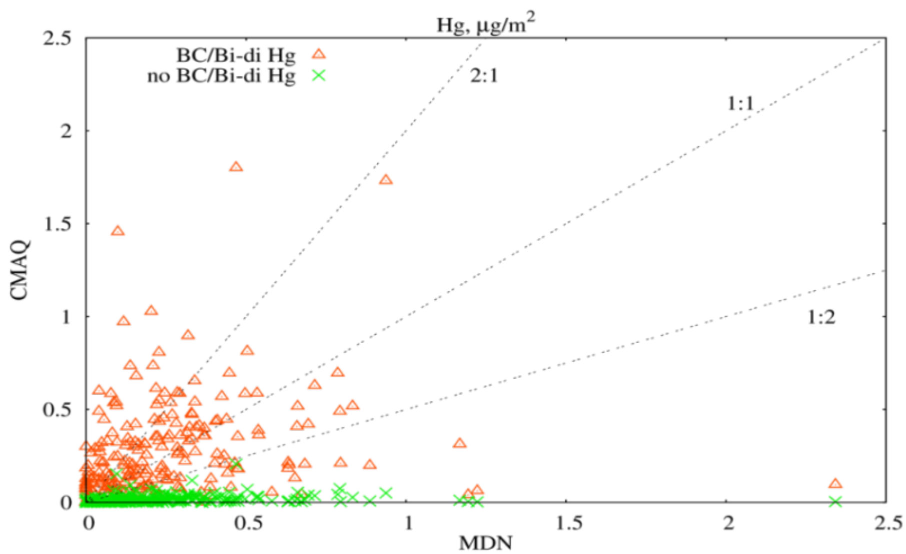

Another runtime shortcut to assess the future 2018 inventory was also taken without altering the purpose of the study. The study envisioned a sensitivity study wherein the impacts from a future NEI would be compared to the 2011 NEI base case acidic deposition results to assess the effects of the potential reductions in emissions due to regulatory actions. As described in the previous section, the 2018 inventory does not represent true projections since the implementation of major regulations (CSAPR and MATS) for specifically the EGUs will not be accomplished in that timeframe. Instead, the inventory more correctly represents a "future" scenario when the implementation of especially the MATS regulations are projected to lead to the shutdown of many of the coal plants included in the 2011 NEI. In addition, the study's approach for the future inventory scenario was to assess the relative reductions in acidic deposition impacts due to changes in the overall domain emissions, including in the emissions from NYS power sector point sources. For mercury, the reductions in NY's point source sector were noted in the previous section to be 23 percent from the 2011 to 2018 NEIs. In addition, the latter "future" inventory contained very few and low quality Hg emissions data for the sources in or outside the modeling domain. Thus, for mercury, the only defensible comparison that can be made between the 2011 NEI results and possible reductions in 2018 are qualitative discussions of the effects of emissions reductions from the NYS point source or "power" sector.

Therefore, it was determined at the study planning stage that the effort level of the sensitivity study should be limited practically to only the modeling of the acidic deposition for 2018 emissions for comparison to the 2011 NEI results. In addition, since the EPA 2018 emissions data were readily available on the 12km grid scale, the CMAQ modeling performed for this 2018 NEI were compared to the corresponding results for the 2011 inventory at the 12km grid scale based on the same platform. That is, since the interest was in relative and not absolute reductions in deposition from 2011 to a future year scenario, the task of assessing these future reductions was accomplished by considerably reducing the CMAQ runtime by using the 12km grid results instead of projecting the 2018 emissions onto the 4km grid.

The effect of grid resolution on deposition patterns was addressed by comparison of the 4km vs. the 12km results for the base case 2011 NEI. Examples of CMAQ/WRF predictions are presented in Figure 5-2 for precipitation and NO3eq (NO3eq is particulate NO3 plus gas phase HNO3).

Figure 5-2. CMAQ predictions of precipitation and NO3 on 4km vs. 12km grid scales

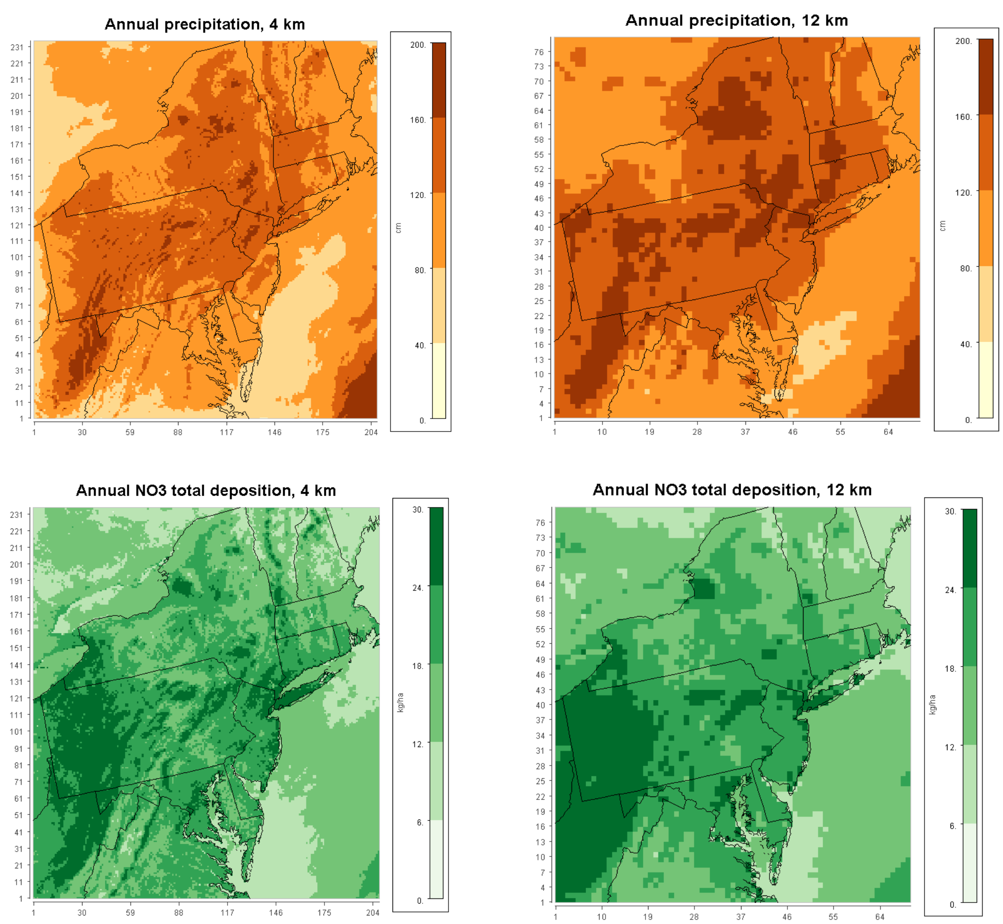

The NO3values are annual total deposition of wet plus dry components. Similar patterns were found for other pollutants. These plots indicate a better spatial resolution by the refined 4km grid, as would be expected. The 12km grid results are more broad brushed, especially at the higher values. The similarity between NO3 and pecipitation patterns is due, in part, to the importance of wet deposition in the totals discussed in the next section. Whether the refinement by the 4km grid leads to better model performace is addressed by comparisons to available wet deposition observations, as discussed in Section 5.3.

5.1 Acidic deposition results for 2011 NEI

A set of CMAQ predictions for the 2011 NEI base case and the "zero-out" case, the latter reflecting NYS power production point source contributions, was generated and reviewed to identify the consequent total deposition patterns. Some additional patterns were generated for the summer and winter months to assist in the understanding of the annual results. Deposition patterns over the modeling grid were simulated for the following defined components: sulfate=SO4, SO4eq (as sulfate equivalent) = particulate SO_4 plus gas-phase H_2SO_4, total sulfur (TS, as sulfate equivalent) = SO_4 plus 1.5 times gaseous SO_2), nitrate (NO3), NO3eq (as nitrate equivalent) = particulate NO_3 plus gas-phase HNO_3, reduced Nitrogen (NHxeq as ammonium equivalent) = particulate NH4 plus gas phase NH3, and ammonium=NH4. In addition to the patterns for annual totals of these acidic deposition species, the wet and dry components were plotted to discern their respective contributions. A large set of combinations of these variables were generated for review and only the pertinent, and interesting patterns are presented in this section.

Figure 5-3 presents the annual total and wet SO4eq results over the domain. Deposition is in kilograms per hectare (kg/ha) and it is important to note that these represent the accumulated amounts over the time period simulated; in this case an "11-month" value since CMAQ simulations were not done for March due to missing meteorological data, as noted previously. The graphs were made to have essentially the same scales, but some minor variations appear due to the plotting software, which sets some of the endpoints. The graphs show the importance of wet deposition in controlling the total deposition for SO4eq. The plot for dry deposition (not shown) essentially indicates a "constant" value below the nine kg/ha cutoff of Figure 5-3 over the whole domain. The dry fraction of the total sulfate deposition is found to be about 10 to 15 percent over NYS and somewhat higher in the southeastern part of the domain. The SO4eq result reflects the same general pattern as for precipitation in Figure 5-2, but is likely influenced by other important considerations such as the spatial distribution of SO_2 emissions, especially EGUs depicted in Figure 4-7. The SO4eq pattern over NYS is more spatially smooth indicating the likely dominance of long range transport of chemically formed species over localized influences.

Figure 5-3. Annual accumulated total (left) and wet (right) SO4eq deposition

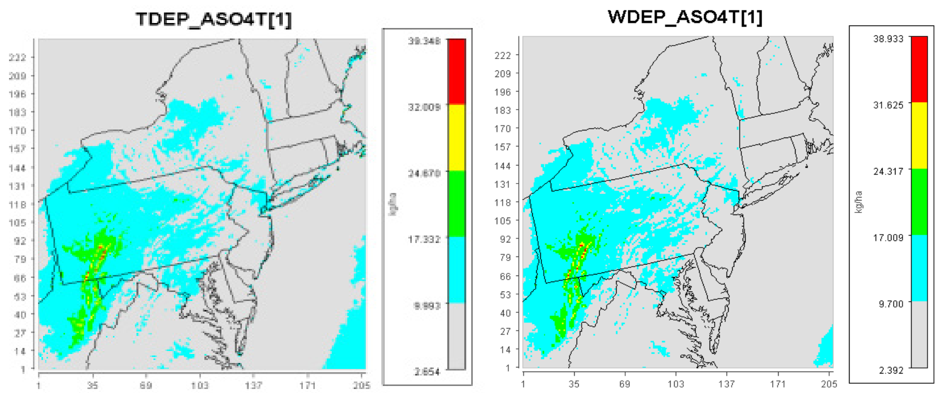

The low dry deposition of SO4eq reflects the corresponding low dry deposition velocity for sulfate particulate over the annual time scale. By definition, total sulfur (TS) deposition includes the gas phase SO_2 deposition, which has a higher dry deposition velocity. Thus, total wet and dry annual TS plots were generated and are shown in Figure 5-4. The important influence of dry deposition for TS is apparent, with levels on par with wet deposition values over NYS and even higher contributions in the areas of maximum impacts in PA. In comparison to the sulfate results in Figure 5-3, total TS deposition is increased by at least two fold over NYS with the inclusion of SO_2 deposition. It is also seen that certain areas in NYS indicate higher localized total TS deposition, in contrast to the sulfate results, due to the dry deposition component that reflects the likely influence of localized SO_2 sources. It is not clear why more areas with such influence are not prominent, but the results of the "zero-out" modeling provide further information.

Figure 5-4. Annual total (top left), wet (top right) and dry (bottom) TS deposition

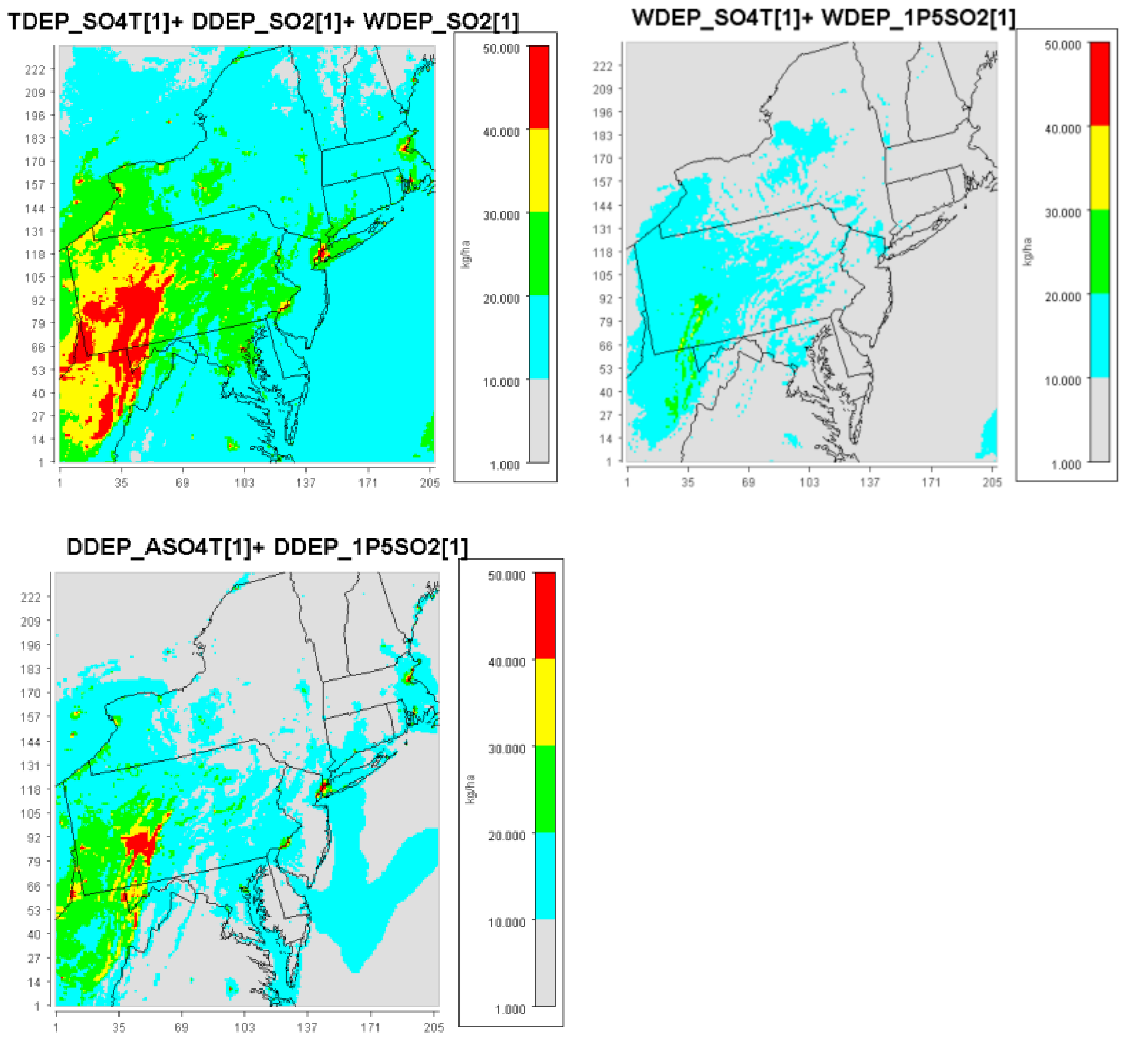

To quantify the contribution of wet and dry components to the total TS results, plots were generated from the ratios of the components to the total and are presented in Figure 5-5 as a fraction of wet and dry deposition divided by the totals. These fractions are provided over the same range scale for ease of comparison. It is seen that total sulfur is influenced by both components significantly, with generally higher than 50 percent due to wet deposition in the eastern sector of NYS, including the Adirondacks, and the reverse dominance of dry deposition in the western areas of the State. The influence of localized SO_2 impacts due to dry deposition is seen in limited areas. For the rest of the U.S. portion of the domain, dry deposition of TS seems to be the dominant component.

Figure 5-5. Fraction of annual TS deposition due to wet (left) and dry (right) components

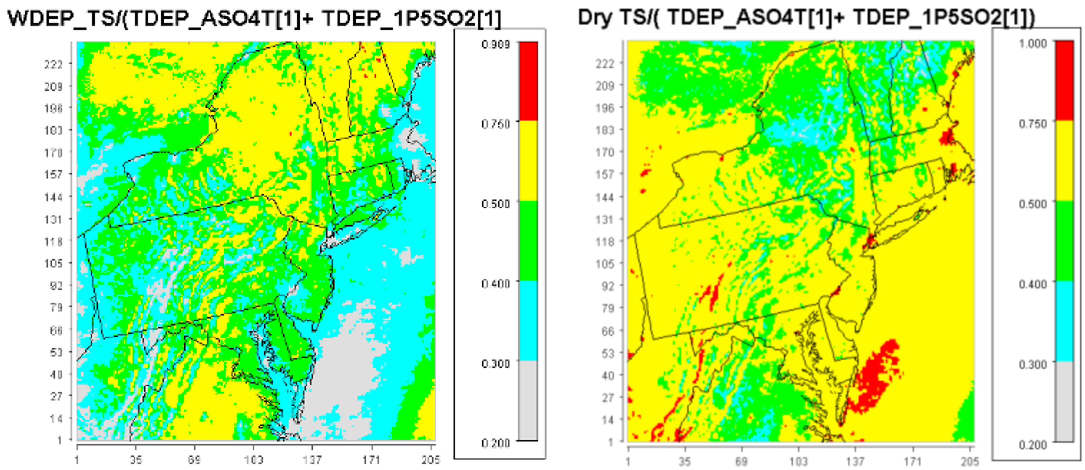

The resultant deposition of total NO3eq was previously depicted in bottom left side of Figure 5-2 and shows a similar pattern of impacts in the domain as for SO4eq in Figure 5-3. However, unlike sulfate, the dry deposition contribution to the totals is much higher for nitrates, as depicted in Figure 5-6 as fractions of wet and dry components. This result is related to the inclusion of gaseous nitric acid (HNO3) in the definition of NO3eq, which has a relatively large dry deposition velocity. For NYS, the wet component of NO3eq is over 50 percent for most of the area, but there are extended areas with a dominant dry component such as the Catskills. For the rest of the U.S. portion of the domain, the dry component plays a significant role, especially for the region south of PA.

Figure 5-6. Fraction of annual NO3eq deposition from wet (left) and dry (right) components

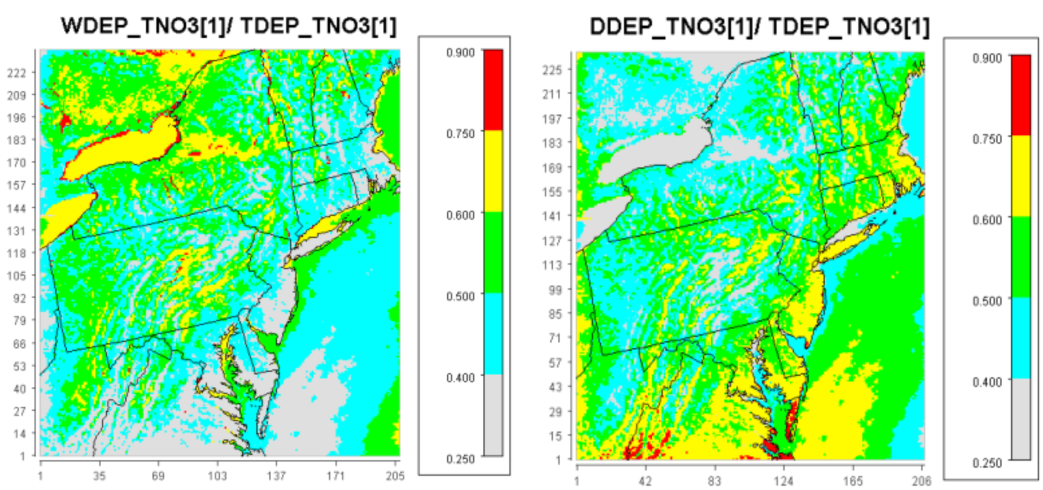

The next acidifying component plotted was total reduced nitrogen (NHxeq) with the total annual deposition depicted in the left panel of Figure 5-7 and the fraction due to dry deposition on the right. The absolute values of NHxeq impacts are seen to be much lower than for NO3eq (Figure 5-2) and SO4eq (Figure 5-3) and appear to be maximized in areas of agricultural activities such as in southeastern PA. However, it is important to recognize that in terms of Nitrogen acidifying, NHxeq has four times the effects of NO3eq. The dry component fraction also indicates the general areas where agricultural activity has a large influence, such as in western NYS. As noted previously, the emission inventory for NH3 is relatively poor for number of the sectors and, therefore, the modeled results should be viewed as tentative.

Figure 5-7. Annual total (left) and dry (right) deposition fraction of NHxeq

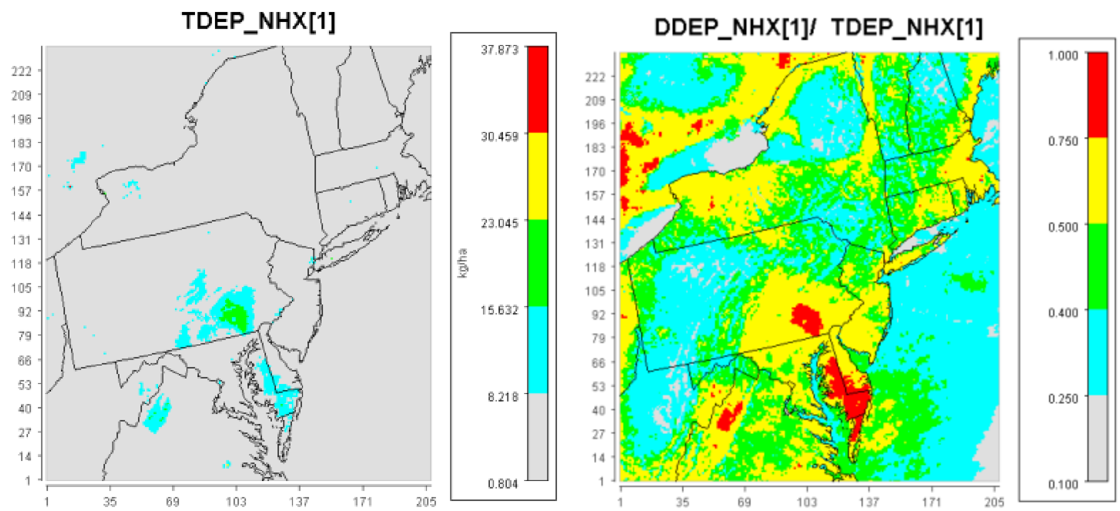

The relative contributions of wet and dry components to the SO4eq, TS, and NO3eq annual deposition can be compared to a limited extent to previous model assessments in recent years as a check of the CMAQ simulations. A model to observed comparison of wet sulfate and nitrate deposition is presented below in Section 5.3. The importance of dry deposition of SO_2 vs. SO4 and its contribution to total TS values was also noted in the study[73] by the EPA in CMAQ simulation comparisons between 2002 and 2010. Also, the study found that total N deposition had a large impact by the dry component, as in this study. Similarly, a study[74] of multiple years (2002–2011) of deposition by CMAQ indicated that for sulfur as well as nitrogen, dry component was more important than wet for many of the years, but in 2011 these were compatible. There was a steady decrease in both components over the years due to the reductions in SO_2 emissions, but an increase in the importance of dry deposition was seen in some years due to low precipitation in these years. For reduced Nitrogen, the dry component was more important for the oxidized form while for reduced N, wet deposition was more importance. Thus, there is a sense of confirmation of the current results.

For sulfate/SO4eq, the dominance of wet deposition was noted in the current CMAQ results. However, the relative contribution of the wet component is somewhat lower than those noted at the CASTNET sites (e.g., Huntington Wildlife Forest[75] [HWF]) where dry component is modeled with another resistance approach for deposition velocity in determining total values. At many of these sites, wet deposition is noted to be well over 90 percent of the total. As noted in the section on previous study findings, it was thought that the low dry deposition could be associated with the rather low annual average wind speed (U) reported and used at these sites. Specifically, at the HWC, the average U was noted to be 0.6 m/s which is rather low and questionable. Thus, the hourly data for 2011 was reviewed using the "validated" data set which eliminated missing and other data coded invalid. The average U determined was still low at 0.85m/s (scalar) and 0.53m/s (vector), but it was also noted that the "validated" set still contained questionable data such as negative values and those below the instrument threshold of 0.53 m/s. Eliminating these data resulted in an average scalar wind speed of 1.2 m/s, which is more reasonable and consistent with the average at Whiteface lodge of 1.8 m/s. Since the dry deposition model used for the CASTNET calculations is proportional to and uses the vector U, it is concluded that the relative contribution of the dry component is underestimated by a factor of about two to three, thus producing the very large fractional wet deposition contributions to the totals. A visit to this CASTNET site indicated the additional possible influence of a nearby tree line in reducing the average wind speed. Thus, it is concluded that the relative wet sulfate deposition component predicted in the current CMAQ modeling of about 10 to 15 percent is a more reasonable estimate.

In order to gain some further understanding of the results on the annual timescale, limited plots were also generated for the summer and winter months of 2011. These plots provide a sense of the relative importance of the seasons in term of precipitation and dry deposition factors. Plots of sulfate deposition for the summer and winter are presented in Figure 5-8. Note that the upper limits in the scales are set by the software package, but do not affect the comparisons. Comparison to the annual results in Figure 5-3 shows the overall importance of the summer months, but in NYS the contribution from both seasons seems similar. These results are also controlled by the wet components, as in the annual totals of Figure 5-3.

Figure 5-8. Summer (left) and winter (right) total SO4eq deposition

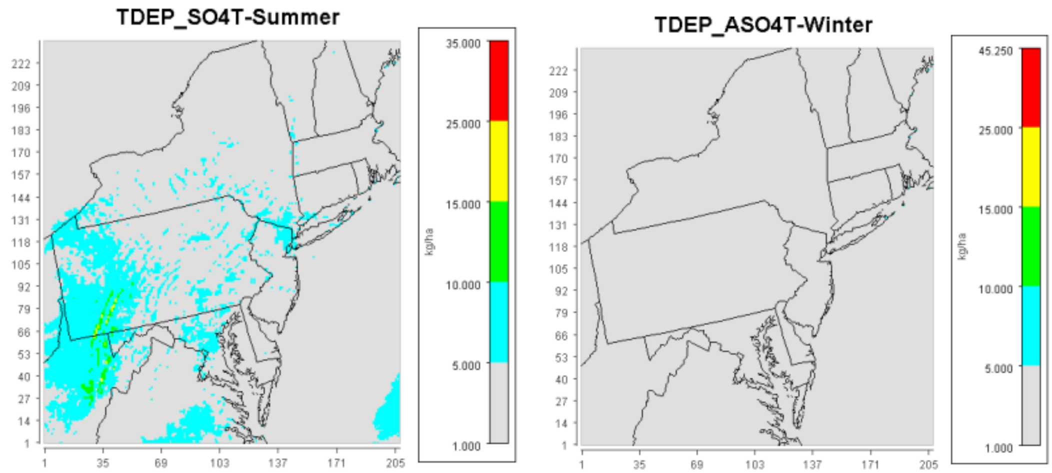

To get a better quantification of these seasonal contributions to the annual results, plots of the corresponding fractions are provided in Figure 5-9. These results are more detailed representations of the importance of the summer months relative to the winter period in determining the total annual deposition for sulfate. Summer contribution ranges from a quarter to half of the annual deposition in NYS, while winter contributes to less than a quarter of the annual values throughout the modeling domain. It is also seen that during the summer months, the impacts are relatively higher in areas such as the Catskills vs. the Adirondacks, which can be attributed partly to the corresponding precipitation patterns described further in Section 5.3.

Figure 5-9. Summer (left) and winter (right) fractions of annual total SO4eq deposition

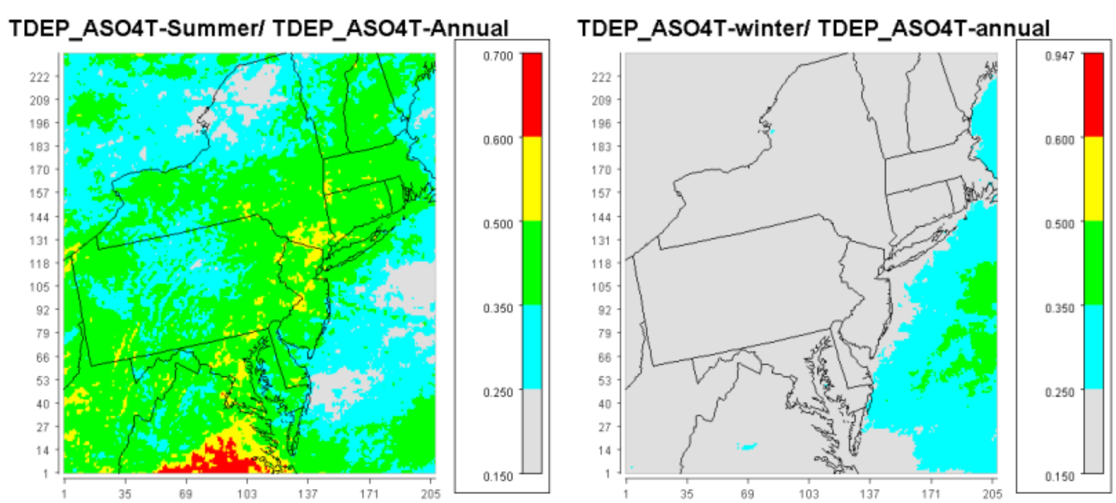

Similar seasonal plots were generated for NO3eq and are shown in Figure 5-10. In contrast to SO4eq, these results indicate the importance of both seasons in determining total deposition. Furthermore, the higher summer deposition in the area around Catskills is contrasted with higher wintertime deposition in the Adirondacks. The localized peak in the NYC area is likely the result of higher NOx emissions of non-point sources and has been previously noted to be an overestimation by CMAQ.

Figure 5-10. Summer (left) and winter (right) annual total NO3eq deposition

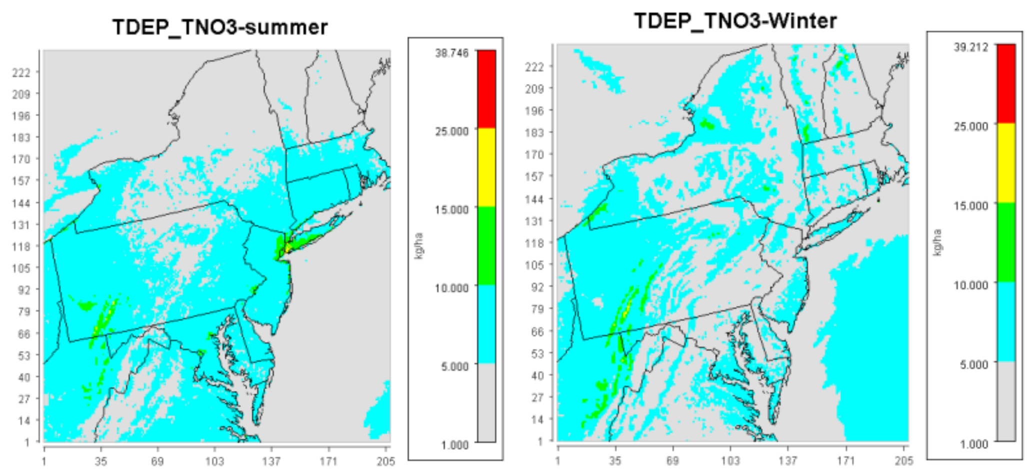

Turning now to the study's germane consideration of the relative contribution of the NYS power sector major point sources to the total modeled impacts, similar plots were generated for the "zero out" CMAQ simulations. These plots were supplemented by additional graphs reflecting the power sector contribution by the use of the relative difference = ([base case - "zero out" case]/base case), which represents the fraction of the deposition due to the eliminated power sector sources in the "zero-out" CMAQ run. Thus, the larger the difference, the larger the contribution of the power sector to the specific deposition. The "zero-out" CMAQ simulation maps for SO4, TS, NO3, and NHx were compared to the base case maps to get a first order view of the potential differences. Based on the anthropogenic emissions estimates in Table 4-7, it was anticipated that SO_2 from the power sector would play a bigger role in the deposition differences than NOx, followed by NHx based on the relative size of the power sector vs. the rest of the NYS and domain emissions. Whether the expected effect would be realized in the deposition of sulfate and TS, as an example, depends on not only the emissions, but on the deposition and chemical processes in CMAQ. It was found that for all four acidic components, only small differences were observed by simply comparing the maps. Thus, the relative difference maps provided more appropriate quantifications of the power sector effects.

Figure 5-11 presents plots of SO4eq deposition for the base case and the “zero-out” case. Note that the base case is the same as in Figure 5-3, except the scale range has been reduced to provide detail in impact gradients over NYS. In addition, the effects of eliminating the NYS power sector point sources were not seen in other areas of the domain and, thus, the maps have been limited to the NYS and to adjacent and downwind areas. A comparison of the two maps shows very little difference in the patterns with and without the NYS power sources. Thus, the relative difference was calculated and plotted in Figure 5-12. The influence of the power sources is relatively low, with essentially all areas experiencing less than 7.5 percent effect. There are limited locations in NYS of somewhat higher reductions, at twice this amount, which are possibly due to localized effects from the set of power sources.

Figure 5-11. Annual total SO4eq deposition for base case (left) and zero-out case (right)

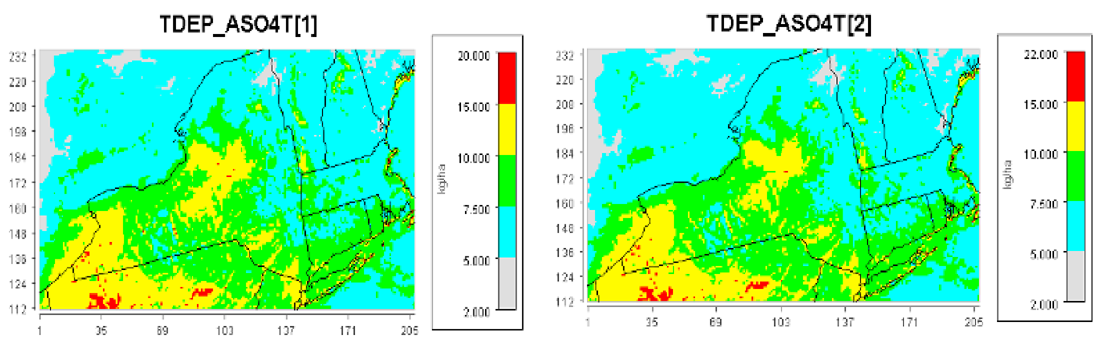

Figure 5-12. Relative difference in total SO4eq deposition from base to “zero out” cases

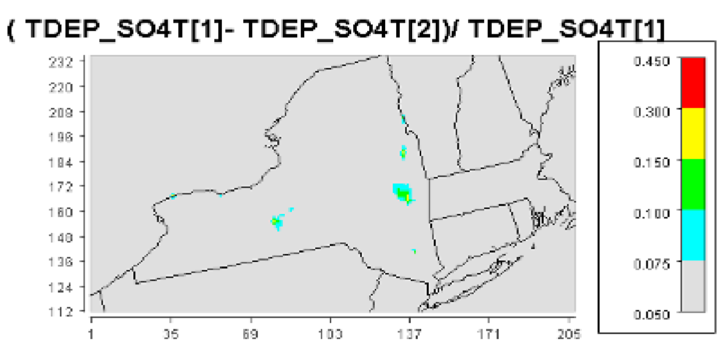

A better representation of the localized effect was anticipated for TS based on the previous finding of the importance of the dry component of SO_2 in shaping the TS deposition pattern. Thus, Figure 5-13 presents the relative difference between the base case and the “zero out” case, as well as the dry deposition contribution to this difference to more clearly indicate the consequences of eliminating the power sector sources. Unlike SO4eq, the power sector has a significant contribution in reducing the total sulfur deposition. In addition, the pattern of reduction is replicated in the relative difference in the dry component which confirms its dominance. The reductions are upwards of half the deposition stating on a very local scale with less, but still significant, drops over large areas away from the maxima. The rest of the State and other areas experience only a 7.5 percent reduction in TS similar to the result for sulfate. A look at the location of the “eliminated” major point sources in Figure 4-5 and the discussion of the current disposition of these sources in subsection 4.4 demonstrates that these reductions are associated with large drops in SO_2 emissions as a consequence of the elimination or major cuts in coal burning at facilities (e.g., Danskammer, Cayuga, Huntley, Dunkirk) located where the largest drops in deposition are seen in Figure 5-13. Thus, these reductions in total sulfur deposition have in fact occurred since the 2011 base case, but cannot be verified by direct observations of ambient deposition due to limits in measuring dry deposition. The comparisons of CMAQ projections to observed wet sulfate, presented in the next section, only partially addresses the likely drops in TS deposition. The modeling of the future 2018 case in Section 5.4 further confirms the reductions presented for the “zero-out” case.

Figure 5-13. Relative difference in annual total TS deposition (top) and the contribution of the dry TS component to this difference (bottom)

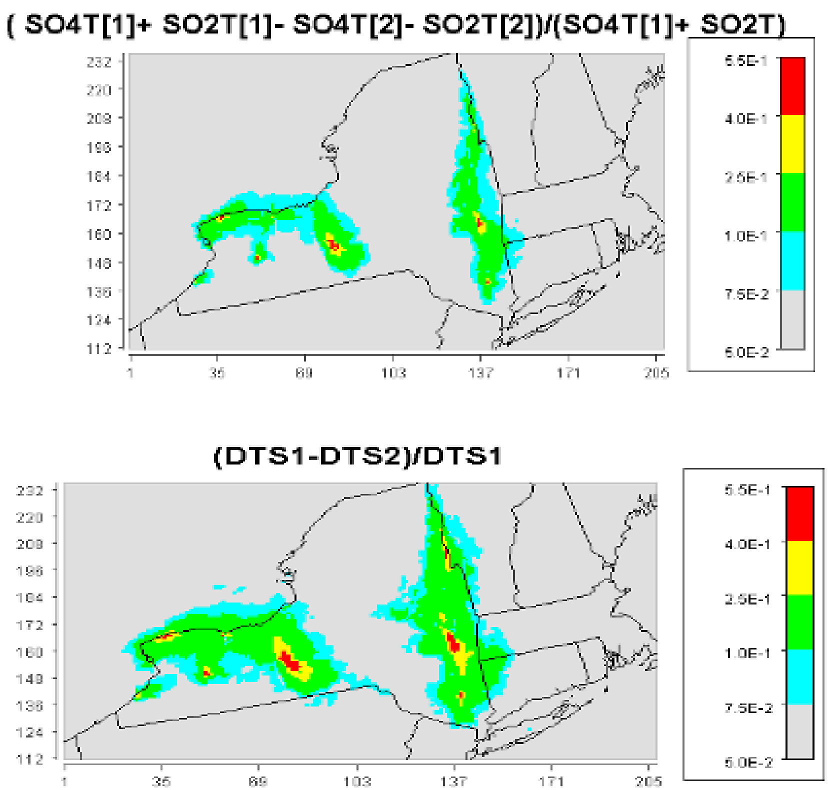

Tuning to the results for the NO3eq component of acidic deposition, Figure 5-14 provides the pattern of impact for the “zero-out” case and the relative difference in NO3eq deposition from the former to the base case. The plot for the NO3eq base case is not presented, but is essentially identical to the “zero-out” map in Figure 5-14. The scale of the total NO3eq deposition is the same as in Figure 5-10 for SO4eq for ease of comparison. It is seen that for the base case (and zero out case) NO3eq impacts are higher over the whole area depicted. On the other hand, the relative difference in total NO3eq deposition in Figure 5-14 indicates that the elimination of the power sector has a relatively low impact on the base case with reductions of the order of less than 7.5 percent over the whole area.

Figure 5-14. Annual total NO3eq deposition for the zero-out case (top) and the relative difference between the base case and zero out case (bottom)

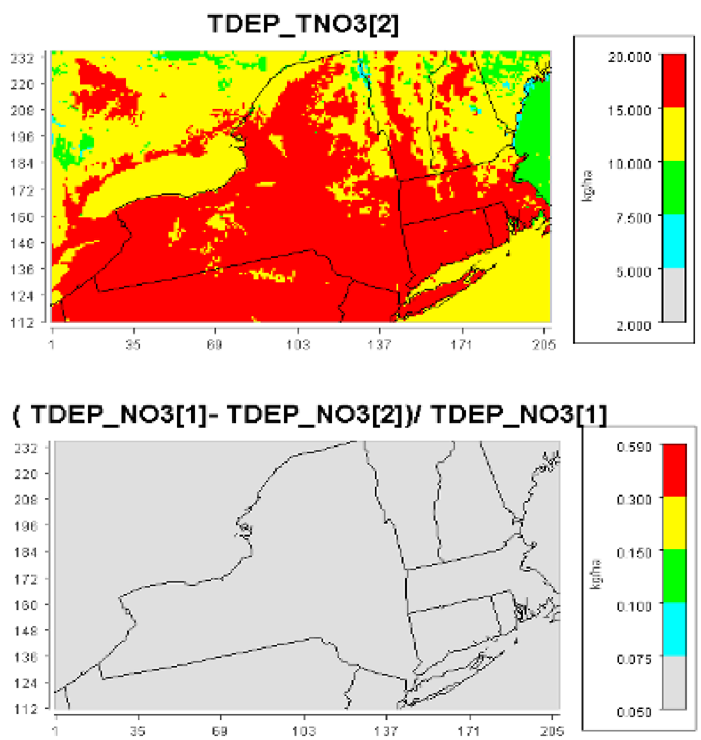

The plots for NHxeq did not indicate any difference between the base case and the “zero out” case and are not presented. This is not surprising due to the low level of NH3 emissions for the power sector sources relative to the NYS area sources and the domain emissions in Table 4-7.

5.2 Mercury deposition results for 2011 NEI

Similar to the acidic deposition results, maps of deposition patterns for total mercury and its three species were generated for the base case and "zero out" case from the respective CMAQ runs. In addition, limited supplemental plots were created to better understand the potential seasonal and wet vs. dry component contributions. The set of maps presented in Figure 5-15 shows the annual deposition of mercury species (Hg0-elemental, Hg2-oxidized gaseous, and HgP-particulate) and the total (THG) on the same scale for ease of comparison (again, the upper limit is set by the plotting program, but has no influence on the comparisons). The deposition levels are in the standard units of ug/m2 used to report mercury results.

It is found that the total deposition of mercury over the domain is contributed mainly by the Hg2 form, followed by the Hg0 and then HgP species. These results are in line with the relatively lower wet removal factor (Henry's law constant) and dry deposition velocity for elemental mercury vs. the oxidized form, which surpass the influence of higher emissions of the former in the speciation profiles assigned to source types in Section 4.3. For HgP, the lower contribution is due mainly to the low (few percent) emission factor for the particulate form in determining the emission rate. The spatial pattern for THG over the domain is somewhat similar to the sulfate and nitrate results above, at least with respect to the maximization of impacts in southwest PA and the relatively smooth coverage over NYS. The exception for mercury is the rather high, but localized total and Hg2 deposition in the NYC area. This effect is undoubtedly related to the relatively large emissions from the area source types discussed in Section 4.2 at the county level in the NYC Metropolitan area associated with scrap metal processing and crematories. It is likely that these projections suffer from the same level of over prediction for these very low elevation area sources types, as was noted previously for NO3 from mobile and area sources.

Figure 5-15. Annual species (Hg0, Hg2, HgP) and total (THG) Hg deposition for base case

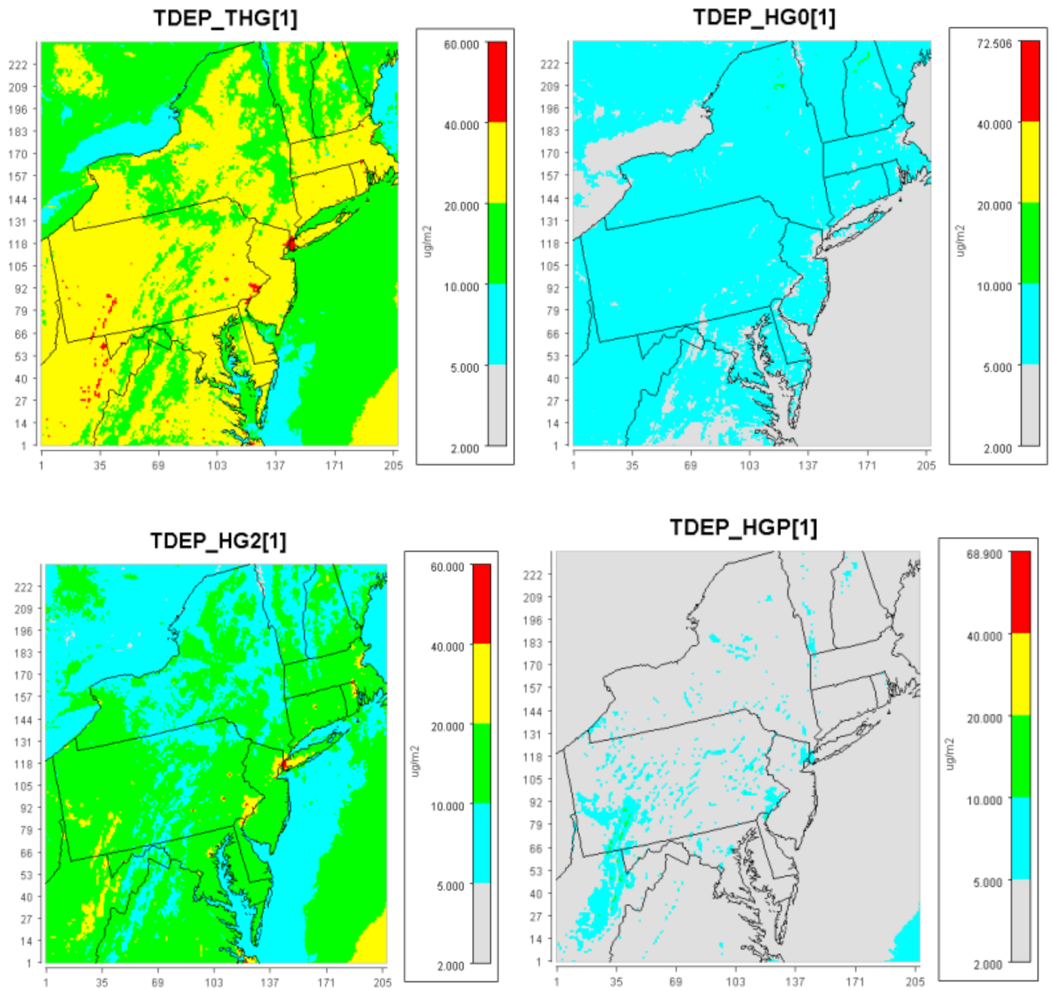

To determine the wet and dry components of the total Hg and its species, plots were generated of these contributions using the same scale as in Figure 5-15. In addition, the fractions of the wet and dry deposition from the total were calculated. The results for the annual THG deposition for the base case are presented in Figure 5-16. The distribution over NYS of both components is relatively uniform, with the dry component contributing to over 60 percent in large areas of the State. Somewhat lower, but still over 50 percent contribution is seen by dry deposition in many parts of the domain south of NY. These are in contrast to the "crude" modeling done for NYS in 2002, which showed wet deposition as more important. There appears to be a large wet component over the large lakes and the ocean (opposite for the dry component), but it could not be readily determined if these reflect the expected low dry deposition velocities over water or some spurious result as a consequence of CMAQ simulation or data limitations. The same pattern over the water bodies was seen in the corresponding plots for Hg2 component noted in Figure 5-16.

Figure 5-16. Annual wet deposition (top left) and its fraction of THG (top right) and dry deposition (bottom left) and its fraction of the THG (bottom right) for the base case

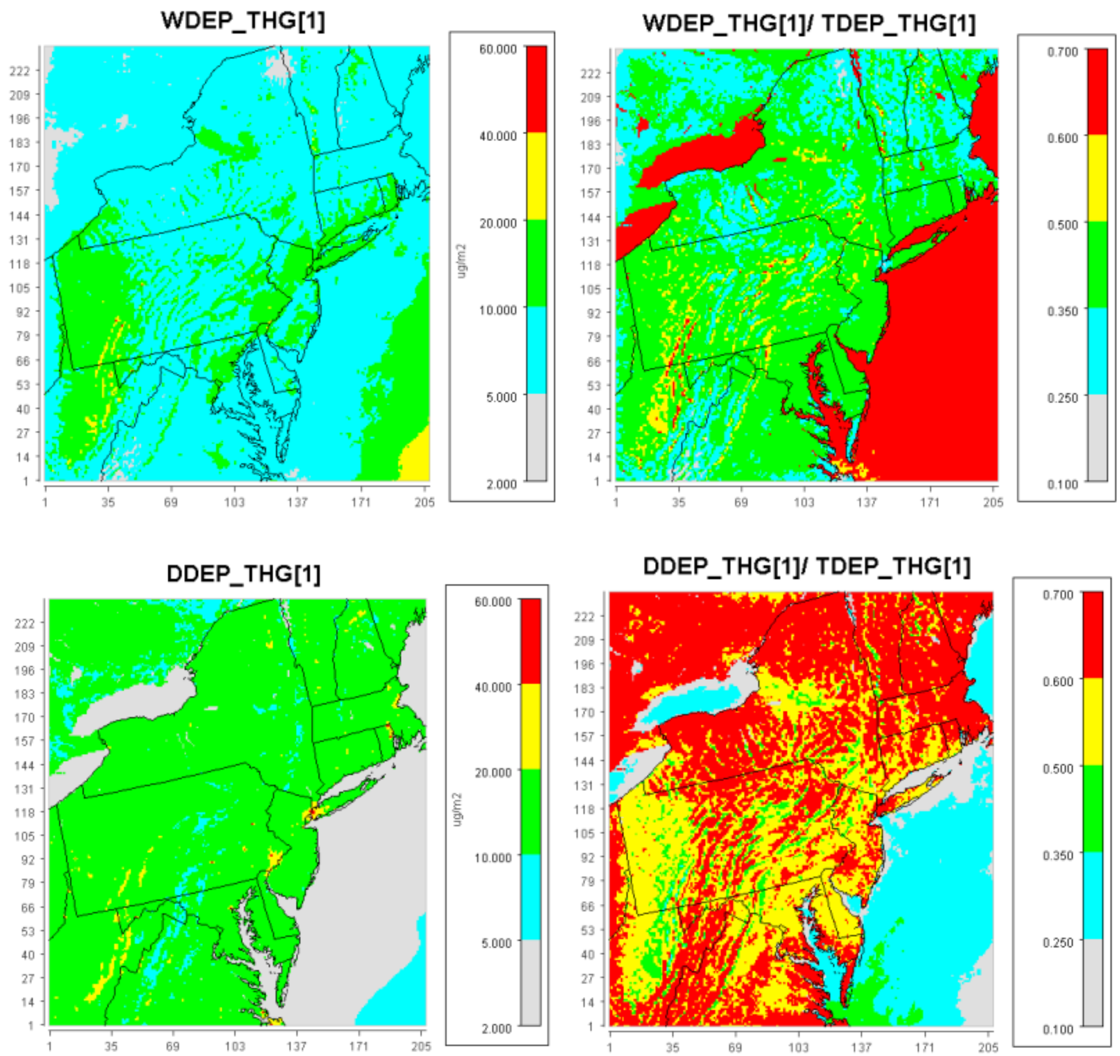

The Hg2 fractional plots similar to those for THG are presented in Figure 5-17. In this instance, it is noted that the dry and wet components over the whole domain and in NYS have larger gradients, but essentially contribute equally to the total Hg2 deposition. The larger dry deposition contribution to the THG plots in Figure 5-17 was determined to be due to the dominance of the dry component for the elemental (Hg0) mercury (not shown), which has an important contribution to the THG values.

Figure 5-17. Annual wet fraction (left) and dry fraction (right) of Hg2 for the base case

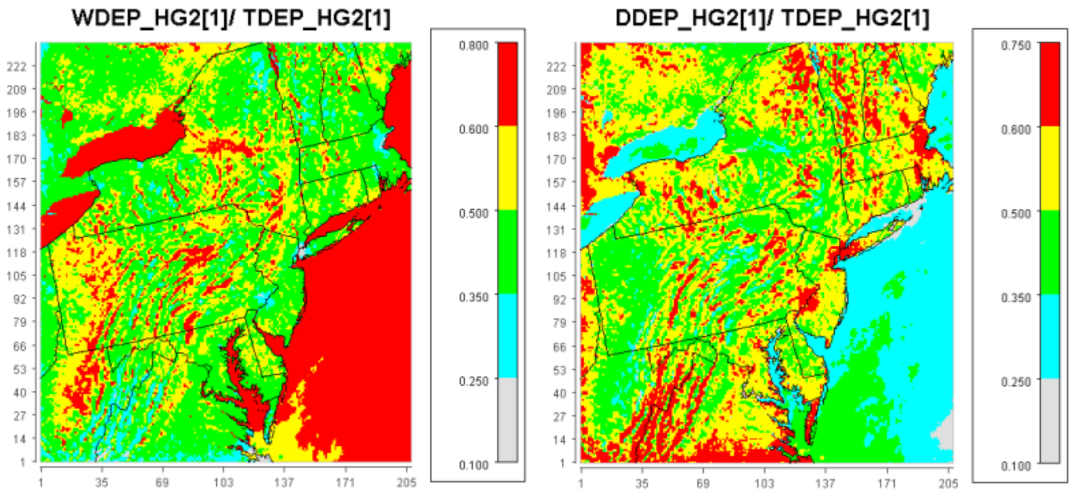

To determine possible seasonal effects on the annual results, maps for the summer and winter months were generated. For total mercury (THG), the results indicated the same level and pattern of impacts for the two seasons. The summer map is presented in Figure 5-18, with the winter plot being very similar (not shown). It is determined that unlike sulfate deposition, no distinct differences are projected by CMAQ for the different seasons, with all contributing essentially the same levels to the annual results. Plots for the Hg2, the largest contributor to THG, show the same seasonal results. However, there is a distinctly higher Hg2 wet deposition in the Catskills area vs. northern sector of NYS, as seen in Figure 5-18, which is similar to the SO4 results above.

Figure 5-18. Summer total mercury (THG-left) and summer Hg2 wet fraction (right)

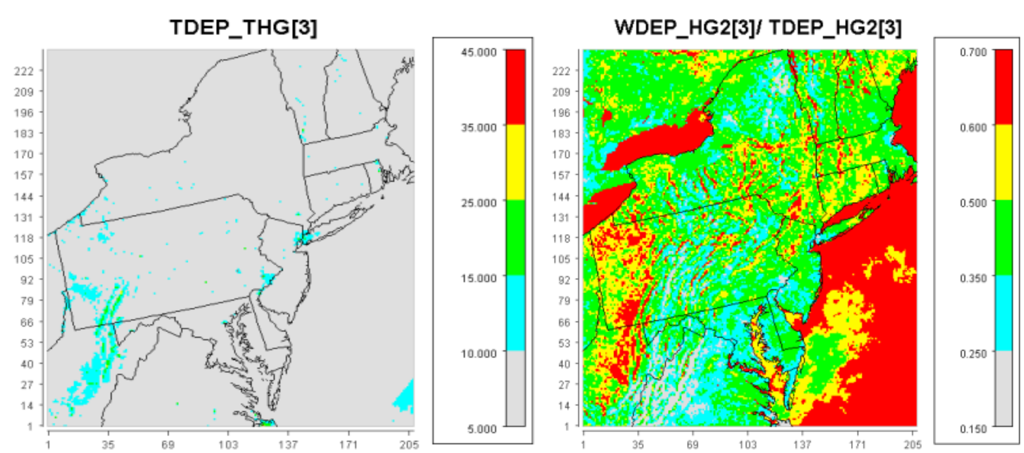

A comparison to other recent CMAQ simulations of mercury deposition supports the general findings of the study. Some of the simulation studies were on much larger areas and scales or have made adjustments to the modeling inputs and results, or only provide total deposition, such that a full comparison to the study results is not feasible. One example of a similar CMAQ simulation is the EPA national modeling of Hg by CMAQ[7] which used a previous version without some of the updates in the current study version. The CMAQ simulations in the EPA study indicated the dominance of the oxidized gaseous form for the total deposition similar to the current findings, although the assumption was made that the wet deposition of the Hg0 was nil. However, this is not a significant factor for the comparison since wet deposition of Hg0 was noted to be relatively small in this study. In addition, deposition of Hg0 was higher than for the HgP, as in the current case. Seasonal total Hg deposition indicated some variations, with summer showing lower levels, but this could be due to the omission of wet Hg0 deposition in the EPA CMAQ simulations.

The next set of plots deal with the issue of the NYS power sector and other large point source contributions to the overall levels. As in the case for acidic deposition, the relative difference was calculated between the base case and the "zero out" case with results normalized by the base case. In addition, these results were again confined to the NYS and adjacent area since impacts from the power sector was not seen outside this area. It was anticipated that, similar to the acidic deposition results, the general plots for the zero out case would be very similar to the base case. This was in fact noted in sample plot for THG and Hg2, which are not presented. Instead, Figure 5-19 shows the relative difference in deposition for the annual as well as for the wet and dry component of Hg2 over the NYS area of the CMAQ domain. The differences on the annual levels are contributed to by both the wet and dry deposition differences, but are clearly dominated by the dry component. No differences are noted on the same scales for Hg0, but differences are noted for the dry component for HgP and are shown in Figure 5-20.

Figure 5-19. Relative difference in annual total (top), wet (bottom left) and dry (bottom right) Hg2 deposition between the base and "zero out" cases

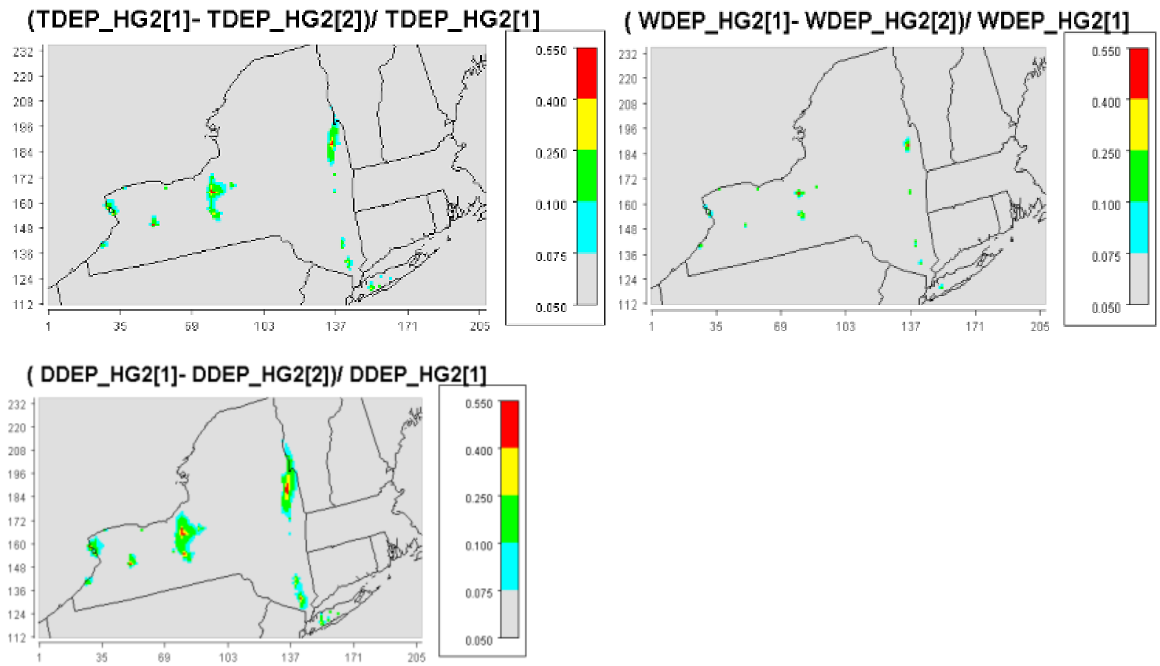

Figure 5-20. Relative difference in HgP deposition between the base and "zero out" cases

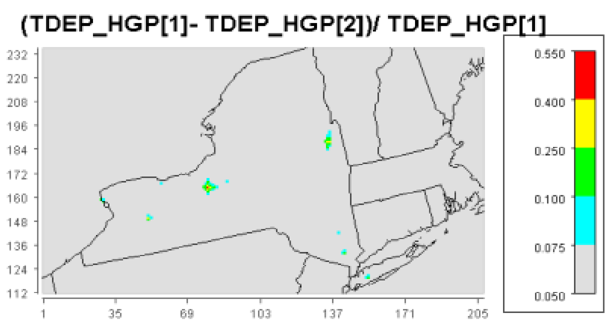

These results, especially for Hg2, are transferred to the THG differences since the former species has the larger contribution to total mercury levels. The relative difference plots for THG on an annual level and its dry component contribution are shown in figure 5-21. These relative differences are depicted on the same scale as those for acidic deposition species in the previous section. A comparison of the two forms indicates generally the same areas of reduced deposition for total mercury and total sulfur as a result of mainly the dry component of Hg2 and SO_2, respectively. However, the areal extent of the mercury reductions due to the elimination of emissions at the power sector point sources is considerably less than for acidic reductions. This is partly due to the NYS source Hg emissions and impacts being much smaller than the total overall emission and deposition modeled. It is also the case that some of the sources that contribute to reductions in Hg deposition are different from the modified coal plants, as a review of Table 4-10 and the maps of relative differences would indicate. That is, the WTE sources with large Hg emissions reductions (Hudson Falls, Westchester) are likely contributors to the localized Hg deposition reductions.

Figure 5-21. Relative difference in total annual (left) and dry component (right) of THG deposition between the base and "zero out" cases

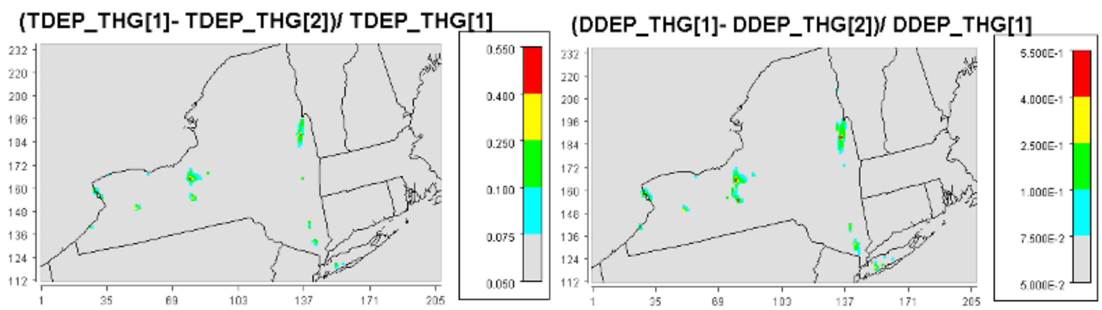

These results for mercury deposition are another indication of reductions in deposition levels around the facilities with relatively high emissions, which have reduced emissions since the 2011 NEI base case. These reductions are also reflected in the future case 2018 inventory and their consequences are further discussed in Section 5.4.

5.3 Comparisons of CMAQ to observed 2011 wet deposition

An important consideration in using model predictions for policy guidance and decisions or research approaches to specific pollutants is an evaluation of how well the model performs against actual observations. These evaluations range from detailed "validation" performances with adequate monitor coverage around single or multiple sources in a limited area to instances of long-range transport from regional scale emissions with limited spatial or temporal monitoring data. In the case of regional scale modeling of acidic or mercury deposition, additional factors come into play that make model evaluations much more difficult even beyond the significance of basic model limitations due to uncertainties in emissions, chemical and physical transformations, and transport simulations. Specific for the current study of deposition, two considerations related to the monitored observations must be understood before model evaluation results are understood and used.

First, there cannot be any substantive and adequate evaluation of total deposition of acidic or mercury deposition due to lack or robust and detailed observations of the dry deposition component. As noted in the previous sections, the dry component is projected to be a significant fraction of the species, as well as total acidic and mercury deposition. As such, its observations are essential for model testing. The second limitation to monitoring data is the relative sparsity of the locations over the rather large geographical area of simulations and is, understandably, due to practical consideration of both the number and location of where monitoring is undertaken. In addition, available data of wet deposition is based on extraction of specific component for acidic deposition (for example, the sulfate ion) or to total mercury in precipitation, which limits the modeled species to be evaluated. Attempts to monitor dry deposition or its surrogates have a number of limitations that have been discussed in the literature and will not be addressed herein. At times, the dry deposition component is only an estimate using observed concentrations of the pollutant to which modeled dry deposition velocity is applied.

In instances where dry deposition data is used for model testing, the approaches are essentially the use of passive sampling methods of the species/surrogates or the collection of litterfall or throughfall under a forested area surrounded by an open area where "background" wet deposition is used to adjust the former in calculating the "dry" component. For example, the use of passive samplers and their limitations is discussed in a recent attempt[76] to determine source areas of mercury. Other examples have used Hg litterfall data for comparison to dry deposition estimates and recognized the qualitative nature of such an assessment[77] or have used throughfall data to compare to modeled estimates of sulfur and nitrogen data with the recognition of the former representing a lower limit to the modeled results. Furthermore, these studies and others note the rather site specific nature of these data and the fact that such data is limited to forested lands, with the rest of the area in need of model estimates[78] of dry deposition.

Thus, CMAQ predictions of wet deposition of sulfate, nitrate, ammonium, and total mercury were compared to available observations at monitors throughout the modeling domain from the National Atmospheric Deposition Program (NADP), Mercury Deposition Network (MDN), and NTN/AIRMON (National Trends Network/Atmospheric Integrated Research Monitoring Network) sites. In addition, WRF projected precipitation data were compared to data from these same sites. Only concurrent and valid data of chemistry and precipitation from each site were used in the comparisons. The locations of the sites used are depicted in Figure 5-22. Data from 47 NTN/AIRMON and 27 MDN sites were used, including precipitation totals, to generate season and annual (i.e., 11-month) accumulated deposition of various species. It is seen that monitor locations in NYS are relatively limited, especially for mercury with only four sites. Thus, spatial coverage of the large geographic area is limited and very likely not chosen to reflect areas of projected high impacts, but rather sensitive areas of interest to the research and regulatory groups.

Figure 5-22. Locations of NADP mercury and acidic deposition sites for model comparisons

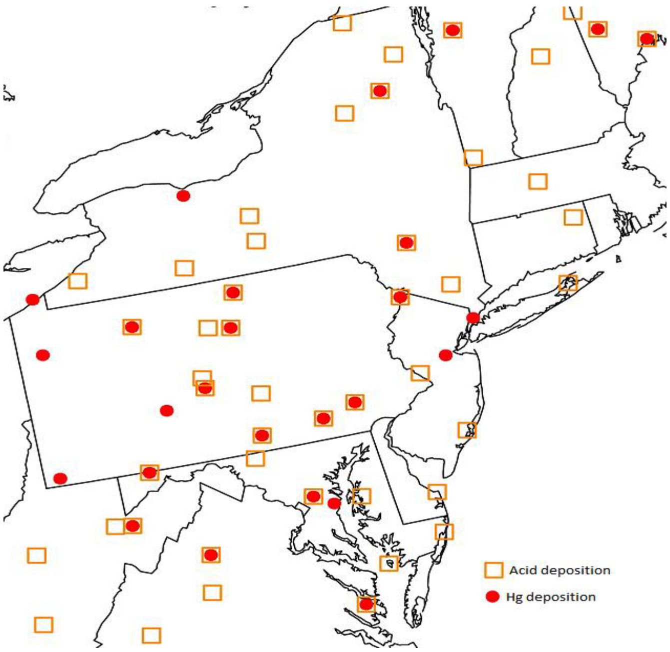

The data from these sites for 2011 were used to generate seasonal and "annual" deposition and precipitation and compared to corresponding CMAQ predictions. Again, these values are the cumulative deposition of a species over the timescales noted. Figure 5-23(a) presents the seasonal and annual sulfate (SO4) wet deposition comparison, while 5-23(b) presents the seasonal nitrate (NO3) and ammonium (NH4) results. The corresponding annual results for NO3 and NH4 are similar to the SO4 plot and are not shown. The results of comparisons indicate a general underestimation by CMAQ of observed wet deposition for all acidic deposition species on an annual level which appears to be driven by the clear underestimation during the summer and, secondarily, by the spring results. Comparisons during the fall and winter seasons appear to be much better, except for NH4 where the tendency for underestimation is seen in all seasons. The latter results are no doubt partly related to the much larger uncertainties in the emission inventory for NH4 and its dominance by non-point source emissions.

The model to observed comparison for mercury at the MDN sites in the domain are presented in Figure 5-24(a) on a seasonal and annual basis, while WRF generated precipitation data are compared to corresponding observations from the NTN/AIRMON sites in Figure 5-24(b). Only concurrent valid data from CMAQ and the sites are used in these plots. Data plots for precipitation at the more limited MDN sites are not shown, but are similar to the NTN data results. The CMAQ to observed comparison for Hg is strikingly similar to the acidic deposition results on the seasonal and annual levels, with the highest observed deposition in the summer and spring months which leads to the annual underestimation. It is also seen that the Hg spring/summer plot is an improvement over the similar plot in Figure 5-1due likely to the inclusion of the convective precipitation option in the final CMAQ run. Figure 5-24(b) indicates a similar pattern of underestimation of precipitation by CMAQ and the seasonal negative bias for the warmer months. The overall results are a clear indication of the essential aspect of WRF/CMAQ underestimation of precipitation which no doubt has an effect on the corresponding underestimation of acidic and mercury species.

Many of the previous studies summarized in Section 2 essentially confirm the tendency of WRF/CMAQ to underestimate precipitation and wet deposition. However, more recent EPA studies with CMAQ indicate either good comparison to observations or an overestimation of precipitation, specifically in the summer months for eastern U.S.[79] However, in the latter study, the corresponding wet deposition of sulfur and nitrogen are predicted to underestimate observations that indicate a more complex reliance of the predictions on precipitation as well as other factors. The tendency for the underestimation of precipitation, especially in the summer months, is likely a result of the poor performance of WRF in simulating smaller scale convective activities. As noted in Section 3, although this study invoked the subgrid scale convective option in the simulations based on preliminary results, it is clear that WRF still has trouble simulating the details of such conditions. Another possible factor for the poor performance might be the ability of CMAQ/WRF to simulate the in cloud transformations and resultant deposition. However, a check of the monitor locations for at least all of the NYS sites shows elevations below 850 m, which is well below the heights at which cloud scavenging has been demonstrated to play an important part in deposition observations.

Figure 5-23. Comparisons of CMAQ to observed wet deposition of SO4, NO3 and NH4

(a) **(b)**

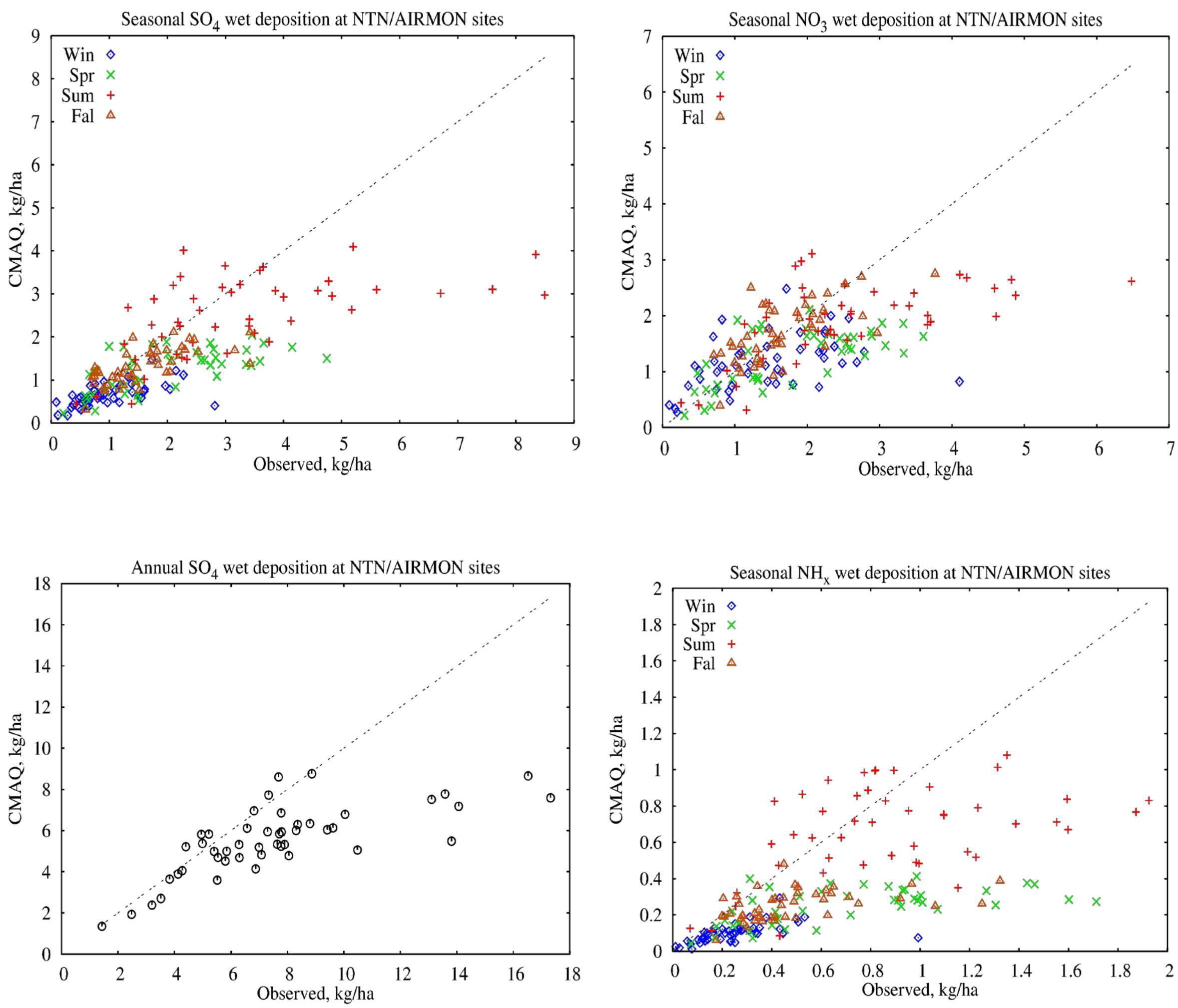

Figure 5-24. Comparisons of CMAQ to observed wet deposition of Hg at MDN sites (a) and precipitation at NADP NTN sites (b)

(a) **(b)**

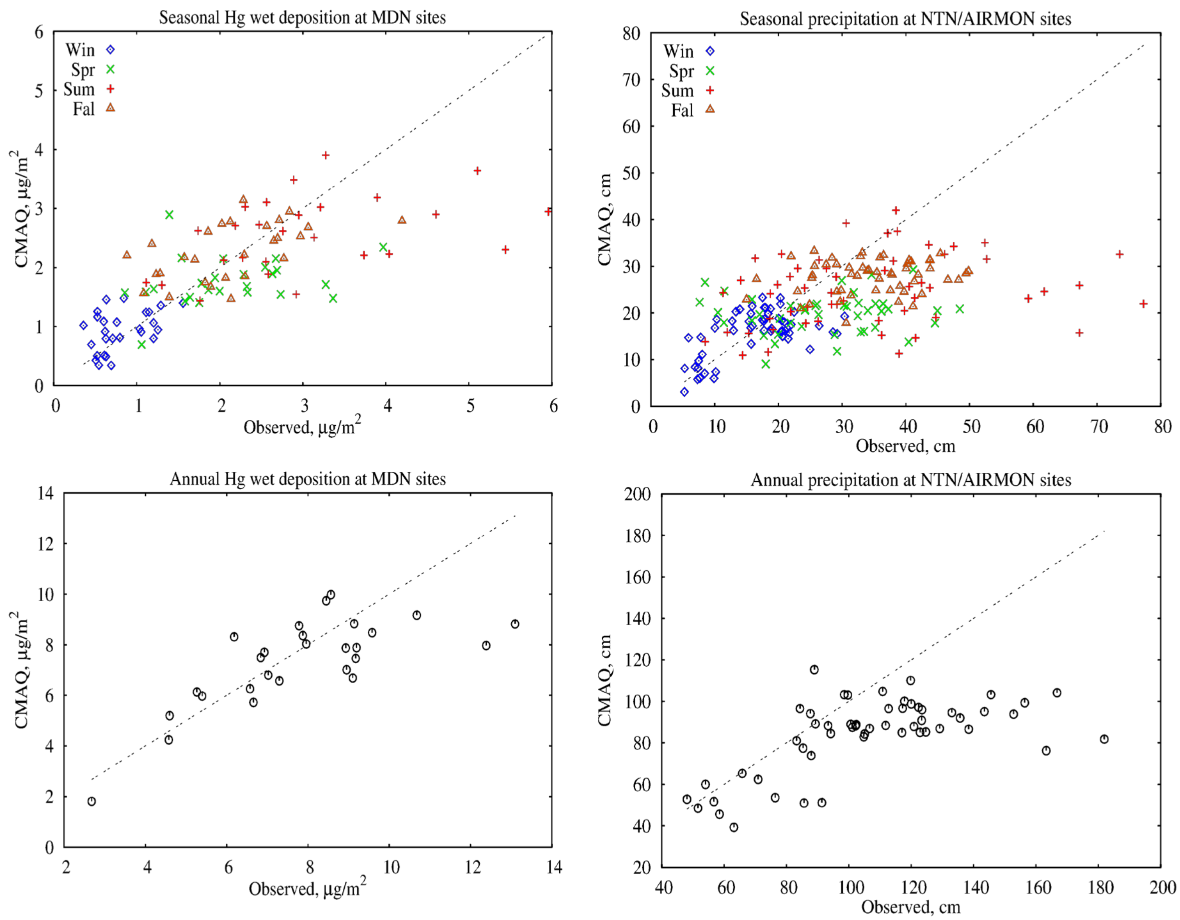

It is also important to keep the ability of CMAQ to simulate acidic and mercury deposition in perspective. The statistics of normalized mean error (NME) and normalized mean bias (NMB) for each season and on an annual level are presented in Table 5-1 for SO4, NO3, and precipitation at the MDN and NTN sites. These statistics give the model's ability to simulate observations in the mean and indicate whether the simulations are underestimating (negative NMB) or overstating the data. The statistics for precipitation at the MDN and NTN sites are about the same which is a good indication of consistency between the networks. Although the highest observed levels occurred in the summer months, model statistics are generally poor in the spring season and the best during the fall months.

On an annual basis, CMAQ simulations are all within 30 percent of observations, with the lowest bias of -6.5 percent for mercury that is somewhat surprising from the standpoint of the relative uncertainty in the emissions inventory. However, a number of other important factors come into play such as the number of monitors and their locations as well as the physical and chemical processes in CMAQ simulations. The NME and NMB for most cases are comparable which indicates that there is more consistent underestimation since NME is defined as the sum of absolute differences while NMB as the sum of negative or positive values. To the uninitiated in modeling assessments, these results might be considered poor, but from the standpoint of the modeling community, these results are remarkably good. It is beyond the current study to detail the number of uncertainties in input data and those inherent in model formulations and evaluation schemes, coupled with expectations in simulating the dynamic and turbulent dispersion system on the regional scales. The study statistics are on par with results noted in more recent studies[3, 80] for acidic deposition using CMAQ on both a 12km and 36km grid resolution studies, but appear to be somewhat improved over studies[8,81] for mercury deposition. However, the latter should not be viewed as demonstrating better model performance using the more refined 4km grid and the latest emission inventory. CMAQ results are not available for the same 2011 NEI on a 12km grid resolution for a proper comparison to the current results. However, previous CMAQ modeling with another EPA 2011 NEI that was generated by the EPA based on significantly different assumptions on the important source categories such as the EGUs was compared to the current results for the various deposition species in Table 5-1 on an annual basis. The model statistics using the current 4km refined grid did not improve on the statistics from the 12km CMAQ modeling, but no detailed comparisons or inferences can be made.

Table 5-1. Statistics of seasonal and annual CMAQ to observation comparisons

NME is normalized mean error and NMB is normalized mean bias

	Winter	Spring	Summer	Fall	Annual
SO_4 wet deposition	NME = 40.7% NMB = -34.7%	NME = 44.2% NMB = -38.7%	NME = 35.7% NMB = -23.4%	NME = 26.6% NMB = -16.9%	NME = 29.6% NMB = -27.3%
NO_3 wet deposition	NME = 41.7% NMB = -20.5%	NME = 40.0% NMB = -30.2%	NME = 35.6% NMB = -23.5%	NME = 21.6% NMB = 1.5%	NME = 22.8% NMB = -18.8%
Hg wet deposition	NME = 34.4% NMB = 15.1%	NME = 30.9% NMB = -16.2%	NME = 28.7% NMB = -15.3%	NME = 23.8% NMB = 6.4%	NME = 15.8% NMB = -6.5%
MDN precipitation	NME = 27.3% NMB = -0.7%	NME = 41.0% NMB = -28.2%	NME = 42.0% NMB = -21.9%	NME = 23.4% NMB = -20.9%	NME = 23.5% NMB = -19.7%
NADP precipitation	NME = 26.1% NMB = -2.9%	NME = 39.1% NMB = -26.7%	NME = 39.2% NMB = -27.6%	NME = 25.8% NMB = -19.8%	NME = 23.4% NMB = -21.2%

One aspect of the CMAQ simulation comparisons for the summer period further investigated was the possible influence of meteorological events such as tropical storm Irene on both the precipitation and wet deposition. Data from certain NYS monitors indicated that some of the higher acidic deposition and precipitation occurred during the summer months. Thus, two monitor sites in NYS were used to plot the weekly sulfate, nitrate, and precipitation totals; one from the western area of the state (Chautauqua) and one in the eastern part near Catskills (Biscuit Brook). The path of Irene was over the latter monitor area during August 27-29, but did not influence western NYS. The results are presented in Figure 5-25(a) for sulfate and (b) for precipitation. It is seen that Irene did contribute to high precipitation values at the Catskills monitor, but not at the western NYS monitor. However, the corresponding sulfate level during August at the Biscuit Brook monitor is not relatively high. Furthermore, the Chautauqua monitor experiences some of the highest annual sulfate and nitrate deposition that were underestimated by CMAQ over much of the year, but the model only had small underestimations of precipitation. These results indicate that there is a more complex relationship between the acidic deposition levels and the corresponding precipitation. This is in line with the results noted above in the EPA study dealing with mercury regional modeling of deposition.

The overall comparison results previously discussed are an indication of the ability of the regional scale models to provide acceptable simulations of deposition over large areas with refined grids. Whether the grid refinement down to 4km horizontal spacing provides a better model simulation cannot be readily answered by the available observational data bases that lack both the detail as well as all components necessary for a robust analysis. It is important to note that more refined spatial simulation of various parameters and specific pollutant deposition can be of great assistance in both policy determinations on a relative basis as well as for research projects. The inability to conduct monitoring studies on both the expansive scale, which models can simulate, and specific limitations for deposition (e.g., dry component) indicates the necessity to rely on these regional scale modeling studies for guidance in both improvements on study design and on policy decisions on practical and effective emissions reductions.

Figure 5-25. Observed and CMAQ modeled weekly SO4 (a) and precipitation (b) at two NYS monitors in 2011

(a) Sulfate

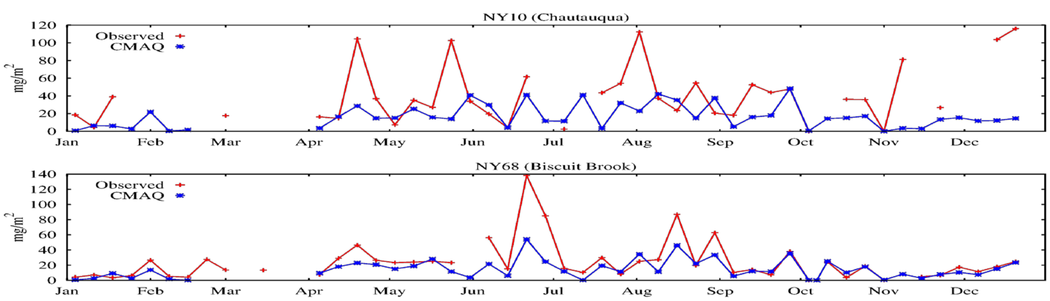

(b) Precipitation

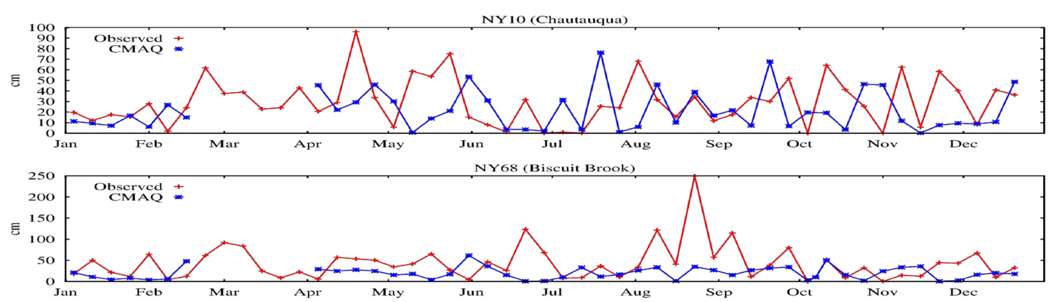

5.4 Comparison of future 2018 inventory case to the 2011 NEI base case

As discussed in the section on the inventory development, the EPA future inventories for the years 2017 and 2018 were lacking reliable mercury data, which the study had envisioned in its plans to only test the consequences of a future emissions reduction scenario on acidic deposition. Data on the acidic deposition precursors was included in the EPA NEIs, but the assumptions used in the emissions modeling resulted in a large number of coal burning EGUs assumed to be shut down in these future scenarios due to implementation of the MATs and CSAPR regulations. Since the 2017 NEI was still being finalized by the EPA as of the study conclusions, the 2018 NEI was adopted for the CMAQ modeling. As noted in subsection 4.4, the timelines for the potential shutdown of the coal plants has been delayed by court decisions. However, the purpose of the current modeling was not dependent on a specific year, but more importantly, it was to test the consequences of future anticipated reductions in emissions of acidic deposition precursors from the important source sectors such as EGUs. Thus, understanding the underlying assumptions in the 2018 NEI provided in subsection 4.4 is important in interpreting the results of the CMAQ modeling.

For Hg emissions, it was noted that the 2018 NEI had inadequate if any information on the sources of importance. Thus, the larger emitters modeled for the 2011 base case for NYS were reviewed by the DEC and resulted in projected reduction of 23 percent in total annual reductions from the EGUs and WTEs, mostly due to coal EGUs being already converted to gas burning or being shut down. No changes were noted for the "other" source category of large Hg emitters. Thus, it can be roughly estimated that this emission reduction from these sources will result in about the same level of deposition reduction and mainly in the localized areas of these sources as noted in the results of the previous section. Furthermore, based on the findings that NYS emissions of Hg and the emissions from all the sources in the modeling domain did not have a large contribution to the overall total Hg deposition, it is concluded that significant reductions in Hg deposition over NYS will likely be associated with future reductions to the overall Hg reductions outside the domain, including continental scale changes.

For acidic deposition, the future 2018 inventory was noted in Section 4.4 to result in significant emissions reductions when the associated rules are in effect. Thus, CMAQ modeling was conducted for comparison to the 2011 NEI base case to quantify potential deposition reductions. As discussed previously, however, this aspect of the CMAQ modeling was based on the 12 km NEI and the modeling grid since it was determined that the effort necessary to cast the 2018 NEI over the 4km grid was both unnecessary and impractical given the specific purpose of this testing of the future scenario. Thus, to assure a valid comparison of the future scenario to the 2011 base case, the latter emissions inventory was also modeled on the 12km grid. The modeling was used to determining the annual impacts of sulfate (SO_4=particulate SO_4 + gas phase H_2SO_4), total sulfur (TS=SO_4+1.5SO_2), nitrate (NO_3= particulate NO_3 + gas phase HNO_3) and ammonium (NHx= particulate NH_4 + gas phase NH_3) on an absolute and relative basis for the two inventory years.

The resultant annual TS total deposition for 2011 and 2018 are presented in Figure 5-26. The largest impacts for the 2011 base case is seen in the western PA and West Virginia areas, as noted in Section 5.1. Impacts in NYS are relatively lower, with the higher levels closer to the larger source areas. These results clearly show the reduction in total sulfur deposition due to the projected reductions in SO_2 emissions in the 2018 inventory associated with CSAPR and MATs rule implementations. The corresponding patterns for total NO_3 (not shown) are very similar to the TS plots for the two inventor years, showing the same general areas of maxima. The annual total NHx deposition for the 2011 base case is shown in Figure 5-27 and indicates the higher levels in the agricultural areas in PA. The corresponding plot for the 2018 inventory (not shown) is very similar in both pattern and magnitude as for 2011.

Figure 5-26. Total annual TS deposition for 2011and 2018 inventories

2011 2018

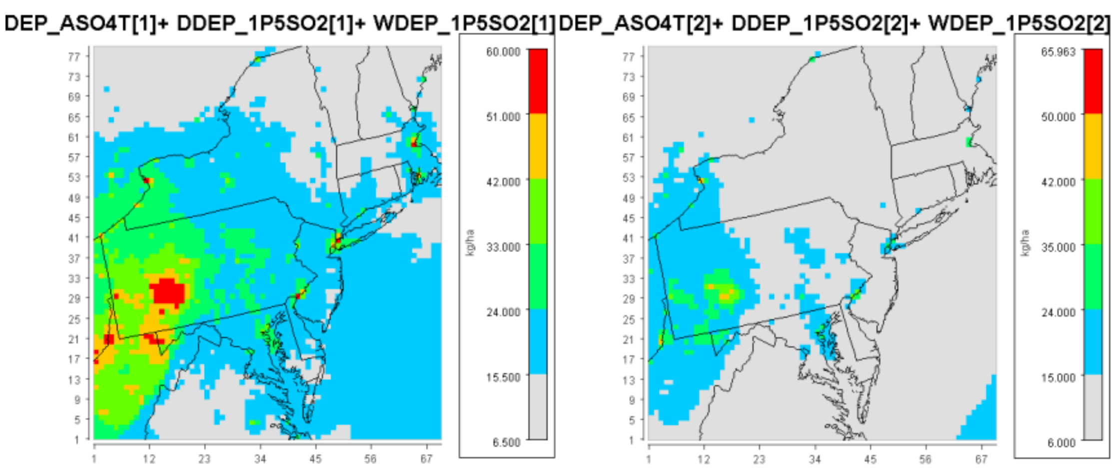

To quantify the difference in deposition between the two inventories, the “normalized difference” was calculated as the base case minus the future case, divided by the base case. This difference ratio provides the fraction of reduction from the 2011 emissions to the future case emissions and was calculated for the three acidic deposition species.

Figure 5-27. Total NHx deposition for the 2011 NEI base case

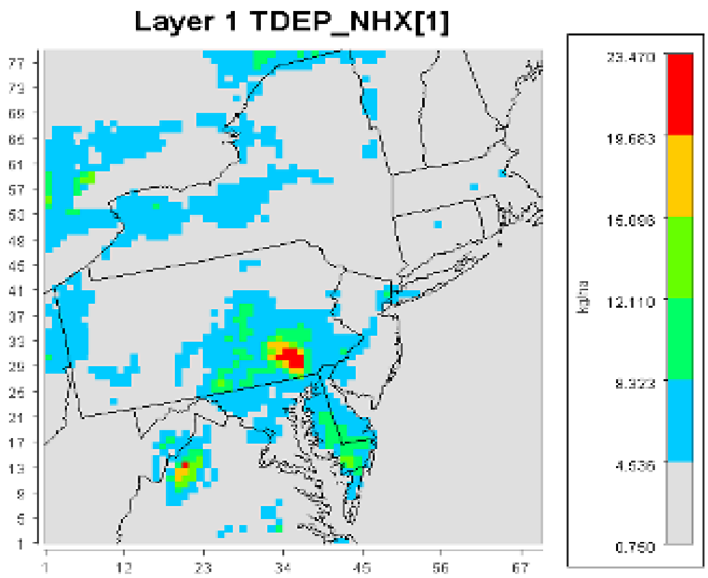

The resultant normalized differences for TS and NO_3 are shown in Figure 5-28. The results show about 40 to 50 percent reduction in TS deposition and about 20 to 30 percent reduction in NO_3 values. Recall that the corresponding emissions reductions noted in the last section were 80 and 70 percent, respectively. These reductions were found to be associated with about equal reductions in wet and dry components for TS (not shown), with slightly higher reductions due to dry deposition over NYS. For NO_3, the reductions were noted to be associated slightly more with the dry component than the wet. Results for total NH_x (not shown) indicated essentially no change in the level of impacts from the 2011 base case to the 2018 case. This is not surprising given that reductions in NH3 emissions are not anticipated from the specific rules used to simulate the 2018 emissions (as noted in section 4). However, it is clear that the implementation of the CSAPR, MATs and other rules in the future, will result in substantial improvements in acidic deposition in the modeling domain and, importantly, in NYS. Interestingly, relatively large reductions are seen for NO3 in NYS in comparison to other parts of the domain.

Figure 5-28. Total annual TS (left) and NO3eq (right) deposition difference between the 2011base case and the 2018 future case inventories

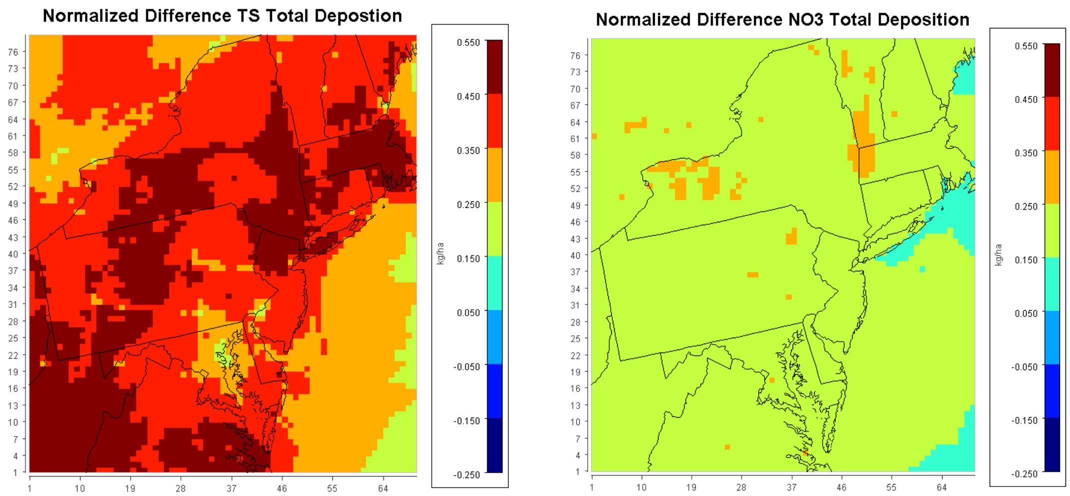

5.5 Example patterns near Whiteface and Hunter Mountains

The plots provided for the whole CMAQ modeling grid and for NYS in the last section were on scales where details on gradients at terrain features were not resolved. Thus, although the refined 4km grid provides an increased level of detail in deposition over the 12km and coarser grid projections, it is interesting to see if the refined grid provides useful gradients over complex terrain areas such as the Adirondacks and Catskills. To that end, example deposition patterns near Whiteface and Hunter Mountains were generated. The results for total (wet plus dry) annual total sulfur (TS) and for total sulfate (SO4) are presented in Figure 5-29 with the centers of the grids at Whiteface and Hunter Mountain and extending 10km from the center in all directions. Each square “block” represents one 4x4km grid area. As a reference, the AERMOD grid in Figure 3-3 covers an area one quarter of the total area in Figure 5-29, extending from the center block to the west end and one block each to the south and north. The results indicate variability in deposition in the vicinity of the two mountains and in the AERMOD grid, although the level of deposition within each block is constant as assumed in CMAQ. However, if the grid spacing was 12km, the deposition level within the nine blocks containing the AERMOD grid area would be essentially the same and one could not discern the variability shown by the 4km grid. The patterns indicate that higher levels are projected in cells mainly south of Whiteface peak, while for Hunter, the higher levels include the peak and south and east of this location. In addition, the levels of deposition for both TS and SO4 are higher in the area around Hunter as opposed to Whiteface. A check of CMAQ simulated precipitation indicates that the difference is not due to differences in wet deposition at these sites, but is likely due to such factors as proximity to source areas and associated transport winds and likely chemical transformation rates in the warmer vs. colder months.

Figure 5-29. CMAQ total sulfur (TS) and sulfate (SO4) deposition around Whiteface and Hunter

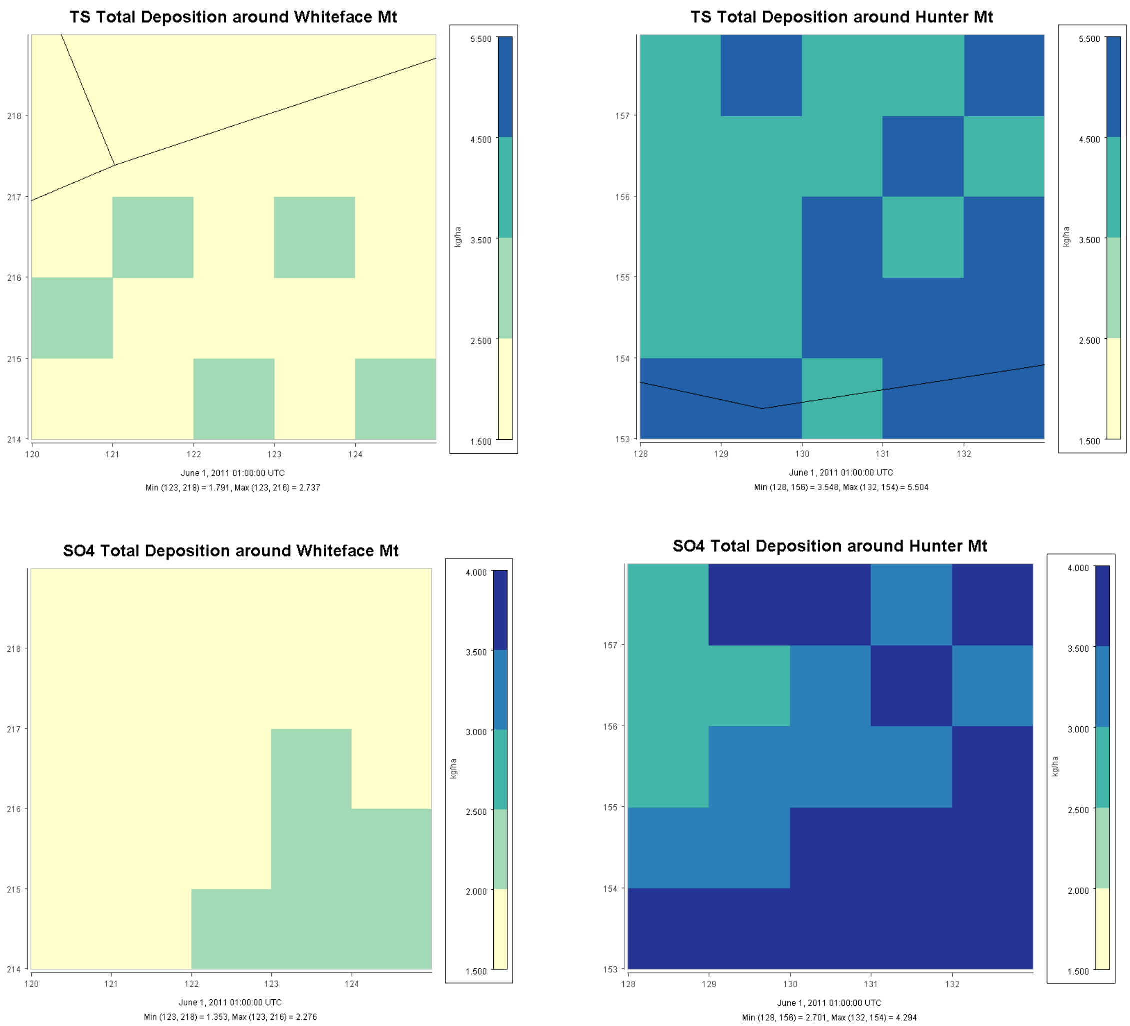

The deposition of THG and Hg2 are depicted in Figure 5-30 for the same grid areas around Whiteface and Hunter. In contrast to total sulfur deposition, these plots indicate broader areas of higher impacts, especially around Hunter, with less distinction in the levels between the two areas. The higher mercury levels are also in the Hunter peak block, but not at the Whiteface Mountain peak, but these higher impact areas are broader around the mountains than for sulfur. It is also seen that Hg2 levels make up over half of the total Hg deposition levels at both locations. Similar plots (not shown) for Hg0 and particulate mercury HgP indicates that most of the difference can be attibuted to the latter form, with Hg0 contributing little to these levels. This is in contrast to findngs in other studies, but it should be remembered that this study's results reflect only anthropogenic emission impacts and do not account for large "background" levels of Hg0 found in atmospheric concentration of mercury.

Figure 5-30. CMAQ total (THG) and oxidized (Hg2) deposition near Whiteface and Hunter

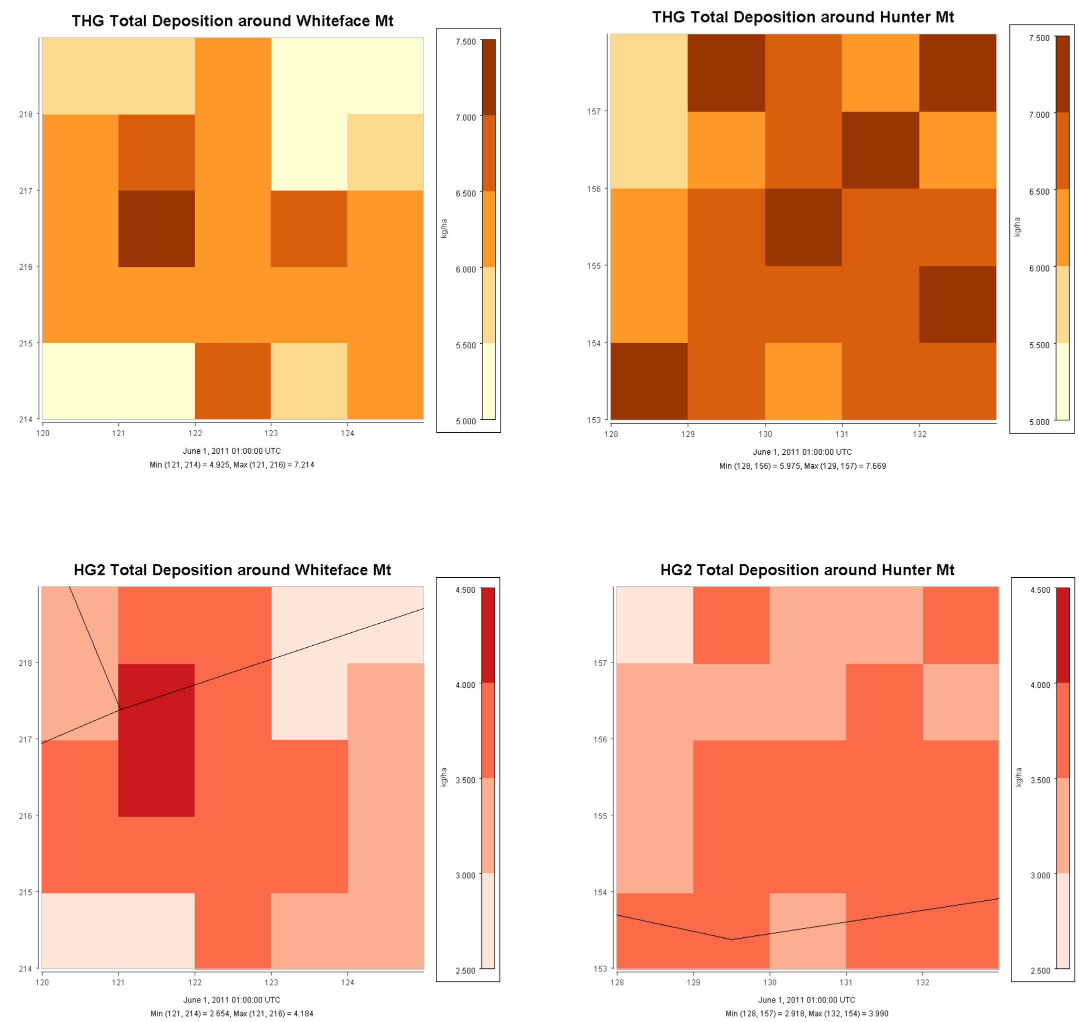

Whether these gradient patterns reflect expectations and observations is hard to assess due to the lack of adequate monitoring data on these scales, especially for the dry deposition component. In addition, observational patterns reflect total ambient loading of the species and site specific conditions at the site studied. For example, studies near Hunter[82] and Whiteface[83] have either inferred or observed gradient patterns for acidic species which generally indicate an increase in deposition with elevation, at least for certain flow directions. This has been attributed to the strong influence of in-cloud scavenging and deposition at the higher elevations,[84] wet canopy increase in dry deposition velocity[85] and the more porous coniferous trees at these elevations, coupled with the higher wind speeds and aerodynamic deposition. It is important to note that pollutant concentrations in the liquid water content are not higher at the higher elevations. Similar gradients have been found for mercury along Whiteface using surrogate litterfall and throughfall data[86] that dominate deposition in the lower and mid elevations, while cloud water is found more important at the high elevations. There are complexities that must be recognized with these results such as the decreased deposition, but not concentration with decreasing height within the canopy due to the wind speed reductions, as documented in previous studies.[87]

6 Findings from AERMOD and AERMET results

The application of the simpler AERMOD model was an attempt to check the patterns of CMAQ deposition specifically at the Whiteface and Hunter complex terrain settings on a finer receptor grid allowed by the model. However, it was clear that because of the limited number of grid points in CMAQ over the AERMOD receptor areas depicted in Figure 3-3 and as confirmed by Figures 5-29 and 5-30, there was inadequate horizontal resolution of CMAQ results to properly evaluate the projected patterns. Therefore, the AERMOD application results only provide inferred findings that might augment the CMAQ deposition pattern, but cannot be used to assess the patterns of gradients of the deposition species. The approach used in these assessments was to place a set of elevated line sources at various heights and a set of distances from the Adirondack and Catskills receptor grids as describes in Section 3. The AERMOD projections are simplification of the transport patterns over the large distances of travel in the CMAQ domain and do not account for the important physical and chemical transformation for acidic precursors and mercury species, nor for the varying fields of winds and land use in the grid areas. Thus, basic findings were limited to projected patterns for limited sources using a “unitized” emission rate for the AERMOD runs. In addition, the deposition estimates were performed for the direct deposition of the oxidized Hg component using representative parameters recommended in the AERMOD guide for dry and wet components, while for acidic deposition, the AERMOD simulations assumed sulfates already available for deposition using corresponding representative parameters.

In addition to the patterns of annual deposition, it was decided to also do limited comparisons of a set of meteorological data generated by the AETMET processor for the AERMOD runs and those generated by the WRF processor for the CMAQ runs. The comparison used the hourly data observed and simulated at the Saranac Lake and Poughkeepsie NWS sites for days of predicted maximum concentrations and deposition from a subset of the AERMOD runs and the corresponding data generated by WRF on these days. The AERMET generated data at the two NWS sites were compared on sample days of 24-hour maxima predicted by AERMOD to corresponding WRF simulations at CMAQ grid locations nearest these NWS sites and, in addition, near the peaks of Whiteface and Hunter Mountains. The basic purpose was to see if and how the expected variability in flows in these complex terrain settings was represented by the NWS vs. the WRF data.

6.1 AERMOD deposition patterns

As described in Section 3, two actual sources from the NYS point sources in Table 4-5 near each of the AERMOD grids were simulated mainly for Hg (2) concentration and deposition patterns. In addition, a set of generic line sources at various heights and distances from both the Adirondack and Catskill grids were modeled. The line sources were mainly placed perpendicular to a dominant annual wind direction such that downwind impacts would be captured for a range of directions. The sources were assumed to be at five elevations ranging from ground level (10m) to top of the average mixed layer (1,000m) to test the dispersion and transport simulations of upwind emissions and plumes into the receptor areas. A large set of simulations were performed for the two grids, ranging from each of the sources separately and in combinations to see if any similarities and differences occurred. For example, a source placed at the edge of the grid, simulating potential influx of concentrations prior to dispersion over the grid, is expected to show more gradients in impact patterns than the same source placed at tens of kilometers away, simulating a broader area of initial downwind spread of emissions prior to impacting the grid. A small number of annual sulfate impacts were also simulated to determine possible differences in deposition patters. No "cumulative" impacts were performed of all NYS point sources of interest for the obvious reasons of a number of AERMOD model process limitations in comparison to the comprehensive and refined analysis performed by CMAQ for all sources in the modeling domain.

The set of AERMOD runs were reviewed and the resultant patterns were found to match general expectations from this simplified analysis, but a few interesting results were revealed and examples of some of these are presented. The set of NYS point sources of main interest to the study were depicted previously in Figures 4-5 and 4-6 which indicated that these sources are either relatively distant or not upwind of the Adirondacks and Catskills grids on an annual wind flow basis. Sample of two of these actual sources were modeled for the two grids; Hudson Falls (nearest) and Cayuga (aligned with general southwest flow) for the Adirondacks and LaFarge and Danskammer (at same distances of about 70km) for the Catskills grid, but with the latter in one of the dominant flow directions according to the Poughkeepsie wind rose. It is recognized that the distance of the Cayuga facility (270km) is well beyond AERMOD's applicability, but the only purpose here was to see the horizontal pattern of deposition projected at this large distance. Some resultant concentration and deposition patterns were reviewed and examples are depicted in Figures 6-1 to 6-3.

Figure 6-1 was generated using the EPA's AERPLOT routine and presents the pattern of Hg2 annual concentrations at each of the Adirondack AERMOD receptors as color coded impacts. No legend is provided for these impacts since the absolute levels are not meaningful due to the normalized emissions, but the "scale" of impacts range from the highest in red to lowest in light blue. What was noted in this and in most other cases was that the total deposition pattern (not shown) was similar to the concentration pattern shown and that it was controlled by the dry deposition component. The purpose of Figure 6-1 is to indicate that there is a predicted pattern of significant horizontal gradient from east to west due to the low wind direction frequencies (Figure 3-4) from this source to the grid, located 70km SE of the grid. In addition, any winds from Hudson Falls to this particular grid seems to impact only the eastern edge with minimal impacts at the higher elevation locations such as Whiteface peak. Addition explanation is that the locations of the higher impact are found to be at terrain elevations around the plume height, a finding more clearly demonstrated in some other plots presented below.

Figure 6-1. Pattern of annual Hg2 concentrations due to Hudson Falls at the Adirondack grid

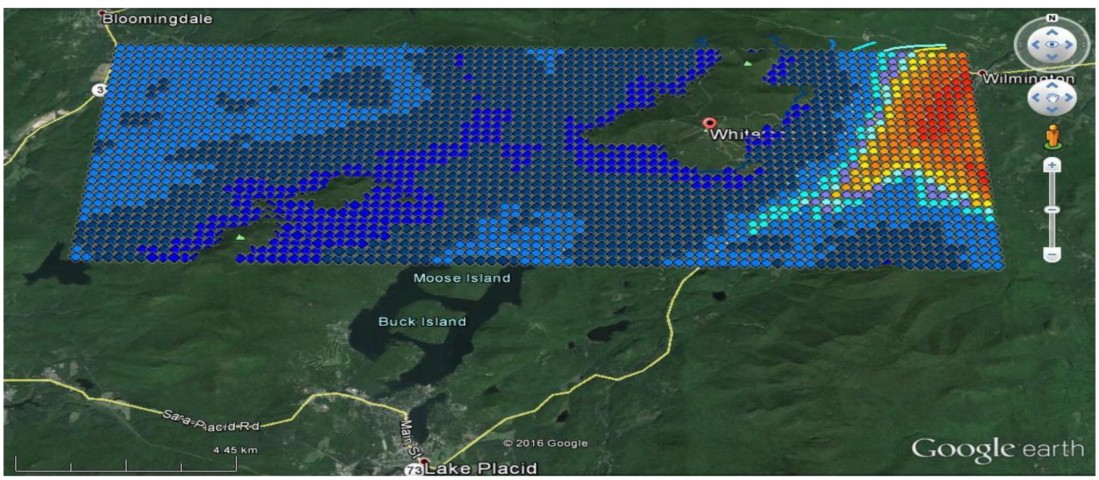

The concentration, total deposition, and wet deposition patterns for the Danskammer facility on the Catskills grid is presented in plots (a) to (c), respectively, of Figure 6-2. These and subsequent plots were generated by the Beeline's BEEST plotting software for AERMOD due to its versatility and ease of manipulation of Google map depictions within the modeling runs. These plots show lines of constant levels of impact, or isopleths, coded from reddish for high to light green for low values. The plot of dry deposition pattern was very similar to the total deposition plot and is not shown. This source is at the same distance (70km) and direction from the Catskills grid as Hudson Falls is from the Adirondack grid, except that there is considerably more wind flow to the former grid, at least as modeled by AERMOD using the Poughkeepsie wind data depicted in Figure 3-4. In this case there is a broad east-west oriented area of higher concentrations and total deposition at the northern edge of the grid, which is rather limited in "width" with a few spots of secondary higher impacts at the southern edge of the grid. The patterns for concentration and total (and dry) deposition are very similar, while the wet deposition pattern is very different, with broader maxima at the southern edge and sharp drop off to the north. The large horizontal gradients in the concentration and dry deposition field are somewhat surprising at this distance of transport, but it was noted in this case also that these higher impacts occur at terrain heights at about the same level as the average plume heights from the Danskammer facility of about 550m (msl). The closer "peaks" are likely as much a consequence of the closer distances to the facility as the terrain height effects. The location of the highest peak at Hunter Mountain is indicated by the "yellow pin" mark and is not as impacted as the surrounding areas. The influence of the simpler terrain approach in AERMOD is likely a significant influence on the pattern outcomes.

The correspondence between concentrations and total (dry) deposition follows expectations from the formulation of dry deposition methods for AERMOD described in Section 3. That is, there is a direct relationship between these two impacts dictated by the dry deposition velocity as a function of the controlling aerodynamic factor determined by friction velocity. The pattern of wet deposition presumably reflects the simplified assumption in AERMOD that at the closer distances, where concentration would be higher from the upwind source, more washout in the column of the pollutant will occur. The broad pattern also reflects the assumption in AERMOD that precipitation is the same over the whole grid. Similar broad wet deposition patterns were found for many of the sources modeled by AERMOD and it is likely due to further limitations of the wet deposition approach at these scales. A better investigation of the wet component is obviously the evaluation of the CMAQ projections using corresponding observed wet deposition data as discussed in the last section.

Figure 6-3 presents the concentration and total deposition patterns due to the Cayuga facility on the Adirondack grid in plots (a) and (b), respectively. The scale on this and subsequent maps relates to the receptor grids depicted in Figure 3-2 (approximately 2okm E-W ad 10km N-S) or as noted in the more zoomed in ones (e.g. Figure 6-5b). Although the AERMOD's steady state transport and dispersion assumptions are unlikely to hold at this distance, the projected patterns appear to still show horizontal gradients and an alignment of two areas of higher impacts with the dominant SW annual flow direction. The deposition pattern is very close to the concentration pattern, as in most other cases modeled. These results also imply that the expected well mixing in the vertical column due to the assumed reflection from the surface and top of the boundary layer in AERMOD might not be occurring even at this travel distance since impacts at elevations at or above the plume height are much less than the higher values at the lower elevations. One way to test the degree of vertical mixing was to model the impacts of five sources with varying heights (10,100,400,700,1,000m) placed simultaneously at a distance of 30km in the dominant SW wind direction with the hope of some interaction and mixing in the transport layer. The result of this run for the total deposition is presented in Figure 6-4. The patterns for concentration and dry deposition for this source scenario were similar to the total deposition depicted. AERMOD runs for some of the individual sources (i.e., 10, 100, and 700m) at this same location indicated that the total deposition maxima were due to the lower level sources, as far as the higher values at the western edge of the grid, while the high elevation source contributed to the levels around Whiteface peak.

Figure 6-2. Annual concentration and deposition patterns by AERMOD from Danskammer facility at the Catskills grid (facility 70km SE of grid)

(a) Concentration due to Danskammer at the Catskills grid.

(b) Total Deposition due to Danskammer at the Catskills grid.

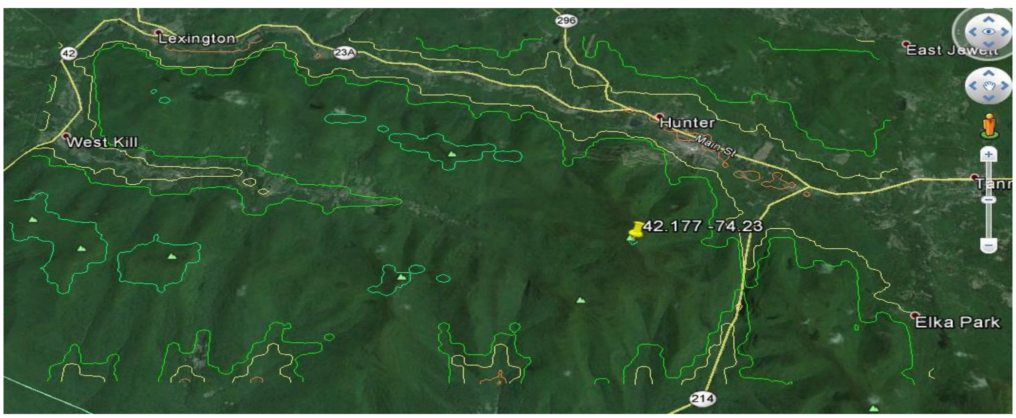

(c) Wet Deposition due to Danskammer at the Catskills grid

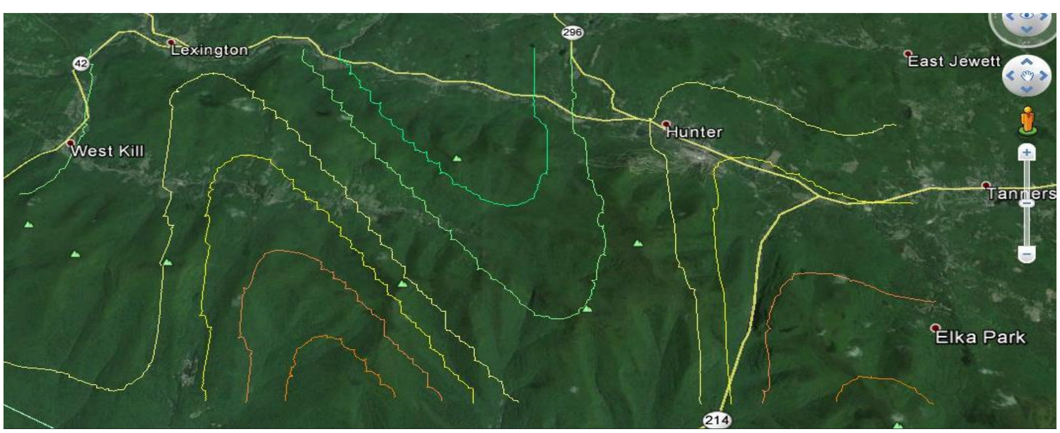

Figure 6-3. Annual concentration and deposition patterns by AERMOD from Cayuga

(a) Concentration due to Cayuga facility at the Adirondacks grid

(b) Total deposition due to Cayuga facility at the Adirondacks grid.

Figure 6-4. Total deposition from all 5 line sources placed at 30km SW of the Adirondack grid

Thus, it is inferred from these runs that for the AERMOD projections, there is limited interaction of the plumes at different layers or at least such interaction cannot be discerned from the annual patterns. A number of additional runs at various distances and source elevations at both receptor grids indicated that the lower source releases had the higher relative impacts which occurred closer to the source and at the edges of the grids with the lower terrain elevations, while the higher sources (700 and 1000m) had much lower impacts and did contribute to the peak areas of Whiteface and Hunter Mountains. These are not unexpected results for AERMOD in general due to the simplified terrain approach incorporated in the model. Another finding that is likely a result of some of the deposition formulations and assumptions was the dominance of dry deposition over wet deposition in determining total impacts at least for Hg2 species. However, in the case of emission releases at the higher elevations in the transport mixing layer (i.e., 700 and 1,000m above ground level), the total deposition was equally contributed to and, at times, dominated by wet deposition. A good example of the latter was a 700m line source placed just upwind of Whiteface peak. The predicted dry and total deposition are presented in plots (a) and (b) of Figure 6-5, respectively. The 4km line source is also show in the figure.

Figure 6-5. Dry and total deposition from a 700m source at 0.6km west of Whiteface peak

(a) Dry deposition isopleths

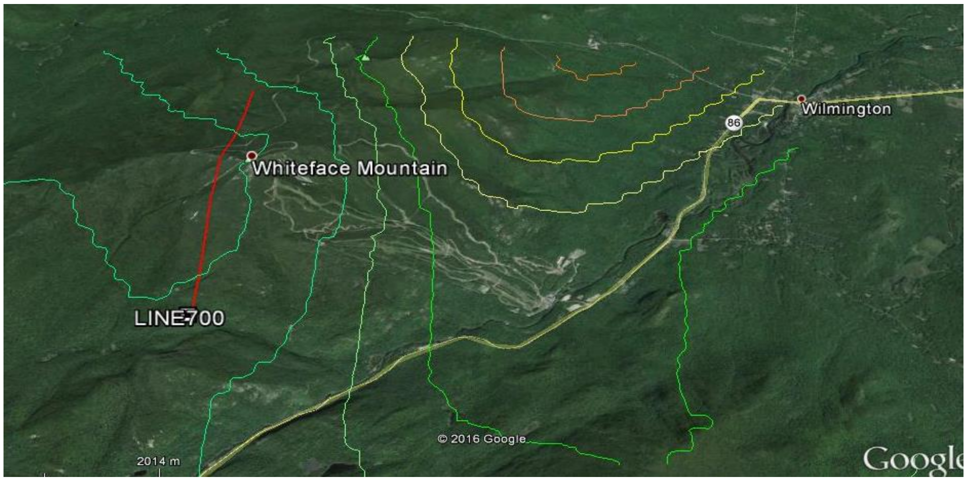

(b) Total deposition isopleths

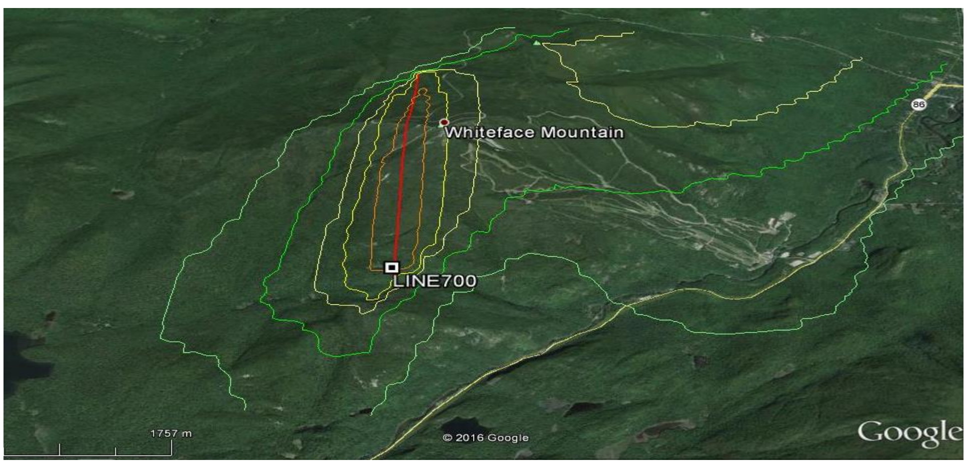

The concentration and wet deposition results (not shown) for this source configuration are very similar to the dry deposition and total deposition plots, respectively. That is, while the dry deposition shows the expected direct relationship to the concentration pattern, which is maximizes downwind of the source, the wet deposition dominated the total deposition and the resultant isopleths “surround” the vicinity of the line source with the areas of maxima. Thus, wet deposition is maximized at the closest receptors on the east and west sides of the source and is not controlled by the dominant wind flow pattern. The 700m line source at this specific location can be thought of as transported concentrations (or emissions) in the upper levels of the mixed layer as it arrives at Whiteface and deposits in its vicinity. That is, the “plume” is yet to be dispersed before impacting the surface of the mountain. These findings are of course dependent on the location of the source from Whiteface as well as the pollutant species. For example, the same pattern would not be seen for the Hg0 component since wet deposition from this source were projected to be essentially nil based on the parameters recommended for AERMOD for this mercury species. Thus, the total deposition for Hg0 resembles the dry deposition pattern.

Furthermore, other plumes transported into the grid from different distances and directions could experience a different resultant pattern for the relative maxima. Thus, as another example, the same 700m line source was placed just west of the Adirondack grid. In this case, the plume would experience an initial dispersion and deposition on the grid before it reaches the Whiteface peak area. The total and wet deposition results for this scenario are presented in plots (a) and (b) of Figure 6-6, respectively. The total deposition shows two areas of maxima; one close to and downwind of the line source and another at the elevations that are at plume level on Whiteface peak. In this case, the total deposition pattern resembles the dry deposition (not shown), except for a subtle higher secondary peak in the northwestern sector of the grid. It was determined that this was contributed to by some of the wet deposition shown in plot (b) maximized next to the source. As noted, the total deposition of other species might not experience this combined effect of wet and dry components. An example is provided in plot (c) of Figure 6-6, which is the total deposition of sulfate for the same 700m line source placed at the west edge of the grid. As seen in this plot, there is no secondary peak of maximum impacts and the maxima at Whiteface show the same pattern as for dry deposition (not shown). It is noted that total sulfate deposition is lower than Hg2 for the same nominal emission rate, while the wet deposition for sulfate is minimal as a result of using the parameters recommended in AERMOD's technical paper. As was seen previously from the CMAQ results, these simplified AERMOD relative deposition contributions could misrepresent the refined modeling results, but still provide an understanding of the level of complexities in the projected annual deposition patterns.

Further complexities which could affect these annual deposition patterns are associated with the combination of wind direction and speed distributions, the flow direction of emissions into the grid, and the relative source to terrain height considerations. A last example of AERMOD projected patterns is shown in Figure 6-7 to demonstrate this point. The dry deposition pattern from a 1000m source placed at the SW edge of the Catskills grid is shown in plot (a) while the corresponding total deposition is shown in plot (b). As for the 700m case in Figure 6-6, the dry deposition follows the concentration pattern, while the total deposition is controlled by wet deposition (not shown). However, in this instance maximum dry deposition impacts do not extend to the area of the Hunter Mountain peak, but are in the general direction of dominant SW wind flow. This result is due to a combination of the specific east to west source orientation, the relatively low westerly flows and associated transport to areas of terrain peaks in the grid similar to plume heights.

Figure 6-6. Total and wet deposition from a 700m source at 1km at the west edge of the Adirondack grid

(a) Total deposition isopleths of Hg2

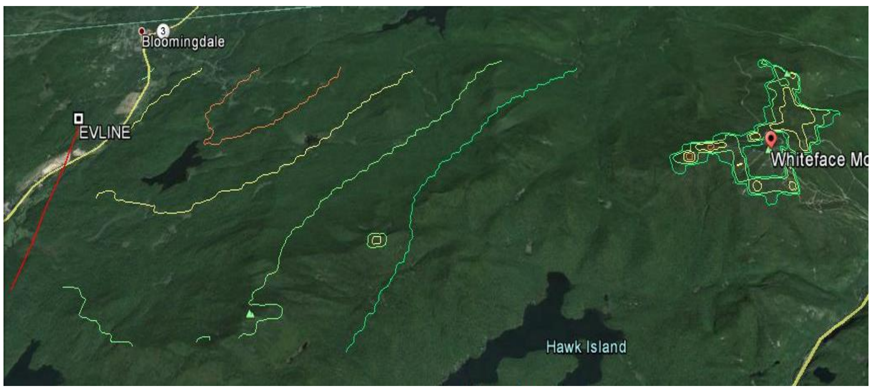

(b) Wet deposition isopleths of Hg2

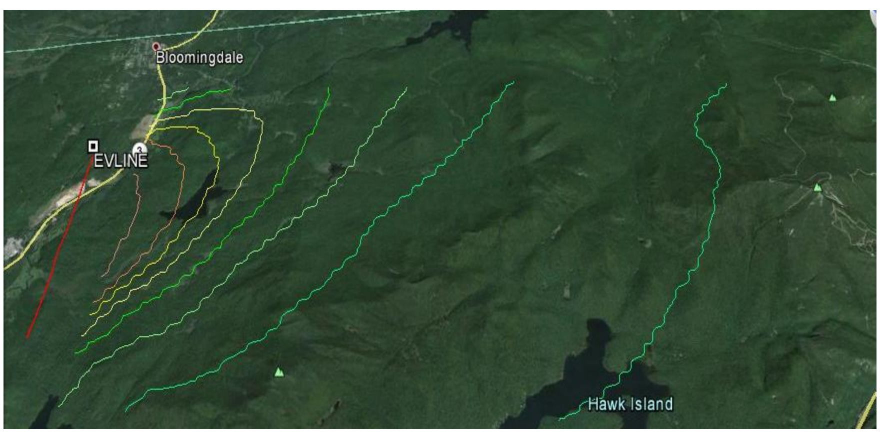

(c) Total deposition isopleths for sulfate

Figure 6-7. Dry and total Hg2 deposition from a 1000m source at SW edge of the Catskills grid

(a) Dry deposition isopleths of Hg2

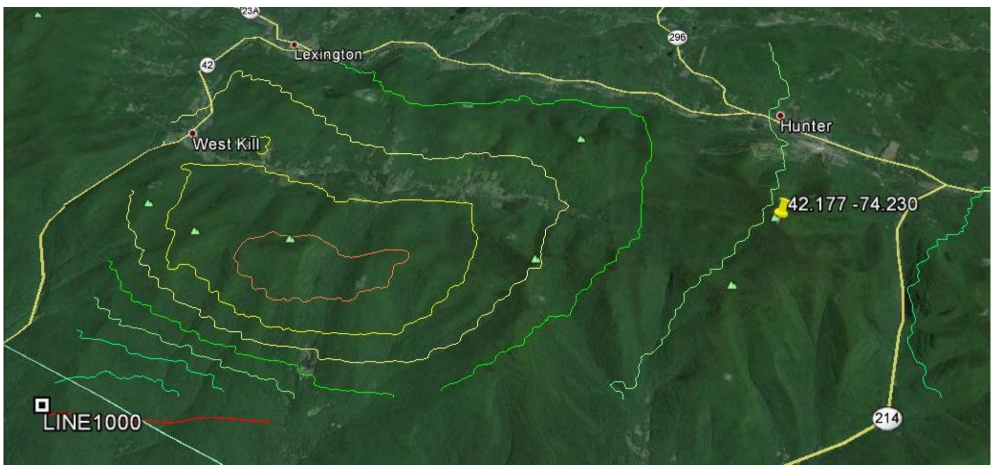

(b) Total deposition isopleths of Hg2

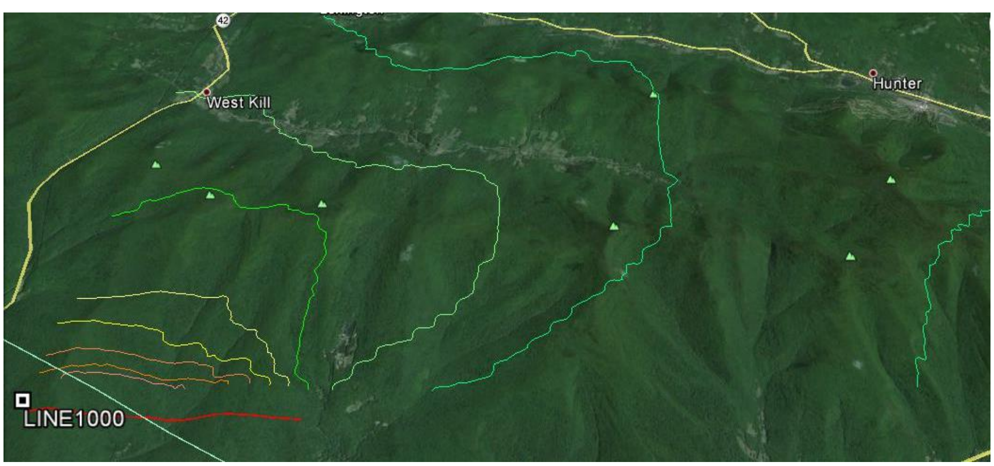

6.2 AERMET and WRF meteorology

It is important and instructive to look at sample meteorological parameters generated by the AERMET processor for the AERMOD deposition estimates to the corresponding set generated by the WRF processor for the CMAQ modeling. The simple approach taken for this comparison was to determine the days associated with maximum 24-hour concentrations and deposition for a subset of the AERMOD modeling results, and then extract the corresponding days of meteorology from the WRF 2011 data. The choice of these days was dictated by factors such as the demonstration of possible effects of variability of controlling parameters (e.g., wind speed, friction velocity, and heat flux and stability conditions), source elevation and distance differences for both the Adirondacks and Catskills AERMOD grids, and the availability of both AERMET and WRF data for the same days. In addition, the emphasis was placed on days associated with total mercury deposition and concentrations for a given source configuration since it was noted previously that in many instances the AERMOD mercury deposition results were controlled by dry deposition and the fact that the occurrence of precipitation on a given day was the essential determinant of the maximum daily wet deposition. Thus, comparisons were mainly for the oxidized mercury (Hg2), but one set of sulfate deposition conditions were also included.

A set of a dozen days of meteorology from each of the Adirondacks and Catskills results were extracted from the AERMET and the corresponding WRF 2011 data. It should first be emphasized that the mere fact of what these two data sets represent, expectations of differences in the parameters generated is a given. One of the purposes of the comparisons was to show potential spatial variability of the parameters when considered from the standpoint of the representativeness of data from a single site, such as the NWS locations, as opposed to data generated over a much larger receptor grid using available observations from multiple nearby locations, coupled with simulation of land use effects, especially in complex terrain of the two grid sets used for the AERMOD simulations. At the same time, it is important to note that the WRF generated data is an average representation of meteorological parameters over the area of the individual grid cells and not at single locations like NWS sites which accents the significance of the refined 4km grid of the current study. That is, while previous applications with a 12km grid represent data over a 144km^2 area, the 4km grid has narrowed that data representation down to a 16km^2 area. In order to compare the AERMET data for the chosen days to the WRF data, it was also necessary to locate a WRF grid point closest to the NWS sites at Saranac Lake and Poughkeepsie. In addition to these two locations, it was decided to also obtain WRF data at grid points close to the Whiteface and Hunter Mountain peaks to determine any variability in the generated data over the distances from the NWS sites to the mountains. Furthermore, for the Whiteface site, observed wind speed and direction data were available at two levels along the terrain adding further information to the comparisons.

For the two dozen days of data from the Saranac Lake NWS site (elevation 500m), the corresponding WRF generated data for the Adirondack grid were extracted from a grid point 1km south of the Saranac Lake NWS site and another grid point at 1.4km south of the Whiteface peak, with elevations of 515m and 773m, respectively, with the WRF heights representing grid average elevations. For the Poughkeepsie grid (elevation 46m), the WRF data were taken from a grid point 2km east of the NWS site and another point 1km west of Hunter mountain peak, with elevations of 75m and 802m, respectively. The WRF data was extracted by the use of the EPA's Mesoscale Model Interface Program (MMIF) run in the "AERMOD mode" that essentially transfers the WRF data to the format ready for input to AERMOD without processing it first through the AERMET program. In addition, observed wind data from two sites on Whiteface Mountain were available from the lodge site on the mountain at 604m and from the peak at 1483m. The data used for comparison were all representative of the nominal 10m height above ground where wind data is usually collected, with the rest of the parameters calculated to represent surface layer conditions. This approach minimizes the potential influence of varying vertical extrapolation and calculations schemes between WRF and AERMET and since these data are more germane to the surface deposition.

The hourly data from these sample days were reviewed to identify general similarities and differences in the basic parameters associated with the daily patterns of concentrations and deposition. Thus, inter-comparisons between days were made of wind speed and wind direction and the calculated friction velocity (u_*), heat flux (H_*) and Monin-Obukhov length (L). L is proportional to negative u_*^3/H_* and roughly represents the height above ground where buoyancy flux overtakes the influence of mechanical turbulence represented by u_*. In addition, z/L is used to determine the relative "stability" of the surface layer, with negative values during convective conditions and positive during stable conditions. When z/L is close to zero, the dominance of "neutral" conditions is implied, mostly driven by mechanical turbulence. The review of these parameters on the sample of the days associated with maximum 24-hour concentrations and deposition were mainly performed for the conditions associated with Hg2 impacts, with a limited look at the AERMOD sulfate projection cases. In general, the data indicated the complexities involved in attempting to show consistency in the set of parameters for the range of source heights and distances modeled. However, some general findings are worth noting in the context of expected relationships between meteorological conditions from these varying set of cases.

It was first apparent that for the two dozen sample days, it was the exception that the same day of meteorology was associated with maximum impacts from the varied source scenarios analyzed. In fact, there were no days which appear to be in common between those associated with concentrations and deposition, with only a few days being in common within the concentration or deposition sets. While the former is not surprising due to the varying source heights/distances, it was expected that some common days would appear for concentration and at least the total (or dry) deposition days for the same source scenarios. As noted previously, the AERMOD modeling results indicated the dominance of dry deposition in the total deposition for most scenarios. For wet deposition, some common days were noted, but this was not surprising due to the relatively limited set of days with precipitation. One interesting and consistent finding in the data was the difference in winds for the concentration vs. deposition days for a large subset of source/distance orientations.

For the Adirondack grid, example graphs were generated for the cases of the same 100m elevation line source (with 4,000m length) placed at the western edge of the grid and just west of the Whiteface peak. Figure 6-8 presents hourly wind data for the day of maximum concentration (max C-8/31) vs. total (and dry) deposition (Dt-8/24) for the 100m source scenario just west of Whiteface peak. All maxima for this case occurred at the same location, but this was not the result for many of the scenarios. The legends note sites of the data from the Saranac Lake NWS site (NWS), the two locations noted above closest to the NWS site (WRF-SL) and the Whiteface peak (WRF-WF) where WRF data was generated, and observed data at the Whiteface lodge (WF-lodge) and peak (WF-peak). The first row plots show a good match, for the days of maximum concentration and deposition, in wind speeds (U) as observed at the NWS site and as generated by WRF at a nearby site, but also the surprisingly good match with WRF data at a higher terrain location 25 km away. The corresponding wind direction (WD) plots in the second row also indicate relatively good match between the NWS observations and the WRF simulations at both SL and WF locations, considering the "artifact" graphical representation in WD as it switches around 0 to 360 degrees for a few hours in both plots. However, the wind speed plots indicate distinctly higher wind speeds associated with the total deposition vs. the concentration days. To see this more clearly, the wind speed was plotted against wind direction for each hour on both days and is shown in the third row of Figure 6-8. It is important to note that in most cases, maximum daily impacts of either concentration or deposition are associated with a subset of the hours in the day during which wind flows to the receptor at which these maxima occur. This is due to the normal diurnal dynamic flow patterns that give rise to varying wind directions.

The AERMOD results for these days indicated that both maxima occurred at a location such that flow from the 4000m long line source could contribute to the impacts with WD in the range from about 200 to 300 degrees. Figure 6-8 plots indicate that for this WD range, U for concentration averages about 1.5m/s, while for deposition case U averages above 5m/s. It is also instructive to look at the winds projected by WRF near WF and the observed data for these days from the WF lodge and at the peak. It is expected that the specific WRF simulated data is more representative of the lodge location due to the similar terrain heights (604m vs. 773m), recognizing that the former represents the "grid cell average" at a distance 1.4km away. The fourth row of Figure 6-8 provides WRF generated U and WD against the observed data at the two WF towers and also includes data from the SLNWS site on the day of maximum deposition (8/24). Observed data for 8/31 at WF were missing for many hours and were not plotted. It is important to note that the WRF simulations did not incorporate these observations at WF. The plots for both U and WD repeat the close match of WRF to the NWS data shown in the first row, but indicate that the simulated wind speeds are lower than at WF peak and higher than at the lodge. The hourly WD data indicate a closer match between WRF and observations and very good match of the observations from the two WF towers. The higher wind speeds on this day likely resulted in a "well mixed" layer and the associated match in the observations. It is expected that winds at the exposed summit of WF at an elevation of 1483m would be higher than at the other two observation towers, even if monitored at a 10m level due to its better exposure to the upwind flow. The WRF simulation and the NWS data exceed the lodge wind speeds, which was not expected.

The overall good match between observed data at the SLNWS site and WRF simulations were not consistent especially for days with lower wind speeds. An example is provided in Figure 6-9 for the days of maximum concentration (10/12) and deposition (5/23) for the case of the 100m line source placed at the west edge of the Adirondack grid. The wind speed and direction data in the first two rows indicate larger differences between the NWS data and the WRF simulations during the low wind speed day (10/12), while on 5/23 the U data and especially WD indicate a much better match, similar to the high wind speed day (8/24) in figure 6-8. There also seems to be a better match between WRF projections of wind speed and direction at the SL and WF sites compared to the NWS observations on both days. The wind speeds on these two days, again, show the higher values associated with the day of the maximum total deposition vs. the maximum concentration. In this case of the 100m source at the grid edge, the maximum deposition occurs at a location associated with the same WD range as for the Figure 6-8 case (i.e., 200 to 300 degrees), but the maximum concentration was located such that flow from around 300 to 330 degrees would be associated with hourly contributions to the maximum. The U and WD plots in Figure 6-9 for day 10/12 indicate that U of about 1m/s during these hours, confined to a few hours in early morning and late night. This was also confirmed by the WD vs. U plots (not shown) for both days. Wind speeds for day 5/23 were much higher. The data for WD also indicates that, in general, there are more hours of flow towards the maximum deposition vs. the concentration; i.e., more persistence as exemplified clearly in Figure 6-9.

Figure 6-8. Hourly wind data for days of maximum concentration (C) - 8/31 and total deposition (Dt) - 8/24 for the case of 100m source at 0.6Km west of Whiteface Mountain peak

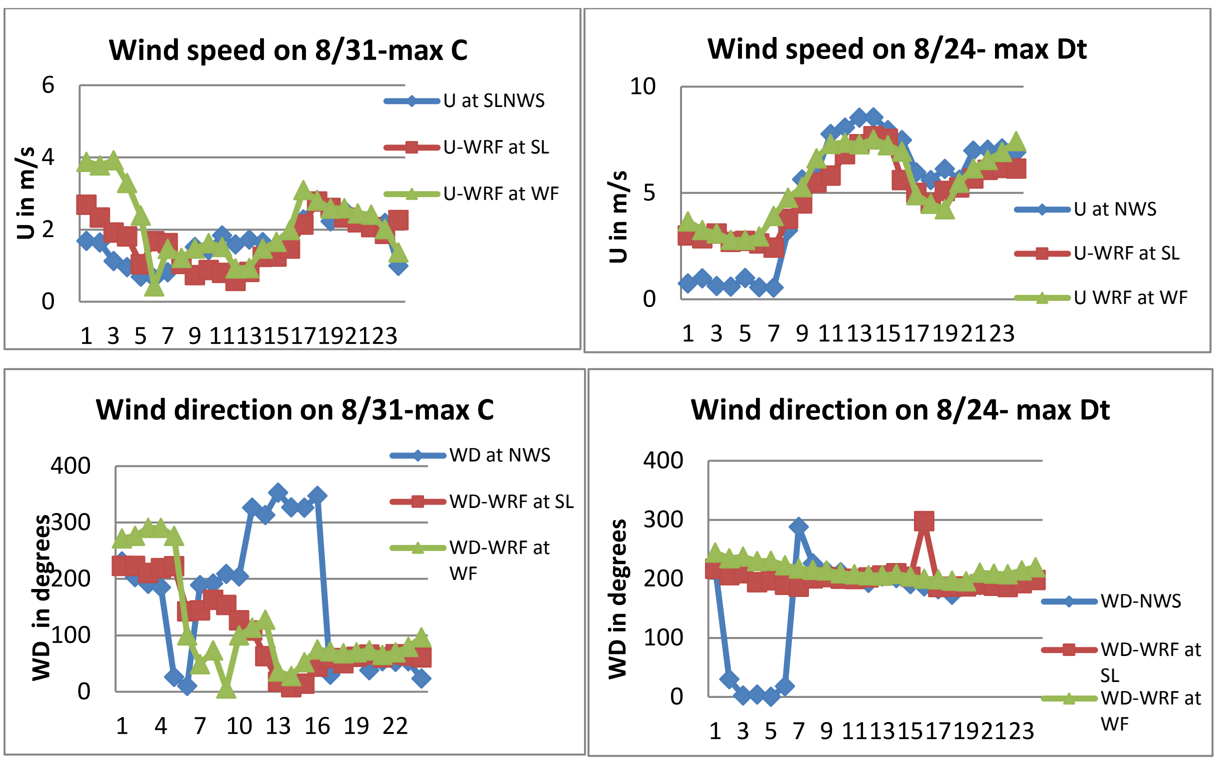

Table 6-8 continued

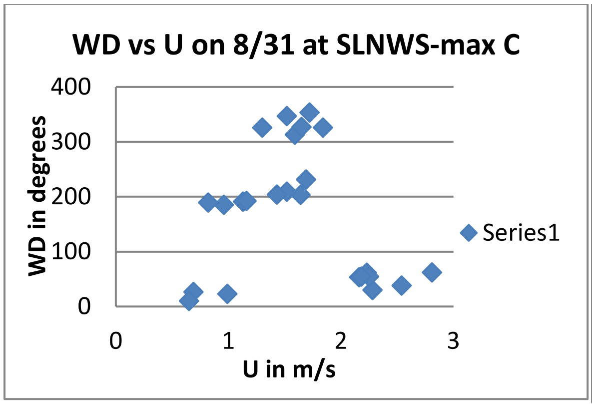

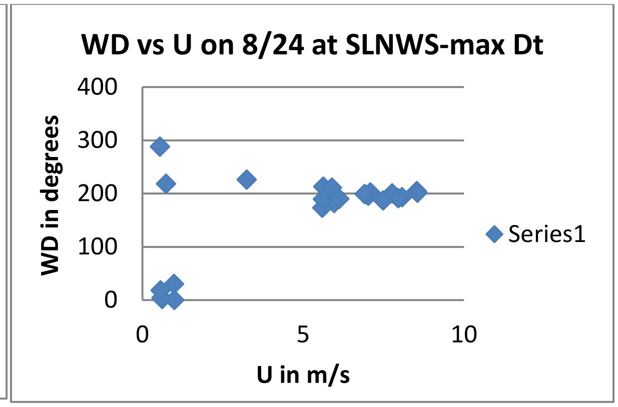

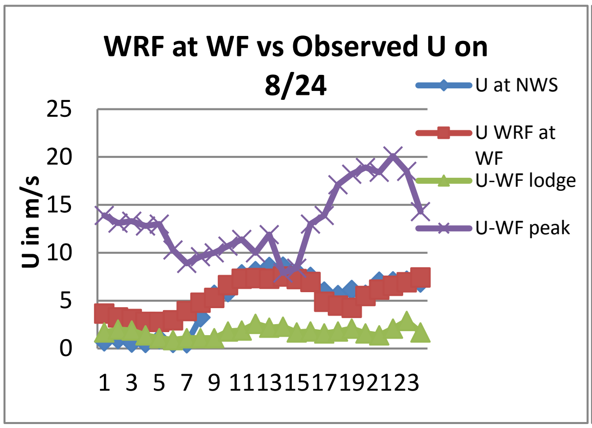

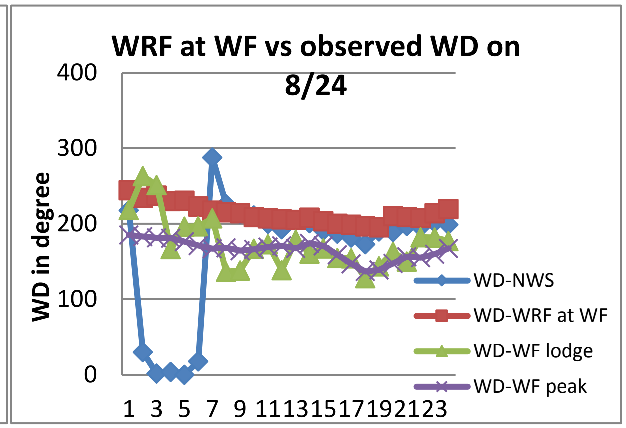

Figure 6-9. Hourly wind data for days of maximum concentration (C)-10/12 and total deposition (Dt)- 5/23 for the case of a 100m source at the west edge of the Adirondack grid

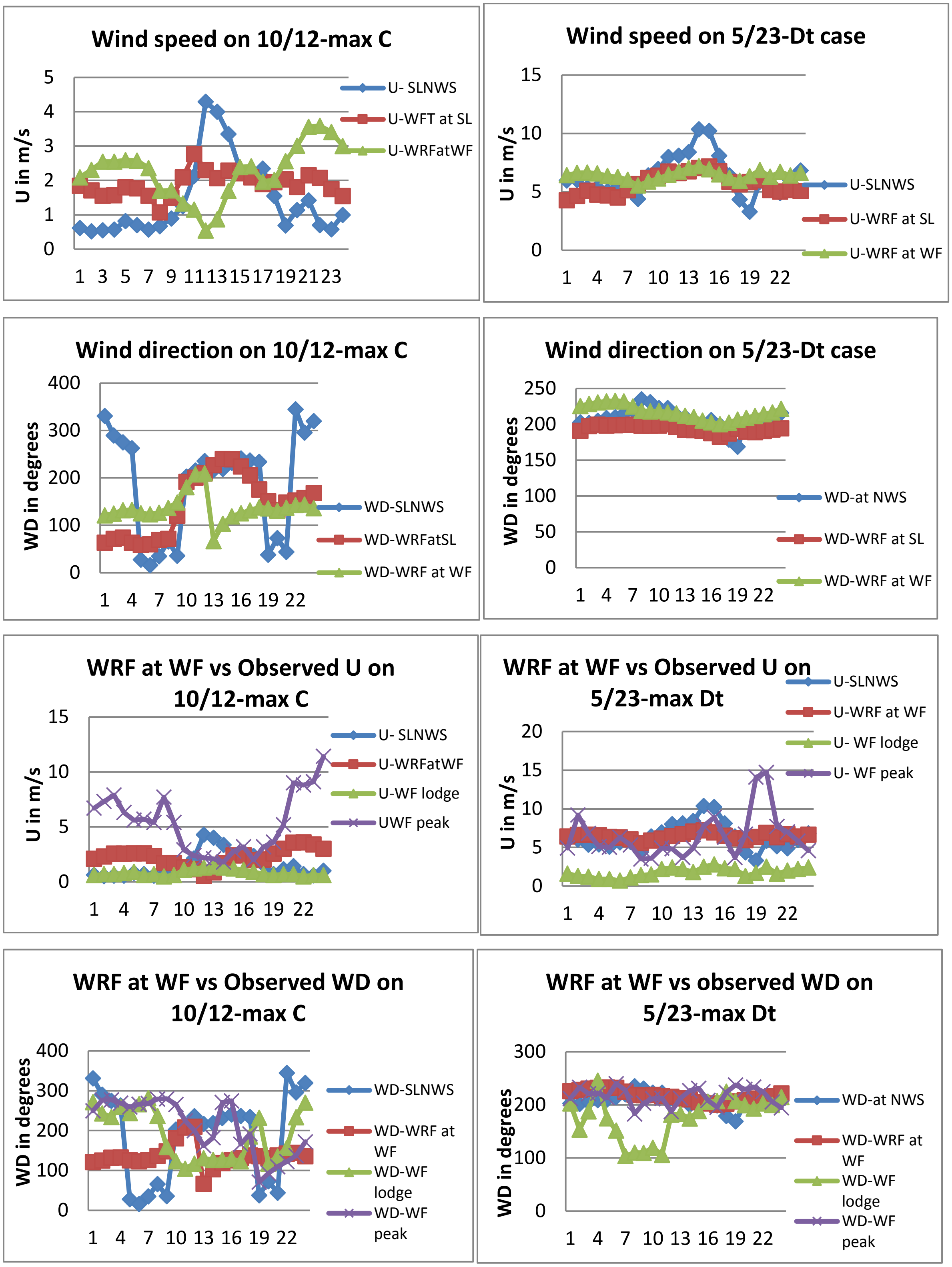

The third and fourth rows of Figure 6-9 show the comparison of WRF simulated wind speed and wind direction, respectively, to the set of observed winds at NWS site and the WF sites for the max C and max Dt days. For the low wind speed day (10/12), large differences are seen in U and WD between both observations as well as in comparison to WRF simulations at WF. Some of the difference in the observed U data might be due to the higher nighttime winds, which might be associated with a low-level jet at the upper levels, as sensed by the observations at the WF summit. On the other hand, for the day with higher wind speeds (5/23), the generally good match in both U and WD is seen between WRF and observations, but in this case the U values at the WF peak are comparable to WF and NWS data, but higher than the lodge site. The relatively low U at the lodge site was also seen for day 8/24 in figure 6-9 even in comparison to the NWS data. The possible influence of the tree sheltering effects on the tower instruments, seen at a site visit, might be partially responsible.

Another important consideration in the comparison of the single point representation of winds at the NWS site, as used in AERMOD vs. the WRF generated spatial variations for CMAQ, is the likely complexities in flow encountered over the large distances and complex terrain settings. It is expected that WRF simulation of the variability of wind speed and direction would better represent the flow patterns affected by variations in land use. Of course, the representation of this variability has to account for the differences in scales of the grid cells. By reducing the CMAQ scale down to a 4km spacing instead of the 12km grid used in previous modeling exercises should lead to better simulation of flow variations. At the same time, it is recognized that the WRF simulations are an average representation over the grid cells and would still have a level of uncertainty. A good test of the WRF simulations would be a detailed comparison to long-term observed data, but is hindered by paucity of valid independent data in the area and is beyond the scope of the current study.

However, the daily observed data from the NWS site and at Whiteface allow for a limited comparison. The wind data in Figures 6-8 and 6-9 seem to indicate that, to a large extent, the WRF data at a grid point close to WF is no better representation of the observed winds at the two heights on the mountain than the NWS data. However, the data in the larger set of days reviewed indicated that this is a fortuitous result not representative of most cases. A more representative day is the wind data for 5/21 that corresponds to maximum concentration day for a 700m source placed at three distances (edge, 10km, and 30km) due west of the Adirondack grid. Plume transport and dispersion at this level is closer to the observation level at WF peak. It is important to also recognize that, by definition, the WRF data is a representation of the average value of a parameter at a given elevation over the area of the grid cell and should not be expected to match the observed levels at specific locations (e.g., two WF sites) within the cell. The diurnal variation in WRF generated wind speed and direction and observed at the NWS and at the two WF towers for 5/21 are presented in Figure 6-10. Also, these data are all taken from or simulated at a 10m height above surface. In general, the WRF data better corresponds to the observed variation in both U and WD and their trends over the day than the NWS data. Although the WRF model simulations of flow are “terrain-following”, it is likely that flow over mountain peaks encounter a level of deformation and speeding-up due to higher approaching wind speeds. The first two graphs indicate that WRF data better matches U at the lodge level and WD at the peak level, while the NWS data does not show consistency in comparison. In the third row, WRF wind speeds are compared to the average of the observed data from the two WF sites to more clearly demonstrate the improved simulation of the average U and its diurnal trend in the grid cell as opposed to the single point NWS data considering that the WF data was not included as part of the WRF simulations.

Figure 6-10. Wind speed and direction for 5/21 by WRF at WF and observed at NWS and WF sites

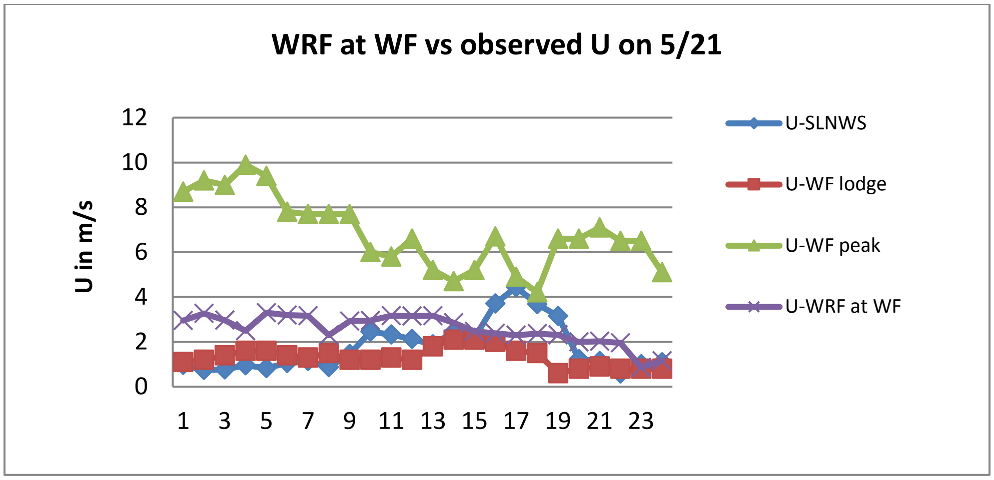

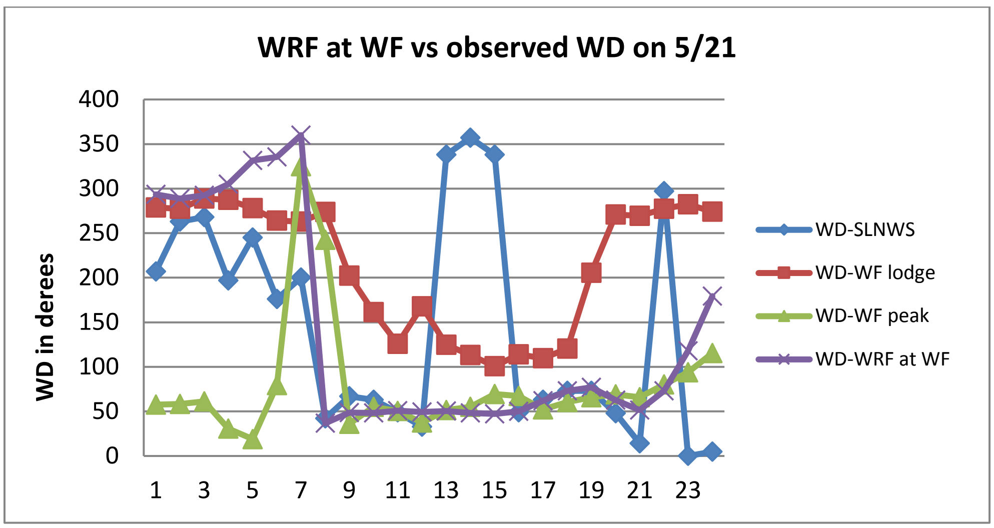

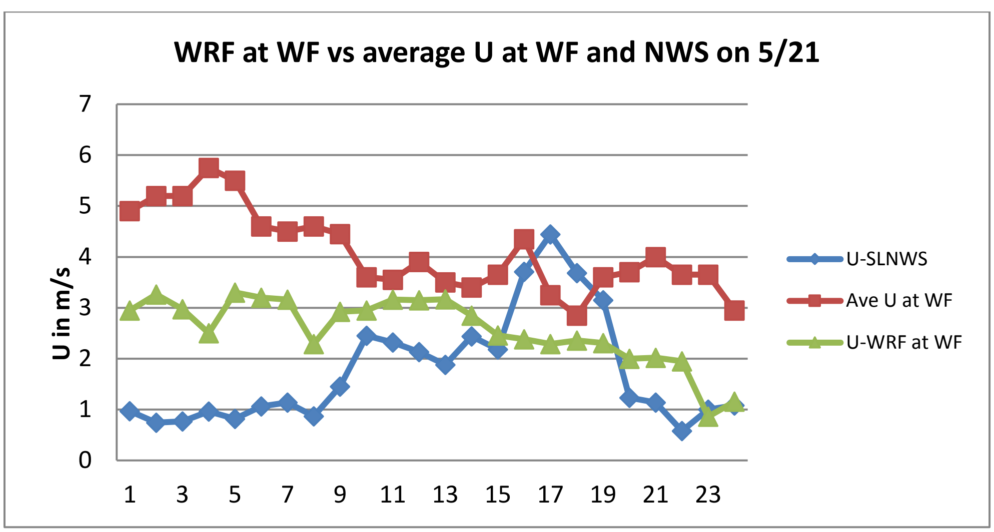

An exception to the finding of higher wind speeds during the 24-hour maximum deposition, as opposed to concentration maxima, was noted for cases with the high source height (i.e., 700 and 1,000m) and some very low-level (10m) sources for both the Adirondack and Catskill grids. AERMOD runs for the 700m case at the west edge of the Adirondack grid was also performed for sulfate impacts, which allowed the comparison of day 5/21 wind data for the Hg2 concentration maximum to the corresponding maximum total deposition for Hg2-day 3/9 and SO4-day 9/15. Since concentrations are based on a nominal emission rate, the same concentration maxima are projected for both pollutants. Plots of wind speeds and directions for the deposition days (not shown) indicated that all three days had essentially the same lower U during most of the day and, importantly, during the hours contributing to the maxima. On the other hand, more persistent wind direction was found for the deposition results, especially sulfate, than for concentration.

If the modeling results are generally indicative of what might actually occur for at least the Hg2 species of mercury, the implications are important from the standpoint of when high concentrations vs. dry deposition (dominating many of the total deposition) are possible, at least on short-term basis. Concentrations are essentially driven by inverse relation to the dispersion or dilution factors, while dry deposition is controlled by the inverse of aerodynamic resistance which itself is inversely related to friction velocity or wind speed (all other resistance factors being equal, which is the case for the simpler AERMOD simulations). Thus, higher winds are associated with higher u* leading to higher deposition via the aerodynamic pathway. In additions, the stability conditions and associated factors during the hours of maximum concentration and deposition are of interest. Thus, some of the interrelationships between the surface layer similarity scales and parameters were investigated and examples presented of the more general findings using data for the days discussed in Figures 6-8 and 6-9.

One aspect of the data from the NWS site and generated by WRF was to test the relationship between wind speed and friction velocity, which is expected to essentially be linear, modified somewhat by stability conditions through similarity functions. For most of the days reviewed, it was found that at both NWS sites and at the WRF grid sites near the two NWS sites and at the Whiteface and Hunter peaks the u* dependence on U was linear to a very good degree. This is not surprising for the higher wind speed days associated with most 24-hour deposition maxima, but was also the case for many lower wind speed days. Some exceptions were found for the data generated by WRF at the cell grid sites. The graphs in the first row of Figure 6-11 demonstrate the relationship between U and u* for the lower wind speed days in Figures 6-8 and 6-9 associated with maximum concentrations. The majority of days of high concentrations and deposition were followed the linear dependence noted for day 10/12. The exceptions were for days similar to day 8/31 by WRF at the WF grid cell and limited to lower U cases and WRF simulations. Some of the latter days had a number of very stable hours, but it was not investigated whether known limits[88] of specific similarity functions under these conditions or formulation in WRF might be responsible for these exceptions. It is clear, however, that essentially all cases indicated that deposition velocity formulations incorporating friction velocity are based on proper mechanical flux relationships.

Another aspect of interest for the cases reviewed was the stability conditions that drive certain of the formulations for deposition estimates. These conditions are indicated by the similarity theory parameter z/L, where L is the Monin-Obhukov length defined from u_* and H_* as:

Equation 7. $$L = -\rho c_p T u_*^3 / kgH_*$$

where c_p is the specific heat of air, ρ is the density of air, T is the temperature representative of the surface layer, g is the acceleration of gravity, and k is the von Karman constant. Thus, under stable conditions with negative H_* (downwards), L is positive and vice versa for unstable cases. When u_* is rather large, leading to large L values, z/L fluctuates around zero. Thus, it is expected that during high wind speed cases, z/L values should tend to indicate neutral stability. Diurnal variations in z/L for the days of maximum concentration (10/12) and deposition (5/23) in Figure 6-9 are depicted in the second row plots of Figure 6-11. The lower wind speed day (10/12) shows a range from stable to unstable to neutral hours, while on day 5/23 the z/L values essentially remain in the neutral to only slightly stable or unstable hours (note the scales for z/L) at both the NWS site and as simulated by WRF at the two cell grid points. The z/L plot for day 8/31 (not shown) follows the plot for day 10/21 of Figure 6-11. On the other hand, for many of the maximum deposition days, the z/L values essentially stay flat around the neutral zero value due to the higher wind speeds.

An unexpected finding for the low U cases is the apparent lack of variation in z/L generated by WRF during hours which are clearly unstable based on the NWS data calculations (e.g. hours 7- 9, day 10/12). On many days, WRF generated z/L values remain at or above zero even when relatively large heat fluxes indicate unstable hours. To investigate possible causes, the example of day 8/31 was chosen since it provided clearer representation and similar variations in some of the parameters of importance. The variation of z/L against its main components u_* and H_* were plotted separately for 8/31 and are presented in the third row of plots in Figure 6-11 for WRF generated data at the WF grid cell. The indicated dependence of z/L on u_* was seen in essentially all cases studied and follows the expectation. That is, as wind speed or u_* increases, the stability class z/L should tend towards the neutral limit of zero.

On the other hand, the expected increase in negative z/L values as positive (or upward) H_* increases is not seen. The indicated increase in positive z/L at very low negative H_* during certain hours is due to the lower u_* during these stable hours. In addition, looking at the z/L and H_* data files for both the NWS and WRF sites for 8/31 reveals a few hours when positive z/L values are found during positive H_* hours in the WRF data, but not in any of the NWS data. This result for the WRF data is contrary to the expectation from the definition of L above; i.e. a positive H_* should lead to a negative z/L or unstable hours.

Further investigation into other days and the MMIF version that generated the WRF data indicated that the calculation of L in MMIF incorporates latent heat flux in addition to the sensitive heat flux. This is contrary to the general definition of L and expectation over land surfaces and was further complicated by the assumption in MMIF/WRF that any latent heat release would be downward, or opposite to the positive heat flux during unstable conditions. The consequences of these assumptions were assessed by choosing a day from the set associated with wet deposition maxima in which case the direction of latent heat transfer cannot be assumed as unidirectional. The H* plots for 8/31 in the fourth row of Figure 6-11 indicates essentially the same values for NWS and WRF, therefore, another day was chosen for clearer demonstration.

Figure 6-11. Meteorological parameters and M-O similarity scales for days of maximum concentration and total deposition for a 100m source at the Adirondack receptor grid

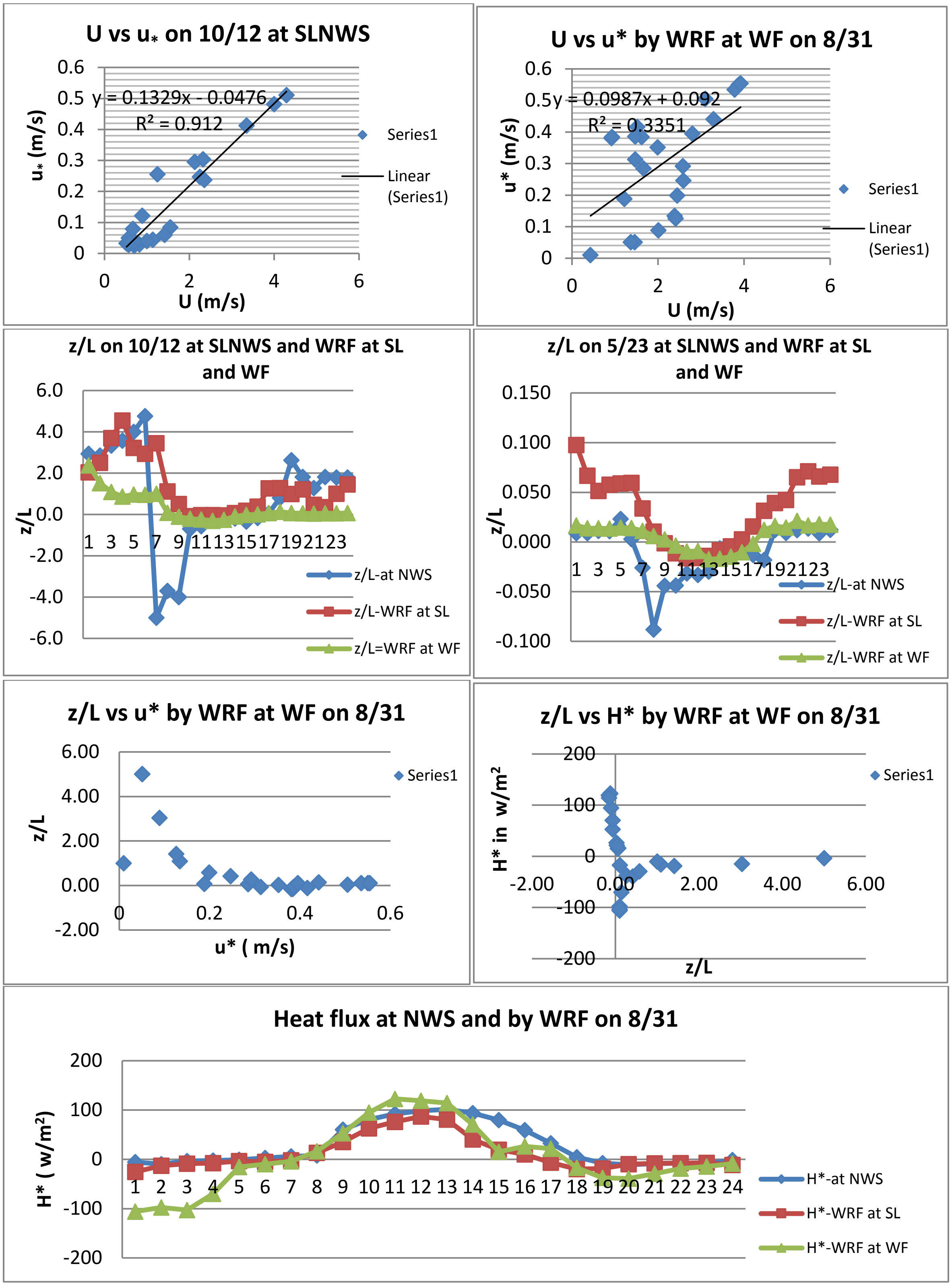

In addition, the chosen day had to display relationships between the similarity parameters as seen in most cases such that the influence of other z/L relationships would not be influential. Thus, day 9/29 was used for the example that corresponded to the maximum wet deposition from the case of all five source heights placed at 10km southeast of the Catskills grid. On this day, the linear relationship between u* and U (similar to 10/12 in Figure 6-4) and the tendency of z/L towards zero as u* increases (similar to 8/31 in Figure 6-11) was seen for both the NWS and WRF generated data. In addition, the day had a variable pattern for u* and H to allow potential testing of the variability in z/L and its expected relationships to these controlling scales.

The plots of pertinent parameters and their relationships are presented in Figure 6-12. The first row of the figure shows the u* and H* diurnal variations at the Poughkeepsie NWS (PKNWS) site from AERMET and those generated by MMIF/WRF at the two grid cells nearby to the NWS site (WRF-PK) and to Hunter Mountain (WRF-HT). The u* variations follow that of the corresponding wind speeds with higher U from WRF, whereas the H* at the NWS site are higher than those from WRF, especially during afternoon hours with positive values. The corresponding z/L calculated at these three sites are depicted in the second row of Figure 6-12 and indicate the expected negative values at the NWS site during these afternoon hours, but essentially a flat line of z/L near zero for the WRF data. The reason for this difference appears to be the difference in the “net” heat flux calculations noted about at the NWS site vs. MMIF/WRF calculated data. A demonstration of the difference is shown in the third and fourth row plots of H* against L for the PKNWS site and WRF calculated values at the nearby PK site, respectively. For the positive heat flux points in the NWS data there is a weak, but noticeable, inverse dependence of negative L on H* as expected. However, in all cases of heat flux including positive afternoon values, the MMIF/WRF data at the nearby site indicates all positive L, or neutral to stable conditions. This is attributed to the effects of the downward latent heat on the H* and L calculations.

Although the data in Figure 6-4 for L vs. H* represents the extreme case of no negative L values for any positive H* values, similar situations exist for other days. This relationship could be a consequence on the stability calculation in the WRF data, but it is not clear, nor further assessed, as to whether it could affect deposition estimates. Furthermore, it is possible that the conditions noted might be a consequence of the MMIF “translation” of WRF data in its AERMOD mode applications. These issues are not of significance to the general modeling approach and the study results and were not further pursued herein.

Figure 6-12. Meteorological parameters and M-O similarity scales for 9/29-day of maximum wet deposition from the set of 5 source heights at 10km SE of the Catskills grid

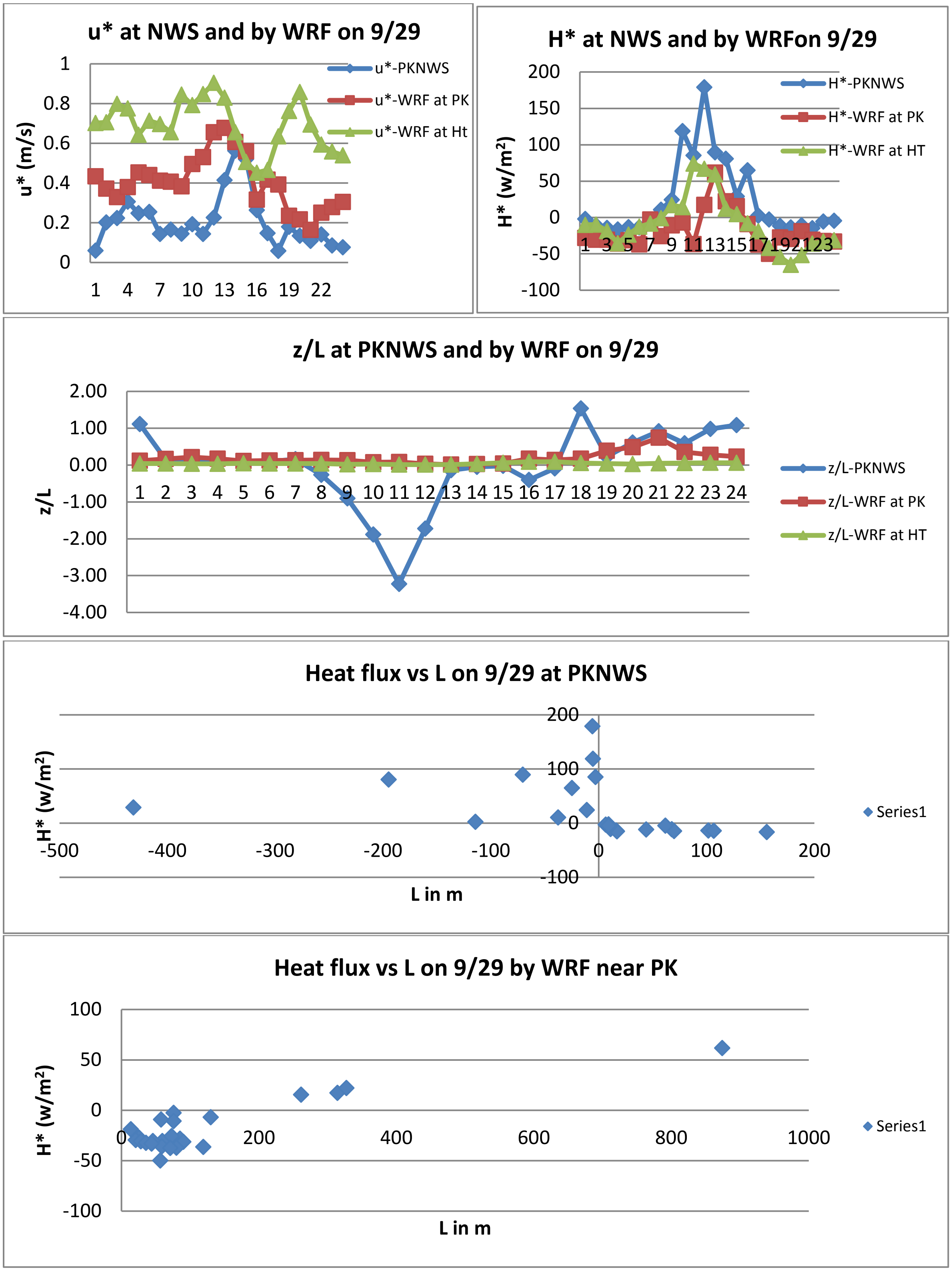

The last comparison for discussion between the AERMET and WRF meteorological data was for precipitation. This comparison, however, was limited to only a few cases since the wet deposition results from CMAQ were evaluated with actual data in the previous section. In addition, it was clear from the previous section that the AERMOD wet deposition assumptions and results are a simplistic representation of the complex spatial varying precipitation in both the horizontal and vertical dimensions. Of the few cases analyzed, it appears that the WRF generated data under-represents the short-term precipitation, at least at single observation locations. An example is provided for day 9/29 of Figure 6-12. The hourly precipitation data for this day at the NWS site and at the two WRF sites are depicted in Figure 6-13. The WRF data misses the two hours of high precipitation (P in millimeters/hour) observed at the NWS site, but when these hours are "zeroed out", the WRF calculations resemble the observations to a good degree (bottom plot), especially as totals for the day, which determine the 24-hour wet deposition. It was noted that the two hours with large precipitation did not contribute to the maximum wet deposition from AERMOD from wind flow considerations to the Catskills grid. What is also seen is that the NWS data is more intermittent than the WRF simulations, likely due to the incorporation of precipitation data in the latter from many sites in CMAQ modeling grid. Other days checked did not indicate as large of underestimation of precipitation by WRF relative to the NWS observations.

Figure 6-13. Observed precipitation at NWS site compared to WRF simulations on 9/29-day of maximum wet deposition (Dw) for the case of all 5 sources at 10 km SE of Catskills grid

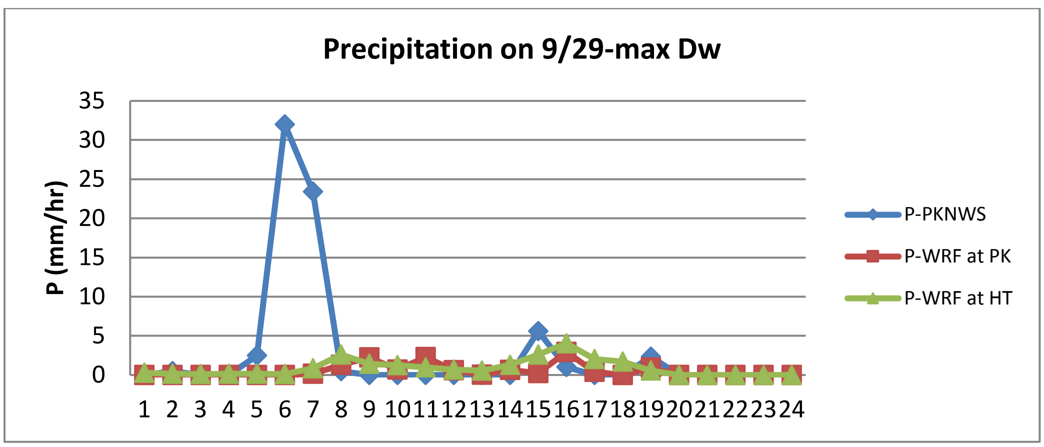

Figure 6-13 continued

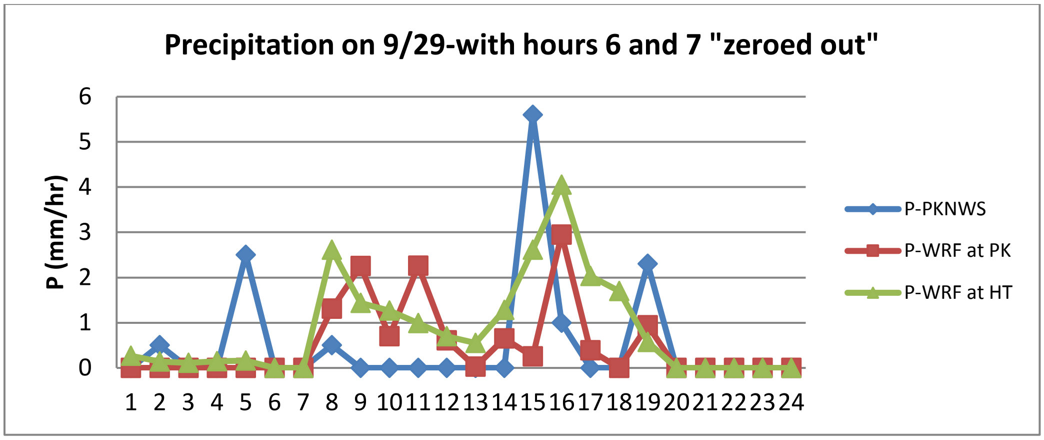

These findings can be summarized as indicting a general tendency for the high 24-hour deposition being associated with higher wind speeds than the corresponding concentration maxima for a specific source height/distance configuration, resulting in different days of importance for at least these 24-hour maxima. To the extent that the annual deposition levels are controlled by these higher 24-hour impacts, the results suggest a means to explain any observed differences in data. For some of the source configurations noted in the above figures, the location of the maximum annual concentrations and deposition were found to correspond to maxima of the 24-hour values. For example, the maximum concentrations and dry/total deposition from the 100m level source placed just west of Whiteface peak or at the west edge of the grid all occurred at the same location for the 24-hour and annual levels. In addition, the wind data, as well as the similarity parameters, show the spatial variability expected over the large distances of transport for the modeling grid. These variations appear to be adequately represented by the WRF simulations based on limited available wind data at Whiteface Mountain, with the understanding that these simulations are representative of average of the parameters in the 4km grid cells. An issue was raised related to the stability conditions in the MMIF/WRF data set for certain hours of the days of maxima, but it was not further assessed whether the issue was due to the specifics in the MMIF processing.

7 References

[1] EPA's Mercury and Air Toxics Standards (MATS). See: http://www.epa.gov/mats/actions.html

[2] EPA's Cross-State Air Pollution Rule (CSAPR). See: http://www.epa.gov/airtransport/CSAPR/index.html

[3] See: http://www.epa.gov/ttn/scram/guidance/guide/Guidance_for_PM25_Permit_Modeling.pdf

[4] See papers by Blackwell on forests and Sauer on songbird Hg levels at the Concurrent Session A - Ecosystem Response to Sulfur, Nitrogen and Mercury Deposition - Part I, NYSERDA EMEP 2011 Conference

[5] See: http://www.gpo.gov/fdsys/pkg/FR-2012-04-03/pdf/2012-7679.pdf

[6] NAPAP Report to Congress, 2011: An Integrated Assessment., dated December 28, 2011.

[7] Wang, Yungang, J. Huang, P.K. Hopke, O.V. Rattigan, D.C. Chalupa, M.J. Utell, and T.M. Holsen (2013). Effect of the shutdown of a large coal-fired power plant on ambient mercury species. Chemosphere, 92, 360-367.

[8] Gratz, Lynne E. and Gerald J. Keeler. (2011). Sources of mercury in precipitation to Underhill, VT. Atmospheric Environment, 45, 5440-5449.

[9] Risch, Martin. R., D.A. Gay, K.K. Fowler, G.J. Keeler, S.M. Backus, P. Blanchard, J.A. Barres, and J. T. Dvonch (2012). Spatial patterns and temporal trends in mercury concentrations, precipitation depths, and mercury wet deposition in the North American Great Lakes region, 2002-2008. Environmental Pollution, 161, 261-271.

[10] Prestbo, Eric M. and David A. Gay (2009). Wet deposition of mercury in U.S. and Canada, 1996-2005: Results and analysis of NADP mercury deposition network (MDN). Atmospheric Environment, 43, 4223-4233.

[11] Air Quality Modeling Technical Support Document (TSD): EGU Mercury Analysis, dated 12/16/11. See:http://www.epa.gov/ttn/atw/utility/utilitypg.html

[12] Yu, Xue, C.T. Driscoll, R.A. F. Warby, M. Montesdeoca, C.E. Johnson (2014). Soil Mercury and its response to atmospheric mercury deposition across the northeastern United States. Ecological Applications, 24, 812-822.

[13] See: http://www.epa.gov/crossstaterule/techinfo.html

[14] See: http://www.wrf-model.org/index.php

[15] Fountoukis, C. and A. Nenes (2007) ISORROPIA II: A Computationally Efficient Aerosol Thermodynamic Equilibrium Model for K+, Ca2+, Mg2+, NH4+, Na+, SO42-, NO3-, Cl-, H2O

Aerosols. Atmos. Chem. Phys., 7, 4639–4659. See: http://isorropia.eas.gatech.edu/index.php?title=Publications#For_citation

[16] http://www.airqualitymodeling.org/cmaqwiki/index.php?title=CMAQ_version_5.0_% 28February_2012_release% 29_Technical_Documentation#Mercury_and_Air_Toxics:

[17] See: http://www.epa.gov/ttn/scram/userg/regmod/ctdmplusfinal_report.pdf

[18] Wesley, M. L., P.V. Doskey, and J.D. Shannon (2002). Deposition Parameterizations for the Industrial Source Complex (ISC3) Model. See: http://www.epa.gov/ttn/scram/7thconf/aermod/aer_scid.pdf (and ISC3 at same EPA SCRAM site).

[19] See: http://www.nyserda.ny.gov/Energy-and-the-Environment/Environmental-Research/EMEP/Conferences/2013-EMEP-Conference/2013-Conference-Presentations.aspx

[20] DEC (1985). The Sulfur Deposition Control Program. Draft Environmental Impact Statement, DEC, June, 1985.

[21] Adams, M.B, et.al. (1991). Screening Procedure to Evaluate Effects of Air pollution on Easten Region Wilderness Cited as Class I Air Quality Areas. U.S. Forest Service General Technical Report NE-151, 9/1991.

[22] Appel, K. W., K.M. Foley, J.O. Bash, R.W. Pinder, R.L. Dennis, D.J. Allen, and K. Pickering (2011). A multi-resolutions assessment of the Community Multiscale Air Quality (CMAQ) model v4.7 wet deposition estimates for 2002-2006. Geoscientific Model Development, 4, 357-371.

[23] Dennis, Robin and Kristen Foley (2014). Characteristics of new CMAQ Deposition series for 2002 to 2011 for critical loads. Presented at 2014 NADP Annual Meeting and Scientific Symposium, Indianapolis, Indiana, October 23, 2014.

[24] Schwede, Donna and Gary G. Lear (2014). A novel hybrid approach for estimating total deposition in the United States. Atmospheric Environment, 92, 207-220.

[25] Communication with D. Schwede: ftp://ftp.epa.gov/castnet/tdep/Total_Deposition_Documentation_current.pdf

[26] Sickles, Joseph. E. and Douglas. S. Shadwick (2013). "Transference ratios" to predict total oxidized sulfur and nitrogen deposition-Part I, monitoring results. Atmospheric Environment, 77, 1060-1069.

[27] EPA Mercury Study Report to Congress. Volume III: Fate and Transport of Mercury in the Environment. Dated December, 1997. See: http://www.epa.gov/ttn/oarpg/t3/reports/volume3.pdf

[28] Siegneur, C. et.al. (2002). Contribution of global and regional sources to mercury deposition in New York State. NYSERDA Report 02-0, prepared by AER, July 2002.

[29] Bullock Russell O. and Katherine A. Brehme (2002). Atmospheric mercury simulation using the CMAQ model:formulation description and analysis of wet deposition results. Atmospheric Environment, 36, 2135-2146.

[30] Bullock, O. Russel, et. al. (2009). An analysis of simulated wet deposition of mercury from North American Mercury Intercomparison Study. Journal of Geophysical Research, 114, DO8301: pages 1-12.

[31] EPA Technical Support Document for the final Clean Air Mercury Rule; Air Quality Modeling. March, 15, 2005. See: http://www.epa.gov/ttn/atw/utility/utiltoxpg.html

[32] Air Quality Modeling Technical Support Document: EGU Mercury Analysis, September, 2011. See: http://www.epa.gov/ttn/atw/utility/epa-454_r-11-008.pdf

[33] Baker, Kirk, R. and Jesse O. Bash (2012) Regional scale photochemical model evaluation of total mercury wet deposition and speciated ambient mercury". Atmospheric Environment. Doi:10.1016/j.atmosenv.2011.12.006.

[34] Bash, Jesse O. (2010). Description and initial simulation of a dynamic bidirectional air-surface exchange model for mercury in Community Multiscale Air Quality (CMAQ) model. Journal of Geophysical Research, 115, D06305, pages 1-15.

[35] NESCAUM (2007). Modeling Mercury in the Northeast United States. Report dated October, 2007.

[36] Zhang,Y. et. al. (2012). Nested-grid simulation of mercury over North America. Atmos. Chem. Phys. 12, 6095-6111.

[37] Weathers, Kathleen, C., S.M. Simkin, G.M. Lovett, S.E. Lindberg (2006). Empirical Modeling of Atmospheric Deposition in Mountainous Landscapes. Ecological Applications, 16(4), 1590-1607.

[38] Yu, Xue, C.T. Driscoll, J. Huang, T.M. Holsen, and B.D. Blackwell (2013). Modeling and Mapping of Atmospheric Mercury Deposition in Adirondack Park, New York". PLOS ONE, volume 8, Issue 3, March 2013.

[39] https://www.cmascenter.org/cmaq/

[40] D. J. Lueckens, W.T. Hutzell, and G.L. Gipson (2006). Development and analysis of air quality modeling simulations for hazardous air pollutants. Atmospheric Environment, V 40, pp 5087-5096.

[41] Shawn J. Roselle, et. al. (2007). Development of a multipollutant version of the community multiscale air quality (CMAQ) modeling system. Presented at the 6th Annual CMAS Conference, Chapel Hill, NC, October 1-3, 2007.

[42] Nancy J. Brown et. al. (2011). Final Report: Fourth Peer Review of the CMAQ Model. Submitted to CMAS by CMAQ Model External Peer Review Panel, dated September 28, 2011. https://www.cmascenter.org/r_and_d/first_review/pdf/final_report.pdf

[43] www2.mmm.ucar.edu/wrf/users/download/get_source.html

[44] Shawn J. Roselle and Francis S. Binkowski (1999). Cloud dynamics and Chemistry, Chapter 11 of CMAQ Technical Document, EPA publication: EPA/600/R-99/030.

[45] Leon Sedefian K. Civerolo, M. Ku., W. Hao, and E. Zalewsky (2015). Refined grid regional modeling of inorganic pollutants in mountainous terrain and coastal areas of New York: Some preliminary results. Presented at the International MAC-MAQ Conference, Sacramento, CA September 16-18, 2015.

[46] Fountoukis C. and Nenes, A. (2007). ISORROPIA II: a computationally efficient thermodynamic equilibrium model for K+-Ca2+-Mg2+-NH4+-Na+-SO42- -NO3- -Cl--H2O aerosols. Atmospheric Chemistry and Physics, 7, 4639-4659.

[47] J. S. Scire, Z Wu, and D. G. Strimaitis (2013). Implementation and evaluation of ISORROPUIA in CALPUFF. Air and Waste Management Conference on Guidelines on Air Quality Models: The path forward. Raleigh, NC, March 19-21, 2013.

[48] EPA (2015). Technical Support Document (TSD). Preparation of emissions inventories for the version 6.2, 2011 emission modeling platform. EPA document dated August, 2015.

[49] https://www.cmascenter.org/smoke/

[50] http://www3.epa.gov/ttn/scram/dispersion_prefrec.htm#ctdmplus

[51] M.L. Wesley, P.V. Doskey, and J.D. Shannon (2002). Deposition parameterization for the Industrial Source Complex (ISC3) Model see: http://www3.epa.gov/ttn/scram/dispersion_prefrec.htm#aermod

[52] http://www3.epa.gov/ttn/scram/7thconf/aermod/aer_scid.pdf

[53] NESCAUM Report to NYSERDA (#10-31): "Determination of Sulfur and Toxics Metals Contents of Distillate and Residual Oil in the State of New York". Final Report, December, 2010.

[54] U.S. EPA, AP 42, Fifth Edition. Compilation of Air Pollutant Emission Factors, Volume 1: Stationary Point and Area Sources. See: http://www.epa.gov/ttn/chief/ap42/index.html

[55] DEC-DAR: Air Guide 36: Emission Inventory Development for Cumulative Air Quality Impact Analysis. Draft, 2005.

[56] Gratz, Lynne E. and Gerald J. Keeler (2011): "Sources of mercury in precipitation to Underhill, VT". Atmospheric Environment, 45, pp 5440-5449.

[57] NESCAUM (June, 2013). Elemental analysis of wood fuels. NYSERDA Final report 13-13.

[58] Huang, J. et. al. (2011). Mercury (Hg) emissions from domestic biomass combustion for space heating. Chemosphere, 84, 1694-1699.

[59] Gustin, Sexaur.M., P.S. Weiss-Penzias and C. Peterson (2012). Investigating sources of gaseous oxidized mercury in dry deposition at three sites across Florida, USA. Atmospheric Chemistry and Physics, 12. 9201-2019.

[60] NESCAUM (2011): Massachusetts State Anthropogenic Mercury Emissions Inventory Update. Dated December, 2011.

[61] Houyoux, Marc and Madeleine Strum, EPA Memorandum, December 1, 2011: Emissions Overview: Hazardous Air Pollutants in Support of the Final Mercury and Air Toxics Standard. EPA-454/R-11-014, November 2011.

[62] Zhang, Y., et. al. (2012) Nested:-grid simulation of mercury over North America. Atmospheric Chemistry and Physics, 12, pp 6095-6111.

[63] EPA (2005). "Emissions Inventory and Emissions Processing for the Clean Air Mercury Rule (CAMR)". EPA OAQPS document, dated 3/15/05.

[64] Edgerton, Eric, S. Benjamin, E. Hartsell, and John J. Jansen (2006). Mercury speciation in coal-fired power plant plumes observed at three surface sites in Southeastern U.S. Environ. Sci. and Technol., 40, pp 4563-4570.

[65] NESCAUM (2007). Modeling Mercury in the Northeast United States. Report dated, October, 2007.

[66] Baker, Kirk R. and Jesse O. Bash. Regional scale photochemical model evaluation of total wet deposition and speciated ambient mercury. Atmospheric Environment, 12, 1-12.

[67] Bullock, David and Shelly Johnson (2011). Electric Generating Utility mercury speciation profiles for the Clean Air Mercury Rule (CAMR). EPA memorandum dated 11/14/11.

[68] Houyoux, Mark and Madeleine Strum (2011) Emissions Overview: Hazardous Air Pollutants in Support of the Final Mercury and Air Toxics Standard. EPA memorandum dated 12/1/11.

[69] Ash Grove Mercury Test Report (2007). Ash Grove Cement Company, Durkee, Oregon, Dated April 5, 2007.

[70] Portland Cement Association (2008). Scrubber Testing Program to Determine Mercury Concentrations and Removal. PCA Summary Report, draft, October 2008.

[71] EPA (2015). Technical Support Document (TSD). Preparation of emissions inventories for the version 6.2, 2011 emission modeling platform. EPA document dated August, 2015.

[72] Sedefian, L., K. Civerolo, M. Ku, W. Hao, and E. Zalewsky (2015). Refined grid regional modeling of inorganic pollutants in mountainous terrain and coastal areas of New York: Some preliminary results. Presented at the International MAC-MAQ Conference, Sacramento, CA September 16-18, 2015.

[73] Schwede, Donna and Gary G. Lear (2014). A novel hybrid approach for estimating total deposition in the United States. Atmospheric Environment, 92, 207-220.

[74] Dennis, Robin and Kristen Foley (2014). Characteristics of new CMAQ Deposition series for 2002 to 2011 for critical loads. Presented at 2014 NADP Annual Meeting and Scientific Symposium, Indianapolis, Indiana, October 23, 2014.

[75] See https://www3.epa.gov/castnet/site_pages/HWF187.html

[76] Huang, J. and M. S. Gustin (2015). Use of passive sampling methods and models to understand sources of mercury deposition to high elevation sites in the Western United States. Environmental Science and Technology. 49, 423-441

[77] Zhang, L. et.al (2012). Estimation of speciated and total mercury dry deposition at monitoring locations in eastern and central North America. Atmospheric Chemistry and Physics, v.12, 4327-4340.

[78] Yu, Xue, C.T. Driscoll, R.A. F. Warby, M. Montesdeoca, C.E. Johnson (2014). Soil Mercury and its response to atmospheric mercury deposition across the northeastern United States. Ecological Applications, 24(4), 812-822.

[79] Baker, Kirk, R. and Jesse O. Bash (2012) Regional scale photochemical model evaluation of total mercury wet deposition and speciated ambient mercury. Atmospheric Environment. Doi:10.1016/j.atmosenv.2011.12.006.

[80] Appel, K. W., K.M. Foley, J.O. Bash, R.W. Pinder, R.L. Dennis, D.J. Allen, and K. Pickering (2011). A multi-resolutions assessment of the Community Multiscale Air Quality (CMAQ) model v4.7 wet deposition estimates for 2002-2006. Geoscientific Model Development, 4, 357-371.

[81] Holloway, T. C. Voigt, J. Morton, S.N. Spak, A.P. Rutter, and J.J. Schauer (2012). An assessment of atmospheric mercury in the CMAQ model at an urban and a rural site in the Great lakes Region of North America. Atmospheric Chemistry and Physics, v.12, 7117-7133.

[82] Weathers, K. C., G.M. Lovett, G.E. Likens, R. Lathrop (2000). The effect of landscape features on deposition to Hunter Mountain, Catskill Mountains, New York. Ecological Application, V 10(2), 528-540.

[83] Miller, E. K., et. al. (1993). Atmospheric deposition to forests along an elevational gradient at Whiteface Mountain, NY, USA. Atmospheric Environment. V. 27A, no. 14, 2121-2136.

[84] Lovett, G. M. and J.D. Kinsman (1990). Atmospheric pollutant deposition to high-elevation ecosystems. Atmospheric Environment. Vol. 24A, No. 11, 2767-2786.

[85] Tsai, J. L, et.al (2010). Observation of SO_2 dry deposition velocity at a high elevation flux tower over an evergreen broadleaf forest in Central Taiwan. Atmospheric Environment. V 44., 1011-1019.

[86] Blackwell, B. D. and C.T. Driscoll (2015). Deposition of mercury in forests along a montane elevation gradient. Environmental Science and Technology. V. 49, 5363-5370.

[87] Bytnerowicz, A., M.E. Fenn, and M.J. Arbaugh (1998). Concentrations and deposition of nitrogenous air pollutants in a Ponderosa/Jeffrey pine canopy. USDA Forest Service General Technical Report, PSW-GTR-166.

[88] Sedefian, L. and E. Bennett (1980). A comparison of turbulence classification schemes. Atmospheric Environment. v14, pp. 741-750.

NYSERDA, a public benefit corporation, offers objective information and analysis, innovative programs, technical expertise, and support to help New Yorkers increase energy efficiency, save money, use renewable energy, and reduce reliance on fossil fuels. NYSERDA professionals work to protect the environment and create clean-energy jobs. NYSERDA has been developing partnerships to advance innovative energy solutions in New York State since 1975.

To learn more about NYSERDA's programs and funding opportunities, visit nyserda.ny.gov or follow us on Twitter, Facebook, YouTube, or Instagram.

New York State
Energy Research and
Development Authority

17 Columbia Circle
Albany, NY 12203-6399

toll free: 866-NYSERDA
local: 518-862-1090
fax: 518-862-1091

info@nyserda.ny.gov
nyserda.ny.gov